Ministry education and sciences Ukraine

KHARKIV NATIONAL AUTOMOBILE AND ROAD UNIVERSITY

TECHNOLOGICAL APPROACHES TO INCREASE PARAMETERS QUALITIES OF A HYDRAULIC HAMMER

Monograph

Kharkiv 2025

UDC 669.017
BBK 34.58
R 62

Recommended for publication by the decision of the Academic Council of "Kharkiv National Automobile and Highway University"

Reviewers: **Ye. Rybka**, Doctor of Technical Sciences, Professor of the Department of Fire Prevention in Settlements, National University of Civil Protection of Ukraine;
O. Beketov, Doctor of Technical Sciences, Associate Professor, Dean of the Faculty of Information Technologies and Mechanical Engineering, Educational and Scientific Institute "Prydniprovska State Academy of Civil Engineering and Architecture";
N. Fidrovska, Doctor of Technical Sciences, Professor, Head of the Department of Construction and Road Machines named after A.M. Kholodov, Kharkiv National Automobile and Highway University.

Autors: **D. Hlushkova,** Doctor of Technical Sciences, Professor, Head of the Department of Metal Technology and Materials Science named after O.M. Petrychenko;
A. Uzhva, Candidate of Technical Sciences, Associate Professor of the Department of Automobiles named after A.B. Hredeskul, Kharkiv National Automobile and Highway University;
A. Suminov, Postgraduate Student of the Department of Construction and Road Machines named after A.M. Kholodov, Kharkiv National Automobile and Highway University;
V. Skripnikov, Postgraduate Student of the Department of Metal Technology and Materials Science named after O.M. Petrychenko.

D. Hlushkova, A. Uzhva, A. Suminov, V. Skripnikov
P62 Technological approaches to increase parameters qualities of a hydraulic hammer / D. Hlushkova, A. Uzhva, A. Suminov, V. Skripnikov. – Kh.: 2025. – 260 p.

The monograph is devoted to a comprehensive examination of the issues of developing new technological modes and the latest coating compositions to improve the parameters of the hydraulic hammer's performance. It covers significant experimental material, as well as a wide range of issues of theory, research methods for new types of materials and technologies, and problems of intensive implementation in production.

Recommended for researchers, practicing engineers, postgraduates and students of higher technical educational institutions.

ISBN

INTRODUCTION

The most important task of modern mechanical engineering is the development of highly efficient technological processes that allow increasing the reliability and durability of critical machine parts.

In modern conditions, to intensify production processes in various industries industry wide use drums mechanisms. The most common are hydraulic hammers – replaceable equipment for hydraulic excavators, loaders or tractors – designed for breaking up asphalt concrete surfaces, destroying concrete and reinforced concrete structures, loosening rocky and frozen soils, compacting loose soil (using a replaceable working element – a rammer), etc.

The hydraulic hammer is installed on the excavator instead of the removed handle or bucket and connected to the hydraulic system. It is indispensable when opening underground structures - heating mains, gas pipelines, pipelines, telephone and power cables. Hydraulic hammer wide use V communal economy, industrial and civil construction, construction of roads, airfield runways, for the destruction of obsolete structures, as well as blast-free excavation of mine workings.

The use of hydraulic hammers, for example, in public utilities allows us to completely abandon the use of the so-called “hot” method of opening frozen soil. There is no need to warm up the ground, which significantly reduces the duration and material costs of earthworks in winter, which is especially important when eliminating accidents in underground utilities; in addition, the environmental situation improves.

Analysis of the operation of hydraulic hammers from various manufacturers in various operating conditions [1] showed that the main reasons for the failure of a hydraulic hammer, provided that the rules for its operation are observed, are fatigue failure of the working tool (peak) and parts of the striking part (piston, axle box, cylinder). It is possible to significantly extend the service life of a hydraulic hammer and avoid breakdowns by additional strengthening and reducing the wear of the main components, increasing their fatigue strength.

To ensure increased wear resistance and fatigue strength of the material of hydraulic hammer parts, it is not always advisable to change the traditional manufacturing technology of the part and, in particular, the methods of its heat treatment. In some cases, it is worth using surface hardening of the product.

Currently, there are a number of surface hardening technologies, each of which has its own advantages and disadvantages. The most common are laser thermal hardening, electric spark alloying, galvanic chromium plating, ion-

plasma hardening, gas detonation spraying, vacuum-plasma hardening, and surfacing of working surfaces.

Study of the influence of various methods of surface treatment on the change in the structure and properties of hydraulic hammer parts strengthening and choosing the most effective method to increase their durability is an urgent task.

1. TERMS AND CONDITIONS OPERATIONS HYDROHAMMER

1.1. Story creations hydraulic hammer

A hydraulic hammer is irreplaceable when breaking hard rocks, concrete, frozen soil and brick structures. The productivity of the replaceable equipment is determined by the energy and frequency of impacts.

In the 1980s, pneumatic and hydraulic hammers with an impact energy of 9000 J. At that time, the world's manufacturers and suppliers of this equipment included Montabert in France,

Furukawa in Japan, MGF, Krupp in Germany, Shand in the UK And other. Many from these companies led developments in this area, which led to an expansion of the range of hammer sizes. Unfortunately, domestic developments in this area were not as fast and were limited to the release of individual series. The reason for this was the technological complexity of conducting developments that require precise processing of parts and the use of high-quality materials. There was another reason: by this time in the USSR there was no urgent need to master this product [1, 2].

The majority of foreign models of hydraulic hammers are produced By scheme, which was for the first time developed And applied by the Krupp company. The differences consist only in the design of individual units and assembly. This trend also applies to some models production CIS, For example, hydraulic hammers

"Impulse", which are produced by enterprises in Russia and Kyrgyzstan. The scheme of the model of hydraulic hammers of domestic production GPM-120 is characterized by low cost and maximum simplicity. Due to their advantages, hydraulic hammers of this brand have stood the test of time and are still in high demand.

Today, a wide range of hammers for different sizes of excavators is available in production. According to the type of execution of the impact part drive, hydraulic hammers are conventionally divided into three groups: hydraulic, hydropneumatic and hydromechanical [2–5].

In hydraulic hammers, the movement of the striking part during the working stroke and lifting occurs with the participation of the working fluid, which is supplied by the pump of the base machine.

In hydropneumatic hammers, the acceleration of the striking part during the working stroke is carried out with the participation of gas, and the lifting of the striking part of the equipment is carried out with the participation of the working fluid of the system.

IN hydromechanical hammers drive shock parts realized from a hydraulic motor through an intermediate mechanical transmission.

A significant part of the range of manufactured hydraulic hammers is occupied by hydraulic hammers with a pneumatic accumulator. In this case, compressed nitrogen plays the role of the energy carrier, and the piston of the working cylinder is used as the striking part of the hammer.

Along with hydraulic hammers, pneumatic hammers are widely used to destroy concrete structures and frozen soils of hard rocks. Pneumatic hammers were the historical predecessors of hydraulic hammers. In pneumatic hammers, compressed air acts as an energy carrier. At the same time, pneumatic hammers have both their own advantages and disadvantages in relation to hydraulic hammers. They are characterized by much more high level of reliability of sealing elements and connections, can be used at high temperatures and are easier to handle repair. The pneumatic hammer effectively copes with its tasks both in powerful pile driving hammers with a striker weighing several tens of tons, and in hand hammers.

However, pneumatic hammers have a number of disadvantages, the main one being that they are bulky and expensive. compressors. When connected to an excavator compressor, the maneuverability of the base machine decreases. The release of compressed air into the atmosphere is accompanied by a high noise level.

The hydraulic hammer, which replaced the pneumatic hammer, soon replaced its predecessor in mobile and stationary applications. cars. AND Although given process refers to To to the beginning 20 centuries,

The first patent applications and inventions began to arrive only in the late 1950s, and in 1957 the US company Ramond was able to obtain a patent for the design of a hydraulically powered pile driving hammer. The company soon tested the new 65CH hammer model on the US Atlantic coast.

Alloy steel of the 38ХН3МФА, 5ХНМА, 5ХВ2С, 9ХС type was used for the production of replaceable tools. According to calculations by the Krupp company, such equipment had a durability of approximately 1000 h when used with medium-hard soils. Nowadays, stronger steels with improved parameters are used. It was noted that when working with soft rocks, the use of pointed working tools is most effective, while flat working tools cope better with hard rocks.

Today, developments in the field of hydraulic hammer designs continue, and modern designs provide for simple And comfortable replacement one type tool to others. At In this case, the choice of equipment is determined by the nature of the work performed (pile driving, soil compaction, development of

frozen soils). The delivery of hydraulic hammers is carried out together with a replaceable tool. These can be caps for driving sheet piles into the ground, asymmetrical wedges, tamping plates, cylindrical tools with a spherical or flat end. and others.

In the 80s, the cost of a hydraulic hammer was approximately 20-50 % of the cost of the base machine. These figures are also applicable to the modern construction equipment market, but the range of choices for the manufacturer of hydraulic hammers has expanded significantly. For example, the price of a hydraulic hammer from the French company Rammer for an excavator is 15 tons is equal to approximately 20% of the cost of the base machine, in relation to a domestic hydraulic hammer production

For MG-300 this ratio is 8%, and for the Delta F-10 hydraulic hammer produced in South Korea it is 11%.

The field of modern construction contributes to the emergence of new models on the market of replacement equipment for excavators. Significant advantages possess gidromoloty

Delta made in South Korea : a winning price-quality ratio, availability of replaceable working tools. Modern list hydraulic hammers form some most bright brands: DAEMO, Delta, Caterpillar, Sandvik, AtlasCopco, IndacoSoosan, Arden, Montaber, Furukawa. In the field of modern construction, two schemes of hydraulic hammer operation are most in demand: the piston type scheme and the diaphragm type. In domestic conditions, piston type hydraulic hammers are widespread, which are produced by Delta, NPK, Furukawa. They have gained recognition from consumers due to their more repairable design and high adaptation to winter working conditions.

Among the domestic developments in this area, the MG-300 design can be singled out . Work on developing the hydraulic hammer was carried out in 1985-1988. The model was supposed to replace the previously produced SP-71A and SP-71. As a result, it was possible to make worker cycle more profitable With economic dots vision and improve the workflow. In this model The hydraulic hammer striker simultaneously functions as the piston of the working cylinder.

1.2. Principle works And requirements To hydraulic hammers

The use of a mounted hydraulic hammer allows you to significantly expand the capabilities of the excavator, turning it into a truly universal machine. Thanks to the tandem with earthmoving equipment, mounted

hydraulic equipment can reliably operate in different climatic conditions, with various soils. However, for more efficient work, it is necessary to know the features of the mounted hydraulic hammers, their operating conditions and maintenance requirements.

With all the variety of hydraulic hammer models produced, there are only a few basic diagrams of their hydraulic drive. The most common diagram is shown in Fig. 1.1, which is used by most foreign manufacturers. The hammer striker is simultaneously the piston of the working cylinder and has two counter-rods, usually of different diameters d_1 and d_2 [5, 6]. The “lower” rod d_1 , which with its end strikes instrument, has more diameter. Camera worker cylinder,

formed around the lower rod, is an idle chamber, i.e. it ensures the movement of the striker away from the tool or idle stroke. This chamber, when the hammer is switched on, is constantly under pressure of the working fluid during the entire operating cycle. The cylinder chamber formed around the "upper" rod (the working stroke chamber) has a larger area than the idle stroke chamber and is alternately connected to the drain line (upward acceleration) and to the pressure line (braking before the top dead center and downward acceleration). The alternating connection of the working stroke chamber to the drain and pressure lines is carried out by a two-position spool valve with feedback according to the position of the striker in the cylinder. Signals for switching the spool are sent to the spool control chamber when the piston passes the corresponding grooves in the cylinder. When the striker is cocked, its piston opens the spool control channel at a certain position, connecting its control chamber to the pressure line and ensuring its switching to the working stroke position.

At the end of the working stroke, immediately before the impact, the piston connects the control chamber of the spool valve with the drain line with its groove, ensuring that the spool valve switches to the cocking position of the striker. The spool valve of the hydraulic distributor of the hydraulic hammer is made with working belts of different diameters, so that the pressure of the working fluid constantly acts on one of its ends, and the pressure acts on it from the opposite end only on phase braking And in time worker move striker.

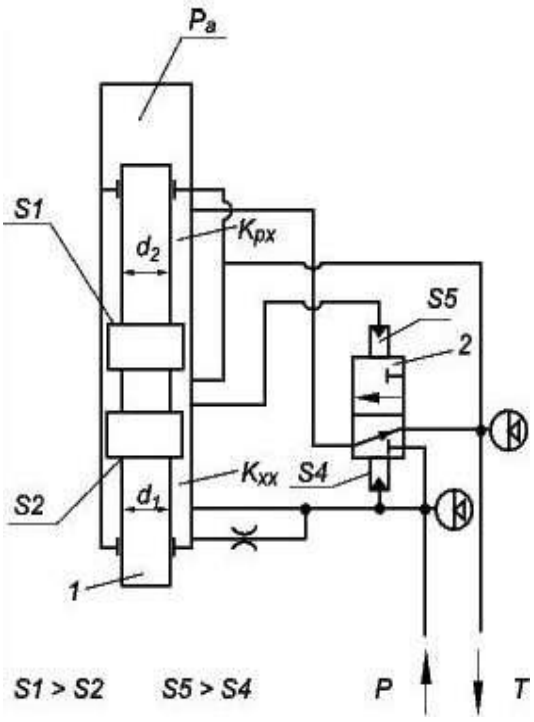

Figure 1.1. Scheme hydraulic Schematic diagram of hydraulic hammer models [6]: 1 – striker; 2 – distributor; Kxx – idle chamber; Kpx – working stroke chamber; Pa – pneumatic chamber; S1 and S2 – areas of working cylinder chambers; S4 and S5 – areas of spool control chambers

The basic diagram of a hydraulic hammer described above is implemented in specific models using various design and layout solutions.

Ultimately, the layout and design solution are determined by the technological capabilities and priorities of the developers. And manufacturers hydraulic hammers, A Also the possibility of patenting individual design solutions.

The choice of a hydraulic hammer for a specific base machine determines its weight. The weight of the hydraulic hammer should be approximately 0.1 of the weight of the excavator, but should not exceed the weight of the bucket with soil. The less the weight of the hydraulic hammer, the better for the excavator in the transport position, the less the load on the excavator's working equipment when aiming the hydraulic hammer at the point where it should work. But, on the other hand, the greater the mass of the hydraulic hammer, the less the force required to press it against the work object, the less vibration transmitted to the base machine when the hydraulic hammer is operating [4, 7, 8].

The next indicator that determines the possibility of using a hydraulic hammer on a given excavator is the flow rate of the working fluid, which

is always given in the technical characteristics of the hammer. This indicator must correspond to the performance of the excavator's hydraulic pump, which will feed the pressure line of the hydraulic hammer. If the performance of the base machine pump exceeds the required flow rate of the hydraulic hammer, then during its operation, pressure peaks may occur, which negatively affect the durability of both the hydraulic hammer itself and the hydraulic units of the base machine. If the pump performance is less than the minimum flow rate of the hydraulic hammer, then the hydraulic hammer may work unstably or will not work at all.

Very important indicator is level worker hydraulic hammer pressure. The pressure that the base machine pump can provide should not be less than the working pressure of the hydraulic hammer. If the maximum pressure of the hydraulic pump is 10-15 times greater than the working pressure of the hydraulic hammer, %, then the pressure line of the hydraulic hammer must be provided with a safety valve that accordingly limits this level [9, 10].

Otherwise, in the event of abnormal situations, some parts of the hydraulic hammer may fail, for example, the pins that tighten the body parts of the hammer, or the bolts that secure the hydraulic distributor, hydraulic accumulator, or the seals may be damaged. The technical performance of the hydraulic hammer is determined by its effective power, i.e. the product of the energy of a single impact and the frequency of impacts. These are the main characteristics of the hydraulic hammer. The greater the strength of the material that needs to be destroyed with the hydraulic hammer, the greater the impact energy has on the performance [11–13].

A hydraulic hammer with greater impact energy allows you to break off larger pieces from the massif, break through thicker layers of road surfaces, and destroy larger concrete structures. If you need to destroy any relatively thin surfaces or structures or destroy strong rocks on relatively small pieces, preferred hydraulic hammers With lower impact energy, but with a higher impact frequency. The impact energy of the hydraulic hammer should be such that the destruction of the material being processed under the tip of its working tool occurs in no more than 15–30 seconds. When destroying viscous materials, such as, for example, frozen soil, various limestones and similar materials, the impact energy has a decisive influence on the productivity of the hydraulic hammer, since in order to form cracks in the material being processed, the working tool must be driven to a sufficiently large depth [1, 3].

The hammer impact energy is usually not specified in the passport data, since it depends on various accompanying circumstances, including the elastic properties of the material being destroyed and the performance of the base machine pump. This indicator can be calculated using the following formula

$$E = mv^2/2,$$

where m is the mass of the striker; v is its speed at the moment of impact with the tool.

Thus, the same impact energy indicator can be achieved due to the mass of the striker or due to its speed. The hydraulic hammer is considered more effective if, when equal impact energy, greater mass of the striker (greater impulse force, those. product mv).

The impact frequency of modern hydraulic hammers ranges from 10 to 40 Hz. Impact energy is from 0.5 to 20 kJ.

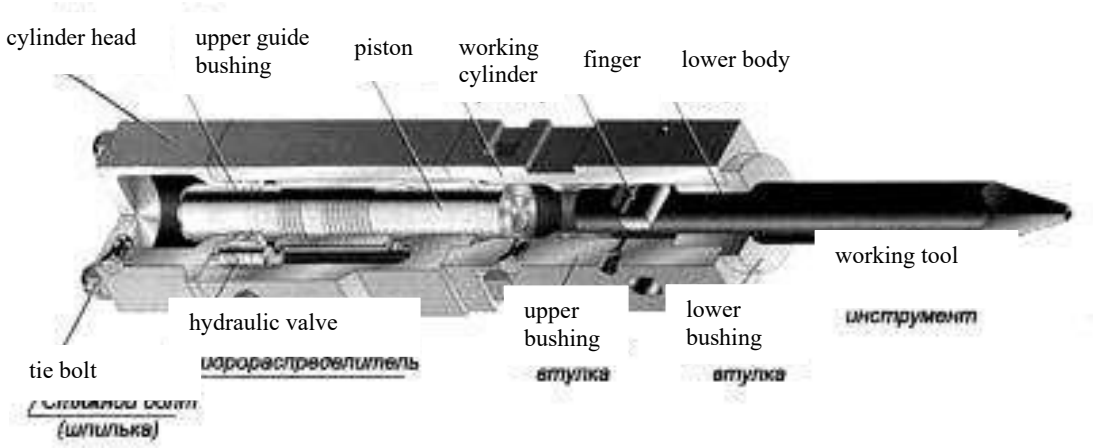

Figure 1.2. General view hydraulic hammer

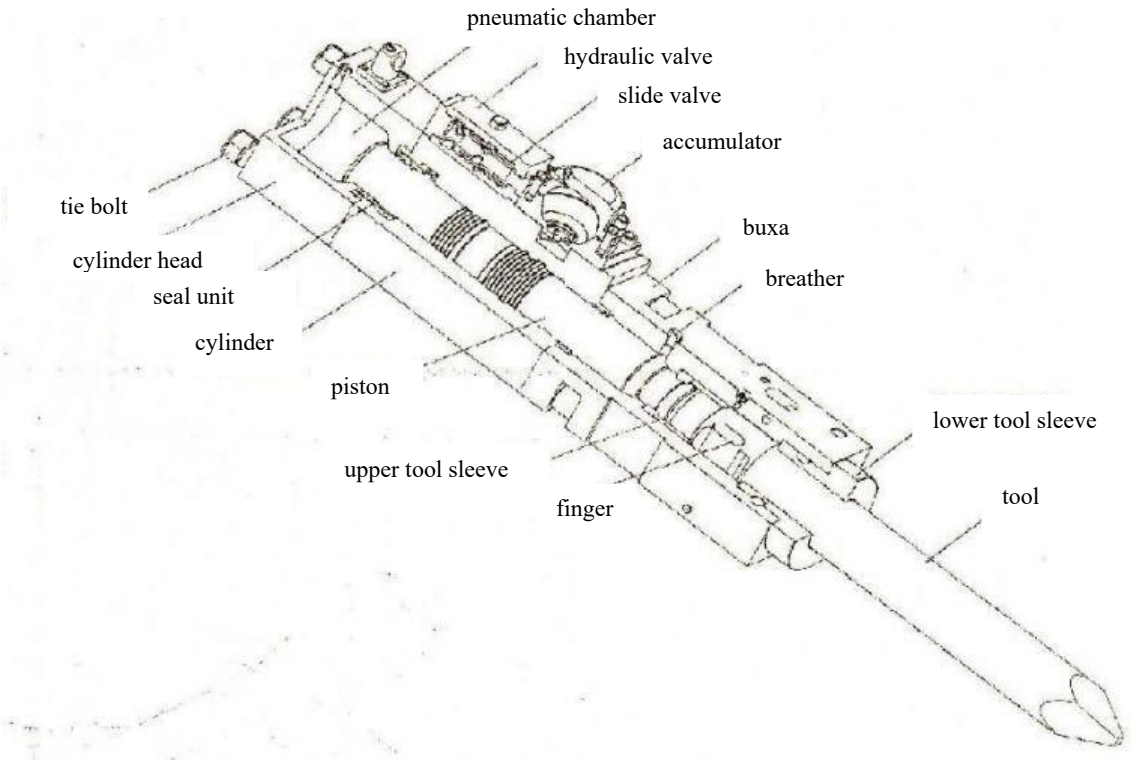

Figure 1.3. Scheme hydraulic hammer (For models Delta F-15, F-20, F-35, F-45, F-50, F-70) [3].

Modern hydraulic hammers use devices for automatic selection of the loading mode based on the energy and frequency of impact, and some models are also equipped with an automatic impact loading system that responds to changes in resistance.

Hydraulic hammers with similar technical characteristics may differ in the way the impact block and the entire hydraulic hammer are secured to the base machine. Most often, the impact block is secured in the bearing jaws located in a box-shaped casing. The elastic shock absorbers used in it reduce the impact of the hydraulic hammer on the excavator. They can be made either in the form of spiral springs or rubber or plastic blocks.

The simplest mounting option is when the impact block is placed between two cheeks, tightened together with bolts or studs. The cheeks can also be attached to the base machine from the side.

A distinctive feature of the DSM light series hydraulic hammers (Fig. 1.4) is the internal structure, which is a monolithic steel block without a tie bolt, which eliminated one of the main causes of hydraulic hammer failure and facilitated their maintenance.

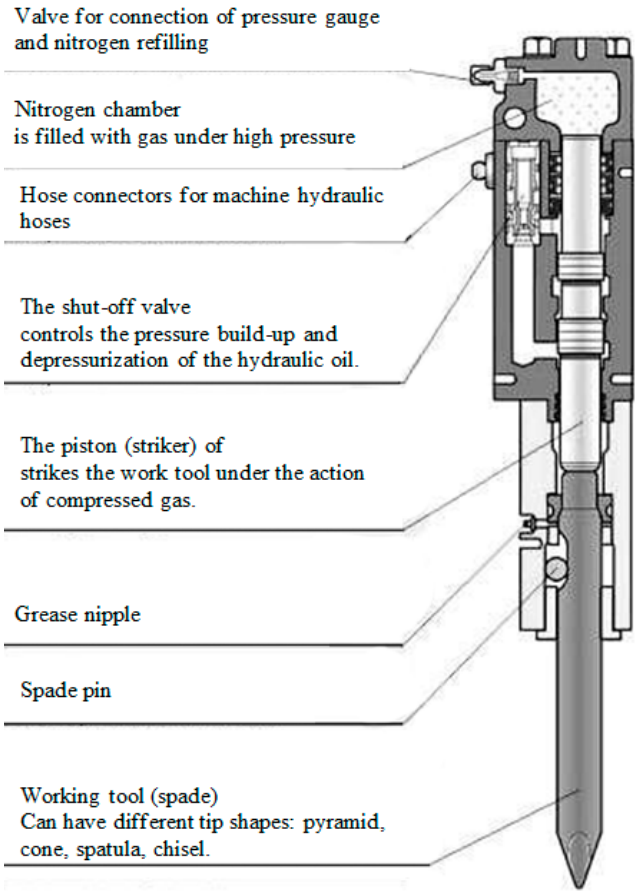

Figure 1.4. Scheme hydraulic hammers easy series DSM [13]

There is a so-called “urban” version with an additional noise protection system: the impact unit is located in a closed box, to the upper end of which an adapter is attached. or an intermediate link, and between the walls of the box and the impact block are being installed noise-absorbing gaskets, reducing noise and vibration. In addition, the outer openings of the casing can additionally close special rubber inserts.

“City” versions of hydraulic hammers are approximately 20% more expensive than basic models.

In general, the main failures in the operation of a hydraulic hammer are the result of violation of the rules for its operation. In order to avoid negative consequences when working with a hydraulic hammer, experts recommend adhering to certain rules for its safe use. First of all, it is necessary to take care about regular lubrication of rubbing elements. Absence or irregularity lubricants can bring To appearance cracks, burrs and, as a consequence, fatigue failure of the structure. In the case of SteelHand hydraulic hammers, lubrication is carried out at least every 3 hours of operation [12].

Of course, in addition to its advantages, a hydraulic hammer can have its own characteristic "weaknesses". And most often they are the result of improper operation or use of the hydraulic hammer for other purposes. However, even under correct operation conditions, the hydraulic hammer is subject to so-called fatigue failure. This occurs because the working tool of the hydraulic hammer - the pick - is driven by a striker, which strikes the shank of the pick under the action of oil supplied by the hydraulic pump. As a result, special tensile and compressive stresses are formed, which lead to fatigue failure of the tool.

The tie bolts, the peak limiter and the piston may be destroyed if the hydraulic hammer continues to operate in idle mode. Therefore, as soon as the object is destroyed, it is necessary to stop the work immediately.

During operation, the hydraulic hammer must be placed strictly perpendicular to the object being destroyed (90° angle, vertically or horizontally). Compliance with this rule will prevent displacement and breakage of the peak. If the hydraulic hammer is not at a right angle to the object being destroyed, the peak is "squeezed out", the load on the studs of the hydraulic hammer increases, and increased wear of the bushing occurs. All this leads to gradual and irreversible destruction of the hydraulic hammer.

It is forbidden use hydraulic hammer Not By purpose, for example, as a lever. This may result in damage to the hammer at the tie bolt, impact tool and front head. It is also prohibited to operate the hydraulic hammer with the boom and handle cylinders extended. This may lead to malfunctions and damage to the excavator.

When operating a hydraulic hammer, special attention should be paid to temperature conditions. At low temperatures, the hydraulic system must be preheated at low engine speeds. Low temperatures can increase the hydraulic hammer's susceptibility to fatigue failure. Such temperatures negatively have an impact And on separate elements hydraulic hammer: for example, rubber seals and cuffs can lose their elasticity, which causes leakage of lubricating fluid and, as a result, wear of rubbing elements.

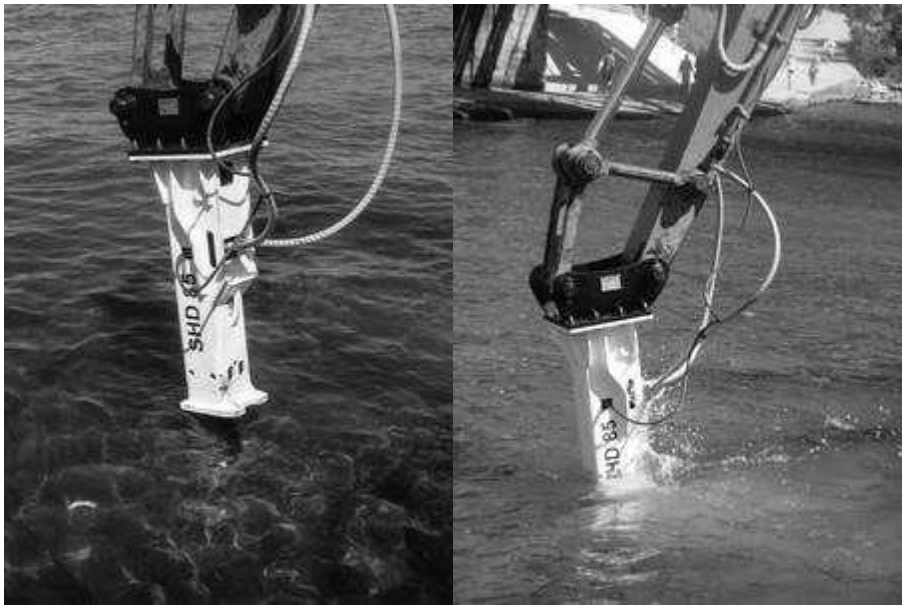

Figure 1.5. Usage hydraulic hammers under water [12]

If you use a hydraulic hammer underwater (Fig. 1.5), you will need to protect it from corrosion, water hammer and other damage. Given the specifics of performing work in such conditions, hydraulic hammers (for example, Steel Hand) are equipped with a ventilation system for underwater work. It allows air to be supplied to the chamber of the hydraulic hammer and prevents water from entering the strike zone of the striker on the peak. For example, at a gas pipe laying site in Sochi, the productivity of the Steel Hand SHD 85i hydraulic hammer, installed on a JCB JS290LC excavator, was 60–80 m ^{3} developed soil in 8 hours of work.

1.3. Modifications of modern hydraulic hammers

The actuator of a hydraulic hammer can be manufactured using a hydropneumatic accumulator or hydraulic accumulators of the "liquid spring" type. Like all vibratory impact machines, hydraulic hammers are characterized by the frequency of impacts And energy single blow. Energy range modern hydraulic hammers 0.5...20 kJ, impact frequency 10...40 Hz. Effective destruction of materials of different strength requires a certain combination of the above characteristics. To destroy stronger materials, greater energy of a single impact is needed.

In the design of modern hydraulic hammers, automatic devices for selecting the loading mode by impact energy and frequency are used for this purpose. In some models of hammers an automatic impact loading

system was used, quickly responding to changes in resistance.

The hydraulic hammer is put into operation at a certain value of tool displacement, which characterizes its correct installation on the processing object.

The drive of most foreign-made hydraulic hammers, as well as domestic ones of the “Impulse” series (I-200 and I-300M), uses hydropneumatic accumulators (membrane and piston), in which compressed nitrogen is used as an elastic element.

The design of the new generation of hydraulic hammers D-600, D-550 of the Delta series (D-250, D-150 are under development) is based on the use of the “liquid spring” effect, which is not widely used in the world practice of producing hydraulic hammers. Executive mechanism hydraulic hammer series "Delta" is capable of recuperating the return or recoil impulse of the working striker that occurs after the impact, and as a result, the energy of elastic oscillations of the liquid in the hydraulic system of the hammer is spent on the useful work of the reciprocating motion of the working tool. The working element (striker) of the hammer simultaneously serves as a piston for accumulating the energy of the hydraulic system during the return motion after the impact. Utilization of the return impulse of the working striker into the useful energy of the "liquid spring" performing a reciprocating motion allows eliminating pneumatic chambers from the hydraulic system of the impact tool [14, 15].

This technical solution significantly simplified the design and increased the reliability of operation of prototype hydraulic hammers, A application hydraulic accumulator With liquid spring simplifies operation – no need to control the battery charge. The streamlined shape of the Delta series hydraulic hammers allows them to be immersed to a depth greater than the working part of the tool.

JSC "Tvertechosnastka" offers four models of hydraulic hammers: NM-120, NM-230, NM-330 And NM-440. The first two are intended for hanging on single-bucket excavator- loaders. Models NM-330 and NM-440 are aggregated with single-bucket excavators on wheels and tracks of the third and fourth size groups. The NM-120 hydraulic hammer can be installed on excavator-loaders. It is used for the destruction of concrete and reinforced concrete structures, asphalt concrete coatings And etc. Hydraulic hammer NM-120 replaces foreign analogues all types works And has the following features [16]: increased resource; opportunity fulfill horizontal And vertical works With provision sustainability basic cars on maximum departure worker equipment, and also more

accurate works when saving highly efficient power hydraulic hammer; exception harmful impacts vibration speeds And vibration acceleration on metal construction basic cars; decrease fatigue operator thanks to reduced level noise And vibrations; minimal requirements To pressure-flow characteristics basic cars; autonomous charger pneumatic accumulator by air. similar By constructions hydraulic hammer NM-230 those same virtues, A performance higher. Hanging hydraulic hammer increased power NM-330 With minimal impact on hydraulic system And metal construction basic cars developed specially For excavators types EO-3323A, EK-14 and their analogues. It replaces foreign analogues in all types of work and along With advantages models NM-120 and NM-230 has the following peculiarities: security circular sectors works basic cars, high efficiency at loosening frozen soils, minimal requirements to pressure-flow characteristics of the base cars. Hydraulic hammer NM-440 calculated to be completed big volumes works on durable materials, his they hang on excavators types EO-4225, EO-4121, EK-18, ET- 2.

JSC TVEKS produces the MG-300 hydraulic hammer for its own excavators [17]. The MG-300 and MG-300.20 hydraulic hammers, which replaced the well-proven SP-71A series, are designed to equip hydraulic excavators weighing at least 12 tons (EO-3323A, EK-12, EK-14, EK-18, ET-14, ET-16, ET-18, ET-25 and their modifications). They are manufactured for moderate climates and are operational in the ambient temperature range of -40 ... + 40 ° C. There are several types of hydraulic hammers replaceable tool: wedge For loosening frozen soil, breaking up road surfaces, concrete structures; a pick (chisel) for crushing oversized solid and rock materials; a rammer for loose soil. The main differences between the MG-300 hammer and previously produced models are increased reliability and impact frequency.

The Delta series of hydraulic hammers are the result of long research in the most difficult conditions and improvements over many years. The new generation Delta equipment is compatible with all types of modern excavators.

In addition to the above-mentioned enterprises, hydraulic hammers for mounted excavators of the second size group of types EO-2621 and EO-2626 are produced by the Krasnoyarsk FSUE SibNIIStroydormash (GPM-150), FSUE Nevyansk Machine-Building Plant (MG-300 and SP-71A) and Zlatoust Excavator Plant Zlatex LLC, previously known as the Bulat plant (Hydraulic hammer GPM-200).

Recently, the company "Tradition-K" has joined the ranks of hydraulic hammer manufacturers. It is one of the largest sellers of construction equipment on the market, which has been selling these units for 10 years [16, 17]. Currently, the company produces three models of hydraulic hammers - Delta-5, SMG-200 and SMG-300. The SMG-200 model is unique in that among hydraulic hammers it occupies a transitional position between the light and medium categories. Of course, it is a good compromise: the SMG-200 can be mounted on excavators with a working weight range of 4–14 t. Hydraulic hammer SMG-300 developed on the basis of hydraulic hammers SP-71, SP-71A, MG-300 taking into account their operation by construction organizations. Its technical characteristics are optimized in order to increase reliability, reduce harmful impacts on hydraulic system And metal structure of the excavator, improving working conditions and reducing operator fatigue, as well as harmful effects on the environment, which allows work to be carried out in urban conditions near and inside buildings and structures.

In construction, many technological operations are associated with the destruction of durable natural and artificial materials. Analysis of modern practice has shown that these operations are effectively performed using explosives and impact machines - mechanical, pneumatic, electric, steam-air and hydraulic hammers. In construction, the scope of application of hydraulic hammers is rapidly expanding due to the development and increase in the power of the hydraulic drive of road construction machines, in particular frontal loaders. Modern Hydraulic hammers produced by various manufacturers have largely similar designs and, in terms of key indicators (energy and frequency of impacts), exceed the indicators of the best pneumatic machines, while having less weight and not releasing oil aerosol into the atmosphere.

Modern foreign-made hydraulic hammers designed for destruction cannot be used for driving reinforced concrete piles, since their pre-impact speed of the striker reaches values of 8-9 m/s. And for reinforced concrete piles there is a limitation of 6 m/s (at high striker speeds, the pile does not sink into the ground, but is destroyed). Such hydraulic hammers are used only for driving metal posts and columns into the ground, for example, fence posts for highways. In addition, there is a limitation on the weight of the elements driven into the ground. If the weight of the element being driven is more than 2-3 times greater than the weight of the hammer striker, the driving process becomes ineffective. In the case of using such hammers for driving posts, the body must be equipped with grips that

ensure the movement of the hammer along special guides along the axis of the element being driven. In addition, to balance the reactive force acting on the hammer body, a special additional load must be provided. For driving reinforced concrete piles used in housing and industrial construction, special-purpose hydraulic hammers with a relatively low pre-impact speed of the striker and high mass. Such hammers include hydraulic hammers of the Finnish company Junttan used in Ukraine

Fig. 1.6 shows the basic diagram of a hydraulic hammer from the Finnish company Junttan.

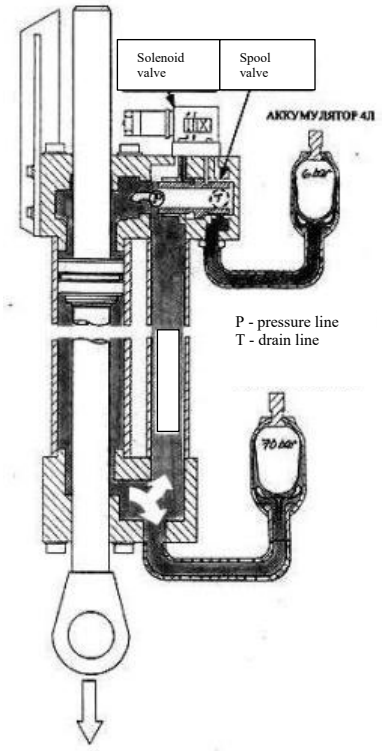

Figure 1.6. Fundamental scheme hydraulic hammer of the Finnish company Junttan

Finnish-made HAMMER hydraulic hammers are designed specifically for operation in difficult and heavy conditions and can be used for intensive operation over a long period of time (Fig. 1.7, Table 1.1). They are designed to solve any problems in road construction and road repair, in the demolition of buildings and crushing of oversized materials in quarries. HAMMER hydraulic hammers have a long service life and are highly reliable under conditions of continuous and long-term operation [18].

Main advantages hydraulic hammers HAMMER:

1. Design hydraulic hammer Hammer is done with a sealed hydraulic accumulator, not a pneumatic chamber. This ensures absence leaks nitrogen,

Not required weekly checking the nitrogen pressure in the pneumatic chamber, there is no need to refill the nitrogen chamber of the hydraulic hammer, and most importantly, there is no need to look for a kit for filling hydraulic hammers with nitrogen.

2. The hydraulic circuit of the Hammer hydraulic hammer provides 100 transmission % of impact energy from a charged sealed battery (constant impact energy), there is no need to press the tool with high force, due to which simple positioning of the hydraulic hammer tool is achieved, while the performance of the Hammer hydraulic hammer does not depend on the hydraulic system of the excavator.

3. High impact energy and reliability of attachments .

4. Fast and high-quality service, timely supply of spare parts and consumables .

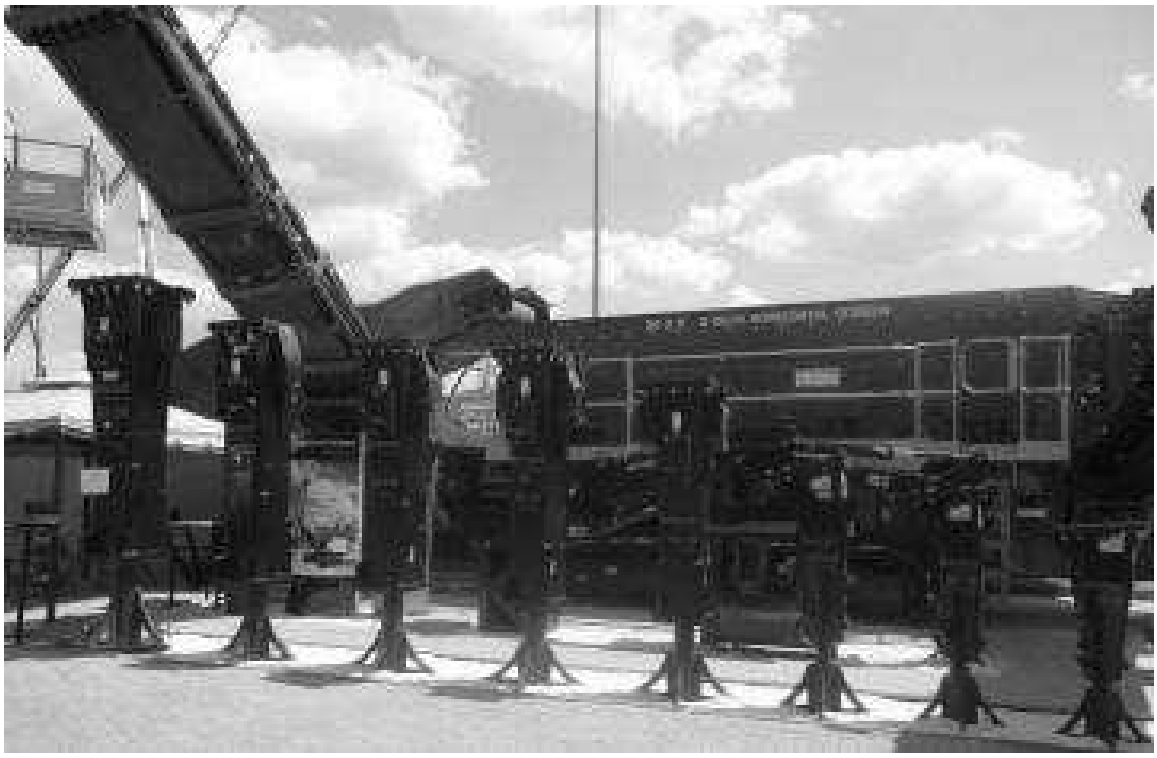

Figure 1.7. Hydraulic hammers companies HAMMER [18]

Table 1.1.

Characteristics hydraulic hammers companies HAMMER [18]

Brand Hammer / Indicators	HB 40	HB 60	HB 80	HB 100	HB 120	HB 140	NV 180	NV 240	NV 330	NV 450	HB 800
1	2	3	4	5	6	7	8	9	10	11	12
Worker weight, kg	150	270	370	505	820	1010	1360	1760	2330	3380	7000
Frequency beats, bpm	1050-2050	500-1700	500-1700	500-1700	500-1000	500-940	430-140	450-700	370-740+	400-700	350-450
Working pressure, bar	100-150	90- 140	90- 140	100-140	125-150	135-145	140-160	135-145	150-160	150-160	150-170
Recommended pressure, bar	145-175	150-195	140-190	150-190	175-200	190	210	190	220	210	220
Max. pressure, bar	220	220	220	220	220	220	230	220	240	230	230
Flow oils, l/min	30- 63	40- 120	40- 120	50- 150	60- 120	100-140	120-180	140-200	160-250	250-350	300-400

End of table. 1.1

1	2	3	4	5	6	7	8	9	10	11	12
Pressure in drain lines, bar	30	20	30	20	10	10	10	10	10	12	10
Consumable energy, kW	10	24	33	35	30	31	41	48	67	93	113
Diameter peaks, mm	50	72	80	90	95	115	125	135	142	166	203
Size pressure line, mm	12	19	26	26	26	26	26	26	32	32	32
Size drain lines, mm	12	19	26	26	26	26	26	32	32	32	42
Optimal. *t* oils, °C	- 20	+40- 60	- 20	+40- 60	- 20	- 20	- 20	- 20	- 20	- 20	- 20
Allowed *t* oils, °C	-20- 80	-20- 80	-20- 80	-20- 80	-20- 80	-20- 80	-20- 80	-20- 80	-20- 80	-20- 80	-20- 80
Optimal. oil viscosity, cSt	30- 60	30- 60	30- 60	30- 60	30- 60	30- 60	30- 60	30- 60	30- 60	30- 60	30- 60
Permission granted. oil viscosity, cSt	20- 1000	20- 1000	20- 1000	20- 1000	20- 1000	20- 1000	20- 1000	20- 1000	20- 1000	20- 1000	20- 1000
Recommended excavator weight, t	2- 6	4- 9	5- 9	7- 13	9- 18	12-20	18- 26	21- 32	27- 40	35- 60	60- 120

According to the operating principle, hydraulic hammers are divided into single- and double-action ones. In the former, the lifting of the striking part is carried out under the action of the working fluid in the hydraulic system, and the working stroke is carried out under the action of its own gravity and the gas pressure in the piston accumulator (pneumatic chamber); in the latter, the action of the working fluid on the striking part of the hammer occurs during the entire operating cycle.

Figure 1.8. Hydraulic hammers V in the process works

Delta F- 3 Delta F -4 Delta F -5

Figure 1.9. Hydraulic hammers series Delta

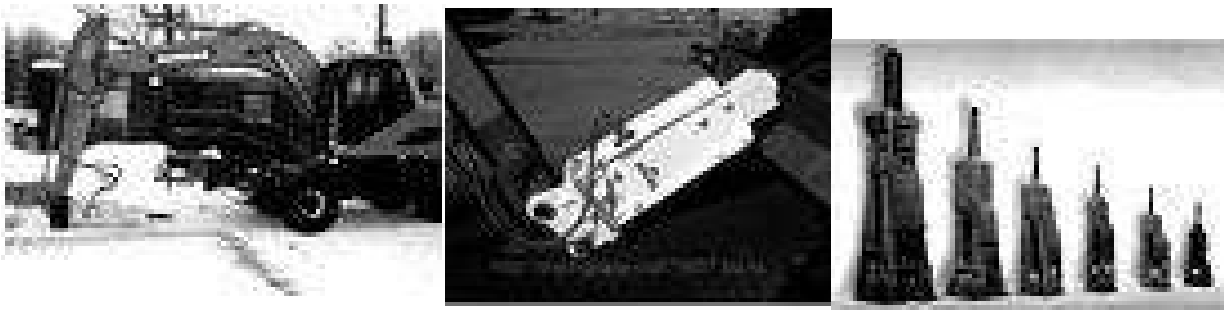

ProfBreaker PB 180 NKOMASIMpulse 300

Figure 1.10. Hydraulic hammers production others firms

The actuator of a hydraulic hammer usually includes hydropneumatic accumulators (diaphragm and piston) or accumulators with a “liquid spring” [19]. Network hydraulic accumulators provide smooth pressure measurement in the hydraulic drive and high efficiency [3, 4].

The disadvantages of diaphragm hydraulic accumulators include a decrease in the elasticity of the rubber membrane in cold conditions, so at temperatures below minus 20 °C, the oil in the hydraulic system must first be heated to operating temperature, and then the entire hammer must be heated. In addition, due to the use of as an elastic element compressed nitrogen time From time to time, refueling is required at special service centers or using separately purchased equipment, which is not always included in the delivery package.

Many hydraulic hammer designs use piston-type accumulators, in which nitrogen is compressed directly by the hammer striker. Depending on the parameters of such an accumulator (gas volume, charging pressure) and the ratio of the working areas of the hydraulic hammer piston-striker, energy is accumulated in it, the share of which in the formation of the impact energy is from 10...15% to 100%. Piston accumulators are less sensitive to negative temperatures, but the presence of compact seals does not exclude the transfer of oil into the gas cavity and nitrogen leakage. Therefore, the nitrogen charge level must be monitored much more often than in diaphragm accumulators.

When choosing a hydraulic hammer, you should consider not only the conditions and the intensity of its use, but also the characteristics of the material being processed. The first thing to pay attention to is the compatibility of the fasteners and the characteristics of the hydraulic system of the base machine and the hammer, as well as the compatibility of the adapter - the intermediate link with which the hydraulic hammer is attached instead of the excavator bucket [19-21].

General selection principle: the weight of the hydraulic hammer should be approximately one tenth of the weight of the excavator, but not exceed the weight of the bucket with soil. A hydraulic hammer with a lower weight is convenient for transportation and creates less load on the working equipment. However more heavy hydraulic hammer required less force to press against the work point. Thus, it creates less vibration transmitted to the base machine [20, 21].

The flow rate of the working fluid must correspond to the

performance of the excavator hydraulic pump feeding the pressure line of the hydraulic hammer. Its value is given in the technical characteristics of the hydraulic hammer. If the pump performance is less than the required fluid flow rate hydraulic hammer, it will either not work or will work erratically. If the pump's performance will be higher, then during operation there will be problems peaks pressure, which negative will have an effect And on the hydraulic hammer itself, and on the hydraulic units of the base machine or can even lead to the breakage of individual parts of the hammer. If this indicator exceeds the operating pressure level hydraulic hammer, a safety valve [21] must be provided in the pressure line of the hydraulic hammer to limit excess pressure from the hydraulic pump.

For more efficient use of the hydraulic hammer in various operating conditions, it is necessary to choose models with additional functions. In particular, with a device for switching operating modes, which is equipped with hammers of medium and heavy class. Switching modes is carried out from the driver's cabin, manually or automatically, depending on the material being processed, or by an “autostop” system, in which the hammer will not work while suspended [20].

Lubrication points and tools for connecting hoses to the filling fittings of hydropneumatic accumulators and pneumatic chambers must be accessible.

The level of vibration impact on the base machine with equal impact energy and hammer mass depends on the frequency of impacts, as well as on the depth of penetration into the material being processed. every hit.

Before starting to operate a hydraulic hammer, two technical problems must be solved [5, 20]:

- Firstly, it is necessary to provide mechanical fastening of the hammer to the excavator working equipment
- secondly, connect his To hydraulic drive excavator.

In most cases, the hydraulic hammer is attached instead of the excavator bucket. by means of intermediate links, which it's called adapter, or mounting plate, or bracket, or simply - suspension. On one side of the adapter, lugs must be formed that correspond to the bucket lugs by the diameter of the holes for the pins, the distance between the lugs and other geometric dimensions that ensure the possibility of installing a hydraulic hammer to the point at which the blows will be applied at the required angle to the horizon. Since there are many models of excavators from different manufacturers, when ordering a hydraulic hammer, the consumer must agree in advance on the necessary

geometric parameters of the adapter with the supplier of the hydraulic hammer [5, 7].

Binding dimensions adapter must comply attachment points formed on a specific model of hydraulic hammer. In most cases, the adapter is attached to the hydraulic hammer along a plane using bolts and nuts. It is preferable to use bolts with a fine thread pitch or use other means that eliminate the possibility of spontaneous unscrewing of the bolts due to vibration that occurs during operation of the hydraulic hammer [7, 11].

The next step is to connect the hydraulic hammer to the hydraulic system of the base machine. In the simplest case, when the excavator has a reserve section of the hydraulic distributor, then The hydraulic hammer supply lines are connected to this section. In this case, again, if necessary, an additional drain line is installed. If the excavator does not have a reserve hydraulic distributor section, then, depending on the basic hydraulic circuit of the excavator, the hydraulic hammer can be connected, for example, to the supply line of any drive of the excavator's working element, which is fed from both sections of the dual hydraulic pump. In this case, one of the pump sections is connected to the hydraulic hammer, and the other remains connected to the working element [7, 11].

On some excavator models it is not possible to separate the flows from a pair of hydraulic distributors that supply power to the hydraulic cylinders of the working equipment, for example, on excavators EO-33211, EO-5124, EO-5126, EO-5225. In this case, additional distributors must be installed to connect the hydraulic hammer. In any case of connecting the hydraulic hammer to the hydraulic system of the excavator, it is recommended to lay the drain line of the hydraulic hammer, bypassing the hydraulic distributors and other hydraulic devices of the excavator and connect it to the general drain line of the hydraulic system directly at the entrance to the hydraulic tank before the filters [3]. Otherwise, hydraulic losses in the drain line can lead to excessive heating of the working fluid, the viscosity of which drops, internal leaks in the working cylinder and distributor of the hydraulic hammer increase, as a result of which the impact energy and frequency of impacts decrease until the hammer stops.

Figure 1.11. Hydraulic hammer And his working Part [3]

Hydraulic hammers are mounted on excavators of size groups 2-5 instead of a reverse shovel bucket; they are connected to the handle by means of a quick-release fastener. An excavator equipped with a hydraulic hammer with a working tool in the form of wedge, pick and rammer, can be used for loosening frozen soil, crushing oversized solid and rock, breaking frozen soil and road surfaces, brick and concrete foundations and other works, as well as for soil compaction. When developing the soil, you can change the angle of the hydraulic hammer to the soil surface. The hydraulic hammer equipment kit includes
(Fig. 1.12) includes: boom 1, handle 4, hydraulic hammer 5 and hydraulic cylinders 2, 3, 6 for lifting the boom, turning the handle and hammer [4]. Hydraulic hammers are driven by the pumps of the hydraulic system of the base excavator, which ensures better use of the installed capacity and reduced operating costs. According to the operating principle, hydraulic hammers are similar to steam-air hammers. Hydraulic hammers create significant impulses of directional force and ensure the lowest energy consumption in the process of developing frozen soils and destruction hard surfaces [7, 11].

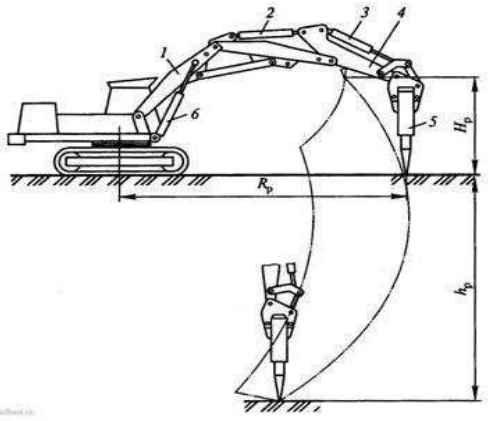

Figure 1.12. Excavator, equipped with a hydraulic hammer [4]

A distinction is made between single-acting and double-acting hydraulic hammers. In double-acting hydraulic hammers, the lifting of the striking part (idle stroke) is carried out under the effect of the working fluid, and its acceleration downwards during the working stroke is carried out under the effect of its own weight and the energy of the working fluid. or compressed gas accumulated during idle running in a hydraulic or pneumatic accumulator. Hammers with a pneumatic accumulator are also called hydropneumatic.

The design of a hammer with a hydraulic accumulator (Fig. 1.13) includes: a working cylinder 6 with a distribution spool 10, a hydraulic accumulator 13 and a pump 12, a housing with a guide pipe 2, striking part 3 and replaceable working tool 1.

The hydraulic hammer operating cycle consists of the upward acceleration of the striking part, its braking before the top dead center, downward acceleration, and impact on the tool shank. The striking part has no sections of steady motion. During upward acceleration, the working fluid from pump 12 (Fig. 1.13) through the spool valve 10 enters the rod cavity 4 of the working cylinder 6 and into the hydraulic accumulator 13, where it accumulates. At the end of acceleration, the spool valve connects the piston cavity 8 of the working cylinder with the pressure line 9, as a result of which the shock part is braked and the working fluid is being displaced V hydraulic accumulator After stops the striking part at the top dead center begins its downward acceleration under the action of its own weight and the pressure of the working fluid acting on piston 5. When the striking part reaches the speed that it would have during steady motion, the accumulator starts discharge, giving away accumulated liquid into the working cylinder 6. At the end of the downward stroke, the striking part strikes the tail of the replaceable working tool 1. Before application blow through back valve 7 liquid from piston cavity 9 enters drain line 11. Then the cycle repeats [11, 12].

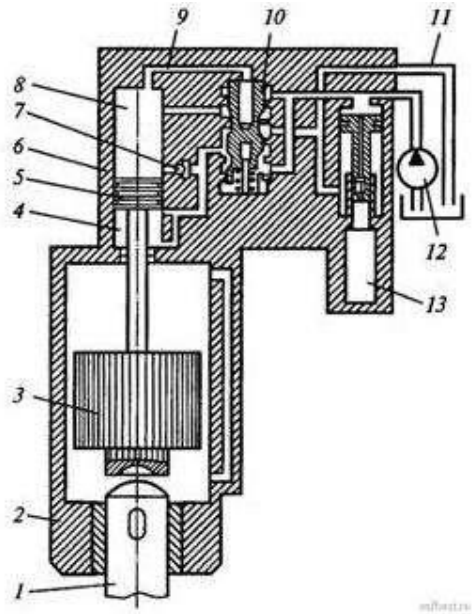

Figure 1.13. Fundamental scheme hydraulic hammer
with hydraulic accumulator [7, 11]

Hammers with hydraulic accumulators are easy to operate and maintain, have a fairly high efficiency (0.55–0.65). They produce little noise during operation, so they can be used in densely populated areas [11]. Hydraulic hammers are developing energy blow 1800– 9000 J, have an impact frequency of 2.5–5 Hz, impact part weight of 100...600 kg, working pressure in the hydraulic system of 10–16 MPa.

U hydropneumatic Molotov pressure working liquid acts on the striker during working and idle strokes. Simultaneous action on the striker of liquid pressure and accumulator gas energy during working in the course allows raise coefficient use of the pumping unit's capacity, reduce the pressure pulsation of the working fluid, improve technical and operational indicators of hammers. The main elements hydropneumatic hammer (rice. 1.14) are: impact block 6, pneumatic accumulator 9, control

camera 7, distributor 1, removable worker tool 15.

The principle of operation of the hammer is as follows. In the initial position (Fig. 1.14, a), the working fluid under pressure is supplied to the cavity A of the distributor 1 and simultaneously to the cocking chamber 3, the control chamber 7 of the impact block 6 and through channels B and B into cavity 12 of spool 14. The discharge pressure acts on stage 13 of spool, moving it to the extreme lower position, and on stage 4 of striker 5, which begins to move upward (idle stroke), compressing the gas in accumulator 9. In

this case, the working fluid from chamber worker move 8 is being displaced through camera 10 spool V drain [10, 12].

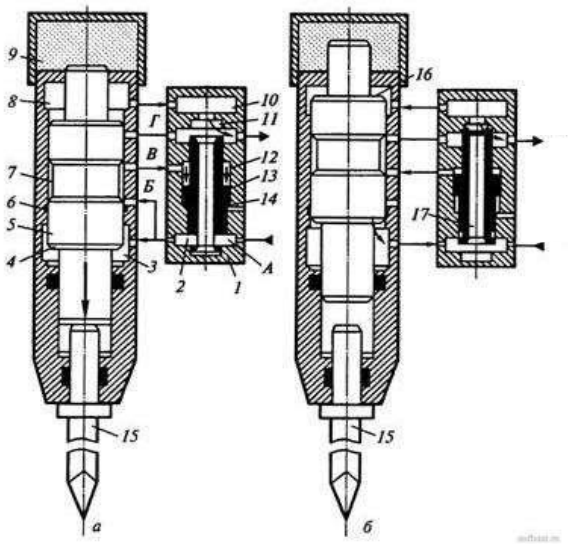

Figure 1.14. Fundamental scheme of hydropneumatic hammer [12]

In the upper position of the striker (Fig. 1.14, b), the control chamber connects channels B and G with each other and simultaneously the cavity 12 with the drain. Under the action of the pressure of the working fluid on the lower stage 2 of the spool, the latter moves upward, with its upper part enters the groove 11 of the distributor body, closes the drain hydraulic line and through the central hole 17 connects the pressure hydraulic line With camera platoon 3 And camera worker move
8. The striker begins to move downwards (working stroke) under the simultaneous action of the accumulator gas pressure and the working fluid (area steps 16 more squares steps 13); working the liquid flows from the cocking chamber into the working stroke chamber. Accelerating, the striker strikes the tool 15, the control cavity connects channels B and C with the pressure hydraulic line, and the spool is thrown downwards. Then the cycle is repeated [3, 10].

Hydraulic hammers can be used in two technological schemes: an excavator with a hammer works continuously, and the soil is excavated by another excavator; an excavator with a hammer performs a specified part of the work, and then the hammer is replaced with a bucket.

When working with hammers, the excavator boom is set to a floating position, which ensures complete vibration isolation of the operator's workplace. The hammers are equipped with a wide range of easily replaceable loosening, crushing, piling, and ramming tools and are launched into operation

automatically when the working tool is supported with a certain force on the object being destroyed (driven).

Hydropneumatic hammers develop impact energy of 500–9000 J and have an impact frequency of 3.5–12 Hz. Charging pressure gas accumulator 0.6–1.2 MPa, working pressure in hydraulic system
10–16 MPa.

Table 1.2 shows the technical characteristics of hydraulic pneumatic hammers [12].

The hydraulic drive system of full-swing excavators is usually made as a two-flow system, in which the working fluid from two or three axial piston pumps (sections pump) of variable capacity is supplied to two pressure lines.

The Delta series of hydraulic hammers covers a wide range of sizes, from which you can choose the one that is best suited for mounting on an excavator, available to the consumer [20]. According to their design and layout, hydraulic hammers F can be divided into two groups. The first (Fig. 1.15, Fig. 1.16) includes lightweight hammers of the F3–F10 models , distinguished by the fact that their pressure feed line does not have a network hydraulic accumulator, and the role of the elastic element is played by the pressure line RVD. The formation of impact energy is carried out mainly due to the energy accumulated in the piston accumulator-pneumatic chamber during the cocking of the striker. These hydraulic hammers are applied on excavators weighing from 1 to 12 tons [5, 6].

Table 1.2

Technical characteristic hydraulic pneumatic hammers [12]

Parameters	Model			
	NM-120	NM-230	NM-330	NM-440
Weight excavator, T	2.5...6	8...13	12...18	18...26
Weight hammer, kg	150	350	750	1100
Energy blow, kJ	0.5	1.0	2.0	3.5
Frequency blows, Hz	12	9	7	5
Consumption working liquids, l/min	20...100	50... 120	80... 160	160...240
Working pressure V hydraulic system, MPa	10	10	16	16
Charging pressure pneumatic accumulator, MPa	0.6...0.8	0.6...0.8	0.6...0.8	0.6...0.8
Diameter tool, mm	70	80	110	135
Working length tool, mm	300	350	450	600

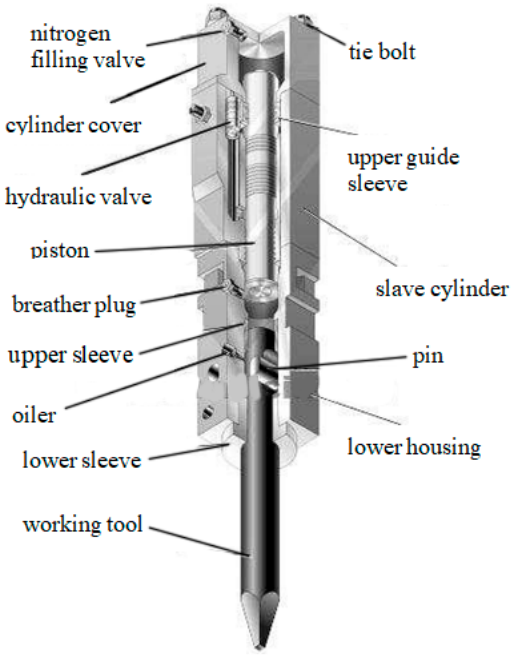

Figure 1.15. Hydraulic hammers Delta easy series [6]

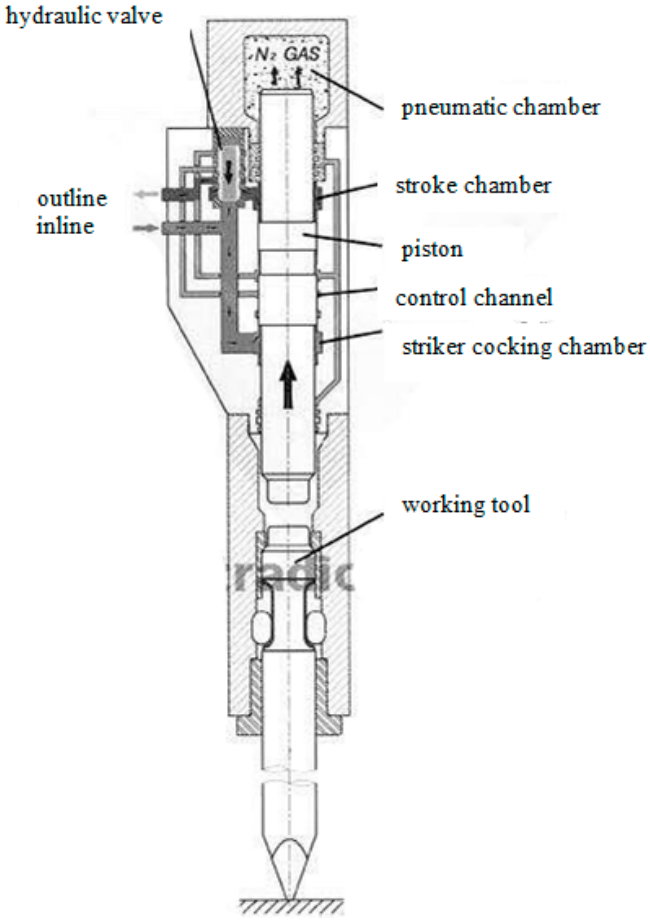

Figure 1.16. Hydraulic hammers Delta easy series: hydraulic line diagram [20]

The second group (Fig. 1.17, 1.18) includes hydraulic hammers F 15… F 50 , mounted on medium and heavy excavators weighing from 13 to 65 tons. The pressure supply line of these hydraulic hammers has a built-in hydropneumatic accumulator, in which hydraulic oil and compressed nitrogen are separated by a rubber membrane.

Design lungs hydraulic hammers Delta extremely simple. Impact block hydraulic hammer consists of from three corpus details [6, 20]:

– axle boxes, which contain the tool bushings, the replaceable tool and the pin that prevents the tool from falling out, as well as a breather valve that connects the space between the striker and the tool with the atmosphere;

– monoblock worker cylinder, V frame whom a built-in hydraulic distributor that ensures the reversal of the piston-striker movement, the upper guide sleeve of the striker with a combined seal;

– the cover of the working cylinder, which contains a piston accumulator-pneumatic chamber and a valve for charging the pneumatic chamber with compressed nitrogen.

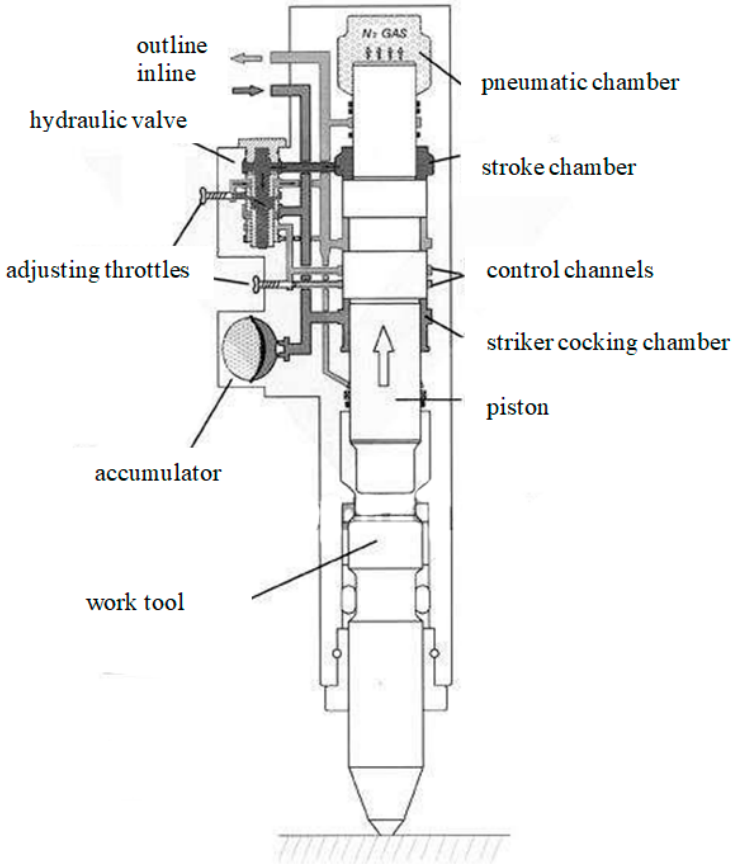

Figure 1.17. Hydraulic hammers Delta second groups: hydraulic line diagram [20]

The upper sleeve of the tool is made with a ring stop, which limits the movement of the tool inside the sleeve when pressed. hydraulic hammer To object work. Bushings tool are made of alloy steel with heat treatment, providing a long service life. A check valve built into the axle box provides air suction when the striker is cocked. During the working stroke of the striker, due to the increase in air pressure in the chamber between the striker and the tool, air is pushed out through the gaps between the bushings and the tool shank along with wear products and abrasive particles that could get into the gap. The axle box also has a grease nipple for periodic lubrication of the tool shank with consistent grease [6, 20].

The monoblock working cylinder with a hydraulic distributor built into its body is made without a sleeve. Thermal and physical-chemical treatment of the cylinder body, reducing the friction coefficient, ensures high durability of the cylinder mirror. Short internal switching channels provide a decrease in hydraulic resistance, which increases the efficiency of the hydraulic hammer and ensures the possibility of long-term operation without interruption. The monoblock design of the working cylinder without a sleeve is less repairable than a sleeve cylinder with a docked hydraulic distributor, but this drawback is compensated by the high precision of the mating parts, including the hydraulic distributor, which ensures high durability and reliability. In the lower part of the working cylinder body, there are two seals and a wiper, in which the piston rod of the striker moves. A damper chamber is formed slightly higher in the body, in which the piston enters during "slippage" in the event of sudden destruction of the material processed by the hammer [5, 6]. When the piston enters the damper chamber, the pressure in the latter increases sharply, which causes the striker to slow down and protects the hammer from destruction. In order to protect the striker seals from high pressure in the damper chamber, which can reach a value several times greater than the working pressure in the hydraulic system, a groove is made in the cylinder body between the damper chamber and the striker rod seals, which is constantly connected to the drain line. Thus, the seals are always loaded with low pressure, which ensures their long service life. With such a technical decision installation two seals rod striker seems somewhat redundant. The same resource will be provided by one seal [20]. The seals of the upper striker rod are installed in the guide bushing, which is located in the upper part of the working cylinder body. Three seals are located in this bushing. The uppermost one holds compressed nitrogen in the pneumatic chamber and prevents oil from entering the pneumatic chamber. The middle

and lower ones are designed to seal the working stroke chamber of the hydraulic hammer. These seals are separated from each other by a groove connected to the drain line. Thus, the lower seal is loaded with working pressure during the working stroke of the striker (movement towards the tool), and the middle one is always under the pressure of the drain line. This technical solution ensures high reliability of this unit [19, 20].

The basic hydraulic diagram of F hydraulic hammers is similar to most models of many European companies, such as Krupp, Rammer, Montabert, etc. The difference is the design of the hydraulic distributor [3–7]. The distribution spool of light hydraulic hammers (Fig. 1.15) has a tubular shape with belts of three different diameters, made on the outer surface. The belts of the largest and smallest diameters move along the inner surface of the sleeve, and the belt of the middle diameter moves inside the distributor cover.

The internal cavity of the valve and its ends during hammer operation constantly loaded workers pressure. In the lower position of the spool valve, the working stroke chamber of the hydraulic hammer is connected to the drain line, the pressure line is cut off from the working stroke chamber by the lower belt of the spool valve. In this position of the spool valve, the striker is cocked. The spool valve is held in this position due to the difference in the areas of the belts of the lower smaller diameter and the upper average diameter. After the striker has moved upward by a specified amount, the pressure of the working fluid enters the spool control chamber under the belt of the largest diameter through the control channel, which causes the spool valve to switch to the upper position. In this case, the working stroke chamber of the hydraulic hammer is disconnected from the drain line and connected to the pressure line. After the striker has slowed down before the top dead center, the working stroke of the striker begins (towards tool). Tall accuracy manufacturing spool, sleeves, distributor caps and sockets in the working cylinder body allows to do without any seals between the distributor chambers, except for the seal on the distributor cover, which prevents external leaks. The gaps between the distributor sleeve and the body of the working cylinder do not exceed 0.02 mm, the gaps between the belts of the spool valve and the distributor sleeve are within 0.010–0.031 mm, the non-concentricity and non-roundness of the belts of the spool valve and sleeve does not exceed 0.003 mm. Such manufacturing precision ensures the reliability and long-term operation of the hydraulic distributor, which, as a rule, works for the entire service life of the hydraulic hammer without any repairs provided that the requirements for the purity and viscosity of the hydraulic oil are met [20].

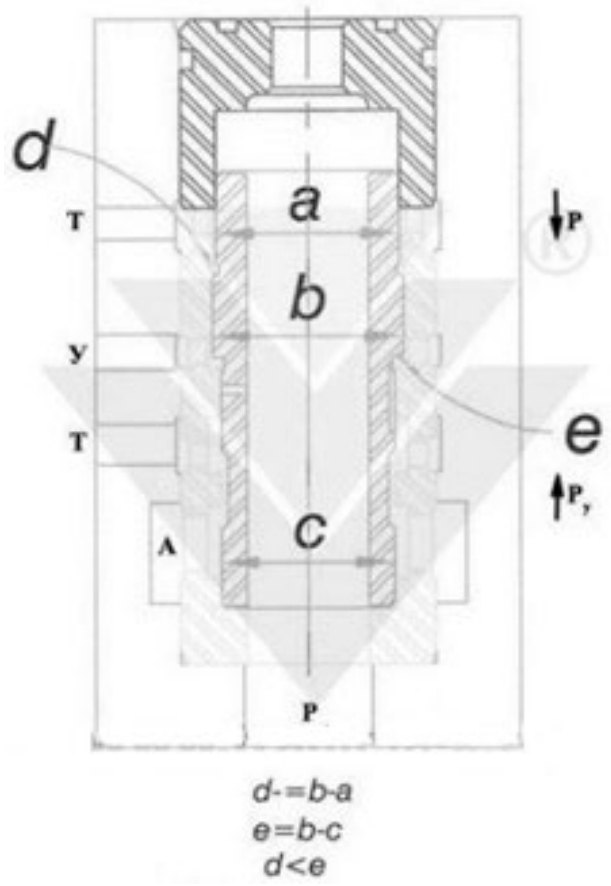

Figure 1.18. Hydraulic distributor diagram for Delta Fine 4- Fine 10 hydraulic hammers [20]: P – pressure line, T – drain line, A – outlet to the working stroke chamber, Y – control line, a, b, c – diameters of the spool necks, d – platform that ensures that the spool is held in the cocked position of the striker, e – platform that ensures switching of the spool valve to the working stroke position

Hydraulic hammers of medium and heavy sizes are equipped with hydropneumatic membrane accumulators, which are included in the pressure line of the hydraulic hammer and provide fairly smooth changes in pressure in the hydraulic system, a high efficiency factor, and reduce the harmful effects of pressure peaks on the hydraulic pump and other components of the base machine's hydraulic system [6, 20].

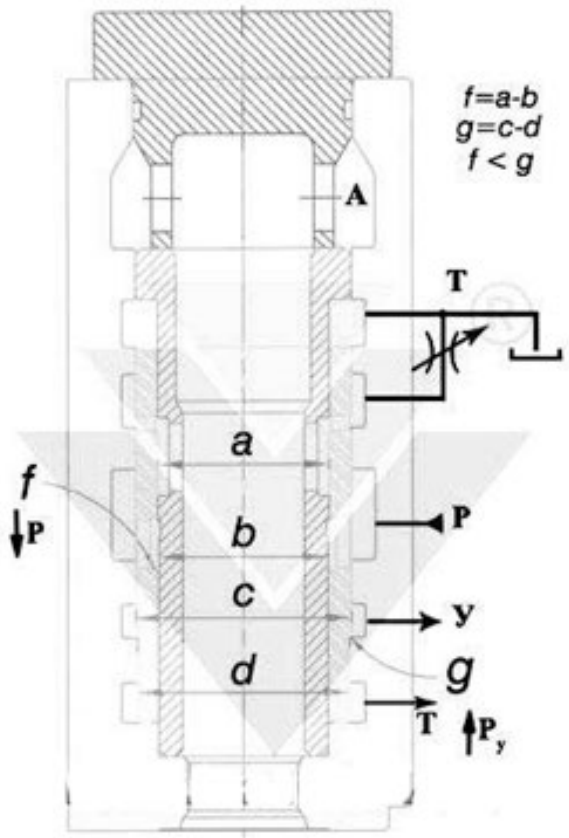

Figure 1.19. Hydraulic distributor diagram for Delta Fine 15- Fine 50 hydraulic hammers [20]: P – pressure line, T – drain line line, A - exit V camera worker move, U - line management, a, b, c, d – diameters neck of the valve, f – a platform that ensures that the spool valve is held in the cocked position of the striker, g – a platform that ensures that the spool valve is switched to the working stroke position

The hydraulic accumulators of the Delta F 15–F 50 hydraulic rotors consist of a housing and a cover, between which a rubber membrane is clamped along the outer contour. To charge the hydraulic accumulator with compressed nitrogen (charging pressure is about 40 bar), a socket for connecting a filling hose and a needle valve is provided, which after charging is tightened and closes the filling hole. The accumulator housing and its covers are tightened along perimeter with bolts from high strength steel. In time works. The accumulator membrane of the hydraulic hammer oscillates around its middle position with a certain amplitude, providing either accumulation of the working fluid when the piston speed of the hydraulic hammer is low, or additional oil supply together with the hydraulic pump to the hammer working cylinder when the piston speed is high. The design of the working cylinder of medium and heavy hydraulic hammers F is similar to the design of light hydraulic hammers. The hydraulic distributor (Fig. 1.19) of these hydraulic hammers is made in the form of a separate block, which is

fixed to the body of the working cylinder with bolts. The basic hydraulic circuits of all models of F hydraulic hammers are similar. However, the design of the hydraulic distributors of medium and heavy hydraulic hammers differs significantly from the design of light ones [20].

The distribution spool valve has a tubular shape and is based in the distributor housing on the outer surface along belts of two different diameters and on the inner surface along a fixed bushing also along belts of two different diameters. The difference in the diameters of the belts on the inner surface of the spool valve ensures its installation in the position of the striker cocking, and the difference in the diameters of the belts on the outer surface ensures its switching to the position of the working stroke when connecting the control chamber to the pressure line. Ends The spool valves in this distributor design are always under drain pressure. The internal cavity of the fixed bushing, along which the spool valve moves, is connected to the working stroke chamber of the hydraulic hammer and is alternately connected to the drain line and to the pressure line.

In medium and heavy F hydraulic hammers, the ability to regulate the hammer impact energy is provided [5, 7, 20]. For this purpose, two grooves are made in the working cylinder of the hydraulic hammer, spaced along the length of the piston stroke, connected to the spool control chamber. In this case, a needle throttle is installed in the channel connected to the lower groove, which can completely block this channel. If the throttle is closed, then the signal to switch the spool from the position of the striker cocking to the position of the working stroke is received at the maximum stroke of the striker. In this case, the maximum impact energy is realized. If the throttle is completely open (two turns), then the signal to switch the spool comes in at minimal working in the course striker, the minimum impact energy mode is implemented, but at the maximum impact frequency. In intermediate throttle positions, modes with intermediate values of impact energy and impact frequency are implemented. The ability to regulate the impact energy allows more efficient use of the hydraulic hammer depending on the operating conditions. For example, when destroying strong materials, it is advisable to work with maximum impact energy, and when destroying relatively weak rocks, it is preferable to work with lower impact energy and a higher impact frequency. In the latter In this case, there are fewer striker “slippages”, which preserves the resource of the hydraulic hammer [20].

The hydraulic distributor has another adjustable throttle, which is installed in the drain line at the outlet of the working stroke chamber. With

this throttle, it is also possible to regulate the energy and frequency of impacts within certain limits under certain operating conditions. If the hydraulic hammer is mounted on an excavator whose hydraulic pump feed rate is lower than that required for normal hammer operation, then when when the hammer is cocked, the pressure line accumulator is not charged sufficiently, and during the working stroke of the hammer, the pressure drops sharply. In this case, both the impact energy and the impact frequency of the hydraulic hammer do not correspond to the passport values. In order to ensure that the pressure accumulator is charged with oil at a low hydraulic pump feed, it is necessary to partially close the throttle. This will increase the pressure in the working stroke chamber during the hammer cocking, accordingly the pressure in the pressure line will increase, the hydraulic accumulator will be charged to the required value, which will provide higher pressure during the working stroke and, consequently, higher impact energy. The frequency of impacts in this case decreases due to the increase in the hammer cocking time. When the hydraulic pump feed, which corresponds to the technical characteristics of the hydraulic hammer, there is no need to close the throttle described above, moreover, closing the throttle will lead to to overloading the hydraulic system and increasing heat losses [5–7].

In some modifications of medium and heavy hydraulic hammers, the breather valve is moved from the axle box to the cylinder cover, that is, it is removed from zones increased dustiness, What reduces probability abrasive particles from entering the hammer. Fresh air enters the chamber between the striker and the working tool through channels formed in the body parts of the hammer [20].

In addition, these hydraulic hammers have the ability to install cartridges for automatic lubrication of the working shank. tool By special channels V corpus details, which simplifies the operation of the hydraulic hammer and saves time spent on its maintenance.

Table 1.3

Comparative characteristics hydraulic hammers Delta (Delta Fine) [20]

Model of hydraulic hammer	Excavator weight , T	Weight of hydraulic hammer, kg	Energy blow, J	Frequency beats, bpm	Consumption oils, l/min	Working pressure, MPa	Working length of the tool, mm	Diameter tool, mm	Length g/hammer, mm
FINE - 4	1- 3	160	480	550-1200	20-50	9- 12	345	55	1306
FINE - 5	2- 7	260	849	450-900	30-50	9- 13	407	68	1684
FINE - 7	7- 9	473	1764	450-800	45-90	13-15	408	85	1979
FINE - 10	9- 11	765	2443	450-800	80-110	15-17	615	100	2298
FINE - 15	13- 18	1400	4234	400-900	90-120	15-18	700	120	2480
FINE - 20	18- 26	1790	5290	400-800	130-150	16-18	764	135	2773
FINE - 35	28- 35	2450	7200	350-700	150-190	16-18	799	150	3046
FINE - 45	35- 50	3280	9970	300-600	190-250	16-18	884	160	3281
FINE - 50	45- 65	3870	13125	250-450	250-310	16-18	884	175	3870

Delta hydraulic hammers with the same technical characteristics are produced in various modifications, differing in the method of fixing the impact block and the entire hydraulic hammer on the base machine:

The most common and cheapest modification is the one in which the impact block is secured between two cheeks, tightened together with bolts or studs. The cheeks are provided with keyway projections that fit into the corresponding nests on bux hydraulic hammer. These protrusions and They absorb mainly all vertical and horizontal forces that arise during the operation of the hammer, including when turning out chipped pieces of the material being processed [20].

The upper ends of the cheeks are provided with platforms with holes for fastening the adapter with bolts. The type of adapter is determined by the parameters and connection dimensions of the base machine.

Figure 1.20. Hydraulic hammer piston type [4]

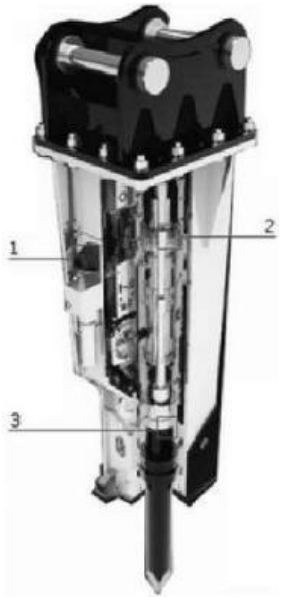

Figure 1.21. DAEMO hydraulic hammers: the attachment is equipped with a hole for supplying grease, allowing the installation of an automatic lubrication unit (models DMB 700 and above) [6]

Figure 1.22. Development of rock mass: the average daily capacity of the quarry is 1000 m3 (750 m3 in the original); is provided by the simultaneous operation of four hydraulic hammers [4]

In another modification, the cheeks are made in such a way that the connection to the base machine is carried out from the side.

AND, finally, V So called "urban variant" The hammer's striking block is located in closed box [5–7]. The adapter is attached to the upper end of the box. Various elements are installed between the walls of the box and the hammer's striking block to reduce noise and vibrations that occur when work hydraulic hammer. One of the problems that mining companies are increasingly facing enterprises With open way developments located in developed industrial areas and places of unique nature, is limitation or ban on carrying out blasting operations, which requires the search for new non-traditional ways developments, A Also new technical funds [4–6].

In mining operations, powerful hydraulic hammers with an impact energy of 8-15 thousand joules, mounted on hydraulic excavators with a working equipment "reverse shovel", are increasingly used for blast-free development of rock masses. If until the first half of the 80s they were widely used in construction work and crushing oversized material in quarries, then with the creation of powerful hydraulic hammers, A Also V connections With tightening environmental requirements, this equipment began to successfully compete with the traditional drilling and blasting method and was used in the direct development of rock masses in both

underground and open-pit mining operations [5–7, 21]. When deciding on the development of the Savinsky magnesite deposit (Russia), we proceeded from the characteristics of this region, located in the Baikal region, and the requirements for minimizing the negative impact of mining operations on the environment. As a result, a decision was made to build and develop it using blast-free technology.

The deposit is characterized by the following mining and technical features that determine the technology of mining operations:

– the mountainous nature of the deposit's relief makes it possible to open working horizons directly from the surface;

– the complex nature of the internal structure of the deposit with contact dip angles of 50–85° and alternation of different grades of magnesite, substandard ores and host rocks requires selective development of the deposit;

– The use of traditional technology for the development of ores and host rocks is only possible with drilling and blasting loosening.

The conducted studies of the physical and mechanical properties of magnesite from the Savinsky deposit showed that the rocks are highly viscous and have a variable strength nature. Thus, the spread of values of compressive strength was from 58 to 190 MPa in cores with average values of 141 MPa, respectively. Based on these conditions, in May 1993, construction of the highway route was started, carried out in semi-trenches on a slope with a slope of 10-30° using blast-free technology with the use of a hydraulic hammer. models NM-2500 CS companies KRUPP With energy blow 8-

10 thousand joules [21]. The specified hydraulic hammer is mounted on an EO-5221 excavator weighing 38.7 tons, with an engine power of 125 kW and a hydraulic pump capacity of 218 l/h. The rocks being developed were individual large pieces of magnesite rocks dumped in Quaternary deposits, as well as their rock outcrops. The destruction of the rock outcrops was carried out quite successfully. The following technological schemes were used:

• with the excavator located on the roof of the approach and the hydraulic hammer primarily operating below the standing horizon;

• with the excavator positioned on the base of the bench and the hydraulic hammer operating above the excavator installation horizon.

Significant difficulties arose when destroying individual pieces enclosed in quaternary deposits. It should be noted that due to the specific nature of construction work, the faces were scattered along the highway at

distances of 200 to 1000 m from each other with fairly steep climbs. In these conditions, significant time was spent on preparing the faces, moving the excavator from face to face, and other preparatory operations.

In order to obtain data on productivity, the operation of a hydraulic hammer was investigated when mining a separate monolith, enclosed in Quaternary sediments, with approximate dimensions of 2.8 ξ 3.5 m [21]. Surface The area where the excavator was located was uneven and consisted of loose material. The timing of the main and auxiliary operations, as well as the measurements of the pieces separated during the work, showed that 7 cycles were completed before the monolith was completely destroyed to a depth of 0.7-0.8 m. The time for deepening the working element and separating a piece or pieces from the monolith averaged 1.38 min. The monolith was destroyed from two excavator positions. On average, it took 1 min 17 s to reinstall it. The volume of rock mass destroyed was about 8.2 m^3 with a total recorded time of 13.5 min. The productivity of the hydraulic hammer was determined as the ratio of the total volume of pieces separated from the massif and destroyed to a given size to the total time spent and amounted to about 37.8 m^3 /h in the specified area. A KOMATSU hydraulic hammer was used in conjunction with the hydraulic hammer, which moved the destroyed magnesite into stacks for subsequent shipment.

At another site, the operation of a hydraulic hammer was investigated in the destruction of rock outcrops with surface dimensions 8 × 3.5 m [21]. The above-described work schemes were used. Initially, excavator was installed on approach, A the hydraulic hammer worked below the installation level, moving pieces of rock mass separated from itself. The platform had limited dimensions, and the excavator was partially located on loose material. Its unstable placement led to unstable operation. As a result, the operator was advised to change the work scheme and move down to the bottom of the platform. After this, the work became more productive. Time for insertion of the tip and separation pieces from the massif varied from 38–40 to 70 s. Complete destruction of the monolith to the design mark was accomplished in 12 cycles. The total volume of destroyed rock The mass was about 17.8 m^3 with the time spent being 11.17 min. The estimated hourly productivity during this period was 95.4 m^3 / h. Thus, at the Savinskoye deposit, within two months, without the use of drilling and blasting operations, a highway route with an ascent to a height of about 120 m above the valley level was constructed using the NM-2500 CS hydraulic hammer in a set with RBA.

The experience of using blast-free mining at one of the quarries in Italy is of interest [21]. In connection with the ban Since 1988, the blasting operations at the Capaci quarry of GIUSEPPE SENSALE (Sicily) have been switched to mechanical breaking using hydraulic hammers from KRUPP. The developed deposit is represented by hard limestones used as fillers in concrete, as well as in road construction. There are 8 hydraulic hammers in operation, four of which are used as the main equipment for preparing the rock mass for excavation and loading operations, and four (small-size) are used for auxiliary operations.

In general, for our operating conditions, the use of piston-type hydraulic hammers is justified: Delta , Furukawa , NPK , since they are adapted for winter operating conditions, have a more repairable design and are familiar to our operating organizations [5–7, 20, 21].

The selection of a hydraulic hammer and its purchase should include not only the availability of the equipment itself, but also the availability of replacement tools. And pendants under excavator, A also complex service. In the future, a hydraulic hammer without spare parts and replaceable tools, service support becomes disposable. The main element in which the components of the hydraulic hammer are assembled is the body. The body can be conditionally divided into three parts [5, 20].

IN top parts corps hydraulic hammer is located nitric camera and valve for nitrogen injections And pressure control gas in the chamber. In average parts hydraulic hammer are located his main nodes and channels for hydraulic oils. Valve cutoff controls flow oils. By center corps is located piston (striker). Above And from below piston there are groups seals (seals). The lower part of the hydraulic hammer body is a guide for the working tool (peak). To reduce friction and prevent wear of the body, the peak moves along bushings made of a special material. The locking pin keeps the peak of the hydraulic hammer from falling out of the corps and limits her movement. For lubricants bushings provided oil press (grease bottle).

Table 1.4

Characteristics modern hydraulic hammers [20]

Model of a hydraulic hammer	Weight hydraulic	Impact energy, J	Stroke rate, bpm	Working tool diameter, mm	Oil consumption, l/min	Working pressure, atm
Delta						
Delta F- 3	97	400	600- 1200	46	20- 30	80- 110
Delta F- 4	160	480	550- 1200	53	20- 50	90- 160
Delta F -5	295	849	450- 900	68	30- 50	90- 130
Delta F- 6	395	1210	450- 900	75	40- 80	130- 150
Delta F- 7	473	1764	450- 800	85	45- 90	130- 150
Delta F -10	795	2443	450- 800	100	80- 110	150- 170
Delta F -15	1400	4234	400- 900	120	90- 120	150- 180
Delta F -20	1790	5290	400- 800	135	130- 150	160- 180
Delta F -35	2450	7200	350- 700	150	190- 250	160- 180
Delta F -45	3280	9970	300- 600	160	190- 250	160- 180
Furukawa						
Furukawa F -5	283	710	700- 900	68	38- 65	100
Furukawa F- 6	355	884	650- 1600	75	50- 150	100
Furukawa F- 9	520	1305	400- 1400	90	45- 150	120
Furukawa F -12	835	2320	450- 900	105	100- 130	160
Furukawa F -19	1260	3579	400- 750	120	120- 155	160
Furukawa F -22	1570	4572	360- 700	135	145- 180	160
Furukawa F -27	1710	5118	340- 650	140	155- 190	160
Furukawa F -35	2270	6883	320- 600	150	175- 220	160
Furukawa F -45	3005	8829	300- 500	165	200- 250	160
Rammer						
Rammer BR623 (S23N)	300		400- 2000		20- 100	100- 145

Principle works hydraulic hammer [5, 20].

The hydraulic hammer is connected to the hydraulic system of the excavator (excavator-loader, loader). The hydraulic pump pumps hydraulic oil into the cavity of the hydraulic hammer through the shut-off valve. Under the action of oil pressure, the piston moves upward, compressing nitrogen in the nitrogen chamber.

When the piston rises, the shut-off valve closes the discharge line and opens the drain (return) line. Under the action of compressed nitrogen,

the piston begins to move downwards, pushing oil into the return line of the hydraulic system, and strikes the peak of the hydraulic hammer.

Most modern hydraulic hammers have a piston design that allows hydraulic oil to lift it up, only if the piston is slightly raised. The piston is raised if you push against it with a peak hydraulic hammer into a rock or other object that needs to be broken. This design of the hydraulic hammer allows avoiding idle blows, which lead to rapid wear and tear and breakage of the hydraulic hammer [12, 17].

Knowing the structure and operating principle of a hydraulic hammer, you can easily diagnose most faults (Table 1.5).

Table 1.5

Main malfunctions hydraulic hammer And their reasons [17]

Malfunction	Possible reasons
Weak impact energy	Low pressure nitrogen V nitric camera. Low pressure oils V hydraulic system excavator (loader). High pressure in the return line hydraulic systems excavator (loader).
Low frequency blows	Violation works valves cutoffs. Low pressure oils V hydraulic system excavator (loader). High pressure in the return line of the excavator (loader) hydraulic system.
Leakage nitrogen from a nitrogen chamber	Weakened bolts connections housings. Nitrogen escapes with hydraulic oil through worn out oil seals. Oil V reverse highways Foamed. The nitrogen chamber valve is not tightly closed or is clogged .

1.4. Terms and Conditions works peaks And reasons exit her from building

During operation, the main working tool of the hydraulic hammer, the pick (Fig. 1.23, 1.24), is subject to wear. The pick of the hydraulic hammer can have different shapes: conical, pyramidal, shovel-shaped, chisel-shaped. The choice of the pick shape depends on the type of material being destroyed. For crushing oversized rocks, a significant amount of which is formed during the extraction of minerals by drilling and blasting, a pick with a flat end is considered the most suitable. It is more convenient to install such a tool on the oversized rock being destroyed, since it slips less when the hammer is pressed against the object of impact by the hydraulic cylinders of the excavator's working equipment. However, over time, the working edge of such a tool will tool accepts spherical form. IN 1980s years At the Research Institute of Mining and Chemical Raw Materials, they tested a tool for crushing oversized rocks with a working tip in the shape of a concave sphere rather than a convex one [18]. time tests was noted, What probability The slippage when installing on a point of such a tool is much lower, and the efficiency of destruction of oversized material is not worse than that of a flat tool. Nevertheless, a tool with a concave sphere on the working tip has not received wide distribution for technological reasons. It is easier to manufacture a tool with a flat end, and as it wears out, the entire tool takes on a shape close to a convex sphere, losing its original advantages.

In road construction and during repair work highways, more often total use peaks type "wedge" or

"chisel". Their working Part has two converging edges And allows

"cut" the rock into layers. When using this form, cracks in the treated surface diverge parallel to the planes of the pick, which is convenient when removing old pavement or creating narrow trenches [17]. The "wedge" differs from the "chisel" by the angle of convergence of the planes. In the first case, it exceeds 30 degrees, and in the second, it fits into the range from 20 to 30 degrees. The chisel is most often used when removing old asphalt, and the wedge on frozen and hard soils that must be pre-loosened.

A tool in the form of a double-slanted wedge is preferable if it is desirable for cracks in the material being processed to extend away from the wedge blade, for example, when constructing trenches. A tool is manufactured in which the wedge blade is located both across the axis of

the working equipment and along the axis. When loosening viscous rocks or frozen soils, the highest productivity, all other things being equal, is achieved when using a wedge with a sharpening angle of 20 ... 30 °. For other types of materials, the optimal sharpening angle may be different. Cracks in the soil are formed more easily if the cross-section of the tool is large enough. If the diameter of the working part of the tool is small, then only holes are formed in the soil without cracks.

The forces acting on the hydraulic hammer pick are really very high. Therefore, the material from which it is made has high requirements. Firstly, it should be well-hardened steel containing a high percentage of manganese, chromium, vanadium, and nickel. Secondly, the workpiece for the future pick should not have internal defects - hidden cracks and cavities. Ultrasonic or magnetic diagnostics are used to test them. The pick can only be made of the best, almost ideal metal, then it will be sufficiently reliable and will not break at the first blow [11, 17].

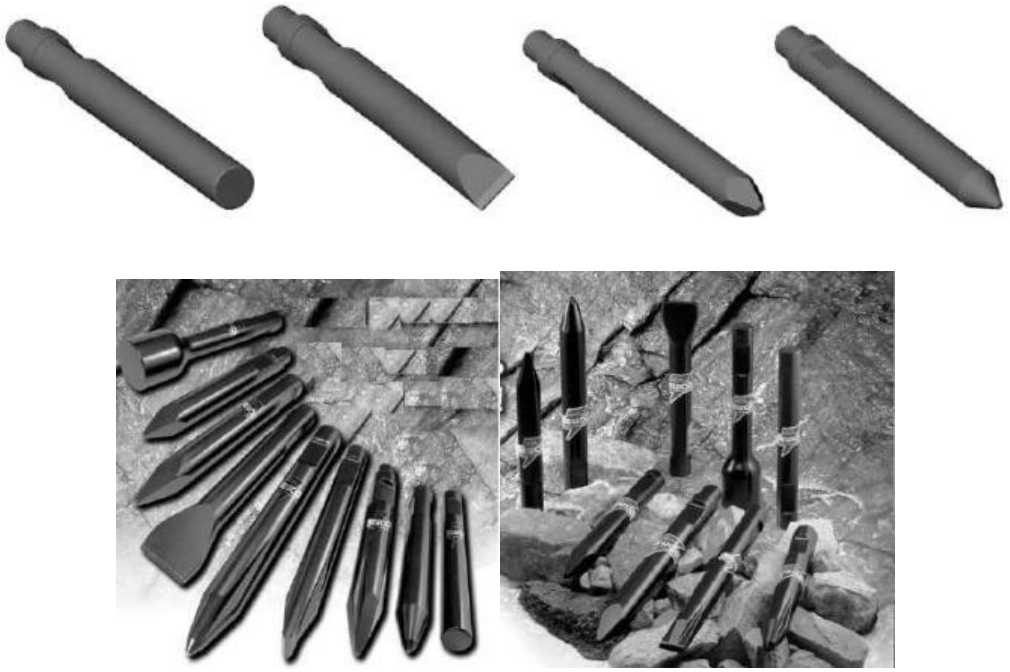

Figure 1.23. Configurations peak hydraulic hammer [17]

Currently, manufacturers offer three main types peak. This is actually a "peak", "wedge" And "chisel" (Fig. 1.23, 1.24). Each of them is intended to perform strictly regulated types of work.

Figure 1.24. Types peak, manufactured by various companies [17]

Usually, a hydraulic hammer is supplied with a "pick" with a round cone at the end. It is not without reason that the name of the entire tool is similar to this shape - for a long time it was considered to be the most universal tool For all types breeds. In At present, a pick with a triangular shape of the working part is more widely used. As shown theoretical research And practical experience works, In most cases, this geometry is the most efficient. In addition, it is cheaper to manufacture [11].

Somewhat less common are picks with a tetrahedral tip or even a blunt working part. The former are used for working with particularly hard rocks, while the latter are very convenient crush large pieces of rock that have been previously broken off from the general mass.

Usually the tool is used even after its tip will accept rounded form. For example, on At the Zaporizhia Ferroalloy Plant, the destruction of oversized casting slag was carried out using a hydraulic hammer model D600. The length of the working part of its new tool, protruding from the axle box, is 790 mm. The tool was used in the work until its working length was reduced approximately to 250 mm. Such exploitation tool is possible only if the tool does not break somewhere in the middle part (Fig. 1.26) before its maximum wear along the length [18].

Figure 1.25. Pika hydraulic hammer (V collection)

No matter how well the hydraulic hammer pick is made, the service life her services in in many ways depends from correct operation (Fig. 1.25). During operation, the hydraulic hammer tool experiences intense impact loads, which create compressive stresses in it, and as a result of the reflection of shock waves from the tool tip and wave interference, tensile stresses. To these stresses are added stresses from the radial components of support reactions, from bending moments, which can arise for various reasons. Factories - manufacturers of hydraulic hammers prohibit work by them How with a crowbar, turning inside out pieces of material, but in practice such working methods are often used. In these cases, the tool is subject to a bending moment, and if the forces of the excavator's hydraulic cylinders are large and the cross-section of the tool is insufficient to withstand the bending stresses, the tool may burst in the area where it exits the axle box [17, 18].

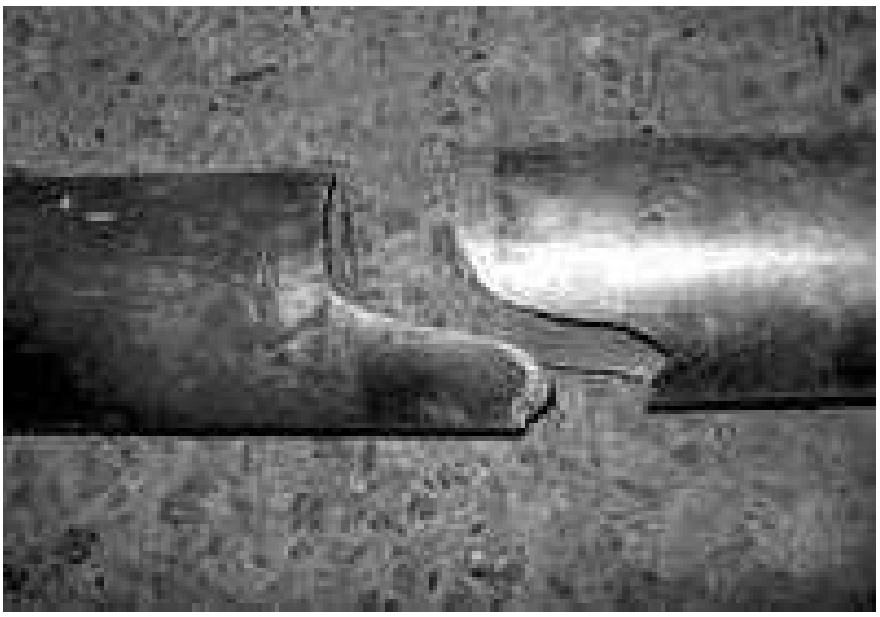

Figure 1.26. Broken peak [18]

It happens that consumers did not work with a hammer as a crowbar, and the tool was destroyed in the cross-section. Unfortunately, this is possible, and there may be reasons for this. For example, the hammer is not installed vertically, but at an angle to the horizon, and at the same time it is pressed to the object of work not along its axis by means of appropriate hydraulic cylinders, but only by the weight of the excavator. In this case, a bending moment acts on the tool, bending stresses appear in its sections, to which stresses arising from the striker impact are added.

Another common reason premature failure of this attachment is too

large a gap between the bushings in which the peak moves with the landing shank. It should be within the range of 0.5 millimeters to 1 millimeters.

The initial gap should not be made smaller due to the risk of the tool jamming in the bushing. The fact is that the gap must be sufficient to remove the inevitable products of natural wear of this loaded pair. When the hydraulic hammer is pressed against the work object, the tool inevitably deviates from the geometric axis of the hammer within the gap. If this deviation is small, then the bending moment from the force arising from the striker hitting the tool is also small. As the gap in the tool-bushing pair increases, the magnitude of the bending moment from the impact force also increases. If the upper limit is exceeded, then when the hammer strikes, the forces are distributed not strictly along the axis of the peak, but with some deviation. This also creates an undesirable bending moment of force, which can lead to breakage of the tool [11, 18]. It is necessary to ensure that the gap between the peak and the bushing does not exceed the established maximum permissible values set by the manufacturer. The Krupp company, as part of the accessories for servicing its hammers, provided a special gauge for monitoring the permissible wear of the tool sleeve [21].

The replaceable tool of the hydraulic hammer is secured from falling out of the axle box by one or two round or oval cross-section pins (Fig. 1.27, 1.28). Half of these pins cross-section enter the grooves on the side faces of the tool.

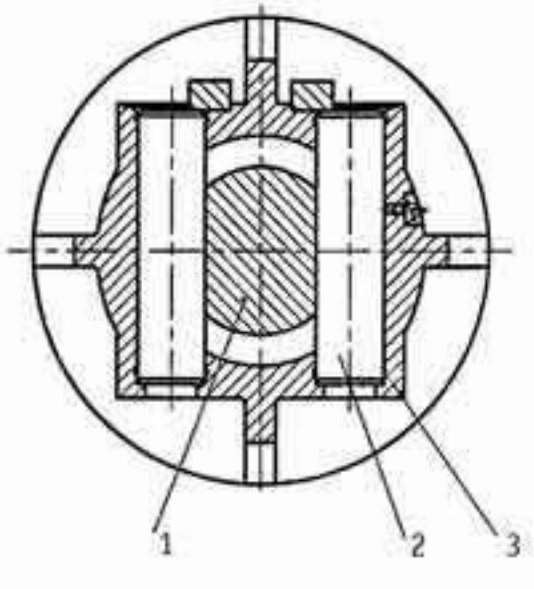

Figure 1.27. Transverse section hammer: 1 - tool; 2 - fixing finger; 3 - box [18]

On most models of hydraulic hammers, the colliding ends of the

striker and the tool are made flat. It is almost impossible to ensure parallelism of the colliding surfaces, especially when the seating surfaces of the tool and its bushings are worn. Therefore, when striking, the contact of the colliding surfaces occurs not in the center, but along the periphery. Part of the kinetic energy of the striker, i.e. the impact energy, is spent on turning the tool to a position where the planes of the ends of the striker and the tool coincide.

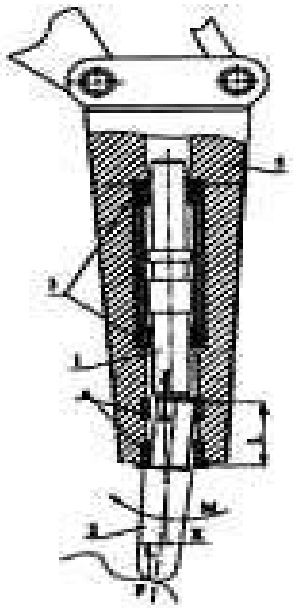

Figure 1.28. Tool loading diagram: 1 – tool; 2 – locking pin; 3 – striker support bushings; 4 – tool bushings; 5 – hammer body; L – length of support part; F – axial load; X – shoulder; M – bending moment [18]

As a result of an off-center impact, both the tool and the most valuable part, the striker, are loaded with additional moments and shearing forces. Sometimes this leads to pieces breaking off from the colliding surfaces of the striker and the tool. In most domestic designs of hydraulic hammers, the upper end of the tool is made spherical. In this case, the center of the sphere is located V in the middle supporting surfaces bushings tool. In this design, the contact point on the flat end of the striker is located practically V center, A diameter contact patches smaller than the diameter of the lower end of the striker. With this technical solution, no chips are observed on the striker and tool [18].

IN designs hydraulic hammers more often total limitation the upper position of the tool in the axle box is provided with a stop of its upper butt or shoulder, located some below, in the limiter V axle box. IN domestic models GPM-120, SP-71, MG-300, "Impulse 300M", SP-62 the tool rests

on the lower end face axle boxes his own with a flange, completed on working parts [18, 21]. When installing the hammer on the point and pressing it with hydraulic cylinders worker equipment excavator the tool inevitably deviates to the side within the gap and is pressed part of the surface of the seat shank to the surface of the sleeve. Radial component forces pressing tool To in the bushing, multiplied by the coefficient of friction, is the friction force to overcome which part of the impact energy is expended. The greater this force, the faster the rubbing surfaces wear out. In the hydraulic hammer model "Impulse 310» applied technical solution, allowing center tool By axes hammer. At the instrument this hammer there are supporting conical surfaces: one on the flange slightly below the upper end, and the second on flange on working parts, which rests V lower edge of the axle box. Because supporting surfaces are made conical when pressed hammer To object works tool strives take up position By axes axle boxes, What promotes increase resource tool.

Usually the working part of the tool along its entire length (except for the tip) is made in the form of a cylinder. There is a proposal [18] to make the working part in the form of a cone, the transverse section whom decreases V direction To working tip, i.e. to the point. The motivation for such a proposal is quite weighty. Firstly, when the cone is driven into the rock being processed, large radial forces arise, which contribute to the occurrence of cracks in the material being destroyed. Secondly, a conical tool is easier to extract from a hole in the ground than a cylindrical one. Thirdly, at loading conical tool bending moment of stress in its working part are more evenly distributed along the length, which means that under equal loads the tip of a conical tool can deviate by a greater amount as a result of bending without breaking. That is, the probability that the tool will break when bent is reduced.

It is not allowed for the hydraulic hammer to operate idle: this will cause deformation And premature wear fingers and bushings, and as a result, play and distortion of the working tool and its breakage in the area of pin attachment and in places of impact with the striker.

Low temperatures and mechanical damage to the surface increase the sensitivity of the tool metal to fatigue loads. Poor-quality surfacing and autogenous sharpening, as well as corrosion due to improper storage, lead to rapid wear and tear and destruction of the pick.

In order to avoid early failure of the hydraulic hammer as a whole, it is necessary to monitor the wear indicators of the pick. Experience in

operating Steel Hand hydraulic hammers (Fig. 1.29) has shown that the rate and degree of wear of the pick depend on the operating conditions of the hydraulic hammer - its service life, density and type of the material being developed [12]. For example, a company that dismantles industrial structures put into operation a Steel Hand SHD150A hydraulic hammer at one of its facilities (St. Petersburg). The hydraulic hammer was used to destroy a concrete foundation. The compressive strength of this material was 30 MPa. As a result, the maximum permissible wear of the pick was recorded after 1,500 hours of continuous operation (3 months, 3 shifts daily for 8 hours). As practice has shown, for equipment such as a hydraulic hammer, this is a completely normal time indicator.

As a rule, the wear limit of the working tool of a hydraulic hammer is set by the manufacturers. For Steel Hand hydraulic hammers, for example, the maximum permissible wear of the peak and bushing is determined depending on the model and weight of the hydraulic hammer.

Table 1.6

Maximum acceptable wear details hydraulic hammer [17]

Model hydraulic hammer	Maximum permissible wear of the peak and bushing, mm
SHD 40i, SHD 45i, SHD 53ib, SHD 68ib, SHD 75ib, SHD 85i, SHD 100i	4
SHD 125i, SHD 135A, SHD 140i	6
SHD 150A, SHD155i, SHD 165i,SHD 175i	8

Figure 1.29. Hydraulic hammers companies Steel Hand [11]

Group hydraulic hammers company Steel Hand today already includes 15 models for excavators and backhoe loaders [11].

In addition to various design features, The strength and durability of the tool are significantly affected by the choice of material from which it is made and how correctly the heat treatment is performed. The tool material must have a high impact toughness coefficient, and its hardness, achieved as a result of heat treatment, must be as high as possible. The steel used must have good hardenability so that high hardness is ensured throughout the entire cross-section. Therefore, high-alloy steels containing chromium, nickel, manganese, and vanadium are used to manufacture strong, wear-resistant tools.

So, main reasons breakdowns worker tool hydraulic hammers are [11, 12, 17–22]:

– diverse lateral loads V in the course works, creating a bend;

– incorrect working angle (the tool is not perpendicular to the surface of the material being destroyed);

– Job "idle";

– low temperatures

– mechanical And thermal damage;

– unskilled surfacing or sharpening;

– flaw lubricants;

– corrosion;

– wear.

1.5. Terms and Conditions works piston (striker) And the reasons for its destruction

The most important parts of a hydraulic hammer are the working striker and the guide bushings (Fig. 1.30, 1.31). Their condition must be monitored very carefully, and most importantly, they must be thoroughly lubricated. This is absolutely necessary to keep the hydraulic hammer in working order. The main rule is that a film of grease must always be applied to the hammer striker. In most cases, the striker and bushings should be lubricated every 2-4 hours of operation. In practice, it is necessary to focus primarily on the operating conditions, and based on this, calculate the frequency of tool lubrication [7].

The striker is the main element of the hammer. The striker is a certain mass m that must be moved some distance from the tool and accelerated to a given speed V towards the tool. In order to accelerate the striker to the desired speed, To him need to attach corresponding strength, the value of which is determined by the pressure of the working fluid and the area on which this pressure acts, as well as the gas pressure in the pneumatic chamber and the corresponding area of the end of the striker on which the gas pressure acts.

Figure 1.30. The striker hydraulic hammer (general view)

The shorter the stroke of the striker, the greater the force that accelerates it must be. However, the same reactive force acts in the opposite direction, i.e. is transmitted to the base machine. Therefore, the force accelerating the striker is limited by the ability of the base machine to perceive it at the maximum reach of the working equipment [1].

At the same time, the shorter the stroke of the striker, the higher the

frequency of impacts can be obtained with the same feed of the hydraulic pump of the base machine. So, the striker of the hydraulic hammer during its operation makes reciprocating movements and in its extreme positions (at the moment of impact and at the top dead center) its speed at some point in time is equal to zero. In the cycle of operation of the hydraulic hammer, the following main phases can be distinguished: acceleration to the side from tool (conditionally "up"), braking before

"upper" dead point And acceleration V side tool to blow.

This means that the consumption of working fluid in the hammer cylinder during the entire cycle is a variable value, while the hydraulic pumps of the base machine provide a constant supply. Therefore, in order to make maximum use of the hydraulic pump capacity and increase the efficiency in the pressure line of the hydraulic hammer, at least on medium and heavy class hydraulic hammers, network hydraulic accumulators are installed that accumulate working fluid under pressure at low striker speed (during acceleration "up" and braking) and release the accumulated fluid in the hammer cylinder when the striker speed is high, i.e. during acceleration "down" (during the working stroke). On light series hydraulic hammers, where the volumes of accumulated fluid are small, the role.

Hydraulic accumulators are often made up of high-pressure hoses that are part of the pressure line supplying the hydraulic hammer [1, 3].

The same amount of energy can be obtained due to the speed of the striker or due to its mass. With equal impact energy, the hydraulic hammer with a larger striker mass will be more effective, since the product mv, numerically equal to the force impulse, is greater for it.

When operating, the hydraulic hammer emits pulsed noise, the source of which is the striker striking the tool. All other things being equal, the emitted noise will be less if the hammer's striking block is not placed between two jaws held together by pins, but inside a closed box-shaped casing, especially if noise-absorbing pads are installed between the striking block and the casing, breaking the sound "bridges" [1, 3].

As for the vibration impact on the base machine, then with equal impact energy and hammer weight, the greater this impact is, the higher the frequency of impacts of the hydraulic hammer. When choosing a hydraulic hammer, it is necessary to take into account not only the indicators given in its technical characteristics, but also the conditions of its future operation, the intensity of its use, the strength of the material being processed.

During the operation of the hydraulic hammer, all its rubbing pairs are

subject to wear: the tool shank - the tool bushings, the sleeve-striker of the working cylinder (or directly the cylinder body), the spool - the distributor sleeve. The amount of wear of the parts is greatly affected by the purity of the working fluid (oil) of the hydraulic system. When working on clean oil, the hydraulic distributor parts usually work for the entire service life of the hydraulic hammer.

The most important and expensive friction pair of a hydraulic hammer is the striker – the sleeve of the working cylinder, the guide bushings in which are moving rods striker. During production these parts, high demands are placed on the precision and purity of the mating surfaces. When the striker moves, its sliding speed relative to the surfaces of the working cylinder reaches values of 8–9 m/s. In addition, these parts are subject to impact loads, which have And radial component, on the value of which is greatly influenced by the wear of the tool- tool sleeve pair.

As a result of all adverse effects on the rubbing surfaces of the striker and mating parts, coarse scoring may occur, which leads to failure of the entire hammer. If not very deep scoring has formed only on the piston part of the striker (there are no contact seals) and the cylinder liner mirror, then such parts can be saved during repair. Coarse scratches can be cleaned by grinding, without eliminating them to the full depth, after which these parts can serve for quite a long time. If the surfaces of the striker rods are damaged (scoring or corrosion), then in this case, when repairing the hydraulic hammer, the striker must be replaced with a new one, since damaged surfaces that are sealed by contact seals disable these seals.

When manufacturing a new striker, it is important to maintain the required clearance values between the rubbing surfaces of the mating parts. When manufacturing repair sleeves for the working cylinder, in addition to ensuring high surface purity, measures should be taken to reduce the friction coefficient. The friction coefficient can be reduced by nitriding the surfaces, saturating the surface with molybdenum disulfite, and other physical and chemical treatments.

When there is a large gap between the tool and its bushings, which appears due to natural wear, when the hammer is in operation longitudinal axes striker And tool cross And the striker interacts with the end of the tool with its edge, not the center. In this case, both the striker and the tool are subject to additional radial forces and bending moments, which can damage the striker. The tool or striker can burst across the cross-section or get chipped in the work of the colliding ends. To reduce the harmful effect of the skew of

the striker and tool axes, it is advisable to make a sphere on the end of the tool with a radius, the center whom lies approximately V in the middle or some below the middle supporting surface of the tool bushings (see section 1.4).

One of the reasons for the destruction of strikers is metal fatigue (Fig. 1.31).

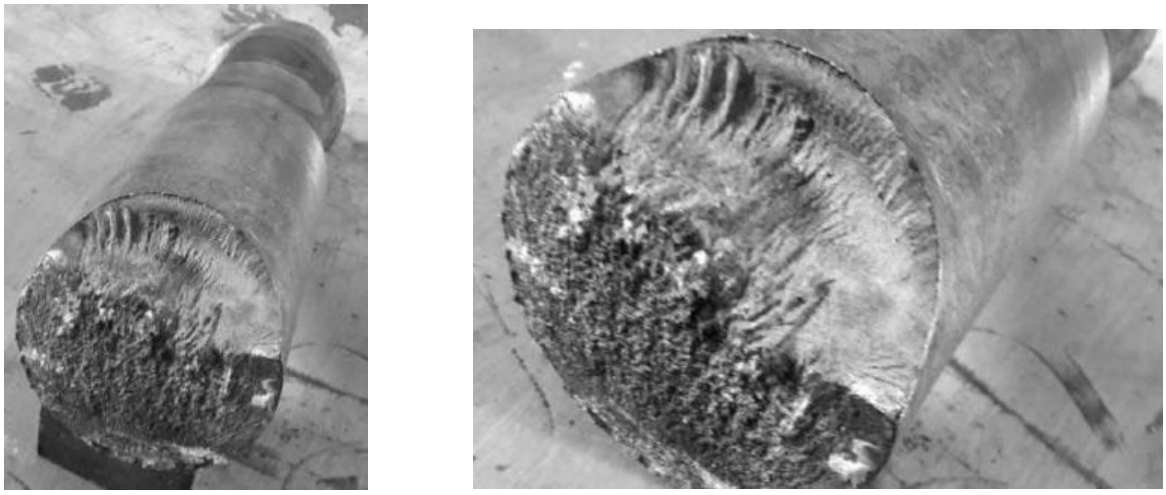

a b

Figure 1.31. Fatigue destruction striker hydraulic hammer during operation

Piston failures can be caused by incorrectly performed forging or heat treatment operations, fatigue, impact loads. The destruction is affected by the formation of scratches and cracks. Scratches appear due to low surface hardness, foreign particles getting into the hydraulic oil, too large a gap between the working tool and the bushings, deviation of the tool axis from vertical. Dents and cracks appear due to low quality steel and insufficient hardness [22–24].

1.6. Bushings frame hydraulic hammer

The lower guide bushing is another vulnerable and particularly wear-prone part of the hydraulic hammer (Fig. 1.32–1.34). Each manufacturer of hydraulic hammers recommends its own method for checking the lower guide bushing. For example, some hydraulic hammers are supplied with a special tool for checking the lower guide bushing and the locking pin, which displays the degree of wear of the hammer during operation. Next stage: weekly check. At her During the inspection, it is also necessary to inspect the instrument for cracks and signs of excessive wear, but this time

more careful attention follows to devote surfaces And shock end face worker striker, as well as fasteners and holes. If signs of wear are detected, special attention should be paid to the corresponding parts. Nuts and bolts should also be checked weekly.

In hydraulic hammers, the replaceable tool - tool bushing pair is a quickly wearing part. In this pair, during hammer operation, large radial forces and, accordingly, friction forces inevitably arise, causing wear of the rubbing surfaces. The situation is aggravated by the fact that abrasive particles from the material destroyed by the hammer, as well as wear products of the rubbing parts, penetrate into the gap between the tool shank and the bushing.

The hydraulic hammer chamber between the ends of the tool and the striker during works continuously changes mine volume. At movement the hammer from the tool (idle stroke) the volume of the chamber increases, a vacuum occurs in it and the surrounding air enters it together with dust and abrasive particles through the gap between the tool and the bushing and through a special hole in the axle box body (breather). When the striker moves towards the tool (working stroke), the volume of the chamber decreases, some excess pressure arises in it and air is released into the atmosphere through the gaps and the breather. However, some of the abrasive particles remain inside the chamber and in the gap between the tool and the bushing. In other models of hydraulic hammers, the breather is made in the form of through holes in the tool axle box [24, 25].

In hydraulic hammers "Impulse 200", "Impulse 300M" the breather is equipped with an air filter made of foam rubber, which somewhat limits the possibility of dust penetration into the above chamber. However, during operation in the vast majority of cases this filter is never changed, it gradually becomes clogged with dirt. However, the operating documents do not say anything about the need for periodic replacement of the breather filter. In hydraulic hammers of Japanese and South Korean manufacturers, a check valve is built into the breather, through which atmospheric air is sucked into the chamber and released into the atmosphere only through the gap between the bushing and the tool. In this case, dust and wear products that have entered the chamber are partially removed from the gap. In some models hydraulic hammers companies Krupp breather steel place Not V bux tool, A V the most top parts hammer - V cover of the working cylinder [26, 27].

Figure 1.32. The striker and bushing

Figure 1.33. Hydraulic hammer bushing

Drawing 1.34. Bushings hydraulic hammer [27]

No matter how high-quality the design of a hydraulic hammer is, its parts are subject to high loads, and friction against hard surfaces has a negative effect on the device. In addition, the outer parts, in particular the body (Fig. 1.35, 1.36), are very worn out under the impact of pieces of material, with which the hydraulic hammer has to deal with. This is the reason why many foreign, and now domestic, manufacturers of such attachments have paid attention on high-strength and wear-resistant steels, capable of increasing service life many times over. Hardox steels are exactly such a material, the use of which can reduce the cost of repair work, increase the durability of equipment [28, 29]. The technologies used in their manufacture make it possible to obtain steels with excellent technological characteristics without affecting the structure of the material.

a

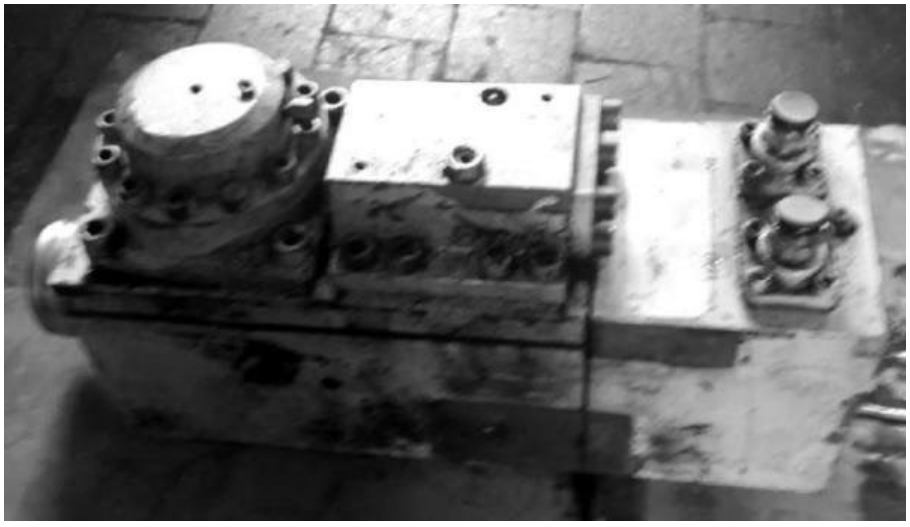

b

c

Figure 1.35. Frame hydraulic hammer: A - new; b, c – after use

Hardox alloys live up to expectations even in low temperature conditions. They retain their properties even at -40 °C. Hardened and tempered, containing a minimum of alloying elements, purified by refining and ladle blowing, Hardox steels provide predictable wear, are easy to weld, cut by laser and arc cutting, and bend on conventional equipment. Therefore, manufacturers of hydraulic hammers have the opportunity to produce equipment of the required shape from these alloys, adjust the body configuration to the internal equipment. Thanks to Hardox steels, hydraulic hammers become more reliable in operation, they can more easily withstand high loads And demand less expenses on repair.

A significant disadvantage is the high technological complexity and cost of the process of producing parts from these steels.

Picks were previously made from tool steels - U7, U8; as well as from steels 65G, 60S2A. Some enterprises producing picks for their own needs use steels 6XC, 9XC. Currently, a significant share of the market is occupied by picks, made of 50 grade steel (common quality carbon steel). It is believed that What in a colliding a pair of pikes and picks striker must be 5–7 HRC units harder than the pick [30]. But the cylinder should be harder than the striker. However, when working on strong concrete, wear and breakage of the strikers and picks is significant, sometimes within literally 1–2 days from the start of work. The reason for failure is the destruction of the striker (work hardening, chipping), its jamming in the body, damage to the body by chipped parts of the striker. The hardness of a pick made of steel 50 is lower than the hardness of the striker; but if you choose a pick in a pair with a striker made of steel 50 from U8, its hardness is 55 units according to HRC, which is 3

units higher than the hardness of the striker, which is the reason for premature destruction.

The tool's resistance to breakage during the operation of the hydraulic hammer is characterized primarily by strength and impact toughness. The tool's wear resistance is determined mainly by hardness. The material of the pick and striker must have maximum hardness on the one hand and sufficient strength and impact toughness (and preferably plasticity) on the other.

When producing working tools, manufacturers have to find a balance of hardness and strength of the material that is acceptable in local operating conditions. Local features include climatic conditions, the main processed material, and the culture of maintenance and operation of hydraulic hammers. Thus, for northern Europe and Canada, the climate is very similar to ours, but developments are usually carried out on very abrasive and hard rock (basalt, granite, gabbro-diabase, etc.). At the same time, the culture of work and maintenance of the hydraulic hammer is much higher domestic. That's why there produce worker tool, primarily focused on wear resistance [31, 32]. However, as a result of using more expensive steels and proven heat treatment technology, it also has high strength properties. characteristics (For example, firm Hammer, which has been on the hydraulic hammer market for over 40 years and is considered the standard in hydraulic hammer construction).

When analyzing domestic conditions, it is necessary to note the combination of the most unfavorable factors, starting with the most unfavorable weather conditions (cold winters) and ending with insufficient maintenance and often improper operation.

Korean manufacturers use very mediocre, cheap steel with a low content of alloying elements, which at the same time (due to proper hardening and low-temperature tempering) has good wear resistance [32].

The Traditsiya-K company believes that the main indicators of a working tool in our operating conditions are strength characteristics, i.e. resistance to premature destruction and fracture. Therefore, it uses high-alloy steel of the highest quality, manufactured according to class A, for its tools. Previously, such steel was used mainly in the defense industry and was supplied for export, including to the Finnish company Rammer (now Hammer). However, it is more than 2.5 times more expensive than steels used by other companies [32].

For the hydraulic hammer cylinder, structural steel 40 X is traditionally used. After quenching from 850 °C in oil and tempering at 520 °C, it has a tensile strength of over 1000 MPa and a yield strength of over 980 MPa with

an impact toughness of at least 59 J/cm2 · and a relative elongation of 9%, a relative contraction of 45 % [33].

For all the investigated parts of the hydraulic hammer (peak, striker, bushing, cylinder) double heat treatment is used: after

Hardening and tempering necessarily involve strengthening the surface to ensure the required wear resistance [30, 32].

In general, the main "failures" in the operation of a hydraulic hammer are the result of violation of the rules of its operation. In order to avoid negative consequences when working with a hydraulic hammer, the service specialists of the Intertekhnika Group of Companies recommend adhering to certain rules for the safe use of the hammer [29, 34, 35].

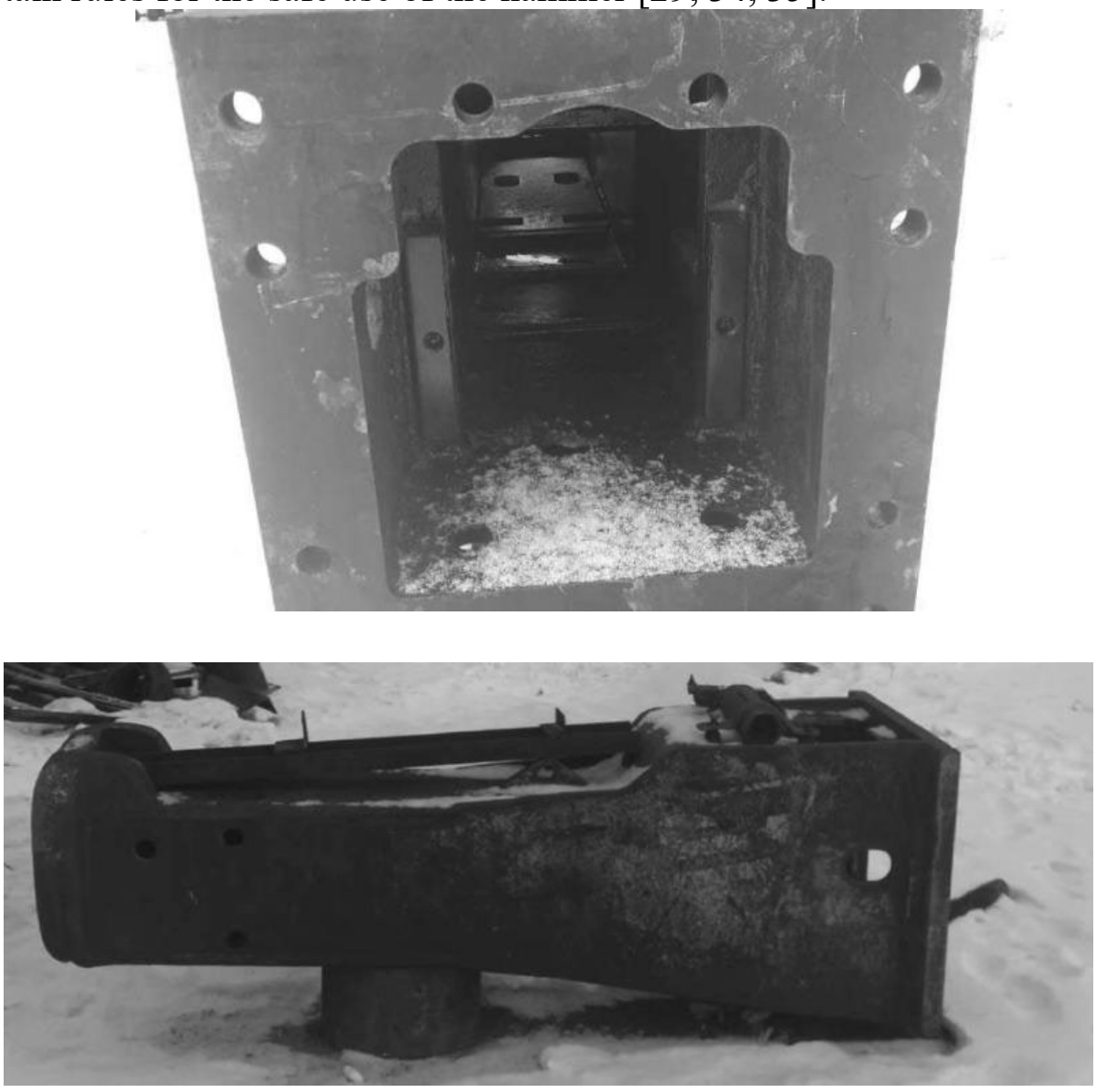

Figure 1.36. Casing (frame) hydraulic hammer after exploitation

First of all, it is necessary to take care of regular lubrication of rubbing

elements. The absence or irregularity of lubrication can lead to the appearance of cracks, burrs and, as a consequence, fatigue failure of the structure. Service specialists of the Intertekhnika Group of Companies advise lubricating individual rubbing elements with a certain value recommended by the hydraulic hammer manufacturer, frequency. In the case of Steel Hand hydraulic hammers, lubrication is carried out at least every 3 hours of operation. In order not to turn process lubricants V labor-intensive procedure, GC "Intertekhnika", as a manufacturer of hydraulic hammers, recommends its clients an additional option: automatic lubrication .

Availability at hydraulic hammer systems automatic lubrication will not only allow you not to involve the excavator operator in the work, but will also ensure uninterrupted lubrication of the rubbing units exactly at the moment when it is really necessary. As a result, the time for equipment maintenance is reduced, the service life of the replaceable parts of the hydraulic hammer (peak, bushing of the working tool) is increased and cases of missing scheduled hydraulic hammer lubrication work. The system (Fig. 1.37) is mounted on the hydraulic hammer body and is independent of the base machine. It is convenient and safe, especially If hydraulic hammer is being exploited on several excavators.

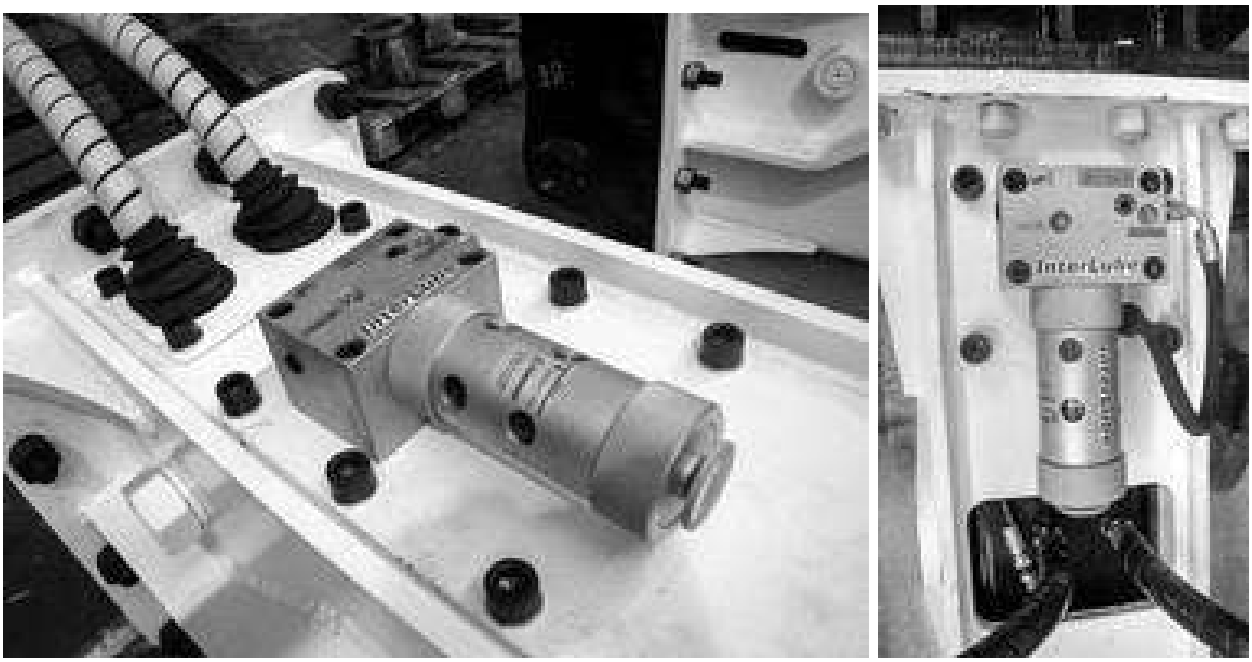

Figure 1.37. System automatic lubricants For hydraulic hammer [35]

The hydraulic hammer will also require lubrication during storage. According to the experts of the Intertekhnika Group of Companies, this will help to avoid the appearance of rust, which can also cause rapid

fatigue failure of the hydraulic hammer [35].

The Delta hydraulic hammer range has recently been expanded with the Delta F-12 Full Hydraulic hammer in a noise and vibration-proof design [36]. IN Delta F-12 Full Hydraulic present record for the industry, the number of innovations that bring it to the same level as the products of such famous brands as Hammer (Finland), Atlas Copco (Sweden), Montabert (France), and other leaders in the global destructive manufacturing industry attachments.

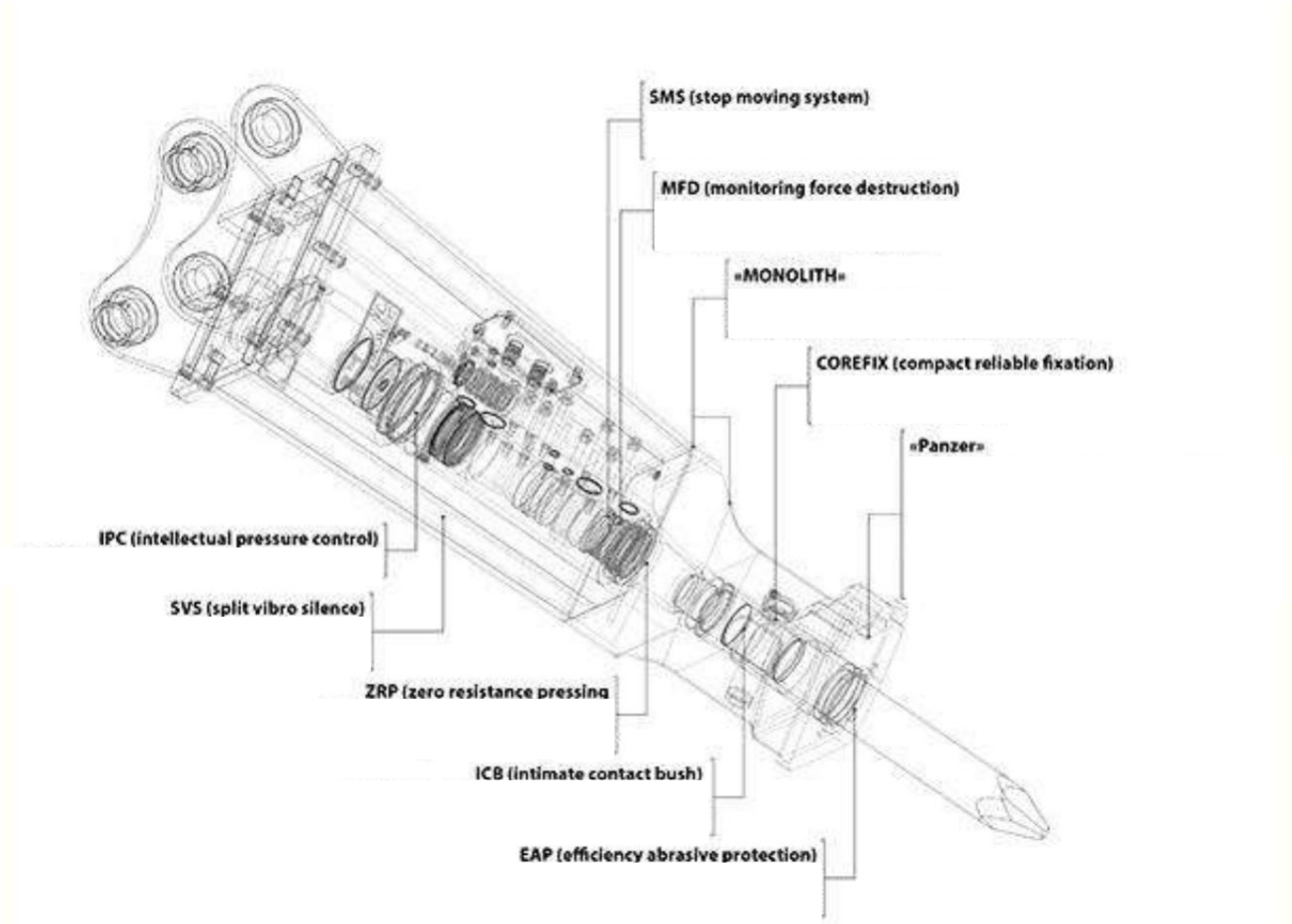

Figure 1.38. Innovations V constructions hydraulic hammer [36]

Structurally, in modern hydraulic hammers, the most common two main schemes for driving the working stroke of the piston (striker). In the first, a pneumatic spring is installed in the hydraulic hammer - in a special chamber, the striker compresses gas pumped to a certain pressure, usually nitrogen. The inconvenience of operating a hydraulic hammer of this design is associated with inevitable gas leaks, which, first of all, leads to a sharp drop in productivity, the need for periodic monitoring of the chamber charging pressure. To fill the pneumatic chamber hydraulic hammer nitrogen to clients have to Always have a set of necessary tools, a special filling device, a

cylinder filled with compressed gas at hand. All this, naturally, creates at exploitation certain inconveniences [22, 36]. The second scheme is based on the accumulation of energy in a membrane-type pneumatic hydraulic accumulator. If there are problems in this unit, the hydraulic hammer loses its functionality, which leads to downtime. In this case, gas leaks, provided that the assembly is of high quality, are unlikely, but the rubber membrane of the accumulator has a relatively short service life and does not tolerate winter operation very well. It should also be noted that replacing it is a rather expensive operation, which requires qualified personnel. Both of the described schemes have been produced for several decades, and the consumer has been forced to put up with obvious serious shortcomings. In the Delta F-12 Full Hydraulic hammer, the energy part does not require maintenance throughout its entire service life (Fig. 1.38, 1.39). This model is equipped with an extremely reliable hydraulic energy accumulator with an IPC (intellectual pressure control) system, which does not contain nitrogen or rubber diaphragms (Fig. 1.39).

It can be said that the automatic adjustment system itself adjusts the pressure in the accumulator, correlating it with the current characteristics of the drive circuit of the base machine and equalizing it to the required value. This operating algorithm leads to the greatest productivity and significantly reduces the load on the components of the excavator hydraulic system. Since this system does not require maintenance, downtime in operation is eliminated, service costs are reduced. The innovation also makes it possible to operate the hydraulic hammer in the harshest climatic conditions, down to -50 ° C, without the risk of damage to parts. and the use of additional options, which is an important parameter. The design of the striker is developed taking into account the features of difficult operating conditions of the equipment. The cylinder, made of a special alloy, is processed by the method of chemical-thermal ion-diffusion nitriding. All changes are made to ensure high reliability, wear resistance when working in contaminated environments, and reduce the requirements for storing the hydraulic hammer [18–20].

Figure 1.39. Hydraulic hammer Delta F-12 Full Hydraulic,
equipped energy accumulator With system IPC [20]

In addition, the design uses the ZRP (zero resistance pressing) system, which does not require the use of a hammer to press the working tool and start the hydraulic hammer. axial force on the equipment. That is, in order to press the tool against the object being destroyed, it is not necessary to overcome the resistance of the air spring. Due to this, the time of preparatory operations is reduced by half, which leads to a significant (up to 32%) increase in equipment productivity compared to hydraulic hammers with similar characteristics [20, 35, 36].

As well as in all previous models, in the design Delta F-12 Full Hydraulic has the SMS (stop moving system) system integrated, allowing the hydraulic hammer to operate if the tool is not pressed against the object. It significantly reduces the likelihood of hard idle blows, preventing premature failure details axle boxes hydraulic hammer V case errors operator. Errors The operator's faults may result in the following situations: the working tool slipping due to imprecise positioning of the equipment, untimely shutdown of the hydraulic hammer - in case of continuing work with a destroyed object, behind which there is a void or softer material. The closed body, made of specially selected, durable structural

steels, has a safety margin designed for long-term operation. This design allowed engineers to achieve a significant increase in the reliability of metal structures as a whole as a result of refusing to use unnecessary fastening elements (ties and studs). It is known that one of the types of failures encountered during the operation of hydraulic hammers is the breakage of the studs that tighten the body parts of the hydraulic hammer, and the studs that tighten the cheeks of the hydraulic hammer, between which the impact block of the hydraulic hammer is located. The studs themselves are designed absolutely correctly: the diameter of the stud body is made smaller than the internal diameter of the thread. In this case, the tensile stresses that occur in the stud during tightening and under operating loads are greatest in the stud body, not where the thread is located. However, studs often break along the thread in the nut end area. Such failure indicates that additional stress occurs in the failure zone due to a local bending moment. This bending moment, in turn, is due to the fact that the surfaces to which the ends of the nuts are adjacent are not parallel. The non-parallelism of the tightened surfaces is due to the fact that the tolerances for deviations from parallelism of the mating surfaces of all parts can be summed up [28, 29, 34, 35]. Therefore, when manufacturing all mating parts, it is usually necessary to tighten the tolerances and ensure their observance, or to introduce some compensators into the design, for example, to use nuts with a spherical end surface and conical washers. The Delta F-12 Full Hydraulic model is free from this need.

The changes made allowed us to expand the list of basic machines; now the hydraulic hammer can be installed not only on wheeled excavators from 12 tons, but also on tracked machines weighing to 22 tons. Thanks to application set «PANZER», manufactured With application durable Swedish steel "HARDOX" significantly increased the resistance to abrasive wear and impact loads of the lower part of the hydraulic hammer, since it is this part that operates in the most difficult conditions [36].

The changes also affected the hydraulic hammer axle box parts. For positioning and fastening the monolithic guide bushing of the working tool applied more one development - ICB (intimate contact bush). This innovation significantly increases the reliability of the unit, as well as the convenience and speed of replacement work. worn parts, while allowing repair work to be carried out on heavily contaminated and corroded elements [36]. The main functions of fastening the guide bushing and the working tool are implemented using just one pin. The axle box also acquired a new protective complex EAP (efficiency abrasive protection), which prevents the penetration

of abrasive dust and small particles into the working area of the striker and cylinder .

As follows from the above material, specialists pay sufficient attention to studying and determining the causes of failure of critical parts of the hydraulic hammer, as well as increasing their reliability and durability. These properties of the hydraulic hammer are greatly influenced by the materials used, production technology and design features.

All other things being equal, the reliability of a hydraulic hammer will be higher the smaller the number of parts, the smaller the number of seals, the fewer threaded connections, the fewer console projections on the outer surface of the hammer, the more smoothly the shape and cross-section of parts subject to impact loads changes.

Another important criterion when choosing a hydraulic hammer is ease of maintenance and repairability. Ease of maintenance is ensured by good accessibility to lubrication points, to tools for connecting hoses to fittings for filling hydropneumatic accumulators and a pneumatic chamber, as well as easy replacement of working tools. Important performance indicators include its ergonomic indicators - emitted external noise and vibration impact on the base machine.

A number of studies have shown that chemical-thermal treatment of the working surfaces of a hydraulic hammer can only solve specific problems.

A study of the experience of using high-energy energy sources suggests the feasibility of using them to increase the service life of hydraulic hammers.
METHOD TESTS

1.7. Material research

For the research, hydraulic drive parts made of steel grades 40, 40X and 9 HS were selected (Table 2.1).

Table 2.1

Chemical compound researched steels

Detail hydraulic hammer	Brand steel	Content elements, % mass.			
		WITH	Si	Mn	Cr
cylinder	steel 40	0.40–0.50	-	0.50–0.80	-
sleeve	steel 40X	0.40–0.50	-	0.50–0.80	0.80–1.10
striker	steel 40	0.40–0.50	-	0.50–0.80	-
peak	9XC	0.85–0.95	1.20–1.60	0.30–0.60	0.95–1.25

Steel 40 is subjected to hardening from 840 °C, tempering at 500 °C; it has a hardenability of 3-4 mm. Hardness HB 197-217, tensile strength 570 MPa, yield strength 320 MPa with a relative elongation of 17%, relative contraction of 45%, KS 30 J/ ^{cm2} .

Steel 40X is subjected to quenching from 850 °C, in oil, tempering at 500 °C; it has a hardenability of 6-9 mm. Hardness HB 217-229, tensile strength 1000 MPa, yield strength 800 MPa with a relative elongation of 8-9%, relative contraction of 40-45%, KS
50–60 J/ ^{cm2} .

Steel 9XC is hardened from 840–860 °C, in oil, and tempered at 140–180 °C; it is classified as a deep hardenability steel (up to 15 mm). Hardness HRC 60-64, tensile strength 790 MPa, conditional yield strength 445 MPa with relative elongation of 26%, relative narrowing up to 54%, KS 39–40 J/ ^{cm2} .

1.8. Conducting metallographic studies

For metallographic studies, an Altami-MET1 optical metallographic microscope was used (Fig. 2.1).

The professional metallographic microscope Altami-MET is indispensable for work in stationary and field (portable modification P) conditions. It allows for the examination of any opaque objects located at any angle to the horizon [37].

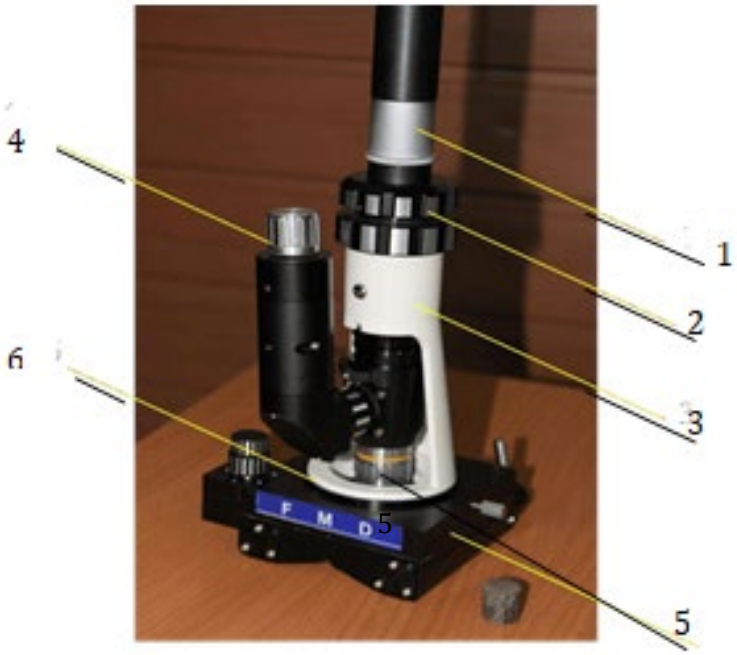

Figure 2.1. General view of the Altami-MET1 microscope: 1 – eyepiece; 2 – focal length screw; 3 – tube; 4 - backlight; 5 - lens; 6 - magnetic table [37]

The microscope has a built-in LED backlight with smooth brightness control, which provides even and contrasting illumination of the object of study even at high magnifications.

The polarization kit, consisting of a polarizer and an analyzer (rotatable by 90°), is supplied as standard with the Altami-MET P microscope and is a unique feature of this type of instrument [37].

A special cutout on the base is designed for installing the microscope on the surface of pipes with a diameter of 10 mm.

The microscope in the basic configuration is equipped with high-quality metallographic objectives with increased distance PL L 10X/0.25 and PL L 50X/0.70 (Fig. 2.2). It is possible to add objectives PL L 20X/0.40, PL L 100X/0.85 and eyepiece WF20X as an additional set, What will give opportunity get increase 2000 short.

a b c

Figure 2.2. Lenses For microscope Altami - MET1 [37]: a – objective lens manufactured by Biomed; planachromat, magnification 4x, numerical aperture 0.10, length of microscope tube, With which lens will work as usual, 160 mm, cover glass thickness 0.17 mm; b – objective lens manufactured by OptiTech; achromatic, magnification 60x, numerical aperture 0.85, length of microscope tube with which the objective lens will work normally, 160 mm, cover glass thickness 0.17 mm; in – objective lens manufactured by OptiTech; plan achromat, magnification 100x, numerical aperture 1.25, length of microscope tube, With which lens will work as usual, 160 mm, cover glass thickness 0.17 mm, oil immersion objective

Altami-MET1 microscope capabilities and characteristics: reflected light research methods: bright field; polarization. Magnification: 100X and 500X (up to 2000X).

Eyepieces: WF10X/18 mm; WF10X/18 mm with crosshair and scale

(100 divisions); WF20X/11 mm.

Objectives: plan achromatic objectives with increased working distance – PLL 10X/0.25 (working distance 11.0 mm); PLL 50X/0.70 (spring-loaded).

The microscope body is made of die-cast aluminum; painted with fireproof enamel; the base has a special cutout for installation on cylindrical surfaces.

Range focusing 25 mm.

Reflected light:

– lighting system with smooth brightness control ;

– source lighting - LED.

IN complete set are located Also polarizer And analyzer.

The kit requires a digital camera or camcorder to capture images of the research samples. A special optical adapter for the camera allows you to obtain excellent quality digital images that can be analyzed in the laboratory.

Additionally, the Altami MET P is supplied with a scanning stage [37], with which it is possible to take a series of photographs of the surface being examined without changing the position of the microscope itself. By controlling the coaxially located handles of the stage, it is possible to perform coordinate movement of the object being examined along the *X* and *Y axes with high accuracy* . This is especially important when working with high magnifications, when smooth movement of the object is required. Magnetic holders are built into the stage for fastening to magnetic materials.

1.9. Conducting measurements hardness

1.9.1. Measurement hardness By Rockwell

The Rockwell method is universal and is used for soft and hard materials [38–43]. In Rockwell hardness measuring devices, the indenter is a steel ball with a diameter of 1.588 mm or a diamond cone with an apex angle of 120 ° . The device has three scales – A, B and C. When measuring with a diamond cone, scales A and C are used and hardness is designated HRA, HRC respectively. At measurement steel with a ball use

scale B, and hardness is designated as HRB. Scale C measures high hardness, for example, of hardened products; scale B measures the hardness of steel after annealing, normalization, etc. Scale A is used to measure the hardness of thin products or thin layers, as well as very hard materials.

Шкала	Индентор	F_0,N	F_1,N	F,N	Шкала	Индентор	F_0,N	F_1,N	F,N	Шкала	Индентор	F_0,N	F_1,N	F,N
HRA	Конус алм	98,07	490,35	588,42	HRLW	Ø6,35тв	98,07	490,35	588,42	HRHS	Ø3,175ст	98,07	490,35	588,42
HRD	Конус алм	98,07	882,6	980,7	HRMW	Ø6,35тв	98,07	882,6	980,70	HRES	Ø3,175ст	98,07	882,6	980,70
HRC	Конус алм	98,07	1373	1471,07	HRPW	Ø6,35тв	98,07	1373	1471,07	HRKS	Ø3,175ст	98,07	1373	1471,07
HR15N	Конус алм	29,42	117,68	147,1	HR15XW	Ø6,35тв	29,42	117,68	147,10	HR15WS	Ø3,175ст	29,42	117,68	147,10
HR30N	Конус алм	29,42	264,8	294,22	HR30XW	Ø6,35тв	29,42	264,8	294,22	HR30WS	Ø3,175ст	29,42	264,8	294,22
HR45N	Конус алм	29,42	411,89	441,31	HR45XW	Ø6,35тв	29,42	411,89	441,31	HR45WS	Ø3,175ст	29,42	411,89	441,31
HRFW	Ø1,588тв	98,07	490,35	588,42	HRRW	Ø12,7тв	98,07	490,35	588,42	HRLS	Ø6,35ст	98,07	490,35	588,42
HRBW	Ø1,588тв	98,07	882,6	980,7	HRSW	Ø12,7тв	98,07	882,6	980,70	HRMS	Ø6,35ст	98,07	882,6	980,70
HRGW	Ø1,588тв	98,07	1373	1471,07	HRVW	Ø12,7тв	98,07	1373	1471,07	HRPS	Ø6,35ст	98,07	1373	1471,07
HR15TW	Ø1,588тв	29,42	117,68	147,1	HR15YW	Ø12,7тв	29,42	117,68	147,10	HR15XS	Ø6,35ст	29,42	117,68	147,10
HR30TW	Ø1,588тв	29,42	264,8	294,22	HR30YW	Ø12,7тв	29,42	264,8	294,22	HR30XS	Ø6,35ст	29,42	264,8	294,22
HR45TW	Ø1,588тв	29,42	411,89	441,31	HR45YW	Ø12,7тв	29,42	411,89	441,31	HR45XS	Ø6,35ст	29,42	411,89	441,31
HRHW	Ø3,175тв	98,07	490,35	588,42	HRFS	Ø1,588ст	98,07	490,35	588,42	HRRS	Ø12,7ст	98,07	490,35	588,42
HREW	Ø3,175тв	98,07	882,6	980,7	HRBS	Ø1,588ст	98,07	882,6	980,70	HRSS	Ø12,7ст	98,07	882,6	980,70
HRKW	Ø3,175тв	98,07	1373	1471,07	HRGS	Ø1,588ст	98,07	1373	1471,07	HRVS	Ø12,7ст	98,07	1373	1471,07
HR15WW	Ø3,175тв	29,42	117,68	147,1	HR15TS	Ø1,588ст	29,42	117,68	147,10	HR15YS	Ø12,7ст	29,42	117,68	147,10
HR30WW	Ø3,175тв	29,42	264,8	294,22	HR30TS	Ø1,588ст	29,42	264,8	294,22	HR30YS	Ø12,7ст	29,42	264,8	294,22
HR45WW	Ø3,175тв	29,42	411,89	441,31	HR45TS	Ø1,588ст	29,42	411,89	441,31	HR45YS	Ø12,7ст	29,42	411,89	441,31

Figure 2.3. Scales For measurements hardness By Rockwell [41, 42]

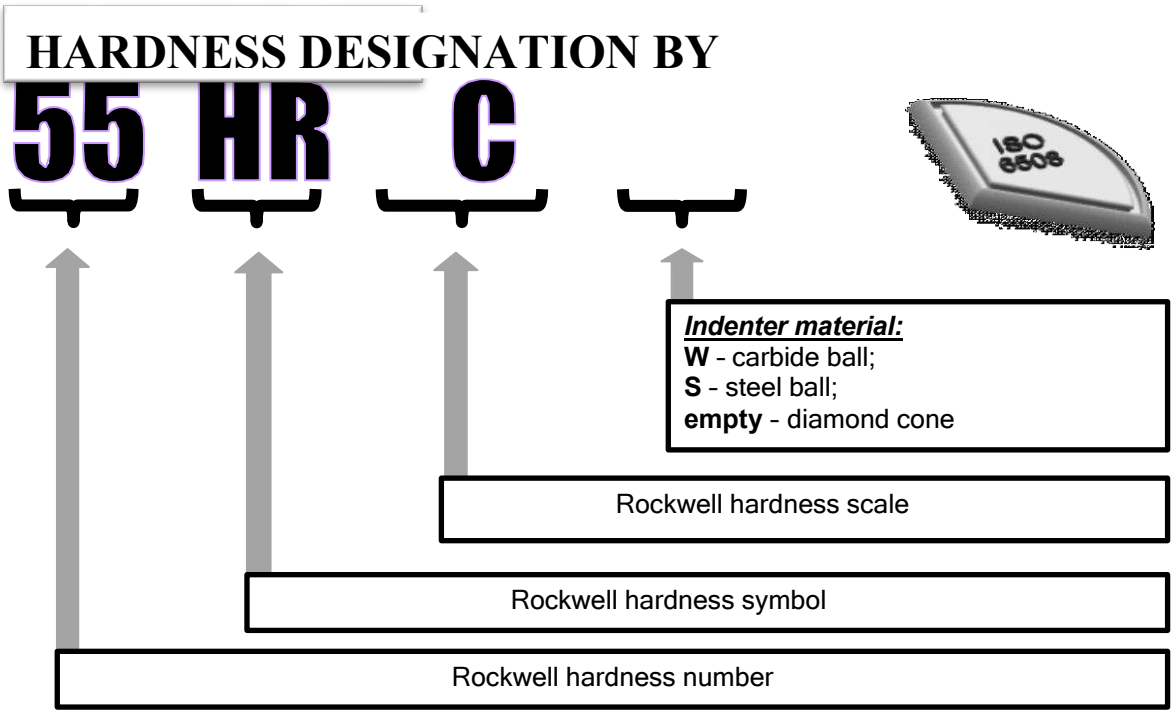

Figure 2.4. Designation hardness By Rockwell [42]

1.9.2. Measurement hardness By Vickers

The Vickers hardness test method involves pressing a tetrahedral pyramid with a square base into the surface of a sample (product) [44–47]. The load *P* during testing can be equal to 5, 10, 20, 30, 50, 100 kg. After removing the load, both diagonals of the imprint are measured (Fig. 2.7–2.9).

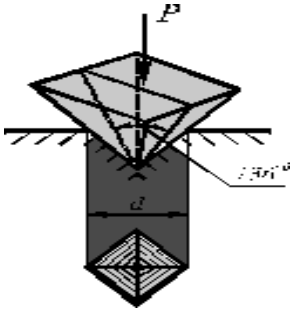

Figure 2.5. Scheme definitions Vickers hardness test [43, 44]

Vickers hardness (F ≥ 49,03 N)		Vickers hardness at low loads (1,961 N ≤ F < 49,03 N)		Vickers microhardness (0,098 N ≤ F < 1,961 N)	
A symbol of hardness	Significance F, N	A symbol of hardness	Significance F, N	A symbol of hardness	Significance F, N
HV 5	49,03	HV 0,2	1,961	HV 0,01	0,09807
HV 10	98,07	HV 0,3	2,942	HV 0,015	0,147
HV 20	196,1	HV 0,5	4,903	HV 0,02	0,1961
HV 30	294,2	HV 1	9,807	HV 0,025	0,2452
HV 50	490,3	HV 2	19,61	HV 0,05	0,4903
HV 100	980,7	HV 3	29,42	HV 0,1	0,9807

Figure 2.6. Scales measurements hardness By Vickers [42, 45, 46]

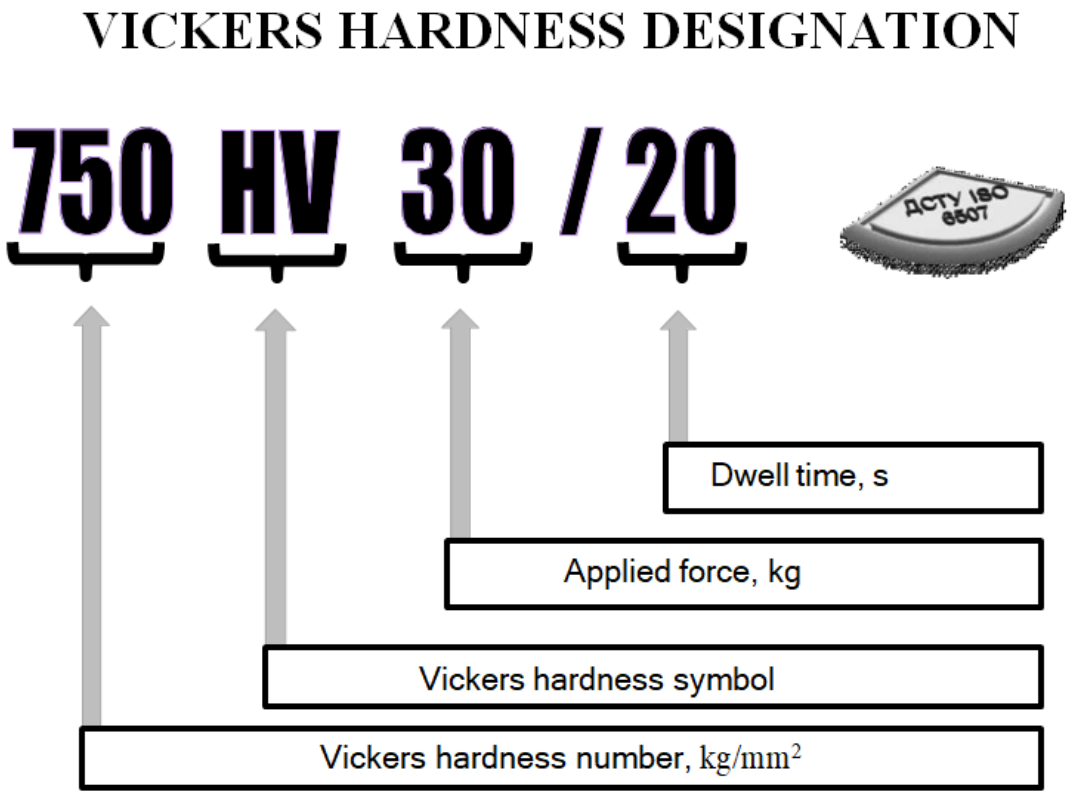

Figure 2.7. Designation hardness By Vickers [42]

Hardness is defined as the ratio of the load to the area of the lateral surface of the imprint. Vickers hardness has the dimension of stress (kg/mm2 or MPa). Using a diamond pyramid allows you to expand the range of hardness measurements to 1000 units, which corresponds to very hard materials.

1.10. Methods tests materials on friction and wear

Testing materials and technologies in real production conditions involves significant expenditure of material resources and time. In addition, it is difficult to fully assess the impact of certain factors on processes friction and wear in real conditions. Therefore, to assess the effectiveness of the use of materials, methods of their processing, design changes to parts and other measures, laboratory and bench tests were carried out, simulating the maximum approximation to real operating conditions.

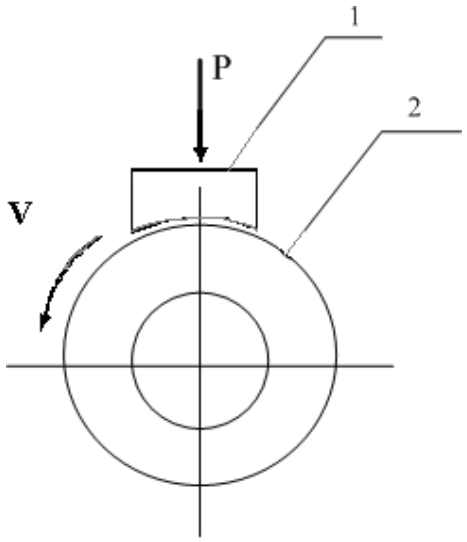

Figure 2.8. Scheme tests on car friction SMC-2 [49]:
1 - fixed sample (block); 2 - mobile sample (video clip)

The main criteria for assessing the performance of materials for details volumetric hydraulic drive And efficiency their surface treatment are tribological characteristics.

In this regard, to carry out this work, test methods were selected that allow modeling the main processes of friction and wear of real parts [48–50].

The tests were carried out on a friction machine SMC-2, which allows for a comparison of the test materials in terms of wear resistance, antifriction properties and properties during the running-in process using the "roller-block" scheme (Fig. 2.8).

Pair friction consists of from rotating roller diameter

50 mm, to the cylindrical surface of which a fixed shoe is ground in a special mandrel. The shoe is part of a ring, the inner surface of which (the working surface) is made strictly along the radius of the roller. The contact of the counterbodies made of cast iron SCh20 during operation is carried out on a surface area of about 2 cm ^{2} to ensure the stability of the shoe during testing. Lubrication was carried out with industrial oil of the I20A brand with the addition of 0.1 % of abrasive particles with a dispersion of up to

5 μm. The rollers were made from the materials under study and after various processing modes.

The sliding time was 5 hours. The wear of the samples was determined by the loss of mass during the test by weighing on an analytical

balance with an accuracy of 10^{-4} g. Weighing was carried out before and after the test. Before weighing, the samples were carefully degreased in gasoline and dried for 15 minutes. For each material variant, at least 3 tests were carried out, based on which the average results for the wear of the counterbodies were calculated. In this case, it is important to know the load capacity, above which, for these materials and operating conditions, critical loads cannot be exceeded, leading to scoring of the counterbodies. Based on the experimental data obtained from comparative wear tests of the specified steel grades, carried out under strictly identical conditions, one can judge their ability to resist wear under the influence of mechanical load [50–52].

Tests to determine friction moments were carried out on the SMT-1 friction machine [49, 53–55]. A roller and block (Fig. 2.9).

The rotation speed was set to 500 rpm and the samples were loaded by 0.2 kN at each step, holding for 75 s at each subsequent loading. After unloading to 0.2 kN, they were held for 15 minutes until the friction torque stabilized. Then they were loaded stepwise until scoring began. The friction torque was recorded on the chart tape of the KSP-4 self-recording potentiometer.

Figure 2.9. External appearance of the friction machine [49] : 1 - mechanism loading; 2 - subject sample

Coefficient friction f calculated By formula [51–53]

$$f = M_{\text{tr}} / (d / 2) \cdot P, \qquad (2.1)$$

Where M_{tr} - friction moment ;

d - diameter movable sample;

R - size loads.

The onset of scoring was determined by a sharp increase in the torque and coefficient of friction and the appearance of scoring on the working surface [52, 54–57]. The measurement error of the friction torque and coefficient friction composed 9 % at R = 0.2 K N to 2 % at P = 1.0 K N.

1.11. Methodology laser thermal processing

Laser heat hardening (hardening) is used to increase the service life of parts that are subject to wear during operation. The essence of the laser hardening process is that a local area of the surface of a massive part is heated using radiation to supercritical temperatures. Heating of the metal is carried out by transferring the energy of laser radiation deep into the material, due to its thermal conductivity. After the radiation ceases to act, this area cools due to the heat being removed into the inner layers of the metal. The high cooling rate leads to the formation of hardening structures in the alloys and to high surface hardness. The depth of hardening depends on the power density of the heat source, the duration of its action, and the thermophysical characteristics of the material [58]. The necessary increase metal temperatures can also be achieved using standard methods – heating in a thermal or induction furnace. However, these methods are often unsuitable due to the non-uniformity of heating. Laser processing satisfies increased requirements for quality, precision, and processing speed in the manufacture of products in conditions of fierce competition in the manufacturers' market [59–61].

In addition, in large-sized parts it is very often necessary to harden only part of the surface, and not the entire volume of the part. Surface treatment of the part can only be done by laser heat treatment, which can be carried out with or without melting the surface layer [62]. Most often, processing without melting is used, while maintaining the original roughness R_a = 0.16–1.25 μm. The depth of the hardened metal layer is determined by the value of the permissible linear wear. Productivity laser strengthening is determined by formula

$$G = \mathrm{Kp}\, V\, \mathrm{d}_0, \quad (2.2)$$

Where Kp - coefficient ceilings;

V - speed movements beam (details);

d_0 - diameter beam (width paths hardening), d_0 = 1–1.5 mm and more [62].

Processing with overlapping and non-overlapping tracks is possible. When a hardening track is applied, partial heating of the previous hardened zone occurs, which can lead to tempering and a decrease in hardness. When processing with non-overlapping tracks, the gap between them is 10–30% of the area of the surface being processed, and wear is reduced by 2–3 times. Laser hardening is used to process engine crankshafts, cylinder liners, gear

wheels, and parts of chemical, oil, and drilling equipment [63, 64].

The laser installation (Fig. 2.10), intended for surface hardening of metal, contains as its main elements a laser with a power supply, an optical system for transporting and focusing the laser beam, a system for positioning the workpiece, a system for controlling and monitoring the processing parameters. Lasers can be electric-discharge CO_2 lasers and solid-state Nd lasers. Electric-discharge CO_2 lasers have a longer wavelength (10.6 μm), electric-discharge excitation, pumping of a gas mixture (CO_2, N_2, He) along a closed circuit, and are used for continuous processing. Their power is 1–25 kW. Solid-state Nd lasers operate from an active element in the form of a rod or plates V intermittent And continuous modes. These lasers have a power of up to 200 W and up to 3 kW, a wavelength of less than 10.6 μm and, therefore, higher absorption in metal. For surface hardening of metal, solid-state Nd lasers are preferable [65].

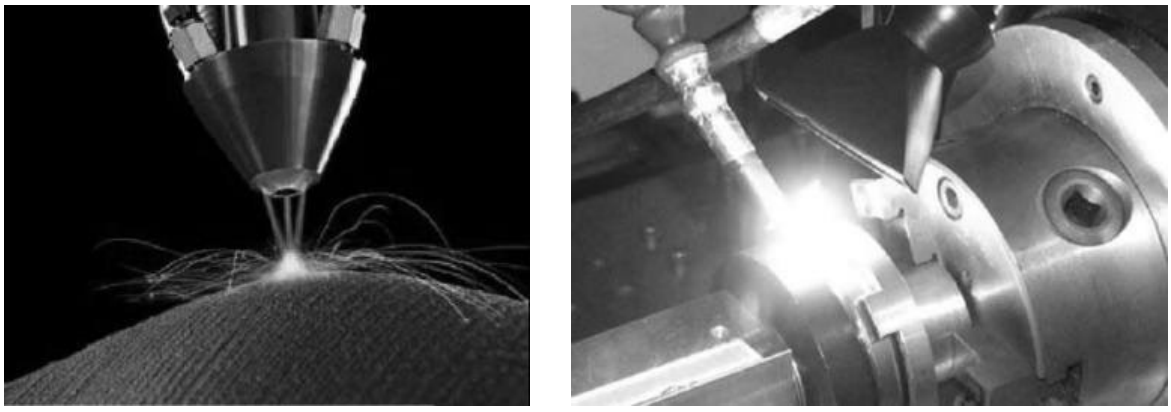

Figure 2.10. Laser strengthening [63]

The use of solid-state systems for metal processing has a number of advantages, including laser heat treatment [63]:

– small dimensions and weight parameters make it possible to use smaller production areas, as well as robotic systems for equipment placement;

– radiation can be transmitted using light guide systems, which allows laser processing in hard-to-reach areas and over long distances (20–100 m);

– long service life with stable parameters of the active environment;

– ease of maintenance and preventive maintenance of solid-state laser systems, as well as replacement of their components;

– it is possible to regulate the pulse energy, repetition rate, their

shape and duration over a wide range;

– use automated coordinate tables of various sizes with a computer control system that allows for precise positioning of parts during laser processing;

– smooth vertical movement of the laser emitter relative to the part expands the tool area processing and efficiency of technological restructuring for new products;

– control of the beam trajectory using a computer. The processing trajectory can be set in a special program for controlling the coordinate table, or drawings created in various design packages can be converted into it;

– the presence of a video surveillance system, a high degree of laser safety when delivering radiation over a distance of several meters.

The HTS-300P unit was used, V in which the laser emitter moves relative to the stationary workpiece placed on the lifting table. This allows processing of heavy, large-sized parts and blanks. The emitter can be turned in the horizontal plane to work with the selected workstation. Monitoring the process processing And control Maybe be carried out operator both with the help of a binocular microscope integrated with the optical system of the laser, and through a video camera with display on the monitor of the control computer. The operator's eyes are protected from the effects of laser radiation and glow in two stages, using a cut-off filter and a liquid crystal shutter operating synchronously with the laser emitter.

Technical characteristics installations models HTS-300P [63, 65]:

Laser

Maximum energy impulse radiation	60 J
Duration impulse radiation	0.2–20 ms
Frequency repetitions impulses radiation	up to 100 Hz
Maximum average power radiation	300 Tue
Maximum peak power radiation	10 kW
Focused beam diameter	0.3–2

mm Optical system

Increase optical systems	15 x
Linear field vision	10 mm
Suppression laser radiation V visual channel	from above 10

7

Positioning system Movement

emitter By axes “z”	
Moving manual coordinate table By axes “z”	

Moving lens By axes “z”	±10 mm
Maximum size of laser processing zone using automated two-coordinate table	1300 × 550 mm
Positioning accuracy of an automated two-coordinate table	±20 microns
Maximum speed of movement of the automated two-coordinate table	40 mm/s

The depth of the hardened zone on metal samples after laser heat treatment without surface melting usually does not exceed 0.2 mm, but this is quite sufficient to increase the durability of products by more than 2.5 times.

Power radiation laser - 0.30 kW, step processing - 2.5 mm, width paths - 2.0 mm. Original roughness surfaces – R_a 0.32–0.8, after LTO the roughness of the hardened surfaces was obtained R_z 10. Reinforced surfaces polished to

achieving a roughness parameter of $Ra_{0.4}$. The depth of the hardened layer is 0.45–0.55 mm, hardness is HV 572–681 (HRC ~ 53–59).

1.12. Technology application vacuum plasma carbonitride coating

When applying a coating using the vacuum plasma method, a source of a substance is used, large particles of which are heated and accelerated to high energy and are embedded or adhered t o the treated surface, forming a layer of the applied substance on it.

A characteristic feature of vacuum ion-plasma methods is the direct conversion of electrical energy into the energy of technological action. It is based on structural-phase transformations in the condensate deposited on the surface or in the surface layer of the part itself, placed in a vacuum chamber [66, 67] . The main advantage of these methods is the possibility of creating a very high level of physical and mechanical properties of materials in thin surface layers, applying dense coatings of refractory chemical compounds, as well as diamond-like ones, which cannot be obtained by traditional methods. In addition, these methods allow:

- provide high adhesion coatings To substrate;
- receive uniform coatings By thickness on big areas;
- vary the composition of the coating over a wide range within one technological cycle;
- get high cleanliness surfaces coatings;
- ensure the environmental friendliness of the production cycle.

Modern vacuum ion-plasma methods hardening of the surfaces of parts include the following stages: generation of a corpuscular flow of

matter; activation, acceleration and focusing; condensation and introduction into the surface of parts (substrates). Generation: of a corpuscular flow of matter is possible his evaporation (sublimation) And spraying. Choice the heating method and the design of the installation depend on the nature of the evaporated material, its initial form (granules, powder, wire), the required evaporation rate, and constancy over time etc. The most widely used heating method is electron bombardment, which allows reaching temperatures of 4000 °C and energy densities in the beam of up to 5×10^{8} W/cm^{2} [66, 68] .

Application plasma coatings carried out on installation "Bulat". The carbonitride coating was applied at a discharge current of 200 A, degrees vacuuming $2–3\cdot10^{-5}$ mm Hg Thickness The coating thickness was 20 μm, the hardness was 15–18 GPa [68–86].

1.13. Methodology detonation spraying

Detonation coatings, being a type of gas-thermal coatings, due to their highest characteristics,
are increasingly used in various industries. Due to its highest characteristics (adhesion strength to the substrate up to 250–280 MPa), detonation spraying can be preferable for strengthening and restoring the most critical and loaded parts and units.

It has been established that coatings based on tungsten carbide from powders obtained by the spheroidization method have the highest adhesion strength to the substrate and high hardness. This is explained by the fact that the dissolution of WC in Co (Ni) partially occurs already during the production of the powder. During spraying, this process continues, as a result of which the solid solution has the maximum degree of saturation [88].

In addition to the dissolution of tungsten carbide in cobalt, during spraying under the influence of an oxidizing environment, a process of monocarbide decomposition occurs, which has a negative effect on the quality of the sprayed coating. In addition, brittle double carbides Co_3W_3C are formed, which also worsen the properties sprayed layer. In powders obtained by spheroidization, the carbide component is better protected. Process modes spraying Also provide essential influence on

structural and phase composition of coatings and, consequently, their properties. The structure of the coating is most strongly influenced by [87–89]:

– compound working mixtures gases;
– place input powder V trunk;
– degree fillings trunk working mixture.

The adhesion strength to the substrate of combined coatings with a VK-25 sublayer reaches 200–250 MPa, and the Rockwell hardness is up to 70 units.

A distinctive feature of detonation spraying is the cyclic nature of the powder feed to the surface of the workpiece at a speed exceeding the speed of sound. The cyclic spraying process is achieved using detonation units, the basic diagram of which is shown in Fig. 2.12 [88].

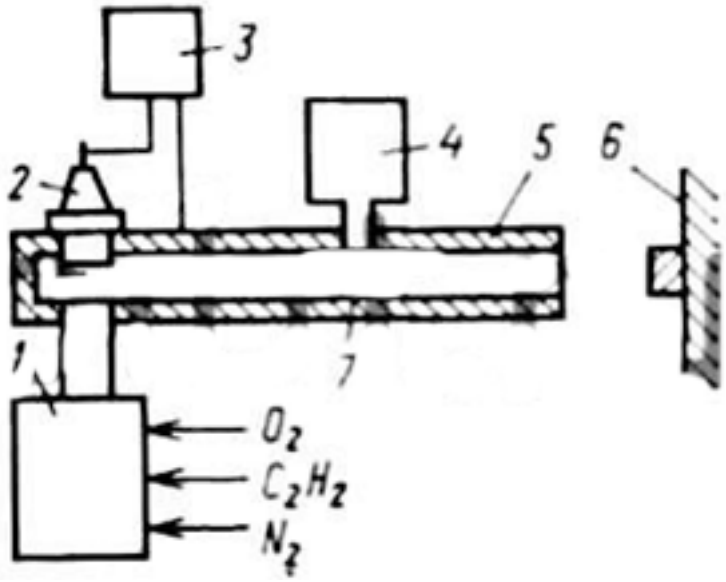

Figure 2.12. Scheme detonation devices [88]

In general, detonation installations consist of a block 4 for feeding spraying powder, including a powder feeder and a dosing device; a block 1, used to form the required gas mixtures and fill the barrel of the detonation installation with them at a given speed; an ignition block 3 and an igniter 2, designed to initiate the explosion of the working mixture; a barrel 5, representing pipe diameter 20-50 mm, 1–2.5 m long and designed to direct the propagation of a blast wave towards the open end of the barrel.

The operating principle of the installation is as follows. From block

1, the gas mixture is fed into barrel 5. At the same time, from the powder feeder through the dosing device (block 4) at specified finely dispersed powder is blown into the gas mixture in portions using gas - nitrogen or air - immediately before its ignition, then the gas mixture is ignited using igniter 2. As a result of ignition and movement of the combustible mixture along the channel, it explodes with the release of a significant amount of heat and the formation of a detonation wave, which accelerates and transfers sprayed particles 7 through the barrel to the surface of the part 6 at a speed determined by the geometry of the barrel and the composition of the gas.

The process of forming coatings by detonation spraying is complex and has not been sufficiently studied. In many ways, it is similar to the plasma spraying process [89, 90]. The similarity lies in the fact that the adhesion of particles to the substrate and to each other can occur in molten, melted, and solid states. The strength of the adhesion is ensured mainly by spraying with molten and melted particles, which spread and crystallize on the surface of the substrate due to chemical interaction. At the same time, the detonation spraying process, unlike the continuous plasma process, is cyclical, imparting higher speeds to the powder particles, which determines the features of the coating formation mechanism.

In detonation spraying, the particle velocity, in contrast to plasma spraying (100–200 m/s), reaches 400–1000 m/s. Therefore, in addition to thermal activation, plastic deformation in the collision zone of particles and the substrate has a significant effect on the mechanism and kinetics of the formation of sprayed layers. However, thermal activation makes the main contribution to the formation of coatings during spraying. Experience in using various spraying methods, including detonation, proves that to obtain satisfactory adhesion of powder particles to the base, it is necessary that a significant portion of them be transported to the substrate in a molten or melted state. The experimental studies on the process of coating formation by detonation spraying presented in [90, 91] they show, What state particles, located V two-phase flow, non-uniformly. At the beginning and middle of the flow they are in a molten or melted state, and the temperature in contact with the substrate reaches their melting temperature. At the same time, due to the heat released when particles with a speed of ~400 m/s hit the substrate, the temperature in the contact zone increases by approximately 100 °C.

When spraying with powder materials with a melting point exceeding the melting point of the base metal, the latter is melted. When

applying coatings with powder hard alloys of the VK type to corrosion-resistant steels, the latter are melted and mixed with the sprayed molten powder particles, thereby increasing the adhesion strength. As with other methods of gas-thermal spraying, preliminary shot-blasting of the sprayed surface contributes to an increase in adhesion [91, 92]. In this case, it is possible to obtain strong bonds between the sprayed material and the substrate with a hardness higher than HRC 60. When spraying the first layer, pores may appear. When spraying the second layer, the powder particles deform and compact the crystallizing first layer, which helps to eliminate or reduce porosity. This phenomenon is characteristic of detonation spraying, and the authors of the work [91] called it the effect of hot impact pressing.

Larger particles from the end (tail) of a less concentrated flow have a lower speed and are applied to the substrate surface most often in an unmelted form. When forming a coating, such particles play a dual role: a useful one - they remove defective areas of the previously applied coating, increasing its density and physical and mechanical properties; a harmful one - with a significant increase in the kinetic energy of large particles. particles V coating may appear cracks And even its complete detachment. These phenomena can be regulated by changing the rate of fire of the installation and granulation of the sprayed powder. From the point of view of the materials and equipment used, the process of detonation spraying is very simple. The main factors determining the nature of detonation spraying are the gas mixture, powders, and the barrel of the installation [93–94].

However, the use of these factors in the spraying process is associated with changing and controlling a number of parameters characteristic of each of them. For a gas mixture, this is the composition of the gas mixture; the dose of the gas mixture per shot; the composition of the gas mixture in the barrel between shots [95–97]. For powder, this is the chemical composition of the powder; granulation of the sprayed powder; the location of the powder in the barrel at the moment of ignition of the mixture; distribution

particles by size. The barrel is characterized by geometric parameters: diameter and length.

In turn, the listed parameters give rise to others that characterize the final state of the process: concentration, temperature and speed of particles; chemical composition of the medium; temperature of the

substrate surface.

Thus, the technological process of detonation spraying is complex, and the quality of the coating formation depends on a set of numerous parameters, maintaining them within optimal limits. Detonation spraying of the powder of the VK 25 hard alloy was carried out on cleaned surfaces without preliminary treatment [99]. Powder with a grain size of 20–100 μm was used; it was melted in an oxygen-acetylene flame and transferred to the surface of the part by a gas flow . The ratio of the oxygen content to the acetylene content was 1.2; the powder loading depth was 300 mm, spraying distance 150 mm, powder charge 200 g, barrel length 1.6 m, barrel diameter 16 mm. The powder used VK 25 is tungsten carbide-cobalt (WC-Co), containing up to 25% cobalt, and is used for work in conditions of fretting corrosion, abrasive wear at normal and elevated (up to 650 °C) temperatures.

1.14. Technology electric spark alloying

The essence of the process of electric spark alloying (ESA) is the transfer of material that meets certain requirements to the surface of the part being treated by an electric spark. discharge. This way provides durable adhesion of the introduced alloying material to the surface of the part; it is easy to implement [100–102].

In electric spark alloying, air or a non-oxidizing gas environment (argon, helium, hydrogen) is used as the working medium. If a pulsed voltage is applied to the electrodes, one of which is the alloyed part (cathode), and the other is the alloying metal (anode), and the electrodes are brought together until a spark discharge occurs, then a high-density pulsed current will flow between the anode and cathode. As a result, at the point of the spark discharge on the surface of the electrodes (mainly on the anode), the metal heats up and partially evaporates. Drops of molten metal from the anode rush to the surface of the cathode under the action of an electromagnetic field. After the end of the current pulse, the movement does not stop and the drops of metal reach the surface of the cathode. Having reached the surface of the cathode, the molten particles anode are introduced into the molten dimple on the surface of the cathode and mixed with the cathode metal, and are partially deposited on the edge of the dimple and welded to it. If you move the anode along some line, you will get a series of dimples with a changed metal composition, i.e. with a new

alloy and a new structure. In order to obtain a relatively smooth hardened surface, the anode must be moved relative to the cathode during the pause between pulses, which is 0.01 s in duration, by no more than 1/4 of the dimple diameter. In this case, the necessary mixing and mutual penetration of the molten metal of both electrodes into each other occurs and the quality of the treated surface improves.

In addition to the purely mechanical mixing of the molten metal particles of both electrodes under the action of high temperatures and pressures developing in the discharge channel, diffusion processes also occur in the surface layers of the electrodes. The alloying process occurs in a gaseous medium, so the molten particles interact with this medium on their way and form a strengthening layer, which differs in its physicochemical properties from the properties of the alloying and alloyed metals [103].

A very valuable property of spark alloying is that it provides a very strong bond hardened layers With alloyed metal. Conducted Studies of hardened parts under alternating loads and temperatures show that the hardened layer does not peel off even when coated with carbide materials (e.g. tungsten carbide or metal-ceramic alloys) due to the formation of a diffusion bond between the hardened layer and the alloyed metal. Various carbide and boride compounds of refractory metals are used as alloying materials, less often tungsten, molybdenum, rhenium and chromium. If it is necessary to apply an antifriction layer to a part or elements of a part, the following are used: tin, lead, bismuth, indium, graphite. These materials are easily oxidized, and therefore alloying is carried out in neutral gases.

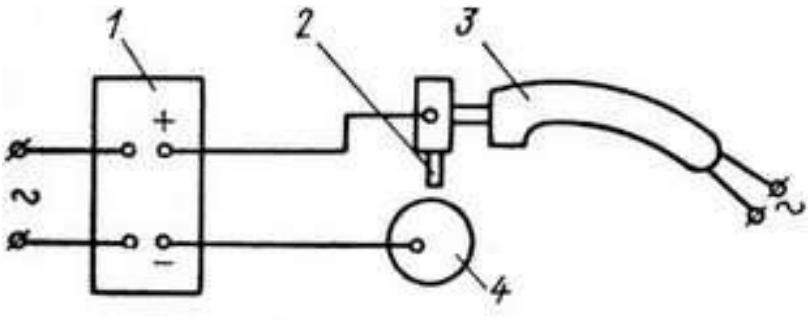

Figure 2.13. Scheme electric spark alloying [103]:
generator impulses 1, electromagnetic vibrator 3, alloying electrode 2
and alloyed electrode 4

Saturation of surface layers during spark alloying with carbide-forming elements (chromium, molybdenum, tungsten) prevents gas

saturation of the metal. Spark alloying increases roughness hardened surface up to R_a 2.7–3.2 [102].

Electric spark alloying was performed on an EFI-46 installation using tungsten and chromium electrodes at a short-circuit current of 3.8–4.0 A and a number of discharges per 1 cm2 of 320–340.

1.15. Methodology galvanic chromium plating

Chrome plating is one of the most common types of galvanic coatings. In technology, chrome plating of products is used For protection from corrosion, wear and tear, sticking onsurface of contacting materials. Depending on the technology and application modes, chrome coatings reach microhardness of up to 950–1100 HV. High hardness and wear resistance, low friction coefficient, high heat resistance and good chemical resistance provide chrome-coated parts with a long service life under any operating conditions [104, 105].

"Hard chrome" coatings are obtained at low temperatures (up to 40 °C) and high current density, they are grey in colour and are characterized by high hardness and brittleness. The quality of the resulting chrome coatings depends on the ratio of chromic anhydride and sulfuric acid. Its value should be 100:1. A decrease in the ratio (50:1) leads to a deterioration in the scattering and covering ability. To ensure good adhesion strength, the parts are kept in a bath without current so that they take on the temperature of the electrolyte and at the initial moment of chroming they give a "current boost" for 0.5-1.0 min, increasing current density 2–3 times compared to the operating one, and then gradually reducing it to the normal value [105].

In chromium plating, anodes made of pure lead or lead alloy with 4-6% antimony were used. Anodes are made of rods with a diameter of 10-15 mm or sheets. The ratio between the surface of the anodes and cathodes should be within the range of 1:2 to 2:3. Lead anodes are covered with a layer of lead chromate during operation, which makes work difficult. Therefore, it is recommended to clean them daily with steel brushes. In between work, the anodes are removed from the bath and immersed in water.

Figure 2.14. Modern galvanic bath [106]

The thickness of the chrome coating can reach 3–500 μm. The wear resistance of the coating is determined by the counterbody, operating conditions And mechanical loads. There is a dependence of wear resistance on the microhardness of the coating, with maximum wear resistance achieved at a microhardness of 8500–
9000 MPa. At lower microhardness, rapid abrasion of the chromium coating occurs, and at higher microhardness, its particles are chipped off, which then work as an abrasive in combination with the counterbody. Parts subjected to wear-resistant chromium plating usually have rigid dimensions, therefore, at a coating thickness of more than 15–20 μm, it is necessary to provide for an allowance for additional mechanical processing to fine-tune the dimensions, and also to use additional anodes, protective screens, and special suspensions. In addition, parts operating under significant mechanical loads must be tempered at a temperature of 180–200 °C for 2 hours to dehydrate them [106].

Wear-resistant chromium plating was carried out at a current density of 70-980 A/dm2 ^{with} a voltage of up to 8–10 V. Electrolyte temperature 55–62 °C. Chrome plating was performed directly on base metal in a standard electrolyte [106, 107]. The resulting coating has thickness from 30 up to 160 microns (V dependencies from details), and a hardness of about *HV* 900.

1.16. Technology ion-plasma application coatings

The ion-plasma method was used. It is based on the physical processes of evaporation or spraying of materials in a vacuum with subsequent condensation of the products on the required surface [108].

This method has near advantages [109, 110]:

– opportunity receipt coatings at temperature substrates 80–100 °C;

– simple technology for producing intermetallic compounds, as well as nitrides and carbides;

– thickness coatings Maybe vary from 0.01 to 20 microns;

– uniform application to parts of complex geometric shapes;

– coating Not needs V finish processing.

Coverings, received by method ion-plasma spraying, can be used to reduce various types of wear, reduce or increase the coefficient of friction, improve anti-seize properties and eliminate seizure, including when operating in conditions of elevated temperatures, vacuum, special environments, etc. [108, 111].

When a vacuum arc is ignited, first the following appear on the end surface of the cathode: rapidly moving cathode spots of the first type, which after a time of about 1–0.5 ms transform into slowly moving cathode spots of the second type. The cathode material, consisting of ionic, vapor and microdroplet phases, erodes from the cathode spots of the second type. The erosion products fly apart almost isotropically over the cathode surface, and due to the movement of the cathode spot and the presence of up to 10 cathode spots simultaneously on the surface, these erosion products form a plasma jet moving away from the cathode surface. The system of magnetic and electric fields additionally processes the erosion products, increasing the proportion of the ionic phase and the kinetic energy of ions, and collimates the plasma jet. At the generator output, the composition of the plasma jet is estimated at the following values: proportion of the ionic phase – 30–95 %, steam phases - 5–65 %, microdroplet phases - 20–0.5 %.

Kinetic energy ions reaches hundreds electron-volt [112, 113].

The plasma jet, leaving the generator nozzle in free-molecular mode, passes through a vacuum chamber, interacts with condensation surfaces and forms a coating. On the detail A negative voltage is supplied through technological devices, which is called the reference voltage in the

sputtering mode and high voltage in the ion surface cleaning mode. Plasma ions accelerate in the Debye layer near the surface under the action of the bias voltage, are usually neutralized and, hitting the surface, transfer their kinetic energy to the surface near the point of impact. Depending on the absolute value of the kinetic energy of the ions, various processes occur on the surface. At energies greater than 10 eV, the processes of ion etching of the surface begin, at energies exceeding the critical energy of implantation, ions begin to penetrate into the crystal lattice, at energies above the energy of displacement of the atoms of the crystal lattice in the solid, displacement cascades occur, characteristic of ion implantation. In this case, the following processes actively occur: formation of active centers of coating growth. Reactive gases are used to obtain compounds. The quality of the coating is determined by the quality of the ion cleaning process of the part and depends on the technological parameters of the arc current, bias potential, gas pressure, temperature of the part and largely depends on the design of the plasma generator, the features of the part and technological equipment, as well as the chemical purity of the materials used.

High-quality coatings from pure metals can be obtained at temperatures of at least 80–100 °C. The initial technological materials for vacuum ion-plasma spraying are cathodes made of sprayed metals, in this case chromium (VKh-1).

The Bulat vacuum ion-plasma spraying unit (see 2.6) (Fig. 2.15) [73] ωασ υσεδ . It consists of a chamber, a vacuum pumping system, evaporators, a rotary device, a water system and a stand.

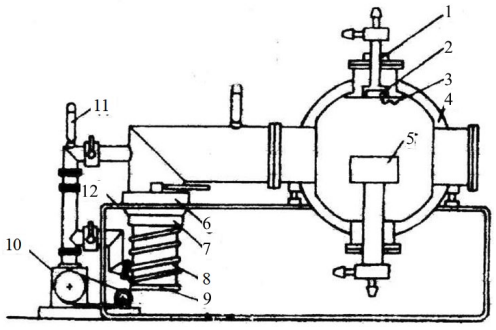

Figure 2.15. General scheme installations "Bulat" [69] :
1 – focusing coil; 2 – cathode; 3 – ignition electrode; 4 - anode chamber; 5 - substrate; 6 - nitric trap; 7 – water trap; 8 – high vacuum unit; 9 – heater; 10 – forming vacuum pump; 11 – monometer lamp; 12 – water cooling system of the unit

The chamber is a cylindrical vessel in which the spraying process

takes place. On the chamber and covers there are six pipes with flanges to which are attached: a viewing window; a rotary device; evaporators and an adapter to the vacuum pumping system.

On the side surface of the chamber there is a nozzle for inlet of working gas and a bracket for fastening the leak to the body of the chamber. Copper tubes through which water flows (hot in the heating mode and cold in the operating mode) are soldered to the covers. The chamber is connected with a high- vacuum unit by an adapter.

All detachable connections on the chamber are sealed with vacuum rubber seals.

The evaporator is designed to create a plasma flow from the cathode material. Cathodes are made of materials that can be restored, and are often cylindrical in shape [69] .

The evaporator works as follows. Upon reaching the chamber necessary worker vacuum on coil arsonist devices is served pulse current. Core with a rod is drawn into the coil and moves the ignition electrode, which closes the gap between the cathode and the ignition device, electrically connected through a limiting resistance to the anode (chamber). At the end of the pulse, the coil of the ignition device is de-energized and the core with the rod returns to its original position, the ignition electrode moves away from the cathode and the electrical circuit between cathode And anode interrupted, exciting a microarc. In this case, an arc discharge occurs between the cathode and the anode. If the arc discharge does not occur, the evaporator control system sends a new current pulse to the coil. After the arc discharge occurs, the supply of current pulses to the coil is automatically stopped.

Cathode spots moving along circular trajectories on the evaporating end of the cathode are the sources of plasma jets. By changing the magnitude of the magnetic field of the coil (changing the strength of the current flowing through the cathode) through the coil), are installing such average radius trajectories of cathode spots to ensure uniform evaporation of the material at the end of the cathode.

When the electromagnetic field is insufficient, the evaporation of the cathode occurs mainly in the center; when the field is large, it occurs at the periphery of the end face.

The high-vacuum unit is designed to pump out gases and create the necessary vacuum in the chamber. It is assembled on the basis of a steam-oil diffusion pump.

The pump operating principle is based on the diffusion of the pumped gases into the working fluid vapor stream due to the difference in partial pressures of the gases in the working fluid vapor stream flowing out of the pump nozzle and in the pumped volume. The gas released from the cooled oil vapor is pumped out by a mechanical forevacuum pump through the outlet branch pipe of the diffusion pump.

The high-vacuum unit is cooled continuously, both in warm-up mode and in operating mode.

Line forevacuum represents by yourself pipeline, connecting the mechanical forevacuum pump with the chamber and with the high-vacuum unit.

The forevacuum line is equipped with electromagnetic valves, throttle valves, a measuring block and a bellows compensator.

The water cooling system provides cooling and heating of all units. Works only with free water drainage.

The electrical equipment of the Bulat unit provides electrical power supply and stabilization of the electric arc discharge; stabilization of the cathode spot of the electric arc on the working surface of the cathode; automatic ignition of the arc when it spontaneously goes out; operation of the unit in the heating, cleaning and condensation modes; control of the necessary parameters of the technological process (arc current, pressure value in the working volume); power supply and control of vacuum equipment [70, 71].

The control of the unit includes the necessary interlocks, signaling and protection of electrical circuits.

According to the technological process, the operation of the electrical equipment of the unit can be divided into three modes:

– warming up;
– cleaning;
– spraying

The required value in the working chamber in all modes is provided by the vacuum system of the unit.

The heating mode of the Bulat unit is designed to prevent condensation and remove water vapor from the surface of the chamber walls, as well as their degassing during the pumping process.

Heating is carried out by hot water circulating through pipes welded to the walls of the chamber. The water, passing through the branches of the

short-circuited winding of the transformer, is heated to a temperature of 80 °C and enters the chamber heating system [69, 72].

The cleaning mode is designed to clean the substrate from contaminants. The cleaning process is carried out by ion etching the surface of the products before spraying, for which a high negative potential is applied to the sprayed product. The cathode metal ions formed as a result of the electric arc discharge, are accelerated under the action of high-voltage potential to an energy sufficient to knock out the atoms of the surface layer from the surface of the sprayed product. In this way, the surface of the sprayed product is cleaned.

IN mode cleaning scheme provides excitation And stable burning of the electric arc between the cathode and the anode, stabilization of the cathode spot on the working surface of the cathode, and the presence of a high negative potential on the substrate. Excitation of the electric arc discharge between the cathode and the anode and control of the movement of the cathode spots on the working (evaporated) surfaces of the cathodes is provided by the evaporator control units; power supply of the electric arc discharges - blocks nutrition; high voltage potential - high voltage rectifier. Control regime Cleaning is carried out from the control unit.

During the cleaning process, using the rotation mechanism, it is necessary to rotate the products to ensure uniform cleaning of the entire surface [73].

The spraying mode is intended for applying a hardening coating to the workpiece. In the spraying mode, condensation of the evaporated cathode material occurs on the substrate, which leads to the formation of the corresponding coating on the workpiece surface.

In the spraying mode, the circuit ensures: excitation and stable burning of an electric arc between the cathode and the anode; stabilization of the cathode spot by the electric arc on the working surface of the cathode; high physical and mechanical properties of the coating on the workpiece; uniformity of the coating over the entire surface of the workpiece; cooling of the working chamber [69, 74–76].

Recently, plasma coating processes have been increasingly used in industry [77–79, 82, 84]. Assessing the overall possibilities of using plasma technology to obtain coatings, it should be noted that their use makes it possible to obtain highly ionized particle flows with energies of up to 100 eV. In such systems, plasma can be obtained from virtually all known metals, alloys, and dielectric substances, while plasma various substances can to join V intense chemical interaction. Under these

conditions, even such chemical reactions occur, which V others Wednesdays or at all Not are being carried out or have small speeds (reactive receiving nitrides, carbides, oxides and others).

At the ion bombardment stage, a high voltage (1.2–1.5 kV) is created between the cathode and the substrate; the duration of the ion bombardment is determined by the thermal properties of the material being processed [82, 85, 86]. The third stage – the direct application of a coating of a given thickness to the processed surface – is carried out at a low voltage. between cathode And substrate (Not more 200 IN). Sputtering of pure metal is carried out in a vacuum; to obtain a compound on the surface of the substrate, the sputtering process is carried out in a controlled gas atmosphere.

Cleaning by ion bombardment, heating and activation of the surface of the part being hardened ensure high adhesion of the coating to it (over 1.5–2 MPa) [84, 85].

The temperature of the substrate onto which the coating was applied was controlled using a Smotrich infrared pyrometer.

The coated parts must have a surface roughness of no more than Ra=1.25 μm, and on the thread no more than Ra=2.5 μm. Visual quality control of the surface preparation was carried out using a magnifying glass and a binocular microscope. The surfaces of the parts must not have traces and stains from moisture and other contaminants, as well as fabric fluff, since they initiate microarc discharges during the ion cleaning process. The parts are assembled on a coating application device. A witness sample is usually loaded together with the parts to measure hardness and thickness.

Vacuum ion-plasma spraying is a finishing operation and the coating does not require any finishing. After spraying, the process is complete and the part can be immediately put into operation [113].

Ion-plasma coating conducted plastic chrome (Option 1) at a discharge current of up to 100 A, a vacuum degree of (4–8) 10^{-5} mm Hg and using improved technology at a discharge current of 100 A, a vacuum degree of (4–8) 10^{-5} mm Hg. When chroming according to option 1, the coating thickness was 10–15 μm, using advanced technology– 50–60 μm.

1.17. Application coatings By Sumy-Swiss jet technology

In the last decade, interest in environmentally friendly vacuum coatings, in particular PVD (Physical Vapor Deposition) coating technologies, has

increased in many industries. One of the most advanced PVD technologies is the deposition of coatings using an electric arc discharge in a vacuum. Vacuum-arc coatings are characterized by high strength of the connection with the base metal, have high resistance to frictional wear, erosion under the influence of cavitation, gas and dust flows, and also good corrosion resistance under conditions of influence of air atmosphere and corrosive environments [114, 115]. Vacuum-arc deposition has been well developed on parts of simple shape.

Experimental equipment for vacuum-arc deposition of molybdenum and chromium coatings on the internal surfaces of parts (Fig. 2.14) has been developed and manufactured, namely electric arc sources that provide the formation of radial flows of metal ions (the lateral surface of cylindrical cathodes is the evaporated surface) obtaining coatings on internal surfaces; as well as coating application technologies. Tests of metal ion sources have been conducted, coatings with a thickness of 30 to 200 μm from molybdenum and chromium have been obtained. The productivity of such a coating application process is quite high and can effectively replace galvanic deposition. The coatings are characterized by high density, absence of cracks, good adhesion to the material of the workpiece and can be obtained at relatively low heating temperatures (~350–400 °C) of the coated products. In this process, the part is not an anode. This allows the energy of the condensing ions to be controlled by applying an electric potential to the part, thus changing the structure and properties of the coatings.

The surface structure of the chromium coating obtained without applying voltage to the condensation surface contains chromium grains elongated perpendicular to the condensation surface (columnar structure). Innings high voltage on surface condensation for some time in the middle of the process leads to a suspension of grain growth and the formation of a fine-grained structure. The reason for its formation is considered to be the beginning of the process [115, 116] of spraying the coating, many local defects arise, which during further application of the coating act as crystallization centers. As a result, a fine-grained structure is formed, which then gradually turns into a coarse-grained columnar structure. The chromium coating obtained by periodically applying high voltage to the condensation surface has a multilayer structure with chromium grains that are significantly smaller than in the coating obtained without its supply to the condensation surface [117]. Such a coating structure has higher

protective properties against corrosion caused by the external environment. In the near-surface layers, there are almost always ready-made nuclei of destruction, and the greater the hardness of the coating and its tendency to brittle destruction, the more dangerous any defects in the form of discontinuities and pores become [115, 116]. The fracture toughness of multilayer chromium coatings is higher than that of galvanic coatings, because coatings obtained by vacuum condensation contain compressive stresses, which increase the fatigue properties of the material, while galvanic coatings contain tensile stresses, which can reduce the fatigue limit of steel by up to 60% [117]. The thickness of the coating layer obtained by jet technology is 30–80 μm.

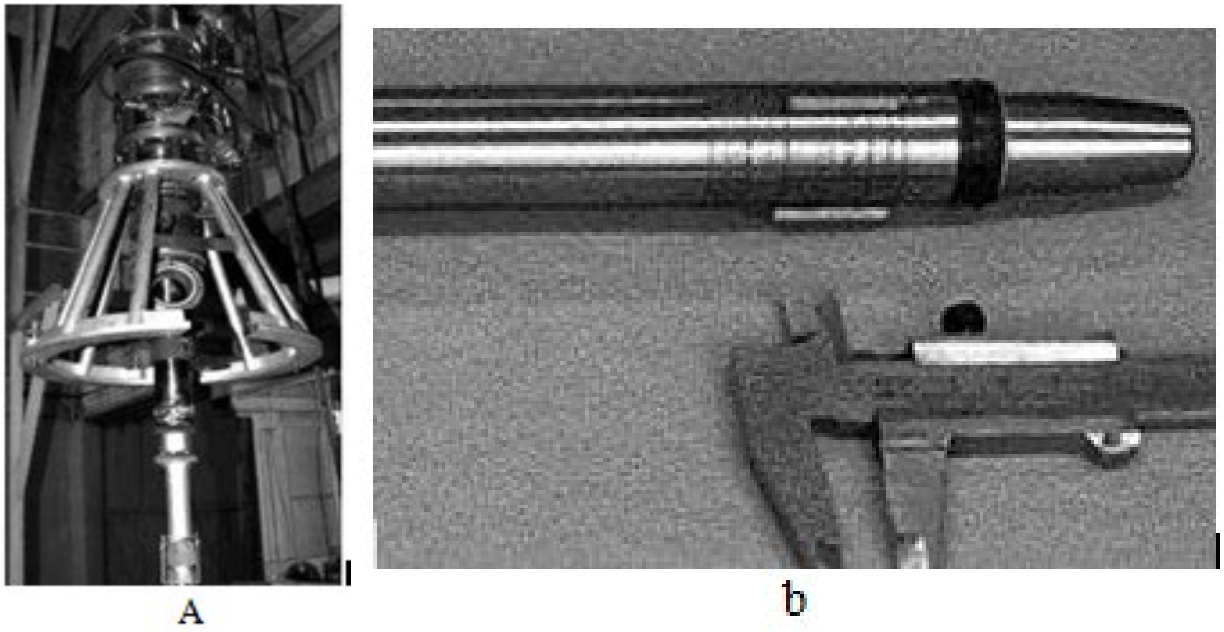

Figure 2.14. Radial-type electric arc evaporator of metals with a movement mechanism (a); devices and sources of metal ions with a diameter of 20 mm (b) [114]

Condensation for some time in the middle of the process leads to a suspension of grain growth and the formation of a fine-grained structure. The reason for its formation is considered to be the beginning of the process [115, 116] of spraying the coating, many local defects arise, which during further application of the coating act as crystallization centers. As a result, a fine-grained structure is formed, which then gradually turns into a coarse-grained columnar structure. The chromium coating obtained by periodically applying high voltage to the condensation surface has a multilayer structure with chromium grains that are significantly smaller than in the coating obtained without its supply to the condensation surface

[117]. Such a coating structure has higher protective properties against corrosion caused by the external environment. In the near-surface layers, there are almost always ready-made nuclei of destruction, and the greater the hardness of the coating and its tendency to brittle destruction, the more dangerous any defects in the form of discontinuities and pores become [115, 116]. The fracture toughness of multilayer chromium coatings is higher than that of galvanic coatings, because coatings obtained by vacuum condensation contain compressive stresses, which increase the fatigue properties of the material, while galvanic coatings contain tensile stresses, which can reduce the fatigue limit of steel by up to 60% [117]. The thickness of the coating layer obtained by jet technology is 30–80 μm.

1.18. Methodology application Hastelloy alloy coatings

The Hastelloy coating was applied according to the invention patent [118] . The technology involves immersion in an electrolyte solution. A potential difference is applied between the anode and cathode, allowing several metals (2, 3, 4 or more) to be deposited on the cathode to form an alloy. The application process the coatings are produced under voltage control conditions, in particular by applying a potential difference between the anode and cathode, which changes over time according to in advance given the law, certain For each alloy. To ensure the operation of the law, the technology with a soluble anode made of the same alloy that is intended for precipitation (to avoid the formation of sediments) is preferable. In this case, the product serves as a cathode.

During the coating process, hydrogen gas is formed, which increases the pH of the solution, which leads to the formation of unwanted sediments and disruption of the alloy composition formed on the cathode. A centrifugal pump is used to eliminate the resulting hydrogen gas and mix the electrolyte.

A potential difference between the anode and cathode is applied, corresponding to a predetermined law. The coating is applied until the required thickness is reached (or until the anode is completely dissolved). In this case, the equilibrium state of the solution does not change over time.

To ensure the required coating composition, an alloy of the following composition was used:

basic component - nickel, chromium – 13.0–14.0%,

molybdenum 0.30 %,
iron 10–13 %,
tungsten 3 %.
IN compositions galvanic baths contained, g/l:
70 NiSO4□ 6H2O ,
242NiCl2□6 H2O ,
30 FeCl2 6H2O ,
60 Hcit,
6 HCl (33%),
68 boric acid,
6 TEA (triethanolamine).

The temperature was 20–50 ° C, the main potential difference was 2.5–3.0 V, the ratio of the anode and cathode surface areas was over 2.5; the pulse duration was 0.23 s.

1.19. Methodology receipt chrome coatings by decomposing the compounds "Barkhos"

Barkhos is a mixture based on organic liquid, which contains 5-30 % weight of dicobalt octacarbonyl, 0.00015–0.0002 mass % of iodine.

The process of pyrolysis of the Barkhos liquid is carried out in a sealed reaction chamber, pre-evacuated to 0.1 Pa, at a temperature of 400–450 °C. The following is formed: a solid phase of the pyrolytic coating, which is deposited on the surface of the product; a vapor phase and a gas phase. The vapor phase consists of the unreacted portion of aromatic hydrocarbons; the gas phase consists of 98% hydrogen and 2% methane. The vapor and gas phases are removed from the chamber by a continuously operating vacuum pump. The vapor phase accumulates in the nitrogen trap of the vacuum post in the form of condensate and is utilized; the gas phase is removed into the atmosphere through the exhaust ventilation system.

The substrate is placed in the reactor and heated to 430–450 °C. The evaporator is heated to 320–340 °C. The coating is deposited by decomposing the organometallic compound “Barkhos” in an inert gas flow at a flow rate of 0.010–0.013 l/min. The pressure in the flow is 1.33×10^{2} Pa. The technical result is increased adhesion (Fig. 2.16).

The prepared substrate is placed in the reactor and hermetically sealed. The reactor is purged with argon to exclude atmospheric oxygen from the reactor volume, the presence of which oxidizes the substrate.

When the required substrate heating temperatures are reached,

And evaporator are installing speed feeds gas from 0,010 to 0.013 l/min and supply a certain amount of MOS "Barkhos" to the evaporator.

The main working unit of the installation is the reaction chamber 1 of the horizontal type. The process of coating deposition is carried out as follows. The coated articles are fixed in the holder 2. The chamber is closed and evacuated. The heating is switched on and the article is heated to the operating temperature. The electric drive 13 is switched on and the articles are moved through the deposition zone in rotational and translational motion. Simultaneously start feeding the working mixture from the dispenser 4 into the evaporator 6, located above the products. The steam-gas mixture from the evaporator 6 comes to the surface products And decomposes With education solid phases coatings and gaseous reaction products. Gaseous products are removed from the chamber using vacuum pumps 7 and 8. The vacuum in the chamber is controlled using a VT-3 vacuum gauge, the heating temperature is controlled by a thermocouple sensor and maintained in a given mode by the control system.

Increasing the heating temperature of the substrate above 450 °C leads to an increase in internal stresses in the coating structure, leading to the possibility of peeling of the coating.

Reducing the substrate heating temperature below 430 °C leads to the formation of homogeneous deposits with greater roughness, which reduces the wear resistance of the coating.

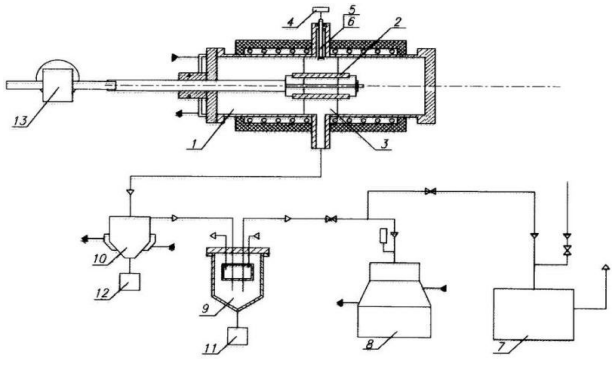

Figure 2.15. Schematic diagram of the installation for applying coating by decomposition connections "Barkhos" [119]: 1 - reaction chamber, 2 - products, 3 - zone precipitation, 4 - dispenser, 5 - feeder, 6 - evaporator, 7 - mechanical vacuum pump, 8 - steam-oil pump, 9 - nitric trap, 10 – water-cooled trap, 11, 12 – containers for draining organic waste, 13 – electric drive

Increasing the feed rate of inert gas results in the formation of on surfaces substrates pyrocarbon, which worsens the resulting coating. This is explained by the fact that the vapors of the MOS "Barkhos" do not have time to react in the area of the temperature field of the substrate and go further into the reactor volume, where the their decomposition.

The decrease in the gas feed rate to less than 0.010 l/min with the formation of pyrocarbon on the substrate surface is explained by the fact that the reacted products reactions do not have time to be removed from the temperature field of the substrate and settle on the surface.

Increasing the evaporator temperature above 340 °C leads to the initial decomposition of the “Barkhos” MOS in the evaporator zone with the formation of a solid phase.

Reducing the evaporator temperature below 320 °C leads to an increase in the precipitation process time.

The coating obtained by the proposed method is characterized by a horizontally layered structure, high adhesion and requires lower costs for the deposition process.

1.20. Methodology stand tests

In order to determine the effect of different types of hardening on the durability of a hydraulic hammer, its parts were tested on a stand after hardening by various methods (Fig. 2.16).

Figure 2.16. Stand For tests hydraulic hammer (general view)

The stand consists (Fig. 2.17) of a stationary frame on which the tested hydraulic hammer 1 is installed, connected by means of flexible hoses 2 to a hydraulic system containing an adjustable oil pump 3, a pressure gauge 4, a safety valve 5, a throttle 6, a filter 7, an oil tank 8 of a measuring system containing a pressure sensor of the discharge line 9, a pressure sensor of the drain line 10, a device for measuring the speed of the striker 11, a measuring container 12, a strain gauge meter 13, oscilloscope 14, thermocouples 15 And 16, connected To
to the writer device 17.

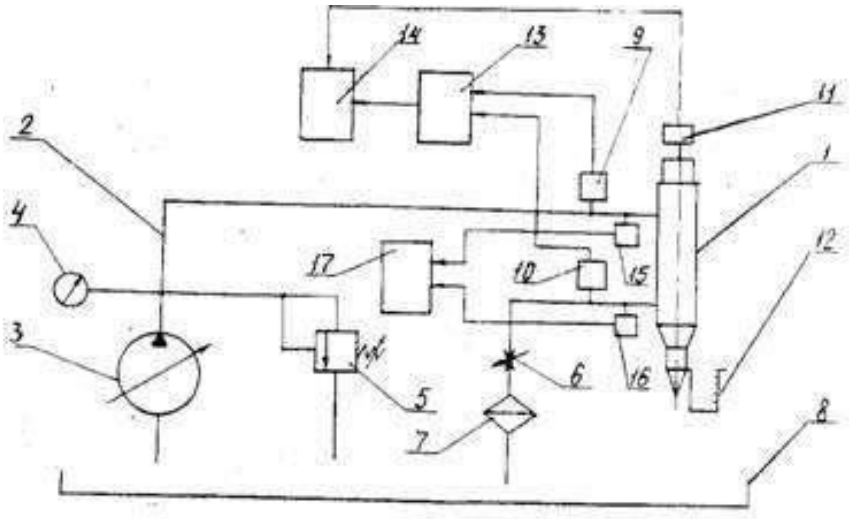

Figure 2.17. Scheme stand For tests hydraulic hammer

The stand operates as follows. Before measuring the parameters of the hydraulic hammer's working process, the pressure sensors of the discharge and drain lines are calibrated on a special stand. Then the oil tank of the hydraulic system of the stand is filled with the required grade of working fluid and the minimum flow rate of the working fluid according to the test conditions is set using the pump's regulating element. At the same time, all the devices of the measuring system are switched on for warming up for the maximum time specified in the passports of these devices, and the drive motor of the pump station. By changing the pump flow rate in steps and changing the throttle opening value at each flow rate, simulating the reaction on the hydraulic hammer tool, all the measured parameters are recorded.

In progress tests in the cavity of the device created pressures from 132 to 620 MPa, the distribution diagram of which, constructed using the slip line method, is shown in Fig. 2.18.

The components were tested in the as-delivered condition (without additional hardening), as well as the components after hardening. Hardening was performed by laser heat treatment, electric spark alloying, application of galvanic and ion-plasma coating based on chromium, detonation spraying, ion-plasma chromium plating using improved technology, application of ion-plasma carbonitride coating, etc. (Table 2.2).

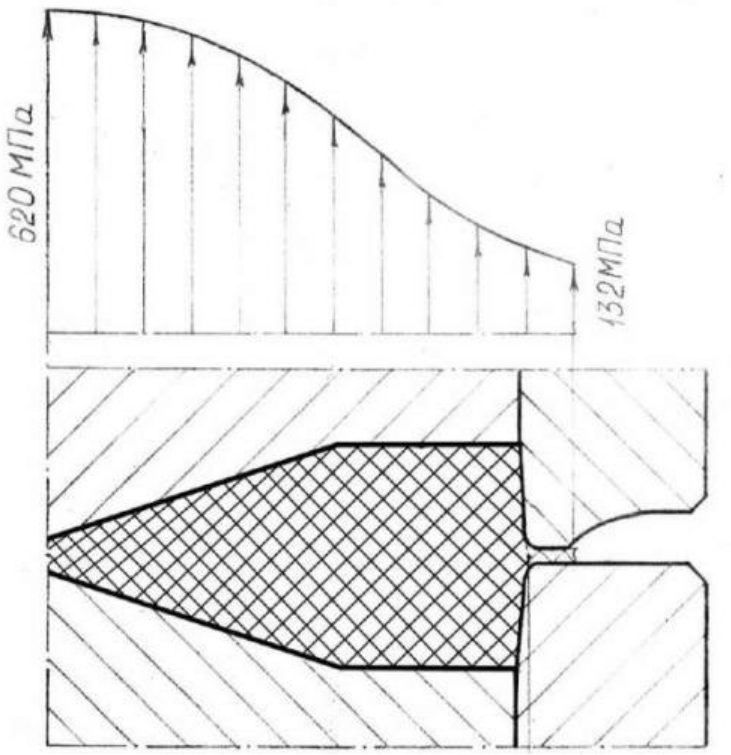

Figure 2.18. Epura distributions pressures V cavities of a hydraulic hammer during testing

Table 2.2

Characteristics tested And researched details cylinder after strengthening in various ways

Way strengthening	Characteristic hardened layers			
	material	thickness (depth)	hardness	parameters strengthening
1	2	3	4	5
Laser thermal strengthening	Basic metal	0.45–0.55 mm	*HV* 570–680	N - 0.30 kW step - 2.5 mm, width paths 2 mm
Electric spark alloying	Tungsten; lower striker additionalchrome	0.05–0.1 mm	*HV* 480–700	N – 1 kW (W) N – 1.5 kW (Cr)
Galvanic chromium plating	Solid chromium	30–160 microns	*HV* 900 HRC 64–66	T-ra electrolyte 55–62 ° Current density 70–980 A/ ^{dm2}
Ion-plasma chromium plating (1 option)	Plastic chromium (Cr3)	10–15 microns	-	Discharge current 100 A, degree vacuuming $4–8 \cdot 10^{-5}$ mm rt. Art.
Gas detonation spraying	VK-25, PT-NA-01	0.1 mm	14.5 GPa	4 blow per second
Vacuum plasma carbonitride coating	System C- N	20 microns	15–18 GPa	Discharge current 200 A, degree vacuuming $2–3 \cdot 10^{-5}$ mmHg
Ion-plasma chromium plating (improved) technology)	Plastic chromium (Cr3)	50–60 microns	-	Discharge current 100 A, degree vacuuming $4–8 \cdot 10^{-5}$ mm rt. Art.

End table. 2.1

1	2	3	4	5
Surfacing work surfaces	"Hastelloy"	35 mm	HB241	Heating of parts before surfacing 400–450 ° C
Multilayered coating	Multilayered chromium	30–80 microns	-	Sumy-Swiss Jet technology
Single layer coating	Wear-resistant chromium	-	-	Decomposition connections "Barkhos"

2. TRIAL AND STUDY HYDRAULIC HAMMER PARTS WITHOUT ADDITIONAL STRENGTHENINGS

2.1. Damage characteristics details devices

The working parts were examined hydraulic hammer, which were manufactured and heat treated for hardness 42–44 HRC. The test was performed on a stand in the volume of 1000 loading cycles. After every 250 cycles, the device was dismantled, inspected and the nature of damage to the working surfaces was recorded.

After 1000 loading cycles, the reduced diameter of the housing channels V zone cut increased to 125.3 mm, striker V zone "N" (see Fig. 3.1) has worn by 0.3 mm, in the "F" zone - by 0.35 mm. The wear of the pick (see Fig. 3.2) is 0.3 and 1.2 mm, respectively.

Initial signs of wear on the working surfaces of the parts in the form of small scratches and nicks appeared at the peak in zone “F” (see Fig. 3.2) after 250 loading cycles, on the bushing in zone “B” after 450 cycles, and on the upper parts (striker and body) after 300 and 500 cycles, respectively.

The tested parts of the device were cleaned of carbon deposits and washed in kerosene and subjected to metallographic examination.

The central part of the striker (zone "F", see Fig. 3.1) has the appearance of a spot with a diameter of 40 mm with a smoothed surface. Around the central spot, annular zones with a relief formed by intermittent short folds with a general radial direction are visible (Fig. 3.3).

Zone "M", adjacent to zone "N", covers about half of the surface (see Fig. 3.1). They show wear of the surface volumes of metal in the form of alternating protrusions and depressions (grooves).

Zone "B" extends to the lower part of the surface and is characterized by intense work hardening of the metal with the formation of a shiny, smooth, flaking surface.

Zone "E" is characterized by wear and work hardening of the surface volumes of the metal.

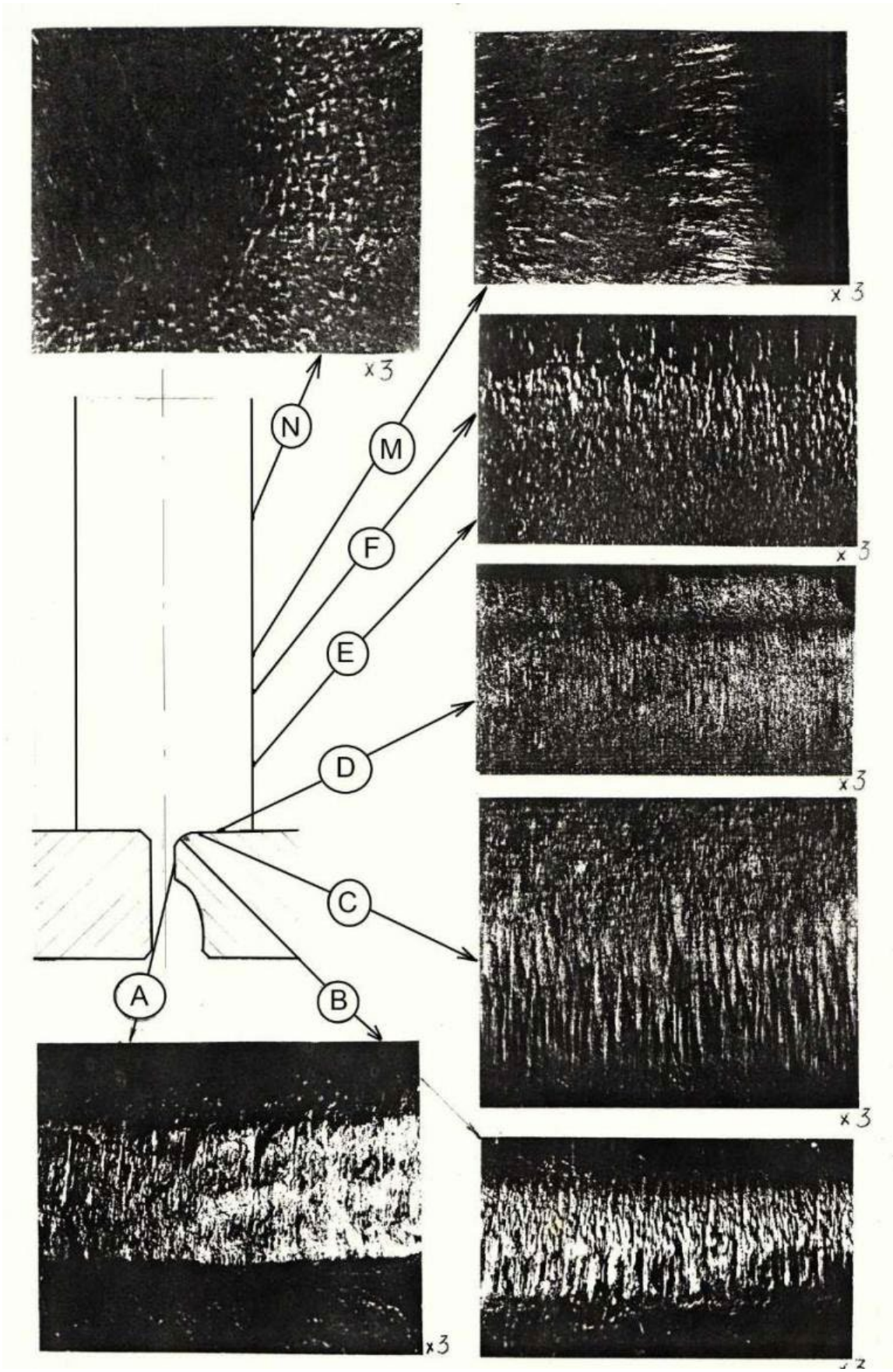

Figure 3.1. Character damage surfaces of the body and striker

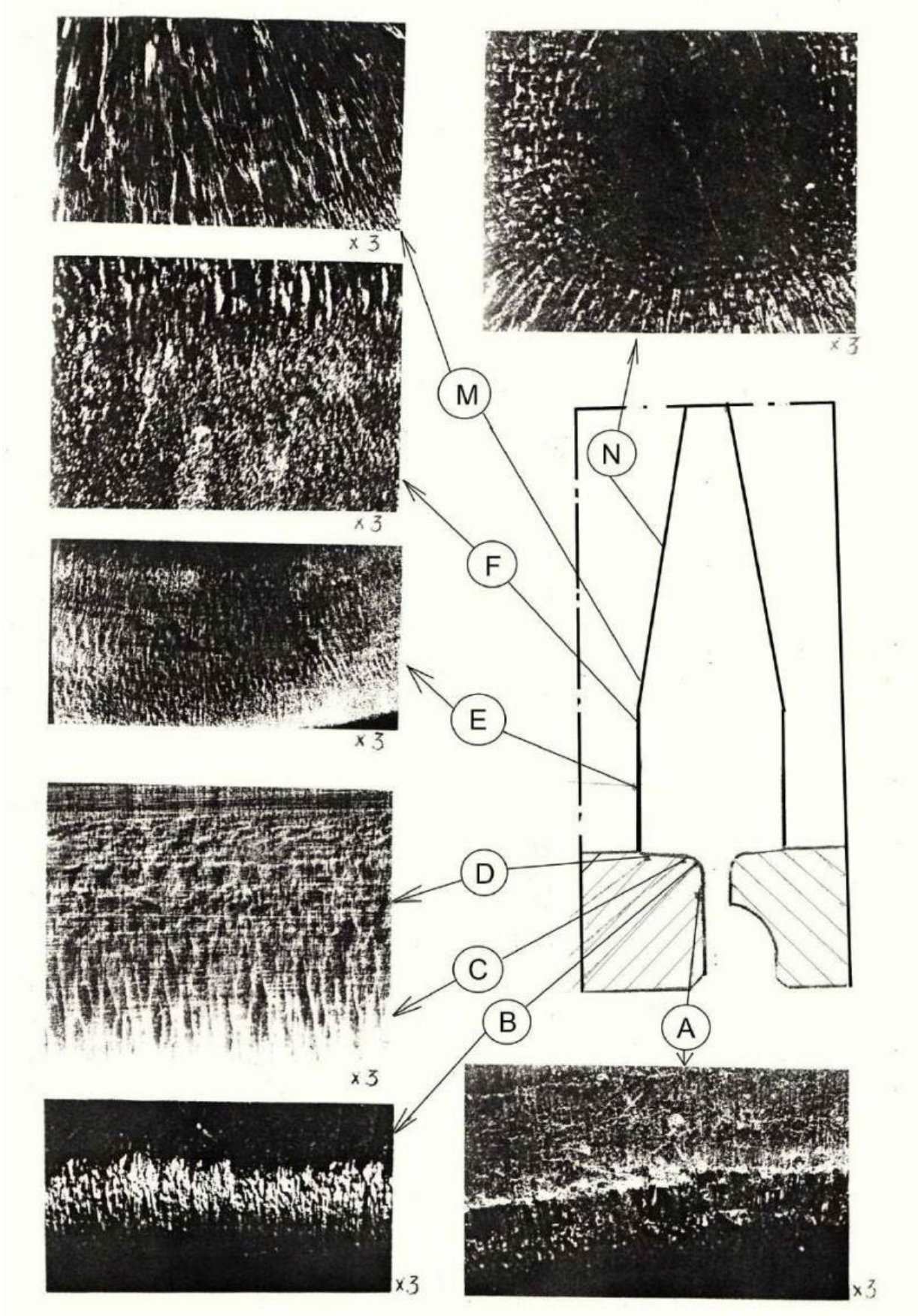

Figure 3.2. Character damage surfaces peaks And bushings

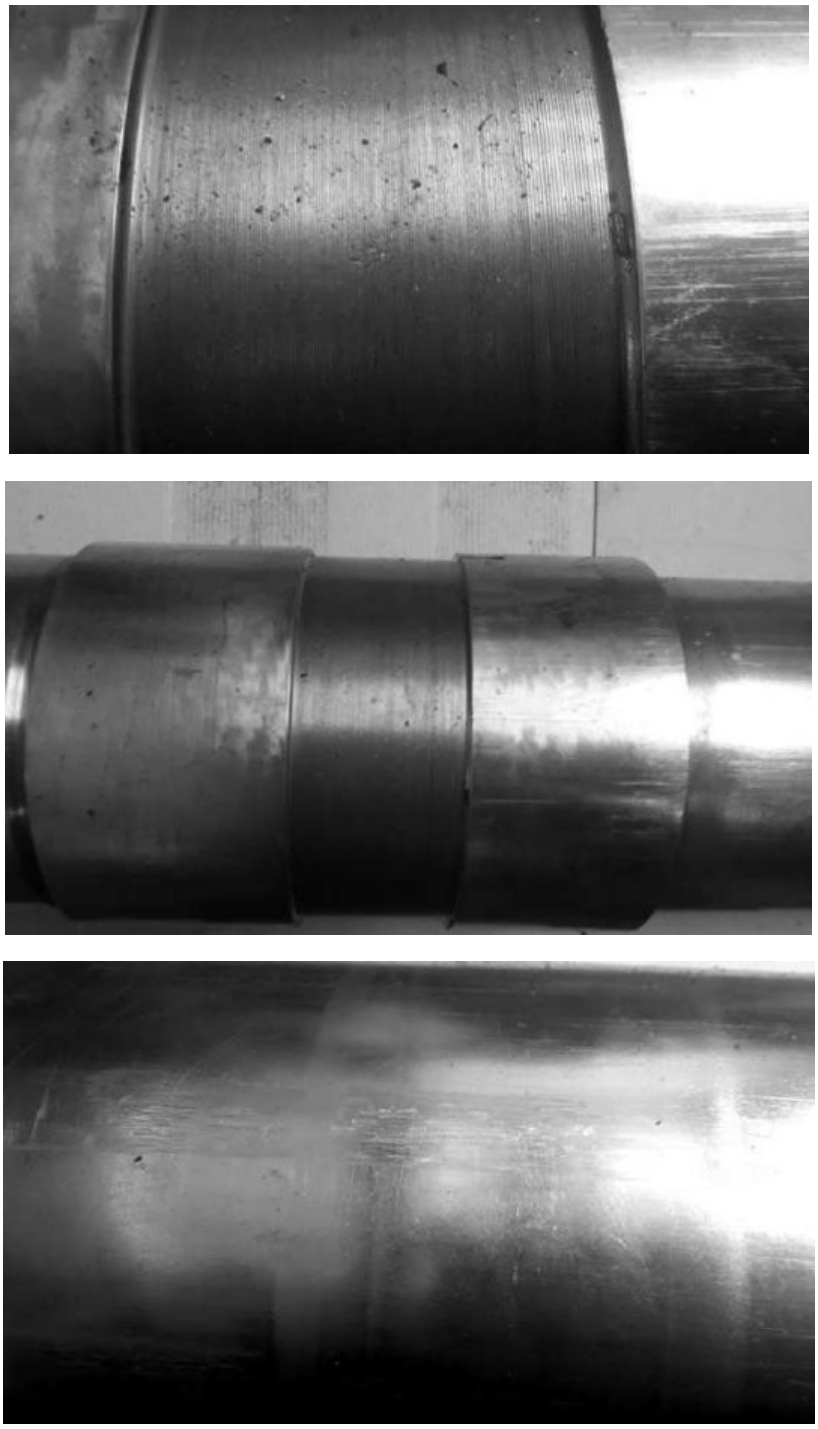

Figure 3.3. The striker after operation: wear surfaces

The formation of adhesion nodes is observed on the section of the body (zone "A") metals, slander And wear superficial layer. IN zones "B" and "C" indicate work hardening and micro cutting of metal the formation of a folded relief oriented along the generatrix of the hull channel (see Fig. 3.1). On the surface of the hull channel (zone "D") wear, work hardening and peeling of the surface of the work-hardened elephant are observed.

On the surface of the housing channel, carbon deposits and tarnish colors are observed.

Ha rice. 3.2. presented picture of damage working surfaces of the pick and bushing. The nature of wear of these parts is practically identical to the damage of the upper parts. More intensive wear of the pick is noted in zones “M” and “F” compared to the corresponding zones of the striker (see Fig. 3.1).

2.2. Study crack formation And structural state of the surface layers of the material of the parts

During the micro-examination and in the fractures of the samples cut from the body and strikers, a significant number of cracks were found V superficial volumes material top parts (Fig. 3.4) and lower (Fig. 3.5).

The upper parts show a greater number of cracks of radial and grid orientation (see Fig. 3.4), while the lower parts show isolated cracks (see Fig. 3.5). The distribution of cracks over the surface of the working zones of the parts is uneven. On the striker, cracks are concentrated mainly in zones “M” and “F” (see Fig. 3.4), and on the body – “B” and “C”. The cracks are most densely located on the striker; they have a radial orientation, while tangential cracks are much less common. In some places, individual tangential cracks merge into one annular crack. In fractures, the cracks look like arcuate sections with a clearly defined border. Walls cracks smooth, significantly ground and have a dark shiny shade. The depth of cracks on the body and striker is up to 0.3 mm, on the bushing and peak - 0.1 mm.

The crack cavities are filled with light-gray oxides almost throughout their entire depth. In all cases, the cracks are located in the structural zone changes And in places extend beyond its limits by 0.1–0.15 mm.

When examining the microstructure, zones of structural changes are observed in the surface layers of all the examined parts. The depth of these zones (see Fig. 3.4, 3.5) on the strikers (“M”, “F”) is 0.15–0.3 mm, on the body and bushing (“B”, “C”) – 0.10–0.18 mm. They contain structures of martensitic and troost-martensitic types. On the rest surfaces structural changes are observed in isolated areas up to 1 mm long and up to 0.03 mm deep.

The microhardness in the zone of structural changes exceeds the microhardness of the base metal of the parts by 1.5–2.0 times and is *HV* 630–680 (HRC 57–59).

2.3. Quality material details

The material of the studied parts meets the operating requirements in terms of chemical composition.

The hardness of the material of the bodies, strikers and peaks is practically the same across the cross-section of the parts and is:

frame - HRC 43–45; striker - HRC 43–44;

sleeve - HRC 42–44; peak - HRC 39–40.

The mechanical properties of the material of the parts were determined on samples cut in the axial and tangential directions at 20 ° C. The results of mechanical properties tests are given in Table 3.1.

Table 3.1

Mechanical properties material parts at a temperature of 20 ° C

Part name	Direction of cutting samples	Mechanical properties				
		σ_{in}, MPa	$\sigma_{0.2}$, MPa	δ, %	ψ, %	KCV, J/ cm^2
1	2	4	5	6	7	8
Cylinder (housing)	axial	1450–1460	1360–1370	14.0–15.0	56.0–59.0	48
	tangen-cial	1460	1360–1370	13.0	45.0	40–42
The striker	axial	1440–1450	1330–1370	13.0–14.0	54.0–56.0	34
	tangen-cial	1440–1490	1350–1410	12.0–13.0	42.0–43.0	34–82
Sleeve	axial	1465–1480	1370–1390	14.0–16.0	54.0–59.0	46–48
	tangen-cial	1475	1400–1410	13.0	48.0–51.0	48
Worker tool	axial	1320	1250–1260	16.5–17.0	62.0–64.0	68–72
(peak)	tangen-cial	1310–1320	1250	15.0–17.0	54.0–56.0	54–58

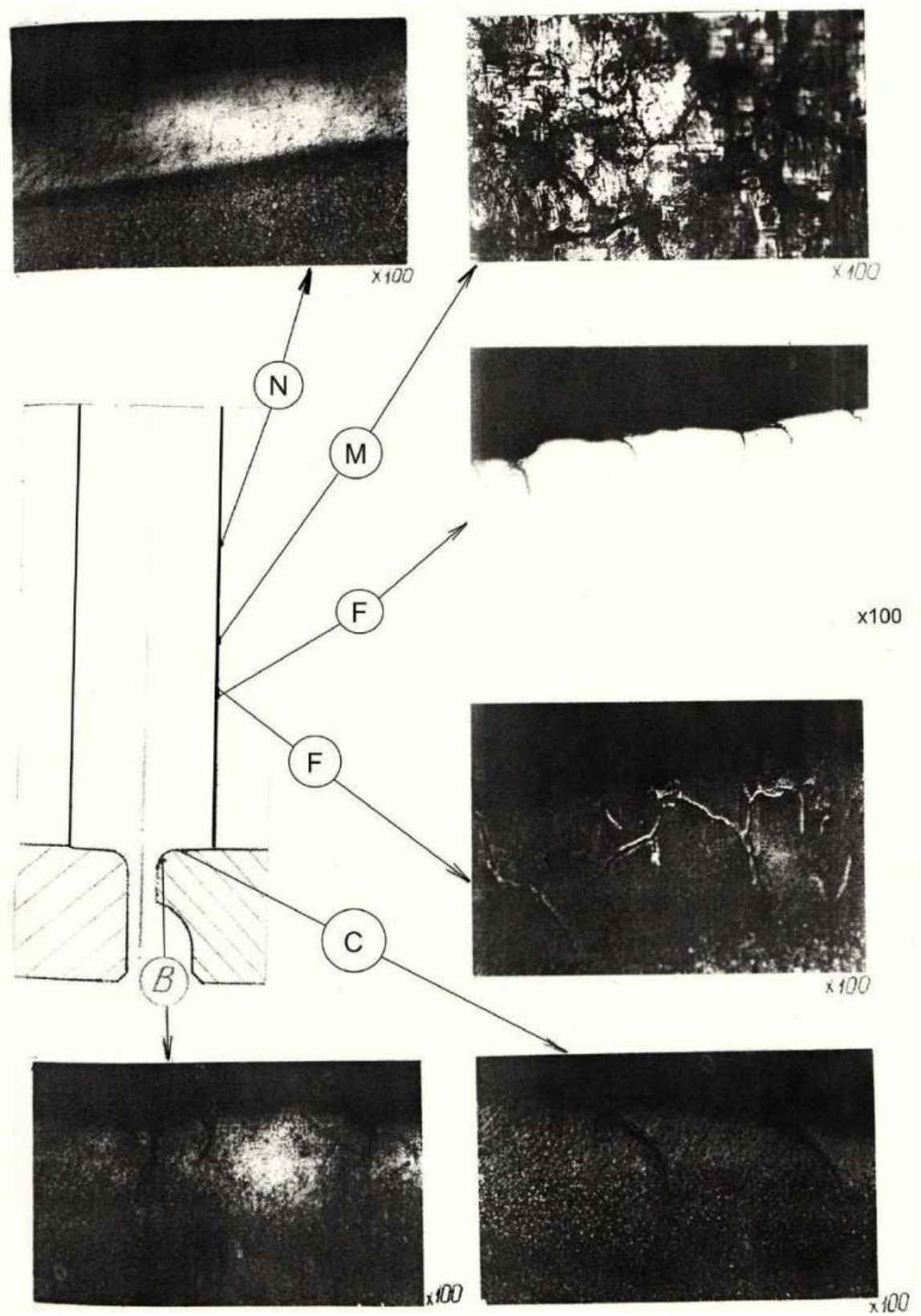

Figure 3.4. Structural changes materials corps And striker

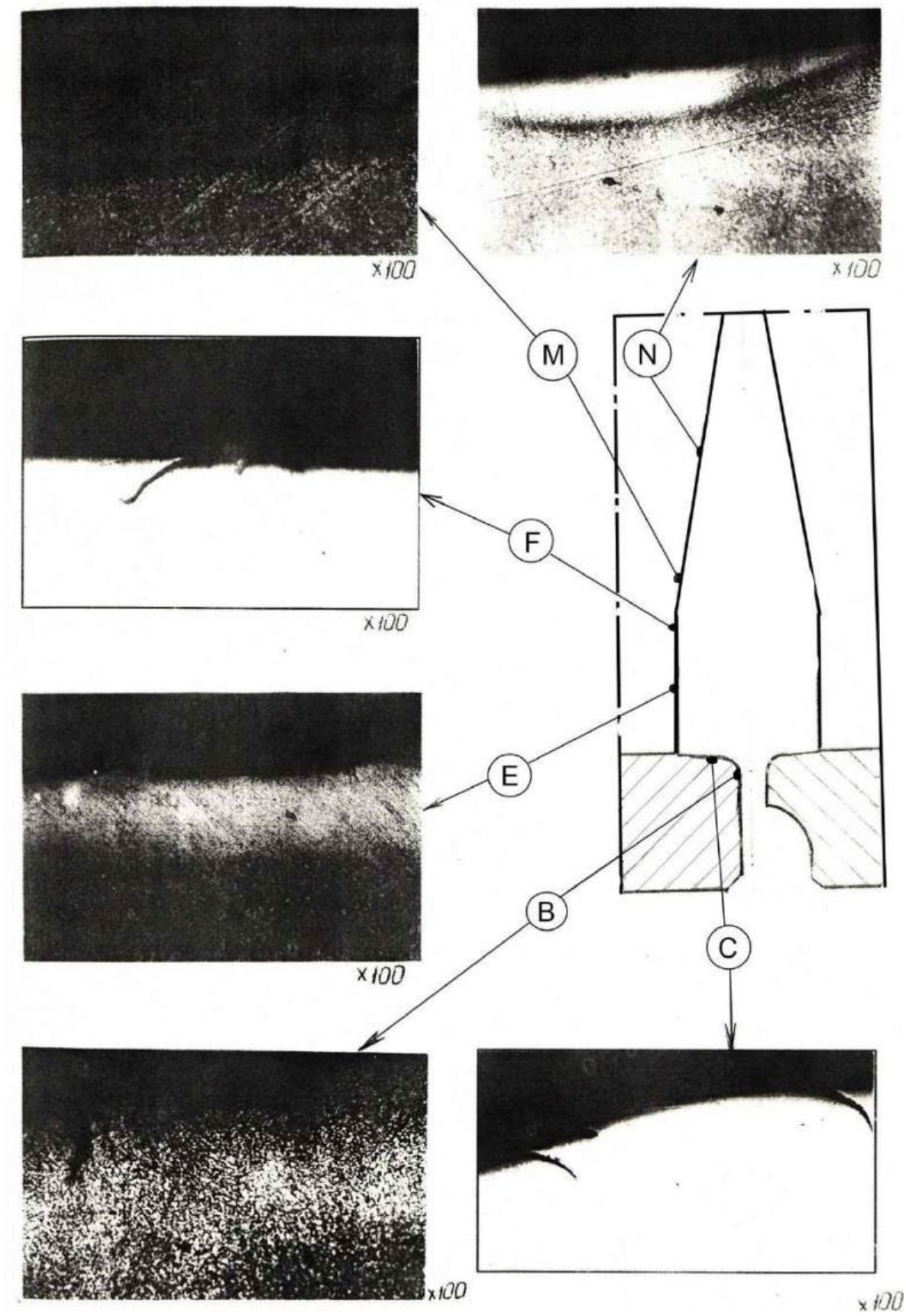

Figure 3.5. Structural changes materials peaks And bushings

An analysis of Table 3.1 allows us to conclude that the mechanical properties of the body, striker, bushing and lance material at 20 °C meet

the operating requirements.

When examining the macrostructure, it was established that the metal of the parts is dense and there are no defects of metallurgical origin (Fig. 3.6, 3.7).

The microstructure is of the sorbitol type (Fig. 3.7), uniform across the cross-section of the parts.

A

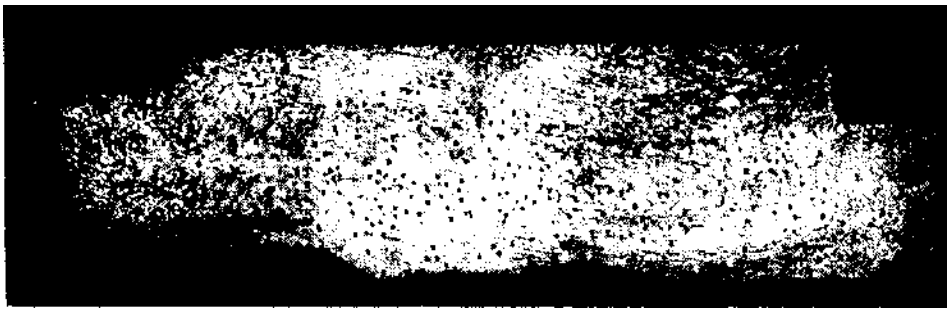

b

Figure 3.6. Macrostructure V diametrical planes: a – housings; b – bushings

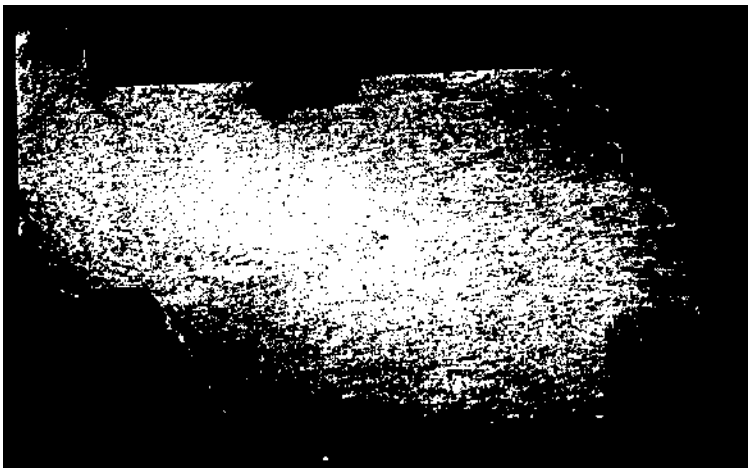

Figure 3.7. Macrostructure peaks

The contamination of the metal of the body, striker, bushing and peak with non-metallic inclusions is almost the same and is estimated at 1.5 points on the GOST 1778-70 scale. Sulfosilicate and oxide inclusions are observed.

2.4. Conclusion

1. The nature and extent of damage development, features of structural changes and type of cracks identified on the body, bushing, peak and striker allow us to conclude that the developed and implemented method of testing models provides comparable loading conditions and, as a consequence, similar structural-phase transformations and damage to the materials of real parts.

2. Damage to the working areas of the body, bushing, peak and striker is of an identical nature with the maximum degree of development on the curved parts of the surfaces of the parts – the areas of the most intense sliding of the counterbody material.

3. The destruction of the material of the device parts includes work hardening, deformation, displacement and peeling of the metal layer, the formation of adhesion nodes and their wear in micro-areas.

4. The degree of damage to the working areas of the body and striker is greater than that observed on the peak and sleeve.

3. TRIAL AND STUDY PARTS HARDENED BY LASER THERMAL PROCESSING (LTO)

3.1. Advantages And choice parameters laser heat treatment

CO_2 gas lasers, which allow the power and time of irradiation to be varied over a wide range, have wide possibilities for surface hardening of machine parts and tools . It is advisable to use a continuous laser only in cases where the use of conventional methods of surface hardening is associated with certain difficulties or is impossible altogether [120–122].

The change in the properties of the surface layers of materials under laser radiation occurred as a result of a high-speed thermal cycle.

Laser processing has a number of advantages over other processing methods [58, 121]:

A) high performance processes;

b) minimal warping And improvement qualities manufactured products; the possibility of selective hardening;

V) opportunity relatively easily process areas surfaces any profiles And high homogeneity reinforced layers.

The nature of the formation of the hardened layer is greatly influenced The distribution of energy in the laser beam has an impact. To increase the efficiency of laser hardening, special coatings are applied to the surfaces being treated that absorb radiation energy well.

The laser processing parameters were selected to obtain optimal values of hardness, depth and structure of the hardened layer (see Section 2.5). LTO on the hardened surfaces of the parts was performed in the form of a system of concentric circles (Fig. 4.1).

Microscopic examination revealed that the laser treatment zones in cross-section have an arc-shaped appearance (Fig. 4.2).

In some cases, the LTO zones overlap. The structure is martensitic, non-acicular. In areas where adjacent zones overlap, some change dispersion structures. IN

The surface layer contains arcuate sections of the troostite type; there are no cracks in the LTO zone.

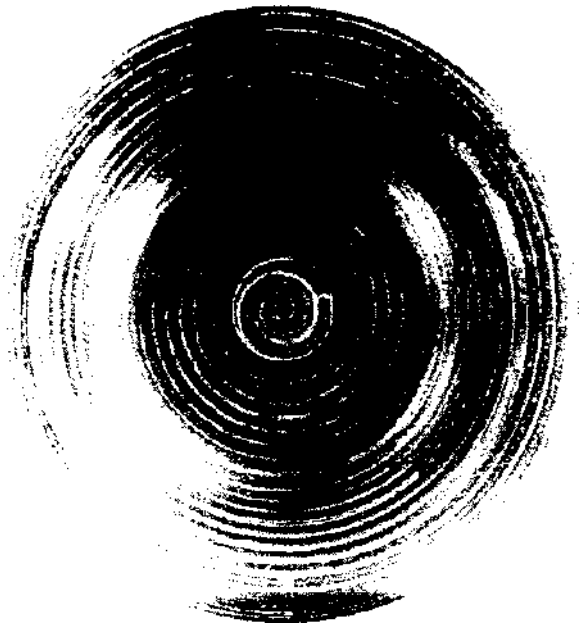

Figure 4.1. View hardened LTO striker

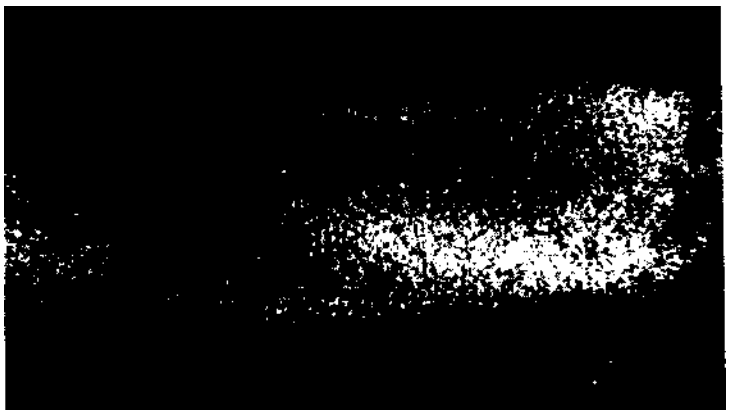

Figure 4.2. Microstructure superficial layers striker reinforced with LTO

Testing of parts hardened with LTO was carried out according to the developed methodology (see section 2).

The test was carried out until wear patterns on the surfaces of the housing and bushing channels appeared in zones “C” and “D”, similar to that obtained when testing parts manufactured without additional strengthening (see Fig. 3.1 and Fig. 3.2).

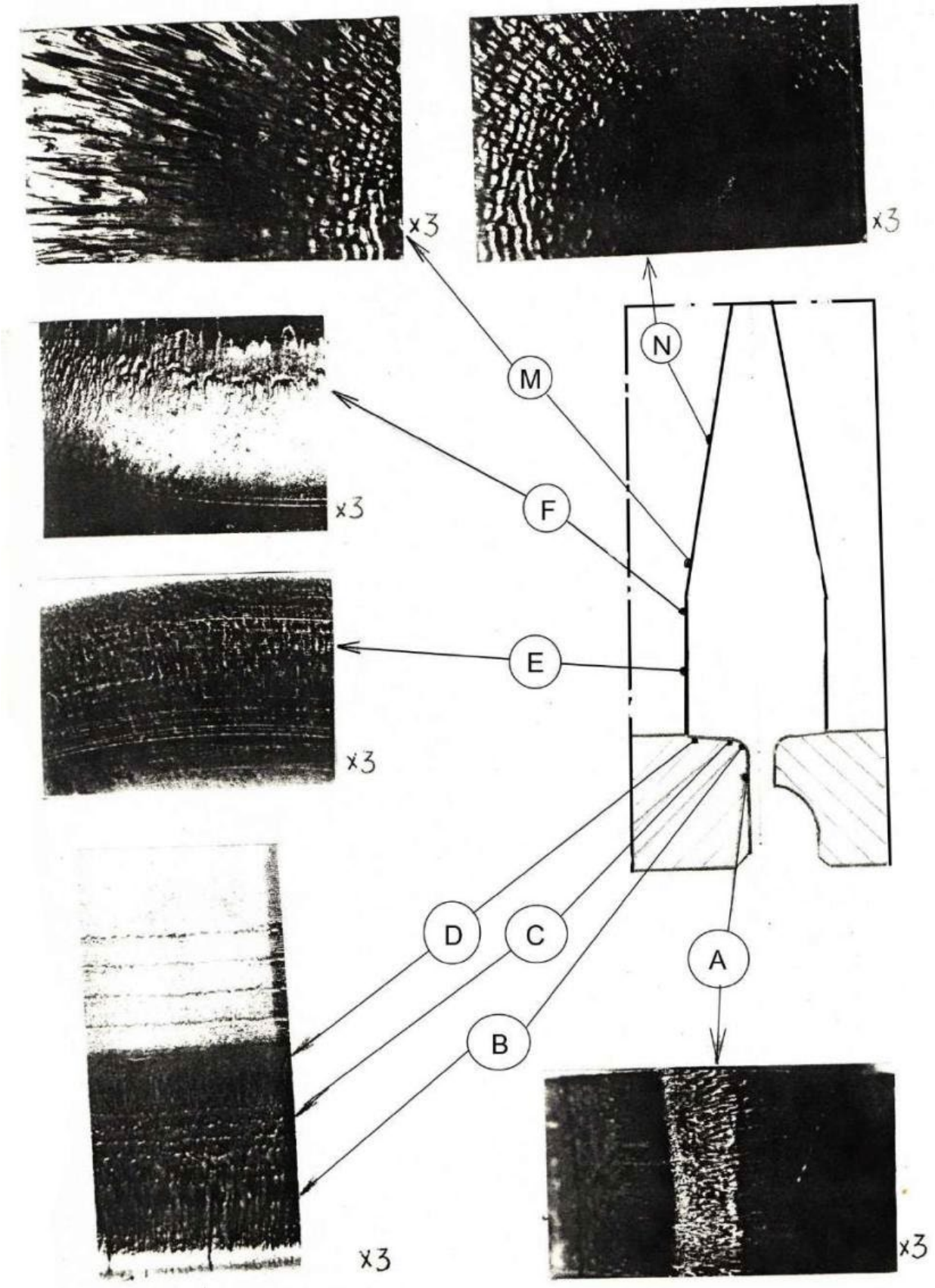

Figure 4.3. Damage surfaces peaks And bushings, reinforced LTO

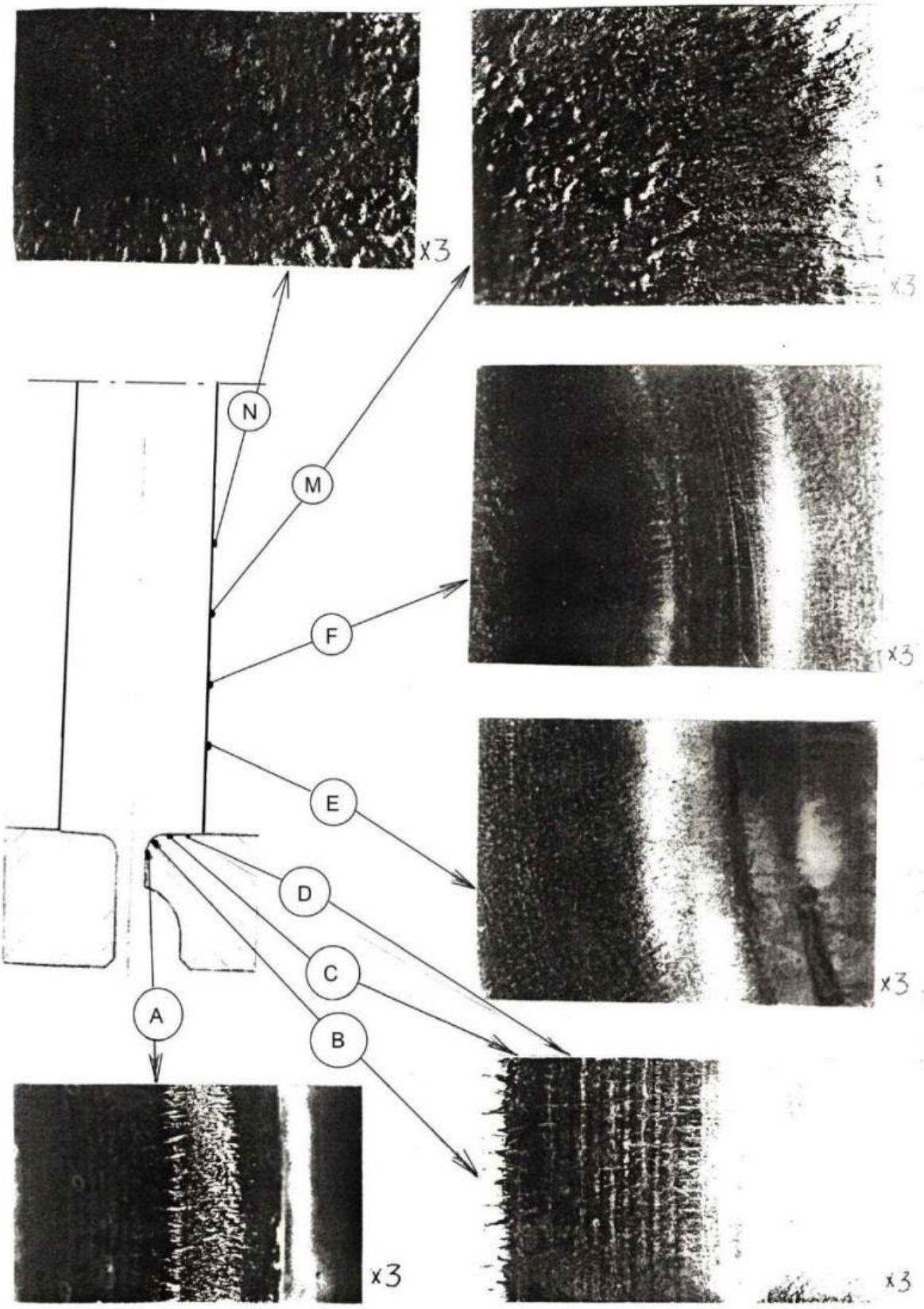

Figure 4.4. Damage surfaces corps And striker, hardened LTO

Initial signs of wear on the working surfaces of parts in the form of small ones risk-scuffs revealed on pique V zones "M" And “F” (see Fig. 4.3) after 350 loading cycles, and on the sleeve after 500 cycles, on the striker and body, respectively, after 450 and 600 cycles.

After 1800 cycles loading character And degree damage to the body, bushing, striker and peak corresponded to that observed in the original version. The given diameter of the body channels and the bushing in the shear zone increased to 125.1 mm, the striker in the “N” zone wore out by 0.25 mm, in the zone "F" - by 0.3 mm. The wear of the pick (see Fig. 4.4) is 0.3 and 1.1 mm, respectively.

3.2. Damage details hydraulic hammer, reinforced LTO

The type of damage to parts reinforced with LTO is shown in Fig. 4.3 and Fig. 4.4.

The damage zones coincide with the corresponding wear zones of parts that were not subjected to additional strengthening (see Fig. 3.1 and 3.2). In zones "A" (see rice. 3.9 and 3.10) work hardening is observed and wear of the surface layers of metal with the formation of characteristic shear lines. Zones "B" are characterized by a folded relief, the grooves of which are oriented along the generatrix of the housing channel. In zones "C" there is intense wear, work hardening and peeling of surface layers. On the body and bushing in this zone against the general background of the worn surface, traces of LTO are visible, to a greater extent this is manifested on the body. Smoothed relief of LTO traces is also noted in zone "D".

The “N” zone of the striker and the peak has the appearance of a round spot with a diameter of about 20 mm on the peak and up to 35 mm on the striker, and is distinguished by a smoothed and riveted surface, turning into a folded relief with a general ring direction.

A clearly defined radial direction of wear grooves is characteristic of zone "M". At the peak, smoothness of the groove surfaces prevails, and wear on the striker. In zone "F" of the striker, intensive metal work hardening With education shiny smooth surfaces dark shade, on pique flakingthe surface is of a lighter shade. Signs of more uniform wear and work hardening are characteristic of zone "E" (see Fig. 3.9 and 3.10).

3.3. Characteristic destruction And structural state of the material of the parts

The working surfaces of the tested device parts have suffered wear of the layer reinforced with LTO. There are rare cracks in the damaged areas. The metal along the crack walls is smooth, covered with a layer of oxides. Some cracks are connected to each other .
(rice. 4.5, 4.6). On in the body And in the bushing cracks are observed V zones
"B" and "C". In zone "B" they are located along the bottom of the grooves formed during the test. The length of these cracks is 0.5–
2.0 mm.

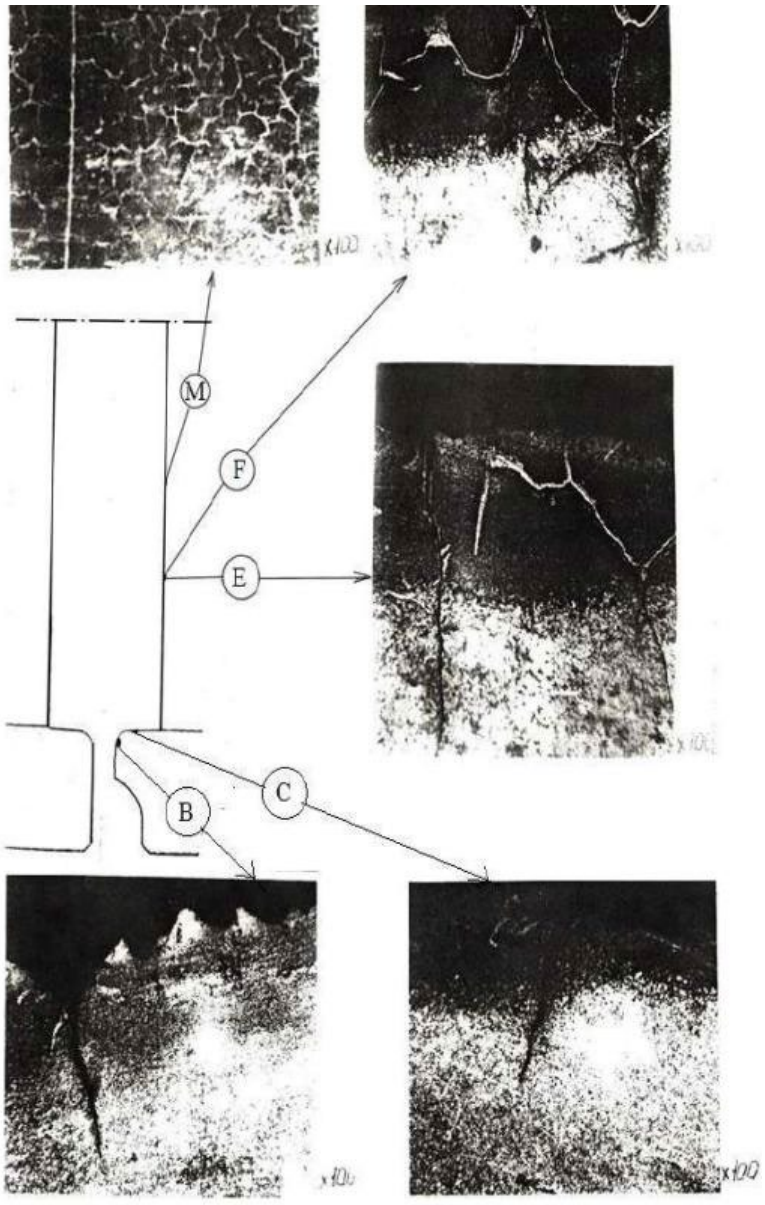

Figure 4.5. Structural changes materials corps And striker

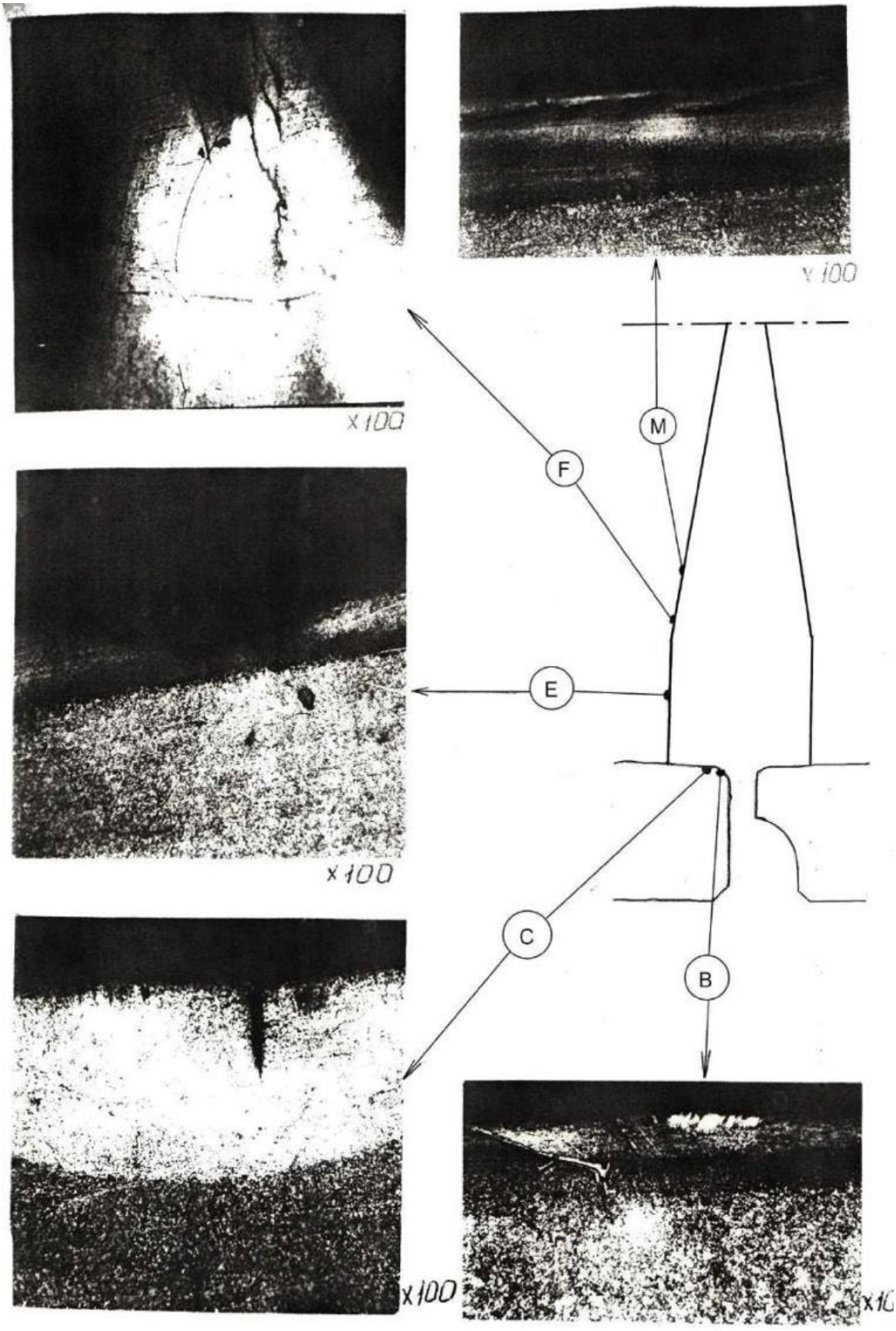

Figure 4.6. Structural changes materials bushings and peaks

In zones “C”, cracks can be observed both in hardened and non-hardened LTO zones and are oriented perpendicular to the surface of the parts.

3.4. Study qualities material details

By section corps striker, bushings, striker And peaks the hardness is practically constant and is:

frame striker - HRC 43–44; firing

pin – HRC 42–44;

sleeve - HRC 43–44;

peak – HRC 39–40.

The mechanical properties of the material of the parts were determined at a temperature of 20 C on samples cut in the axial and tangential directions (Table 4.1).

Table 4.1

Mechanical properties materials details, reinforced LTO

Part name	Direction of cutting samples	Mechanical properties			
		$\sigma_{0.2}$, MPa	σ_{in}, MPa	δ, %	ψ, %
Sleeve	axial	1400–1450	1380–1390	15.0–16.0	56.0
	tangen-cial	1390	1370–1380	12.0–12.5	42.0–45.0
Pika	axial	1240–1270	1210–1250	14.5–15.0	59.0
	tangen-cial	1270	1230–1240	15.0	56.0
Frame striker	axial	1390	1350–1370	13.0	54.0
	tangen-cial	1390–1405	1375–1390	13.0–14.0	51.0
The striker	axial	1370–1400	1350–1380	14.0	56.0
	tangen-cial	1360–1370	1345–1350	10.0–11.0	39.0–42.0

Results tests, presented V Table 4.1, show that the mechanical properties of the material of the parts, according to the parameters studied, satisfy the requirements imposed on them.

3.5. Conclusion

1. Laser heat treatment with a radiation power of 0.30 kW ensures strengthening of the surface volumes of the material details in depth 0.45–0.55 mm and receiving in LTO zones with hardness HRC 53–59.
2. Results of tests of parts hardened with LTO, showed that the wear resistance of the body, striker, peak, and bushing is increased by 1.8 times compared to the original (not subjected to additional hardening) version.
3. The location of damage zones of parts and their nature are identical to those observed on parts manufactured without the use of special strengthening.
4. A study of the nature and extent of damage to parts, the characteristics of structural changes and the type of cracks allow us to conclude that the destruction of the material of the parts occurs in a similar way to that observed on parts that have not been subjected to special strengthening.
5. During the testing process, partial wear of the hardened metal layer of the parts occurred, to a greater extent on the curved sections of the working surfaces of the striker.
6. On the body, striker, sleeve and peak, reinforced with LTO, it is noted significantly more quantity cracks By comparison about the original version, up to 0.7 mm deep, extending beyond the zone of structural changes.
7. The structural changes observed on the damaged surfaces of the parts are of a tempering nature on the striker and peak, while the body and bushing are characterized by secondary hardening phenomena.

4. STUDY OF WEAR RESISTANCE OF PARTS HARDENED APPLICATION CARBONITRIDE COATINGS

4.1. Parameters application coatings

The surfaces of the parts to be strengthened are activated by ion bombardment with a reactive gas mixture, then a carbonitride coating with a thickness of 20 μm and a microhardness of 15–18 GPa is applied to them.

The roughness of the parts surfaces before spraying was R_a 0.35–1.25, and as a result of hardening it increased on the body and bushing to R_a 2.5–2.6, and on the striker and peak to R_a 0.57–0.7. Before testing, the hardened surfaces were polished until the surface roughness was R_a 0.4–0.8.

The wear resistance of parts strengthened by applying a carbonitride coating was studied using the method described in Section 2.

Initial signs of destruction of the hardened layer appeared at the peak after 300 loading cycles in the form of scoring marks in zones "M" and "F". Similar damage to the surfaces of the striker was detected in the range of 400–450 cycles. Scores on the were detected on the bushing after 700 cycles, on the body – 800 cycles. After 800 loading cycles on the bushing in zone “C” there appeared areas 6–10 mm wide, oriented along the axis, on which the coating had almost completely come off. Due to the wear of the coating on almost all elements of the hardened parts, the tests were stopped after 1200 loading cycles.

Measurements of the tested parts show that the reduced diameter of the channels in the cutting zone increased to 125.8 mm. worn out V zone "N" on 0.2 mm, V zone "M" on 0.4 mm. Pika V zone "N" received wear 0.3 mm, V zones "M" And "F" - 0.85mm.

4.2. Character damage details

Damage type of parts hardened by applying vacuum-plasma carbonitride coating during testing shown on rice. 5.1 And 5.2. Damage details By place

the location of the zones of intensive wear and the general character are identical to those observed in the above-studied hardening variants.

On the body and bushing in zone “A” wear, work hardening and vaguely expressed, randomly located shear lines are observed.

Zone "B", characterized by a folded relief, is distinguished by shorter and smaller grooves-burrs. The relief is worn along the tops, to a greater extent on the bushing.

Zone "C" is characterized by the presence of grooves of uneven length. (from 5 to 10 mm). The grooves are small and smoothed. In this same zone, wear, work hardening and peeling of the surface layer are observed.

The bushing is predominantly flaking, the body is worn and smoothed. Zone "D" is characterized by running-in surfaces, uneven around the circumference, wear and minor work hardening.

The degradation of the working surfaces of the striker and the pick is also identical to the previously considered damage to these parts, strengthened by other technologies. A distinctive feature is the sharp difference in the degree of damage in diametrically opposite areas of each zone and the preservation of the relief of the grooves fr
om
wear and tear.

Zone "N", which is a smoothed spot and a relief of furrows with a general ring direction along the peripheral part of the spot, is characterized by an uneven profile of the furrows at the peak.

Different degrees of damage along the surface perimeter are also characteristic of the "M" zone. At the peak, the wear grooves on half the circumference are rough, deep, and not worn at the tops. On the striker, on half the contour, the grooves are short, densely located, and relatively shallow. On the second half, the grooves are smoothed to the base. The wear relief on the striker is rougher than on the strikers of the previously studied variants.

In zone “F” there is wear, work hardening, and peeling of the surface over half the circumference.

In some places, metal dragging is observed in the transition area to zone “E”.

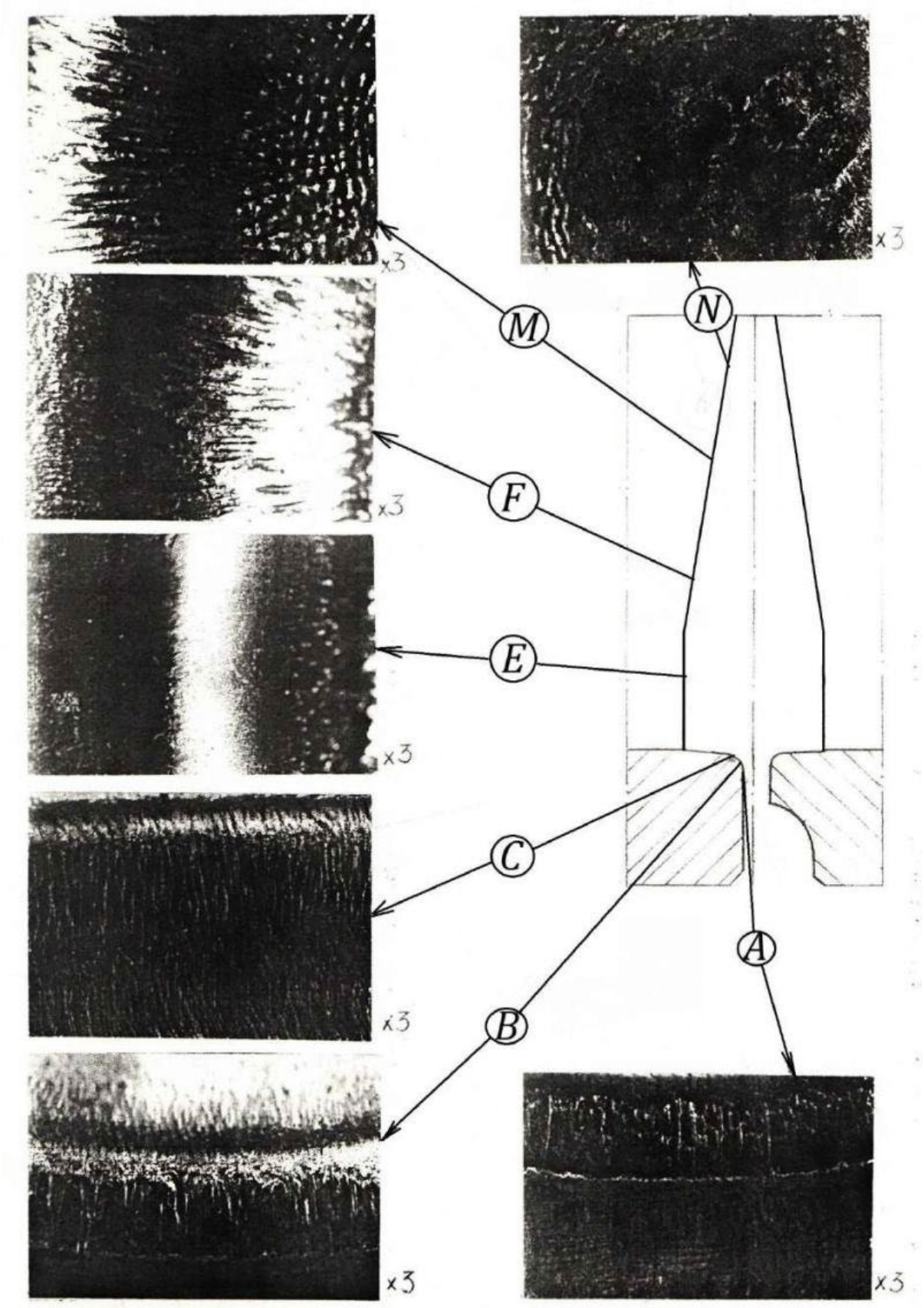

Figure 5.1. Wear peaks And bushings, reinforced application vacuum plasma carbonitride coating

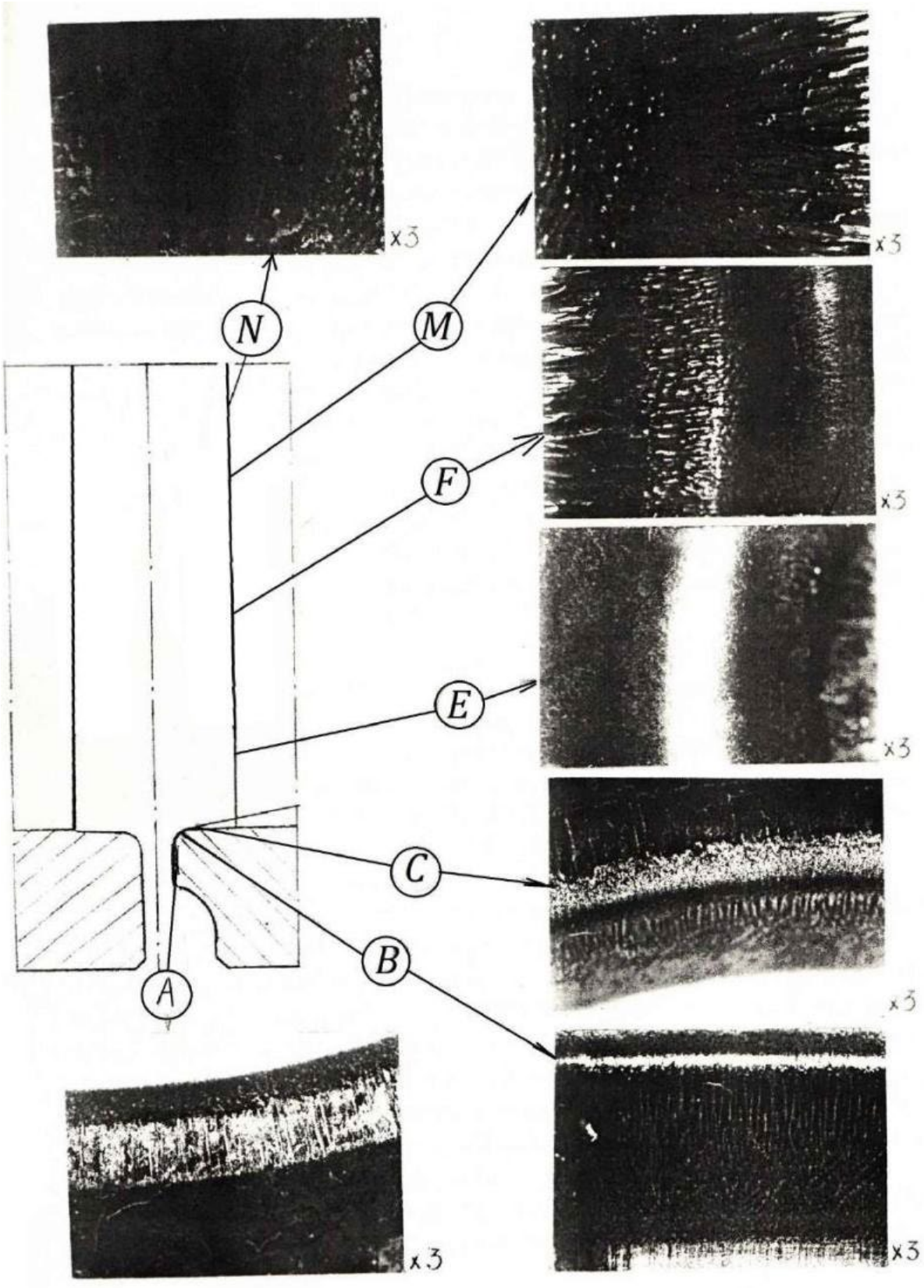

Figure 5.2. Wear corps And striker, reinforced application vacuum plasma carbonitride coating

4.3. Structural state material details

During the testing, the hardening coating on the working surfaces of all parts was almost completely worn out. Coating layers less than 10 μm thick were preserved only in certain areas of the body and bushing (in zones "A", "C" and "D"). No coating residue was observed on the striker and peak (Fig. 5.3 and 5.4).

Structural transformations in damaged layers of parts are unevenly distributed along the circumference and length of working zones. On the body, structural changes are observed in zones "B" to a depth of 0.25 mm, on the striker and peak - in zones "N", "M" and "F" to a depth of 0.2-0.3 mm. The hardness of the material in these zones is HV 510-645, the microstructure is troostosorbital, in places troostos-martensitic.

There are cracks on all parts in the area of damage. On the striker and the peak (especially on the striker) the cracks are developed, have a radial (along the bottom of the grooves) and grid orientation (see zone "M" in Fig. 5.4). On in the body And in the bushing cracks are revealed V zones "A" And
"IN". Depth their on in the body (channel) 0.20 mm, on in the bushing - 0.15 mm.

On striker And pique cracks are observed V zones "E", "M" And "F". Depth cracks on striker 0.3–0.8 mm, on pique - 0.1–0.3 mm.

4.4. Quality material details

Hardness material details is:
bushing – HRC 42–
43; peak – HRC
40; body – HRC 42–
43; striker – HRC
40–41.

On the striker and peak of this manufacturing option, as well as on similar parts hardened by ion-plasma chromium plating, there is a zone 20–30 mm wide, deep from the working surface, which differs from the rest of the section in its reduced hardness (HRC 32–35).

The microstructure of the material of the parts is of the sorbitol type, with a finely dispersed structure.

Results of testing the mechanical properties of the material The

tensile strength of the parts is presented in Table 5.1.

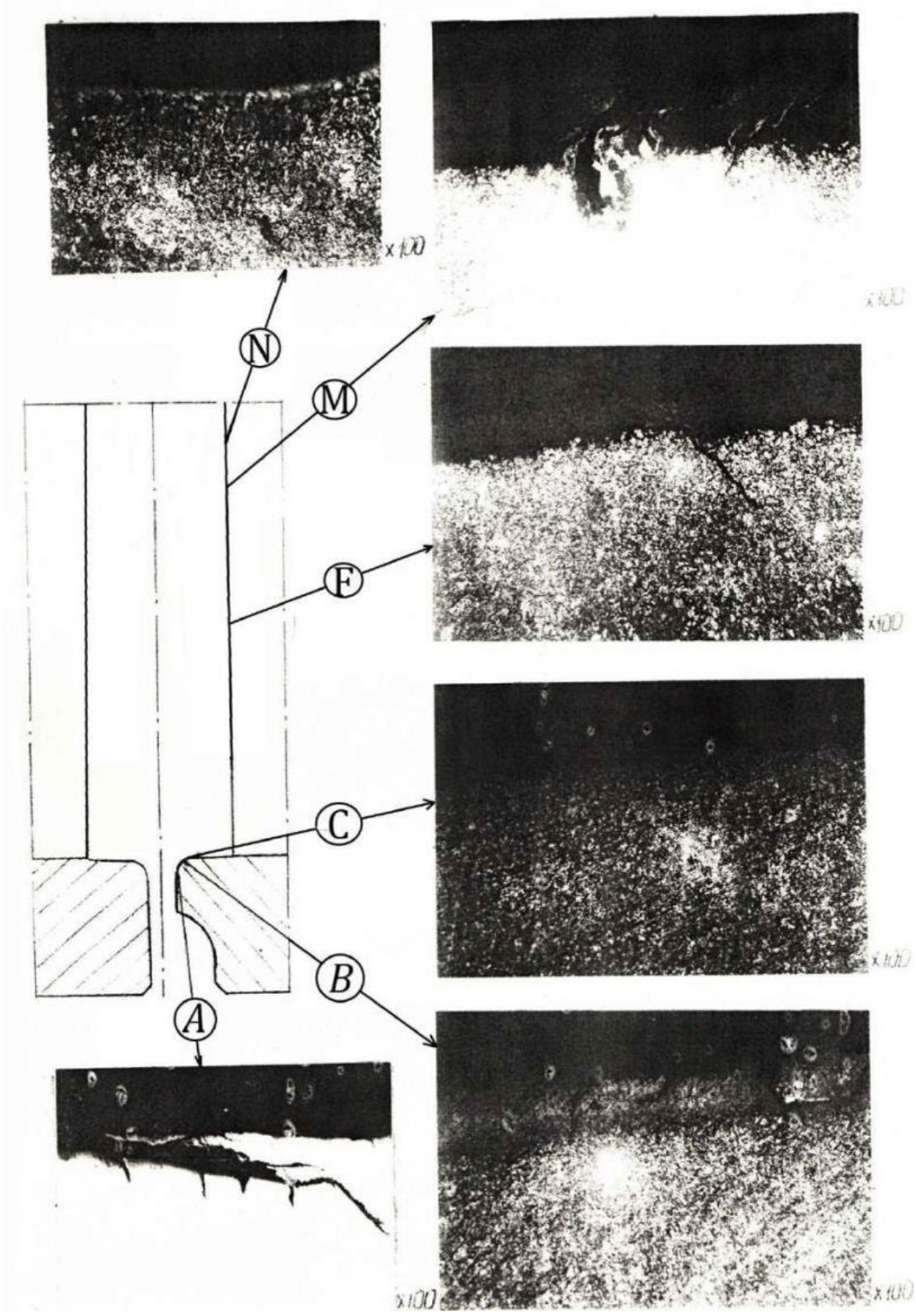

Figure 5.3. Structural changes material corps And striker, hardened vacuum-plasma carbonitride coating

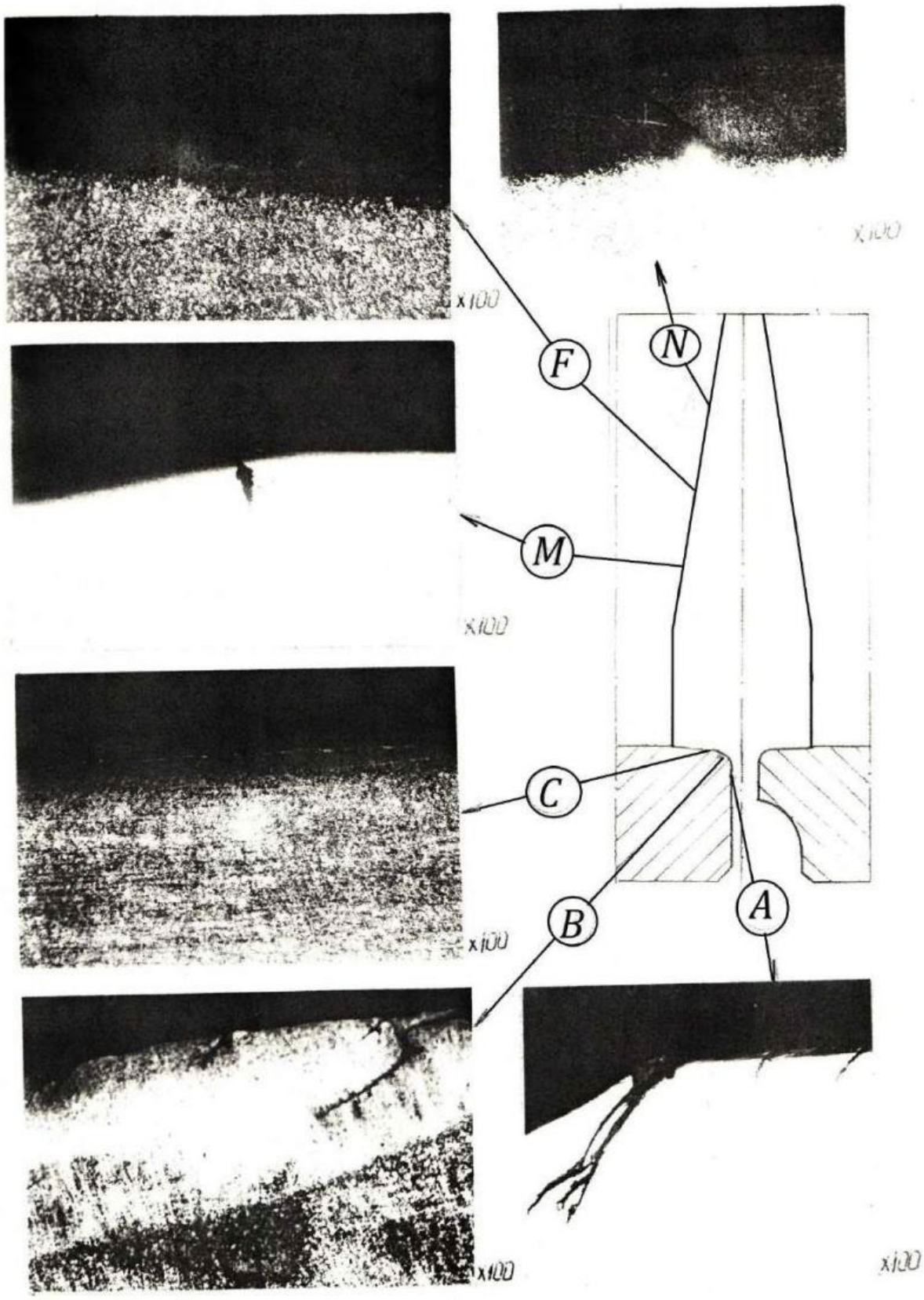

Figure 5.4. Structural changes material of the peak and bushing, reinforced vacuum-plasma carbonitride coating

Table 5.1

Mechanical properties material details, reinforced by application vacuum-plasma carbonitride coatings

Part name	Direction of cutting samples	Mechanical properties			
		σ_{in}, MPa	$\sigma_{0.2}$, MPa	δ, %	ψ, %
frame	axial	1460–1465	1370	14.0–15.0	51.0–54.0
	tangen-cial	1450–1470	1370	12.0–13.0	45.0–48.0
striker	axial	1395–1400	1330	15.0–16.0	54.0–59.0
	tangen-cial	1365–1370	1300–1310	11.0	51.0–54.0
sleeve	axial	1450–1470	1360–1370	13.0–16.0	51.0–56.0
	tangen-cial	1470–1480	1360–1380	11.0–12.0	36.0–39.0
peak	axial (def. (example)	1445	1360–1365	7.0–9.0	19.0–26.0
	tangen-cial	1450–1460	1370	13.0	54.0

4.5. Conclusion

I. Testing of parts strengthened by vacuum plasma application carbonitride coatings, shows, What an increase in wear resistance of 1.2 times is achieved compared to the original (not subjected to special strengthening) option.

2. The location of the damaged zones and their nature are identical to the location and nature of the zones found on parts not subjected to additional strengthening.

3. Along the perimeter of the working part of the striker and the peak, there is uneven damage and the degree of development of the surface relief.

4. Damage details consists of V wear and tear coatings, metal work hardening , education furrows-scuffs And cracks.

5. The hardening coating applied to the striker and the spear wore out completely during the testing process, but remained intact on the body and sleeve. only separate areas coatings.

6. Structural changes are distributed unevenly around the circumference details And characteristic For phenomena secondary hardening.

7. On all details devices there are cracks: on striker and a

dive depth 0.1–0.8 mm; on in the bushing Ikanale corps - 0.15–0.2 mm.

5. STUDY OF WEAR RESISTANCE OF PARTS HARDENED DETONATION SPRAYING

5.1. Terms and Conditions conducting strengthening processing

The working surfaces of the parts were strengthened by spraying VK25 alloy (80%) and PT-NA-01 (Ni 91) binder material %, Al 9 %) [123–125]. The thickness of the sprayed layer was 0.1 mm. The roughness of the surfaces of the parts before spraying was R_a 0.35–2.5. As a result of spraying, the roughness of the working surfaces of the parts increased to values of R_a 4.8–5.4 on the body and bushing and to 2.8–3.7 on the striker and peak.

The wear resistance of parts strengthened by detonation spraying was studied using bench tests (see section 2).

Initial signs of destruction of the hardened layer were detected pique after 400 cycles loading. Bullying risks V zones "M" And
"F" on the striker (see Fig. 6.1) appeared after 1300 cycles, on the bushing after 1050 loading cycles and on the body after 1700 cycles. The tests were carried out in the volume of 1800 cycles.

Measurements of the tested parts show that the reduced diameter of the channels in the cutting zone increased to 125.2 mm. worn out on 0.25 mm, peak in zones "M" and "F" received wear 1.2 mm.

5.2. Damage details devices V in the testing process

The type of damage to parts reinforced by detonation spraying is shown in Fig. 6.1 and 6.2.

The location and nature of damage to the surfaces of the parts are the same as those observed on previously examined sets of the device. The following characteristic signs of degradation of surface volumes are noted on the body and bushing material of parts as wear, work hardening, plastic deformation with education furrows radial directions, oxidation

surfaces. In zone "A" on the body, wear and work hardening are observed, and on the bushing, characteristic shear lines are observed.

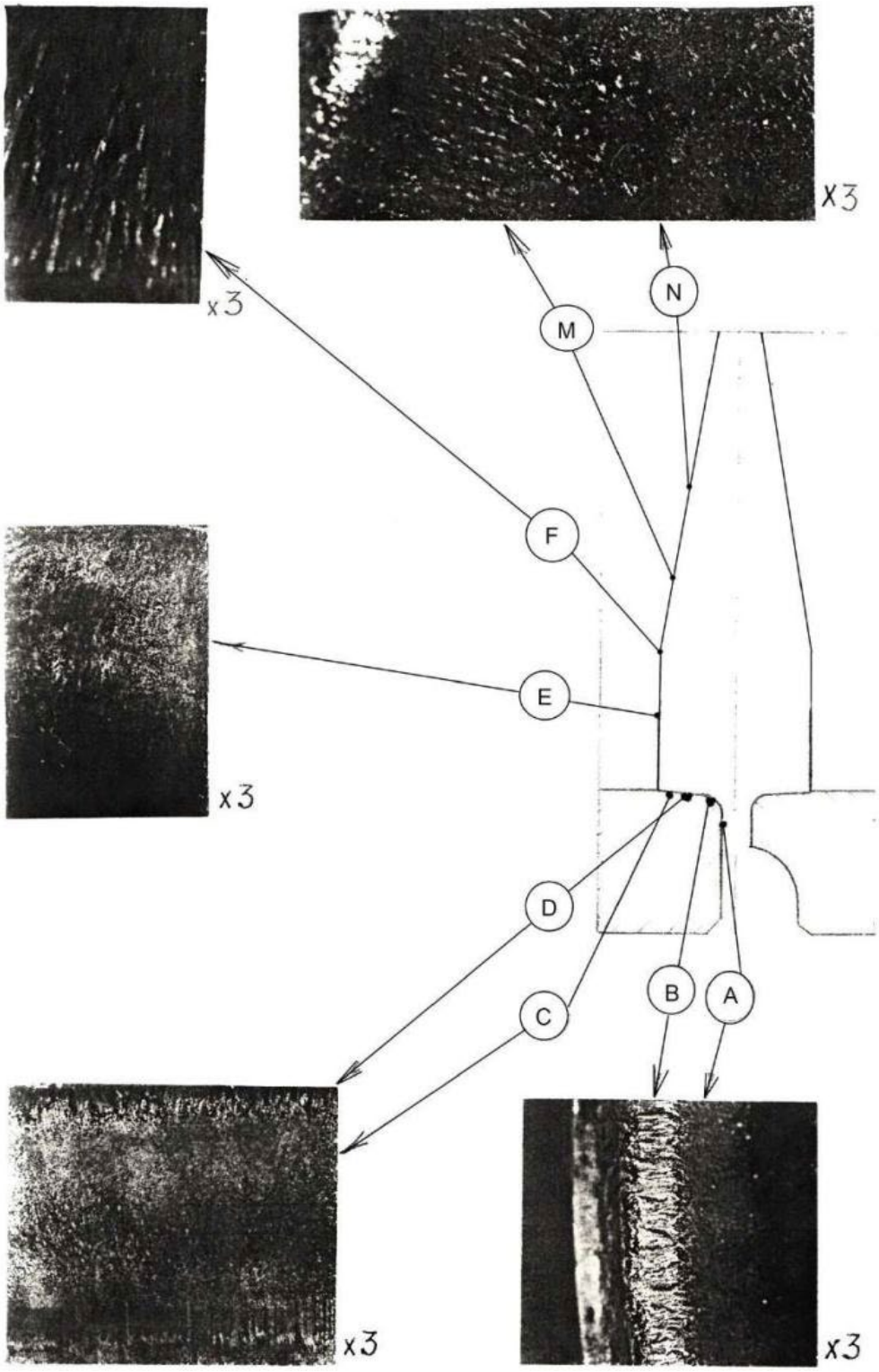

Figure 6.1. Damage peaks And bushings, reinforced by detonation spraying

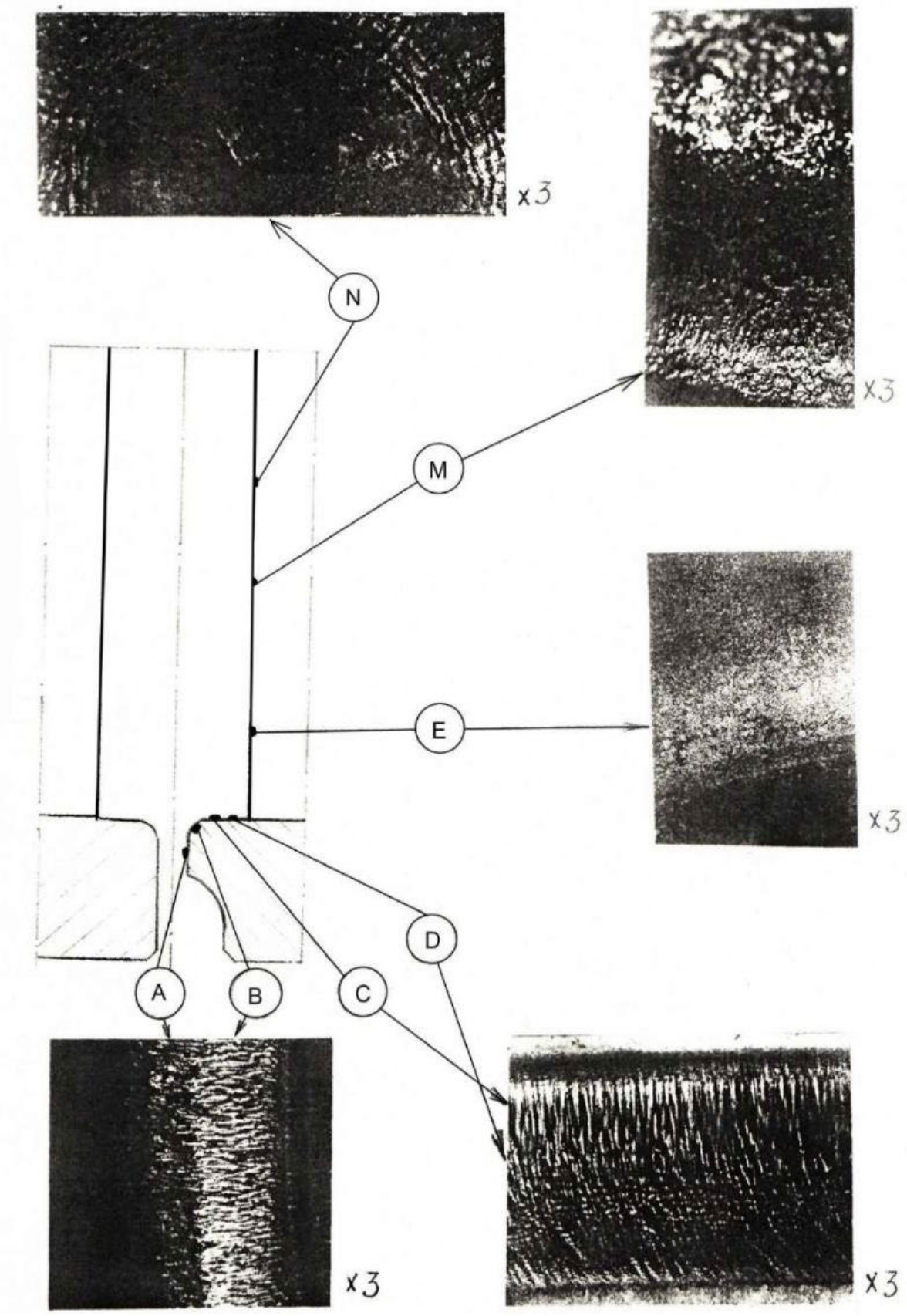

Figure 6.2. Damage corps And striker, reinforced detonation spraying

In zone "B" on the body there is a weakly expressed folded relief, on

the bushing the relief of the grooves is smoothed to the base, so that a picture of wave-like zones of crushing is observed. Peeling of the surface layers of metal in zone "C" is distinguished on the bushing, on body - the surface is smooth. In zone "D" there are traces of surface wear.

The wear pattern of the striker and the pick is typical. In the presence of a central spot and grooves in the peripheral part of the "N" zone, a folded relief of the grooves in the "M" zone, wear and tear plastic deformation with the formation of a rough, peeling surface in the "F" zone and wear with work hardening in the "E" zone, a lesser "roughness" of the relief and greater smoothness is noted for the striker and the peak. The degree of damage on the striker is less.

The body and striker are characterized by the presence of darker tarnish colors on the surface.

5.3. Cracking And characteristic structural state of the material of the parts

During the test, cracks formed on all the examined parts of the device **.** On the bushing, cracks up to 0.05 mm deep are isolated and are observed only in zone "C" (Fig. 6.3). On the body, cracks are visible in zones "A", "B" and "C", with a depth of 0.25 mm, 0.4 mm and 0.1 mm, respectively (Fig. 6.4). There are no cracks in zone "D".

No cracks were found on the striker and peak in the "N" zone. In the "M" zones of the striker and peak, there are cracks 0.3–0.4 mm deep. Cracks 0.1 mm deep are present in the "F" zone of the peak and 0.15 mm – striker. Cracks were found both in the zones of structural changes and outside them.

In the working zones of all the investigated parts of the device, during the testing, almost complete wear of the detonation coating occurred (see Fig. 6.3 and 6.4), only in zone "M" of the body and bushing are coating residues up to 20 μm thick observed. The same isolated areas are present on the striker in zone "F". Structural changes in the base metal were detected in the damage zones of all parts. On the body and bushing, structural transformations are observed in zones "A" and "B" to a depth of about 0.2 mm on the body and 0.15 mm on the bushing

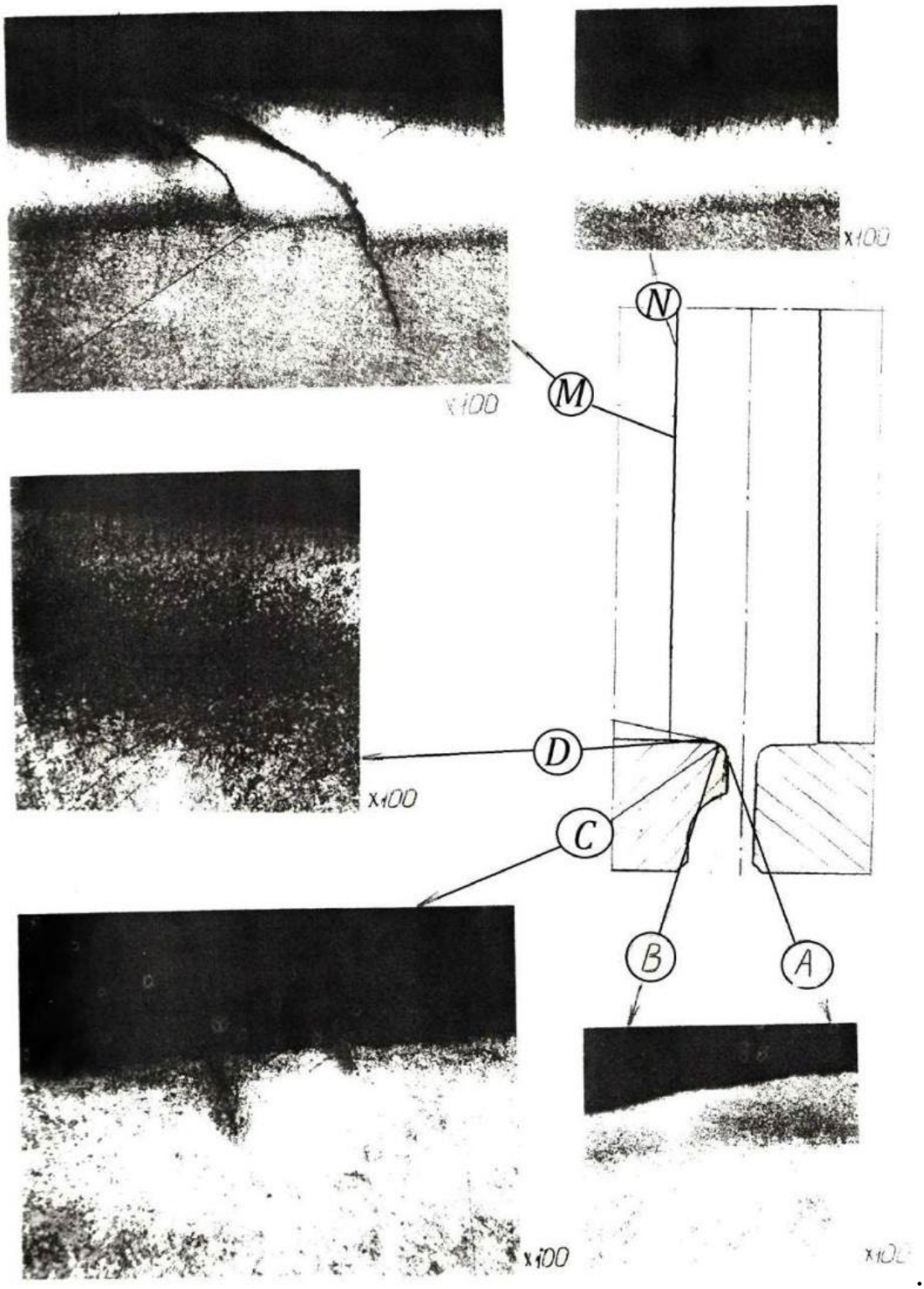

Figure 6.3. Structural changes material corps And striker, reinforced with detonation spraying

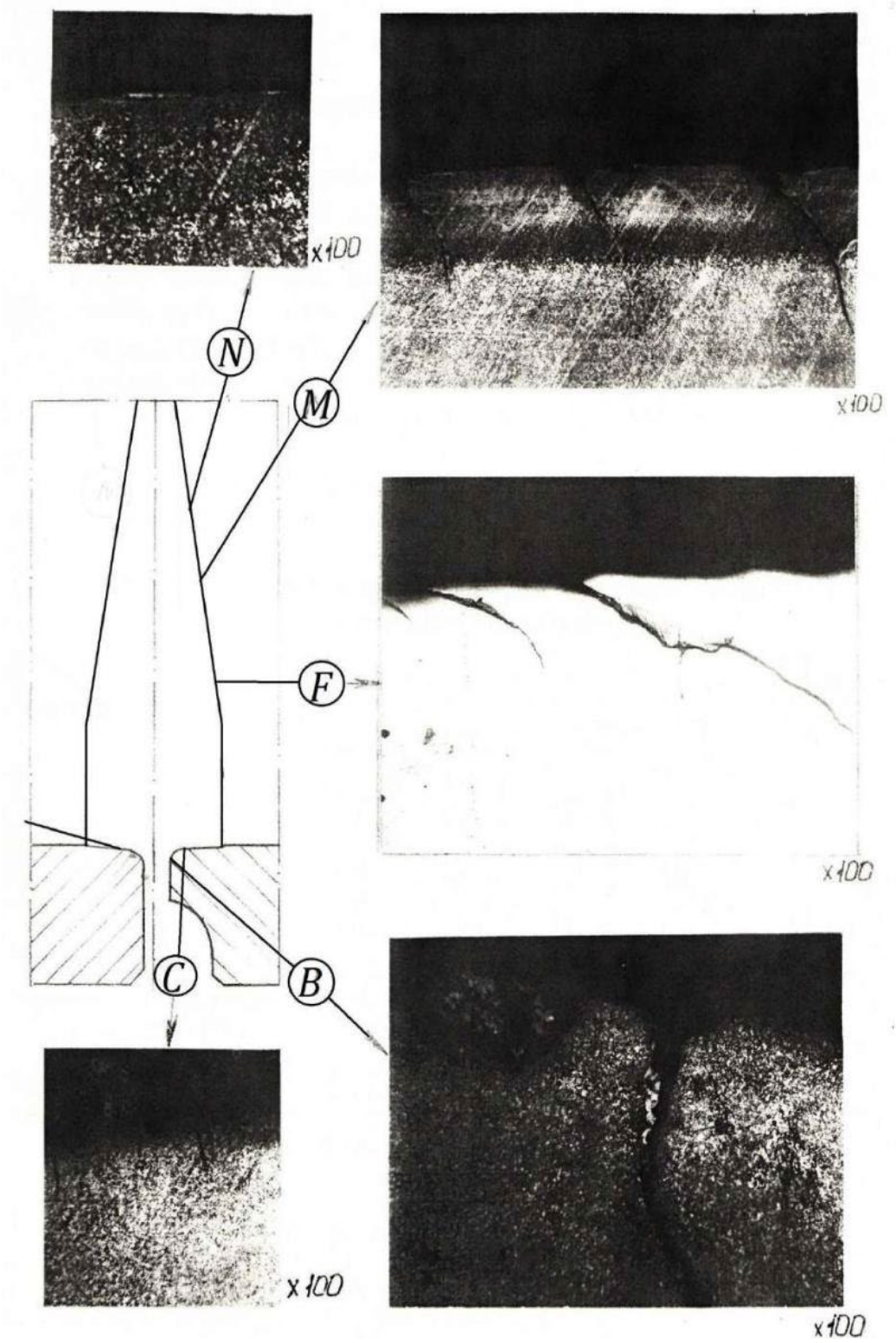

Figure 6.4. Structural changes material peaks And bushings reinforced with detonation spraying

The material hardness in these zones on the body is HV 414–540 and HV 414–645 on the bushing. In zones “C” of the body and bushing, the depth of structural transformations does not exceed 0.05 mm (HV 460–480).

Structural changes in the metal are observed on the striker and the peak V zone "M" on depth 0.25–0.3 mm And V zone "F" on depth 0.1–0.15 mm (for both) with a hardness of HV 340–475 (in places at the peak HV 560–675). In zones “E” on the striker and peak and in zone “N” of the striker, there are no structural changes. At the peak in this zone, the depth of structural changes is 0.15 mm (HV 340–560).

5.4. Quality material details

Hardness material details is:
sleeve – HRC 43; peak - HRC 33–40;
body – HRC 42–43; striker – HRC 43.
The microstructure of the material of the sorbitol -type parts is of a finely dispersed structure.
The results of testing the mechanical properties of the material of the parts for tension are given in Table 6.1.

Table 6.1

Mechanical properties material details, reinforced by detonation spraying

Part name	Direction of cutting samples	Mechanical properties			
		σ_{in}, MPa	$\sigma_{0.2}$, MPa	δ, %	ψ, %
frame	axial	1480–1490	1350–1360	14.0	49.5
	tangen-cial	1490	1360	11.0–12.0	39.0
striker	axial	1490	1390	12.0	39.0–42.0
	tangen-cial	1480–1490	1360–1390	14.0	51.0
sleeve	axial	1470–1480	1390–1400	12.0–12.5	45.0
	tangen-cial	1480	1400	13.0–14.0	52.0–54.0
peak	axial	1320–1325	1250	15.0–16.0	54.0
	tangen-cial	1310	1230–1240	13.0	42.0–47.0

From table. 6.1 it is visible, What mechanical properties material peaks after testing do not fully meet the requirements.

5.5. Conclusion

1. The results of testing parts strengthened by detonation spraying show that wear resistance is increased by 1.8 times compared to the original (not subjected to special strengthening) version.
2. The location of damage zones and their nature on parts reinforced by detonation spraying are similar observed on parts manufactured without additional strengthening.
3. Damage to parts consists of wear of the sprayed coating, work hardening, and the formation of grooves and nicks.
4. Structural changes observed in the surface layers of parts are characteristic of secondary hardening phenomena.

6. STUDY OF WEAR RESISTANCE OF HYDRAULIC HAMMER PARTS, REINFORCED ELECTRIC SPARK ALLOYING (EIL)

6.1. Parameters processing

All parts were strengthened by electric spark alloying with tungsten [126, 127]. The processing current power was 1 kW. In addition to strengthening with tungsten, the pike was additionally processed electric spark alloying with chromium at current power of 1.5 kW. The surfaces treated with electric spark alloying were ground until the roughness of the hardened surfaces of the parts was R_a 0.4–0.8.

During microscopic examination of the areas strengthened by EIL, located outside the loading zone during testing, it was established that in the body And in the bushing reinforced EIL areas have thickness 10–40 μm and a hardness of HV 600–650. On the strikers, the initial thickness of the hardened layer is 20 μm with a hardness of HV 600–650. The hardened zones in the section have the appearance of arc-shaped phases embedded in the surface layers of the metal of the parts. No structural changes are noted under this zone in the base metal.

The study of wear resistance of parts hardened with EIL was carried out using standard methods.

The tests were carried out until a wear pattern similar to that obtained on the parts was formed in the cavities of the housing and bushing, on the striker and peak. manufactured without additional strengthening (cm. rice. 3.1 and 3 . 2) . Initial signs of wear of the device parts in the form of small scratches and nicks were detected at the peak in zones “M” and “F” (see Fig. 7.1) after 300 loading cycles, on the bushing after 450 cycles, on the striker and body after 350 and 500 cycles, respectively.

After 1300 cycles loading character And degree damage to the parts corresponded to those obtained on the non-reinforced set. The given diameter of the housing channels in the shear zone increased to 125.5 mm, striker V zone "N" (cm. rice. 7.2) worn out on 0.35 mm, V zone "F" - on 0.55 mm. Wear peaks makes up respectively 0.35 And 1.15 mm.

6.2. Characteristic damage parts, reinforced electric spark processing

The general appearance of damage to parts hardened by electric spark treatment during testing is shown in Fig. 7.1 and 7.2.

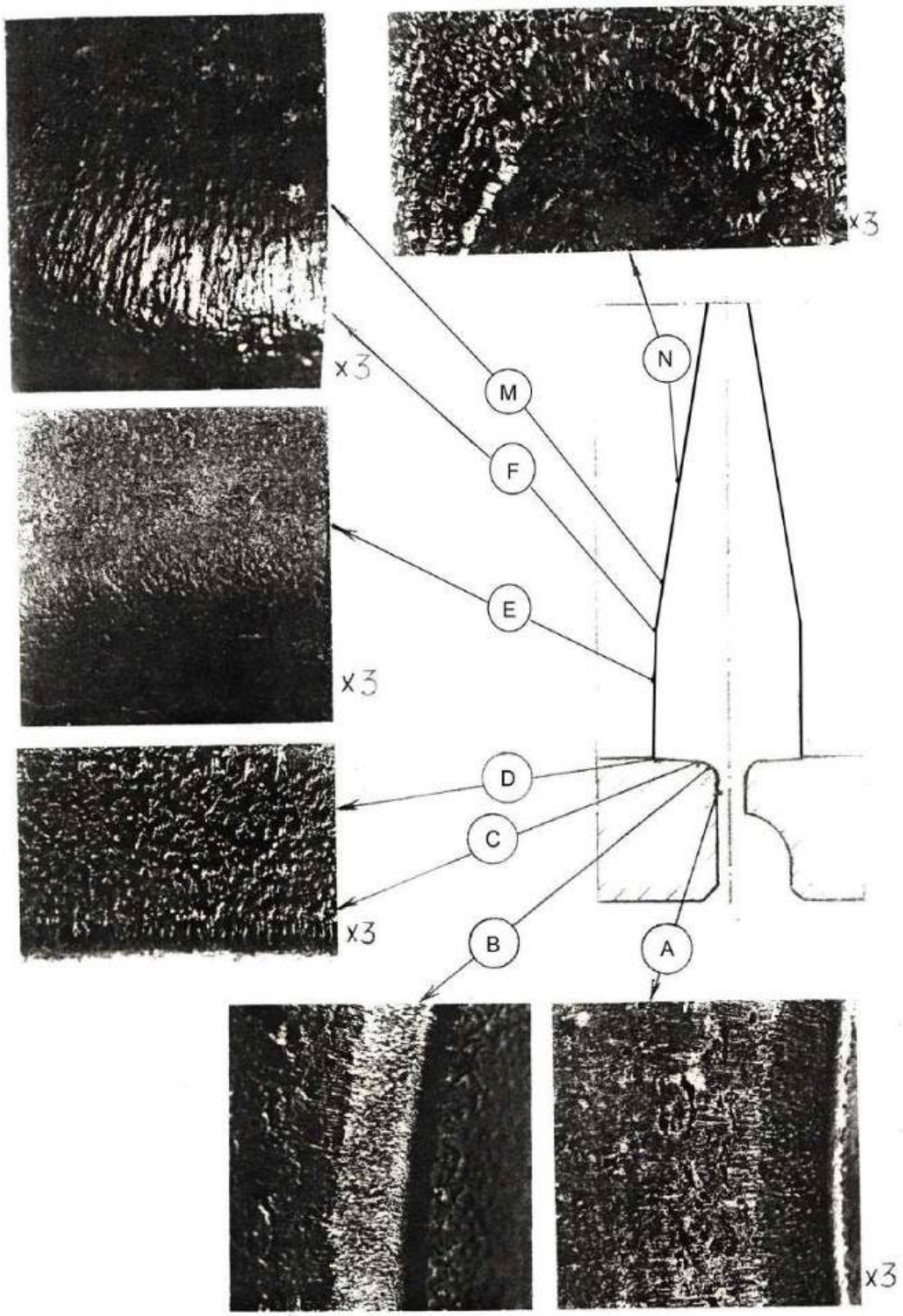

Figure 7.1. Wear peaks And bushings, reinforced EIL

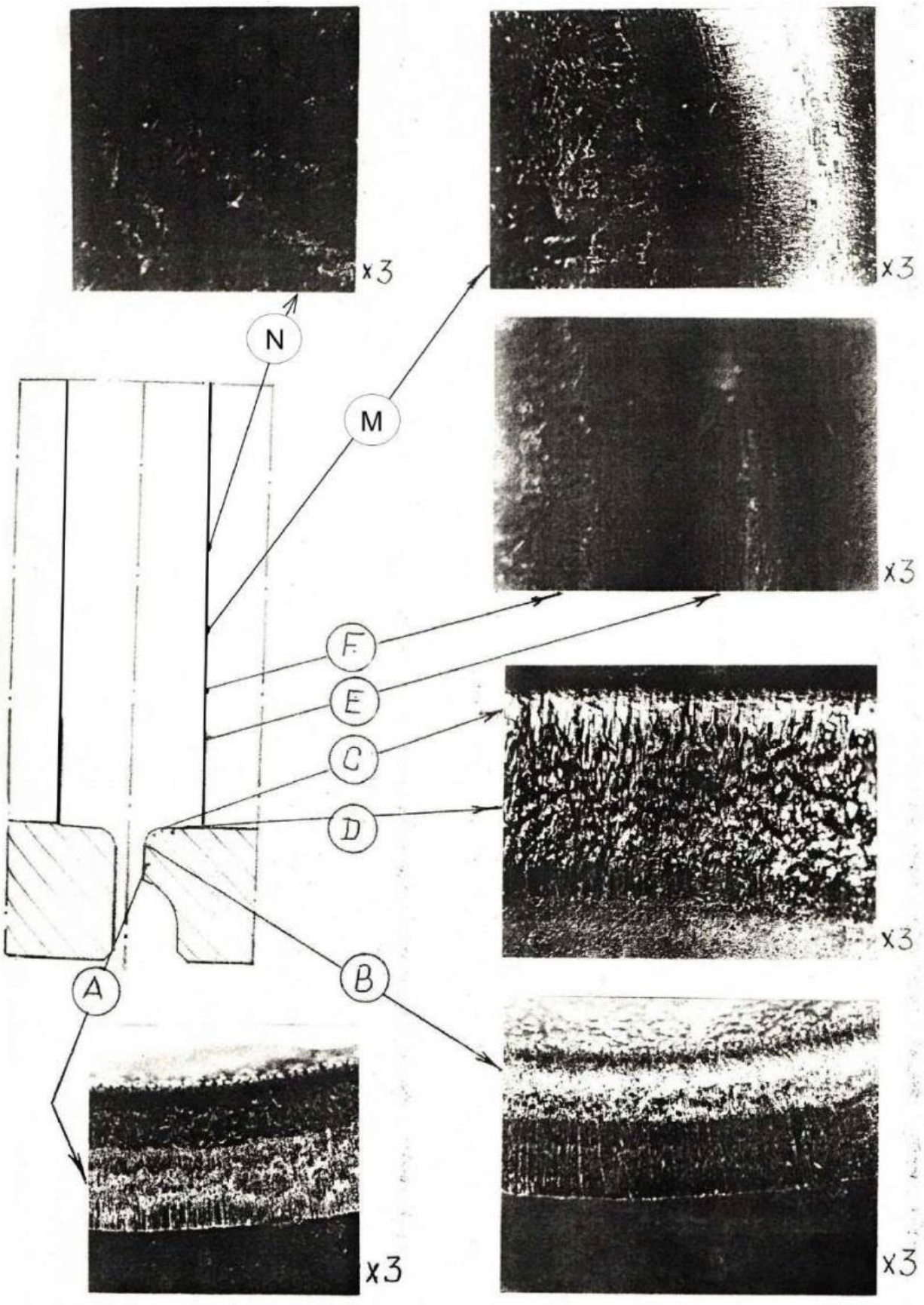

Figure 7.2. Wear corps And striker, reinforced EIL

The damage zones of the housing and bushing coincide with the corresponding wear zones of the housing and bushing, not subjected to additional strengthening (see Fig. 3.1 and 3.2). The nature of the damage is also identical to that observed previously, but the degree of damage (hardening, cracking, plastic deformation of the metal, wear with the formation of grooves) is significantly greater.

Less development of grooves is noted in zone "B" on the striker body compared to the bushing. In zones "C" there is intensive wear with the formation of a relief surface, more developed on the striker body. The abrasion of the original surface in the form of spots is visible in zones "D".

The “N” zone of the striker and the peak has the appearance of a round spot with a diameter of about 14 mm, and is distinguished by a smoothed and riveted surface, turning into a folded relief with a general direction.

A clearly developed relief formed by radial grooves characterizes the "M" zone. At the same time, at the peak, the degree of relief development is higher compared to the striker. The "F" zones, covering about half of the surfaces, are characterized by work hardening and smoothed surfaces.

At the peak, some roughness and peeling of the surface layer of metal is noted. Zone "E" has signs of uniform wear and work hardening.

On the upper parts (body and striker) there are darker colors of tarnish and carbon deposits.

6.3. Structural state material details, hardened by electric spark treatment

On the working surfaces of the tested parts it is noted wear of the surface volumes of metal strengthened by electric spark treatment (Fig. 7.3, 7.4). Cracks are possible; the metal along the walls of the cracks is smooth, covered with a dense layer of oxides. In the body and bushing, cracks with a depth of 0.1–0.3 mm are concentrated in the zones "IN". On striker And pique cracks mesh orientations depth 0.1–0.3 mm are observed in zones “N”, “M” and “F”. The greatest crack depth is observed in zones “M” – 0.3 mm at the striker and 0.1 mm at the peak.

On the working surfaces of all parts, the hardened EIL layer was preserved only in certain areas. On the body and bushing in zones "B" and "C" with a thickness of 5 μm to 0.01 mm. On the striker and peak, the remains of a layer with a thickness of 30 μm to 0.1 mm are observed only

in places on the surfaces "F". In zones "N", "M" and "E" the EIL layer does not appear.

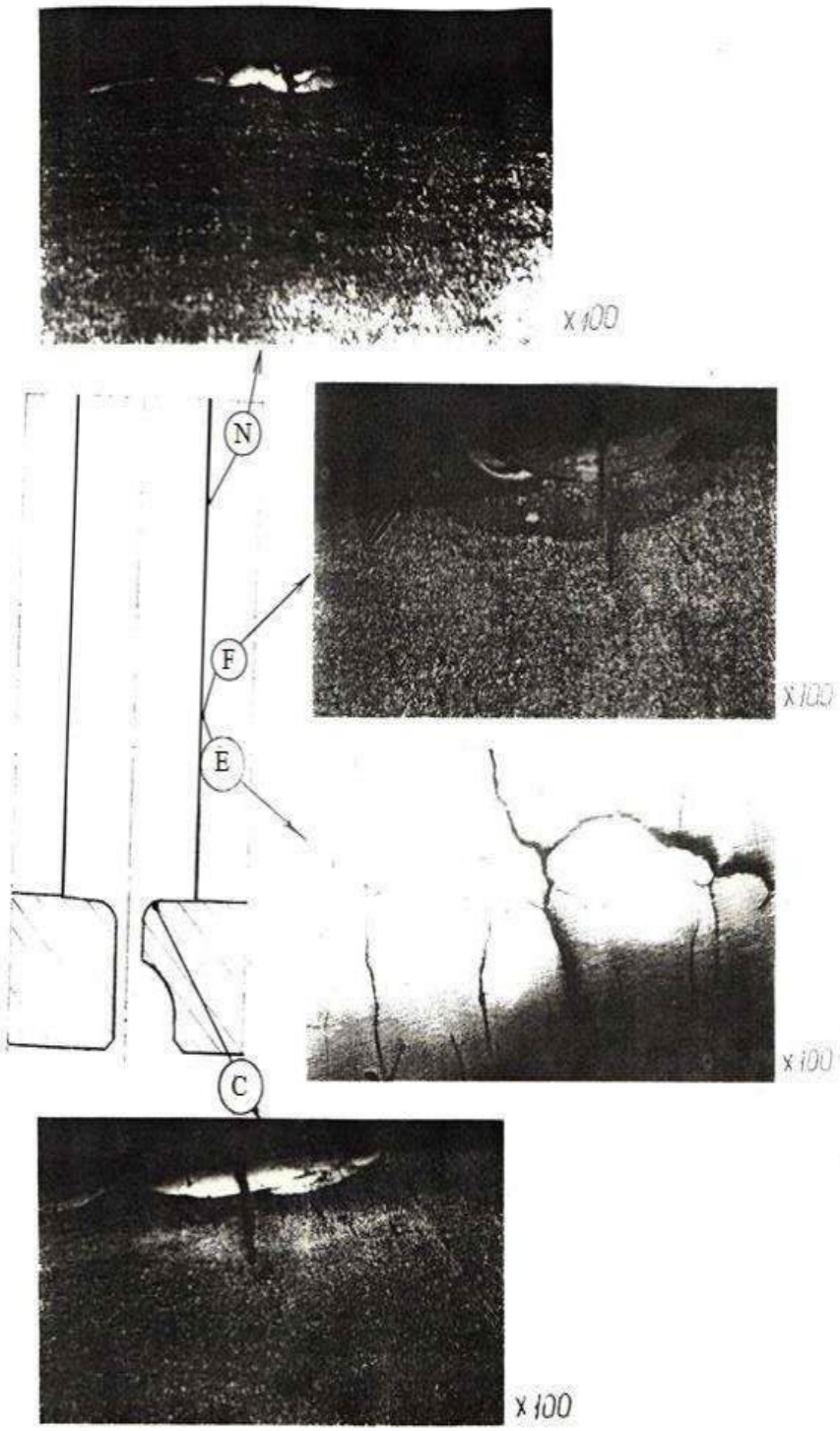

Figure 7.3. Change structures material corps And striker, reinforced with EIL

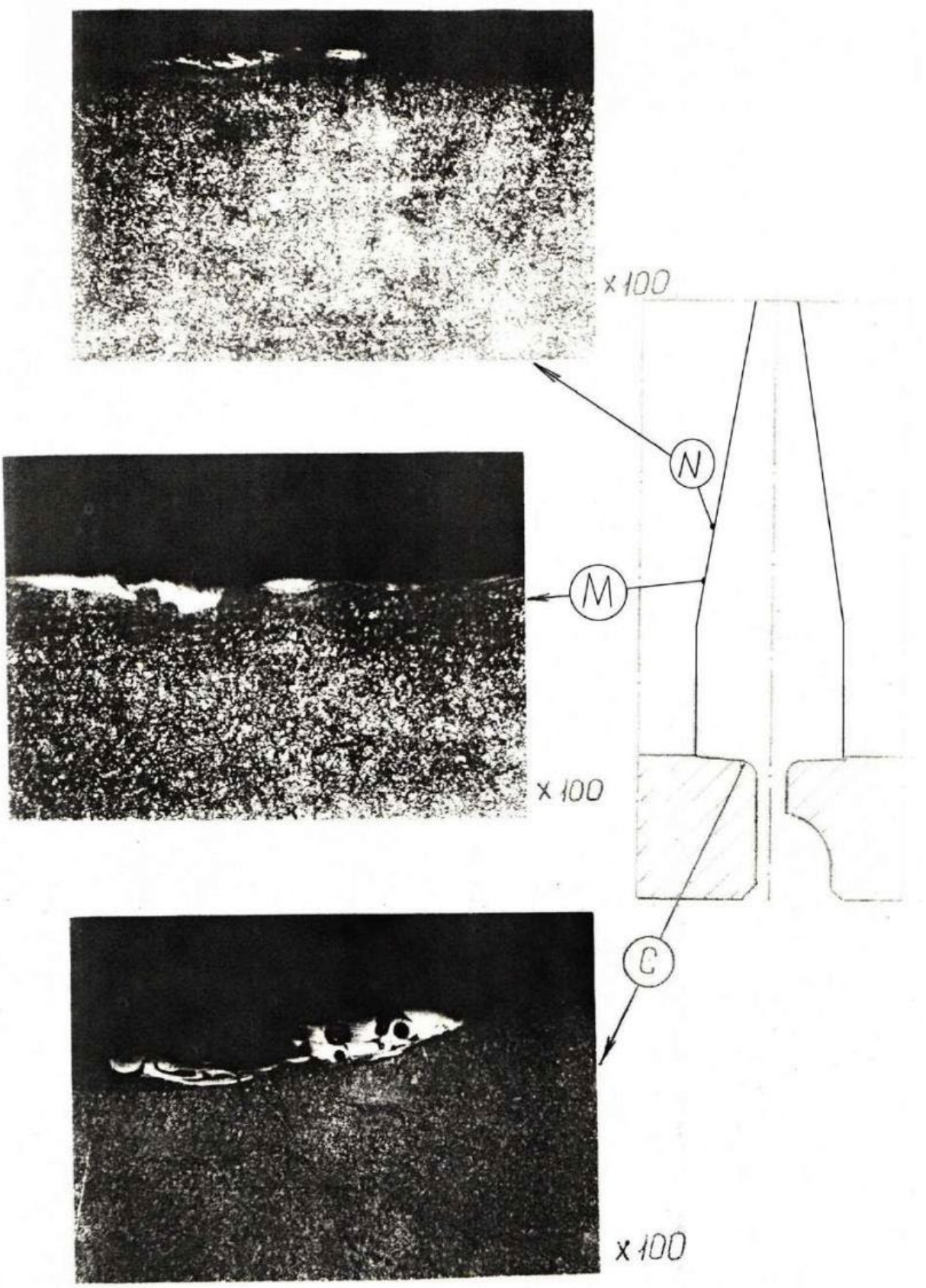

Figure 7.4. Change structures materials peaks And bushings, hardened by EIL

The base metal of all parts of the device directly at the working damaged surfaces underwent changes in structure and hardness. On the body and bushing, changes in structure to a depth of 0.1 mm (HV 400–500) are observed in zones “B” and in zone “C” peaks. There are no structural changes in zones “A” and “D”.

On the striker and the pick, structural changes are absent only in zones "E". In zones "N", "M" and "F", the depth of the zones of structural changes is 0.1-0.3 mm for the striker and 0.05-0.1 mm for the pick. Hardness material V these zones striker HV 420–500, peaks HV 400–460. Metal structure – troost-martensite and troost-sorbite types.

6.4. Analysis qualities material details

The hardness across the cross-section of the parts is practically constant and is:

frame - HRC 45;

striker – HRC 45;

sleeve – HRC 45;

spear – HRC 40.

Microstructure main metal consists of from sorbitol.

The mechanical properties of the material of the device parts were determined at temperature 20 °C on samples, carved in axial and tangential directions. The results of mechanical properties tests are given in Table 7.1.

Table 7.1

.

Mechanical properties materials researched parts reinforced with EIL

Part name	Direction of cutting samples	Mechanical properties			
		σ_{in}, MPa	$\sigma_{0.2}$, MPa	δ, %	ψ, %
1	2	3	4	5	6
frame striker	axial	1475–1485	1430–1510	13.0	56.0
	tangen-cial	1480–1490	1400–1410	12.5–13.0	48.0

End table. 7.1

1	2	3	4	5	6
striker	axial	1485–1400	1360–1375	14.0–14.5	54.0
	tangen-cial	1490	1330–1365	9.0–10.0	29.5
sleeve	axial	1470	1400–1410	12.0–13.0	54.0–59.0
	tangen-cial	1470–1480	1340–1390	12.0–13.0	42.0–51.0
peak	axial	1070–1080	1015–1035	14.0–15.0	64.0
	tangen-cial	1330–1340	1250–1260	14.0–16.0	38.0–59.0

From Table 7.1 it follows that the mechanical properties of the peak material, received on samples, cut out V axial direction, do not fully meet the requirements.

6.5. Conclusion

1. Electric spark alloying with tungsten and chromium at a processing power of 1–1.5 kW ensures local hardening of the surface volumes of the material of parts to a depth of 10–40 μm and a hardness of HV 600–650.

2. The results of tests of parts hardened with EIL indicate that What achieved increase wear resistance parts by ~ 1.3 times compared to the original (not subjected to additional strengthening) version,

3. The locations of damage zones and their nature on parts strengthened by EIL are identical to those observed on tested parts manufactured without additional strengthening and using LTO.

4. For parts of the device reinforced with EIL, a significantly higher degree of development is noted damage by compared to the non-reinforced version. in the body and in the bushing V zones "A" (cut) and "D" (channel) the hardened layer is almost completely worn out, in the rest zones preserved only leftovers layers EIL thickness from

5 μm to 0.01 m. On the strikers, the remains of the EIL layer of the same thickness are noted only in zone “F”.

5. Structural changes occurring during testing in the surface layers of parts are characteristic of secondary hardening phenomena, resulting in a lower level of hardness than in the parts of previous versions.

7. STUDY DETAILS, REINFORCED BY APPLYING GALVANIC CHROME COATINGS

7.1. Parameters processing details

The wear resistance of hydraulic hammer parts strengthened by applying a galvanic chromium coating was studied using the method described above (see Section 2). Tests were performed until the chromium coating on the striker and in the housing channel, on the bushing and the peak was destroyed [128–130].

The thickness of the chrome coating is made within the following limits: body – 40–140 μm; striker – 20–40 μm; bushing – 30–67 μm; peak – 64–150 μm. The roughness of the parts' surfaces before applying the coating was 0.32–0.8 μm. The roughness parameter of the chrome coating is $Ra_{0.57–3.2}$. Before testing, the hardened surfaces of the parts were polished until the roughness specified in the drawing was obtained.

Initial signs of chrome coating destruction in the form of 6–8 mm diameter blisters were detected at the peak after 80 loading cycles. At 150–180 cycles, the blisters began to crumble down to the base metal. With further loading, the areas free of coating increased in size, merging with each other. On the striker, initial scoring marks appeared after 500 loading cycles in zones "M" and "F". Wear of the coating on the striker body and bushing was detected in zones "A" and "B" after 800 loading cycles on the bushing and 900 cycles on the body. After 1860 cycles, the nature and extent of damage to the body and bushing were close to those obtained on non-hardened parts. The reduced diameter of the body channels in the shear zone increased to 125.2 mm, the striker wore out in zone "M" by 0.4 mm, peak received wear V zone "N" on 0.05 mm, V zone "M" - on 1.3 m.

7.2. Wear chrome plated details hydraulic hammer

The type of damage to the device parts, strengthened by applying a galvanic chromium coating, during testing is shown in Fig. 8.1 and 8.2.

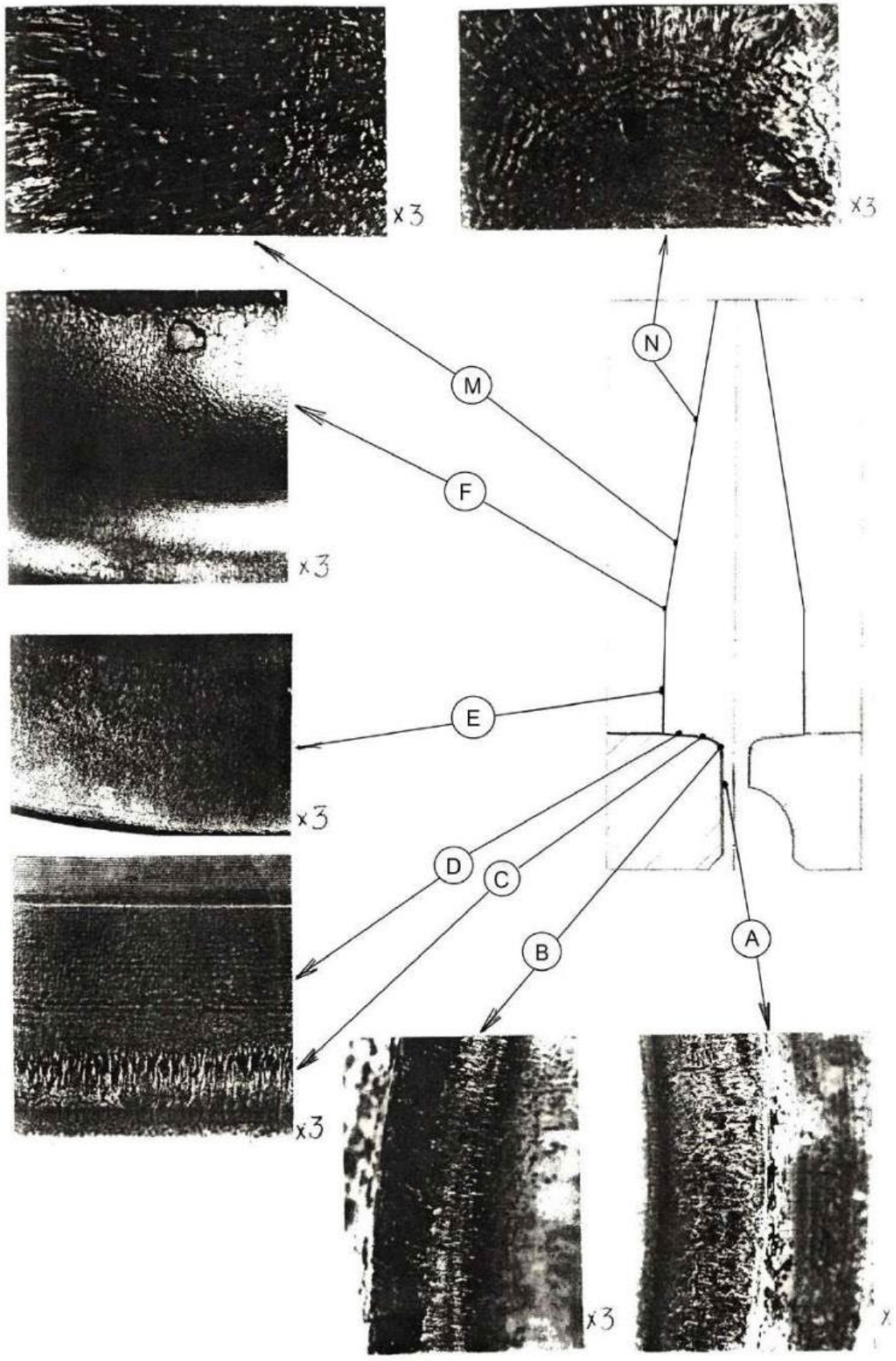

Figure 8.1. Damage peaks And bushings, hardened by galvanic chromium plating

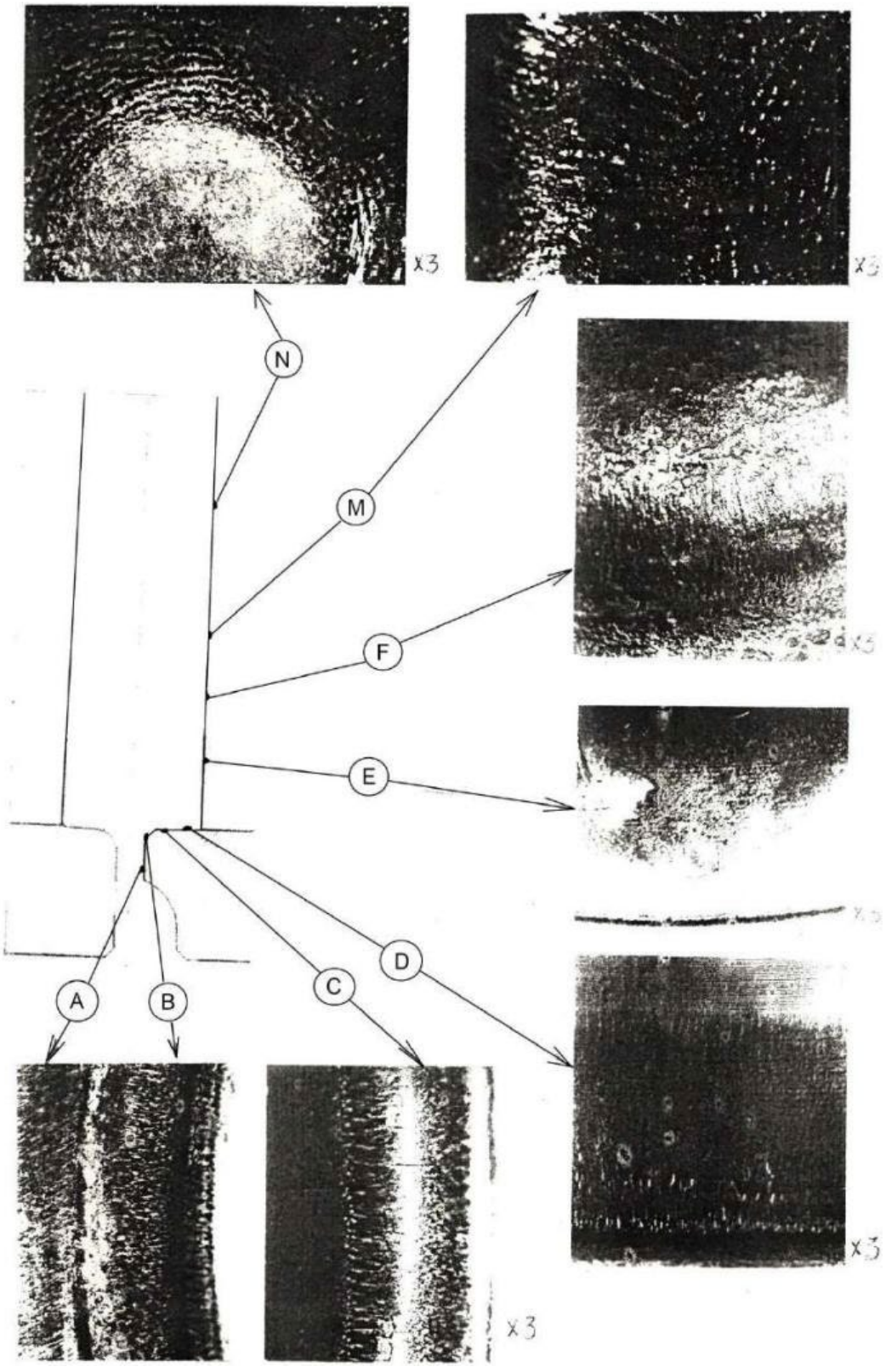

Figure 8.2. Damage corps And striker, hardened by galvanic chromium plating

The damage zones of the housing and bushing are identical in location and linear dimensions to those observed on those not subjected to additional strengthening (see Fig. 3.1 and 3.2). However, the degree of damage development of this set is somewhat higher compared to the original.

A study of the working surfaces of the parts shows that in damaged areas there is wear of the coating, work hardening, plastic deformation of the metal, formation of scuffs, cracking and oxidation (appearance of tempering colours).

In zones “A” (see Fig. 8.1 and 8.2) work hardening, metal wear and shear deformations oriented along the circles equidistant to the cavity of the housing. In this zone, additional grooves-scuffs oriented in the radial direction are noted. On the housing and bushing in zones "B" a folded relief is revealed, formed by wear grooves oriented along the channel of the housing (bushing). This wear pattern is more developed on the bushing. On the housing, the relief of the grooves is somewhat smoothed.

Surfaces "C" are characterized by intensive wear, work hardening and peeling of the surface layer material. The peeling process is more developed on the bushing, wear - on the body. Surfaces "N" are characterized by minor wear and tarnishing colors of light shades.

The "N" zone of the striker and the peak has (see Fig. 8.1 and 8.2) the appearance of a spot with a diameter of 17-18 mm with a smoothed, worn, work-hardened, matte surface. The peripheral area of the "N" zone has a border in the form of annular grooves of deformed metal.

In the "M" zones, there are also grooves of wear of the metal of an annular direction. In these zones of the striker and the peak, the coating is almost completely absent and the relief of the grooves-scratches is observed in the base metal of the parts.

The transition from zone "M" to zone "F" on the striker is smoothed. At the peak, the boundary between these zones is sharp and stepped. The chrome coating, partially preserved in zone "F", has traces of wear and work hardening. There are isolated areas with a diameter of up to 4 mm of chipping of the coating across the entire thickness to the base metal.

IN zones "E" celebrated wear And slander coatings.

7.3. Study structural states material in the working areas of the device parts

On the working surfaces of the studied parts, partial or complete wear of the chrome coating with the formation of local chips occurred during the tests. On the channel and bushing, the remains of the chrome layer are fixed on surfaces "A", "C" and "D". On surfaces "B", the chrome coating is completely worn out. The thickness of the remaining remains of the chrome layer is: on the body – from 20 μm in zone “C” to 50 μm in zone “A”; on the sleeve – from 2–3 μm in zone "WITH" to 60 microns V zone "D". On striker V zone "N" - 10 μm, "F" -
20 μm; "E" - 5 μm. At the peak, respectively, 10, 20 and 200 μm. Unevenness and discontinuity of the remains of the chrome coating layer are noted.

On all parts in damaged areas, structural changes and changes in the hardness of the base metal are observed both on surfaces free from the chromium coating and under the layer. chromium. Mainly structural changes on the body and bushing are observed in zones “A”, “B” and in places “C” (Fig. 8.3 and 8.4). The depth of the zones of structural changes is 0.1–0.2 mm (HV 400–570). On the striker and peak, structural changes with a depth of 0.1–0.3 mm (HV 370–480) occur in zones "N", "M" and "F". The structure of the metal of the parts in the zones of structural changes of the troostosorbite and troosto-martensite types of finely dispersed structure.

All the examined parts have cracks in some places. If there is a chromium layer on the surface, the crack runs along the layer and further is developing By base metal. Cracks in a fracture have an arched appearance with a clearly defined contour, and are distinguished by smooth walls and oxidation.

On the body and bushing, cracks with a depth of 0.1–0.3 mm are observed in zones “A”, “B” and “C”. There are no cracks in zones “D”. On the striker and peak, cracks are not detected only within the smooth part of zone “N”. The depth of the cracks in in the peripheral parts of the “N” zones is 0.1–0.2 mm, in the “M” zones – 0.3–0.4 mm, in the “F” zones – 0.1–0.3 mm and in zones “E” – 0.05–0.1 mm.

7.4. Quality materials details

Hardness material details is:
frame striker - HRC 44;
striker - HRC 44–45;
sleeve - HRC 44–45;
peak – HRC 40–41.

Microstructure of parts is sorbitol type finely dispersed structure.

The results of testing the mechanical properties of the material of the parts at 20 ° C are presented in Table 8.1.

Table 8.1

Mechanical properties material details , reinforced by applying a galvanic chrome coating

Part name	Direction of cutting samples	Mechanical properties			
		σ_{in}, MPa	$\sigma_{0.2}$, MPa	δ, %	ψ, %
frame striker	axial	1450–1450	1420	14.5–16.0	51.0–54.0
	tangen-cial	1455–1460	1395–1410	13.0–14.0	42.0–45.0
striker	axial	1490–1540	1370–1390	14.0–16.0	54.0
	tangen-cial	1495–1515	1400–1410	12.0–12.5	42.0–45.0
sleeve	axial	1470–1480	1420	14.0	48.0–54.0
	tangen-cial	1470–1475	1420–1440	11.0–12.0	42.0
peak	axial	1350–1370	1290	14.0–16.0	59.0
	tangen-cial	1330–1370	1260–1270	12.0–14.0	42.0

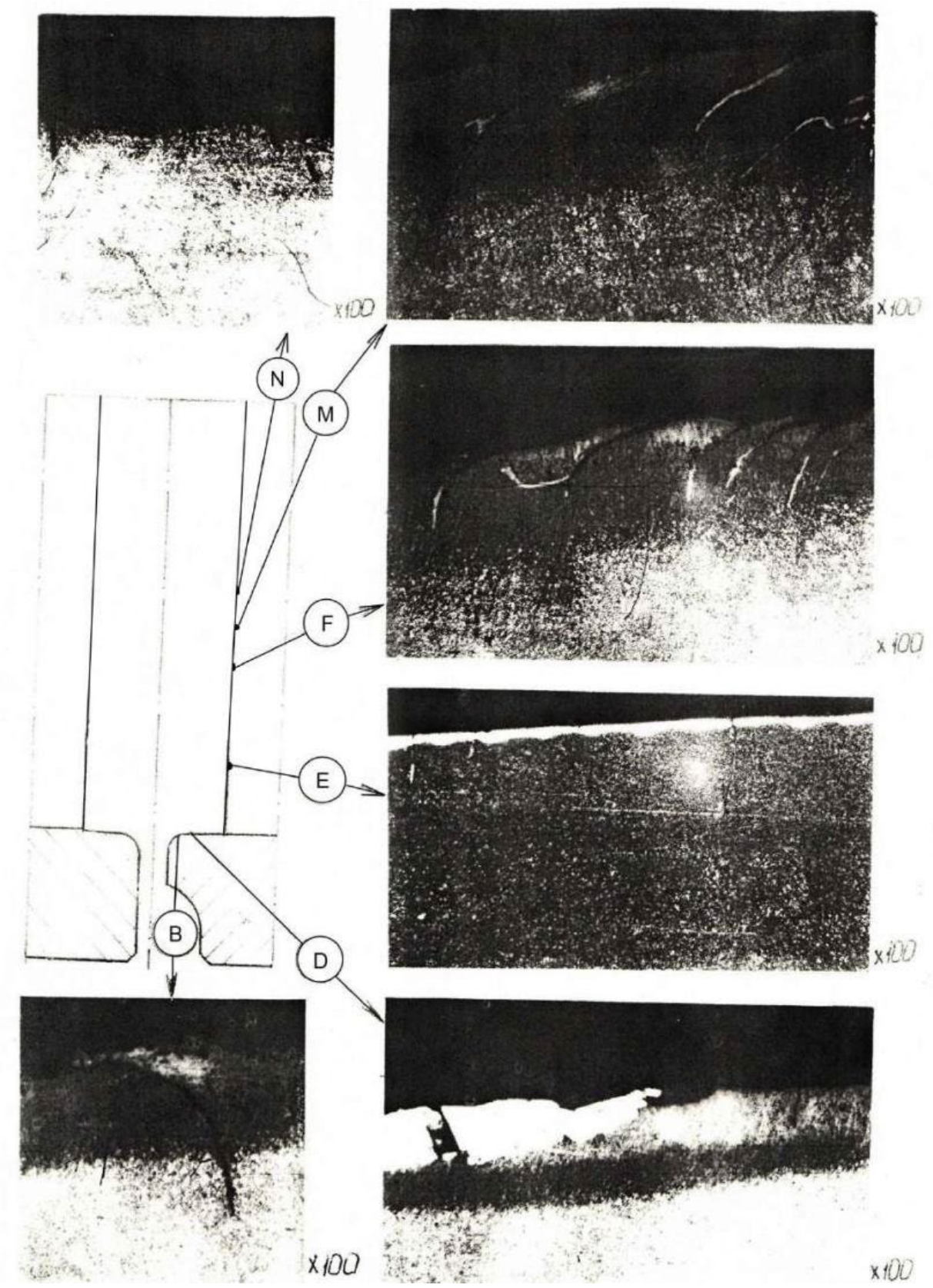

Figure 8.3. Structural changes material corps And striker, hardened by galvanic chromium plating

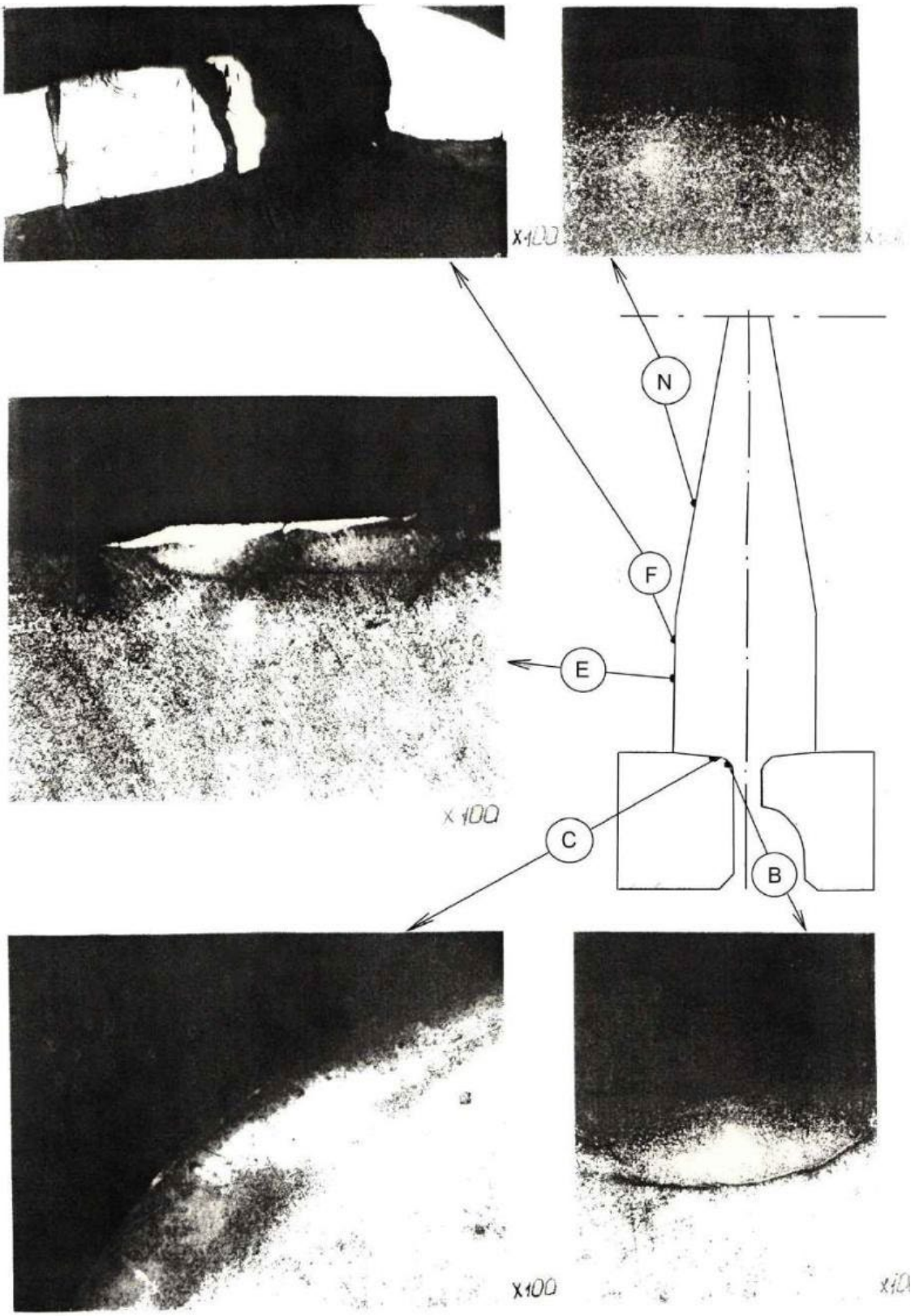

Figure 8.4. Structural changes material peaks And bushings hardened by galvanic chromium plating

From Table 8.1 it follows that the mechanical properties of the material of the parts, obtained during tensile testing, satisfy the requirements imposed on the parts.

7.5. Conclusion

1. Strengthening of hydraulic hammer parts for wear resistance testing of the body and bushing models is performed by galvanic chromium plating with the formation of protective layers on the body and bushing within 30–140 μm; on the striker and peak – 20–150 μm.
2. The results of testing parts strengthened by galvanic chromium plating show that the wear resistance of the housing and bushing models is increased by ~1.86 times compared to the original (not subjected to additional strengthening) version.
3. The locations of damage zones and their nature on parts strengthened by galvanic chromium plating are similar to those observed on parts manufactured without additional strengthening and using LTO.
4. Damage to parts consists of wear of the chromium layer and the base metal in places where the chromium coating is destroyed, work hardening, the formation of grooves and cracks in places.
5. The peculiarity of damage development during testing of parts of this type of hardening consists of significant wear, and in some areas, chipping, of the chrome coating, which caused unevenness of the remaining chrome layer within different zones of the body, bushing, striker and peak.
6. Structural changes occurring during testing in the surface layers of parts are observed both on surfaces free from coating and under the chromium layer; they are characteristic of secondary hardening phenomena.
7. The change in structure and hardness is more pronounced on the body and sleeve.

8. STUDY WEAR RESISTANCE PARTS STRENGTHENED BY ION-PLASMA CHROME PLATING (OPTION 1)

8.1. View damage details

Ion-plasma coating with plastic chromium (Cr3) was carried out by vacuum-arc deposition using radial and end plasma sources [131–136]. The heating temperature housings, bushings And picks camera composed 450 ± 50 °C, striker – 350 ± 50 °C. Thickness coatings: cases – 47–50 μm; bushings – 35–
75 μm; striker – 12–15 μm; peaks – 60–70 μm. Surface roughness parts before coating – R_a 0.4–1.2, after chromium plating the surface roughness parameter changed to values R_a 0.68–3.41. After applying the coating, the parts were polished until the coating roughness was R_a 0.4–0.8.

Study wear resistance details, reinforced ion-plasma chromium plating was performed according to the developed method. Initial signs destruction chrome coatings V in the form of small scratches and nicks appeared at the peak after 200 loading cycles . Bullying risks on surfaces striker (zone "M" And "F") identified after 350 cycles. Wear coatings on in the bushing V zone "B" is marked after 550-600 cycles, on the body - 900 cycles. On the bushing additionally, after 650–700 cycles, at a distance of 5–7 mm from the cut, areas coloring coatings, which To 900 cycle spread throughout the entire perimeter of the channel, which led to jamming devices. That's why after 1000 cycles loading the test was terminated, measurements showed that the reduced diameter channel corps V zone cut increased to 125.1 mm. The striker is worn out on 0.2 mm, peak received wear V zone "N" - 0,1 mm, V
zones "M" And "F" on 0.35 mm.

The nature of damage to the body, bushing, striker and peak, strengthened by ion-plasma chromium plating, during testing is shown in Fig. 9.1 and 9.2.

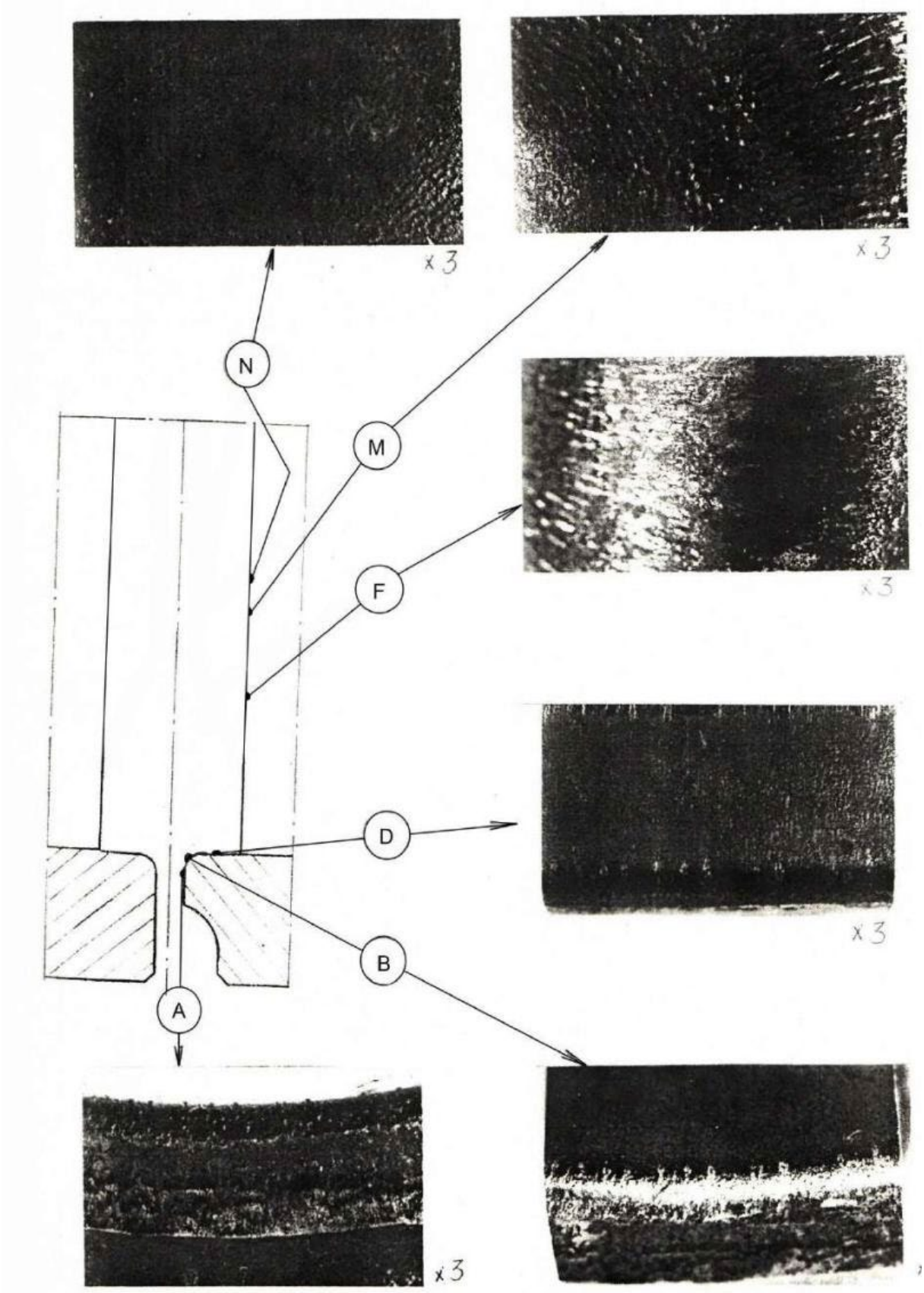

Figure 9.1. Wear corps And striker, reinforced ion plasma chromium plating

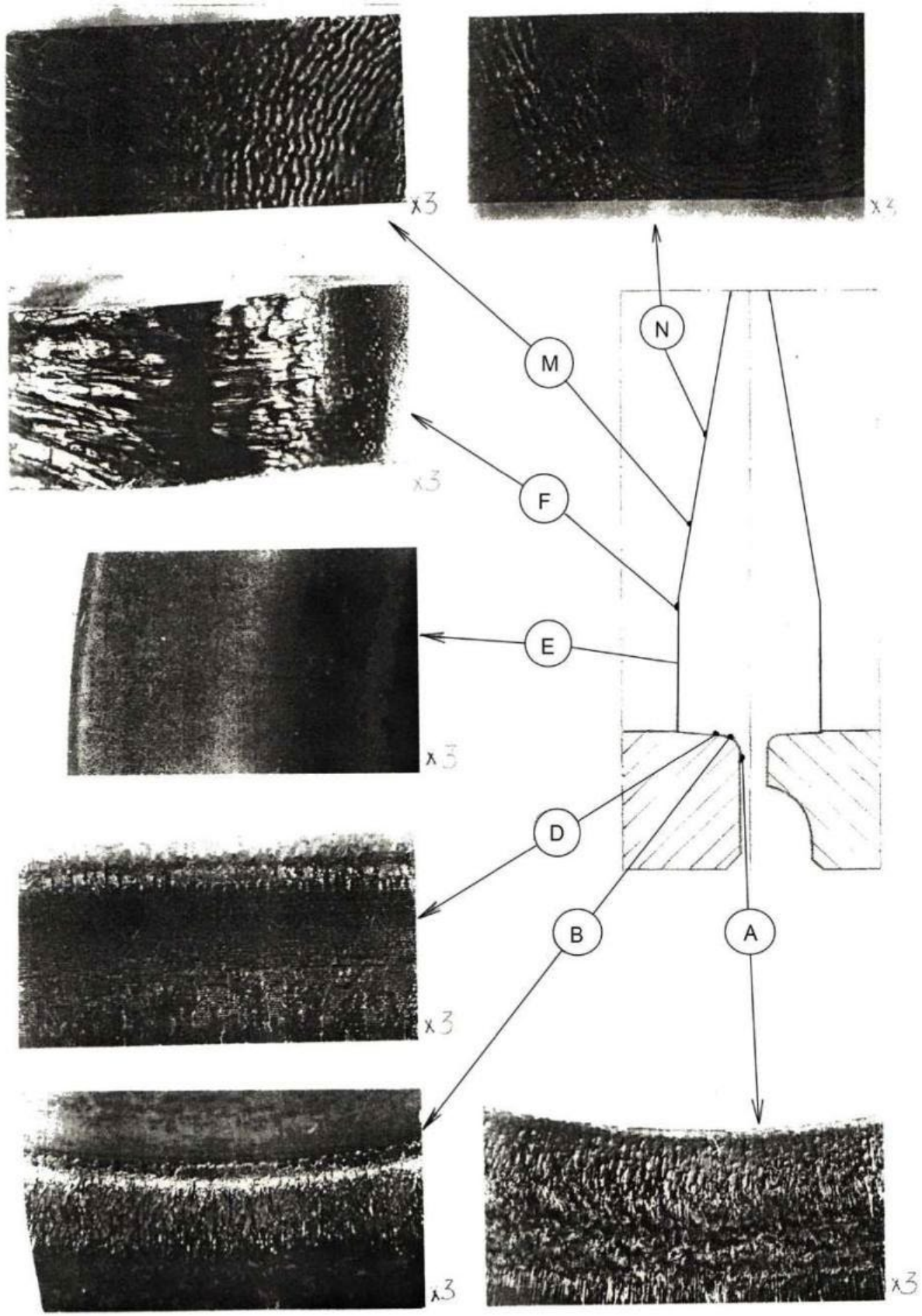

Figure 9.2. Wear peaks And bushings, reinforced ion-plasma chromium plating

The damage zones of the housing and bushing are identical in location and size to those observed in the variants tested above. The difference is in the lesser degree of damage to the working surfaces of the parts. On the housing and bushing, the damage is expressed in the form of wear, work hardening, plastic deformation of the surface layers and surface oxidation.

On the bushing section (zone "A") wear and plastic deformation of the metal are revealed in the form of spots, on the body - plastic deformation is characterized by shear bands. In zone "B" wear and a slightly expressed folded relief are noted. In zone "C" the picture of damage on the body and bushing is different. On the bushing (see Fig. 9.1) a coating chipping is observed, which occupies a large area. In places where the coating chipping occurs, wear is revealed And deformation main metal housings. On in the body V zone "B" (see Fig. 9.2) shows uniform wear and slight peeling of the surface layer, in zone "D" of the body there is running-in and peeling of the surface, on the bushing there is complete chipping of the coating.

The "N" zones of the striker and peak look like smoothed, work-hardened spots with a diameter of 22 mm on the peak and 27 mm on the striker, along the perimeter of which radial grooves of deformed metal with a general ring direction are observed. The "M" zone is characterized by wear in the form of radial grooves of varying degrees of development, more pronounced at the peak. Wear, work hardening, and smoothness of the surface are characteristic of the "F" zones. The relief grooves on the striker are completely smoothed out, and are more clearly visible at the peak. In the "E" zones of the striker and peak, signs of running-in and work hardening are noted.

8.2. Characteristic structural states material details

In the working areas of all parts of the device, significant removal of the coating occurred during the test as a result of wear or chipping (Fig. 9.3 and 9.4). The remains of the chrome coating were 20 μm are observed on the bushing in zones "B", "C" and "D". On the body thickness coatings V zone "B" is 5 microns, in zones "WITH" And "D" – 20 microns. On the striker and the peak the coating is partially preserved in zones "N" and "M" (thickness 5–10 μm) and in zone "E" – 5–20 μm.

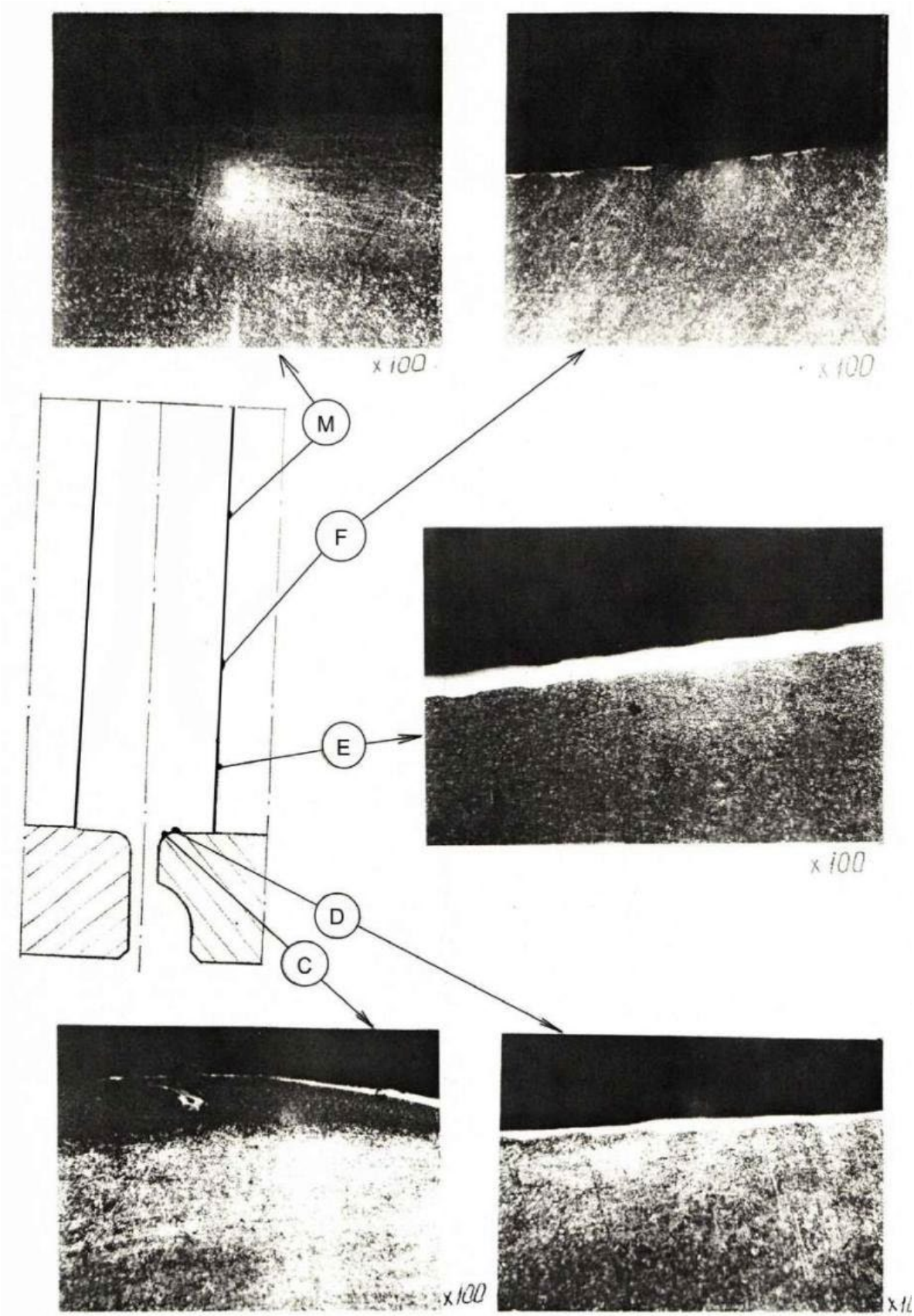

Figure 9.3. Change structures material corps And striker, hardened by ion-plasma chromium plating

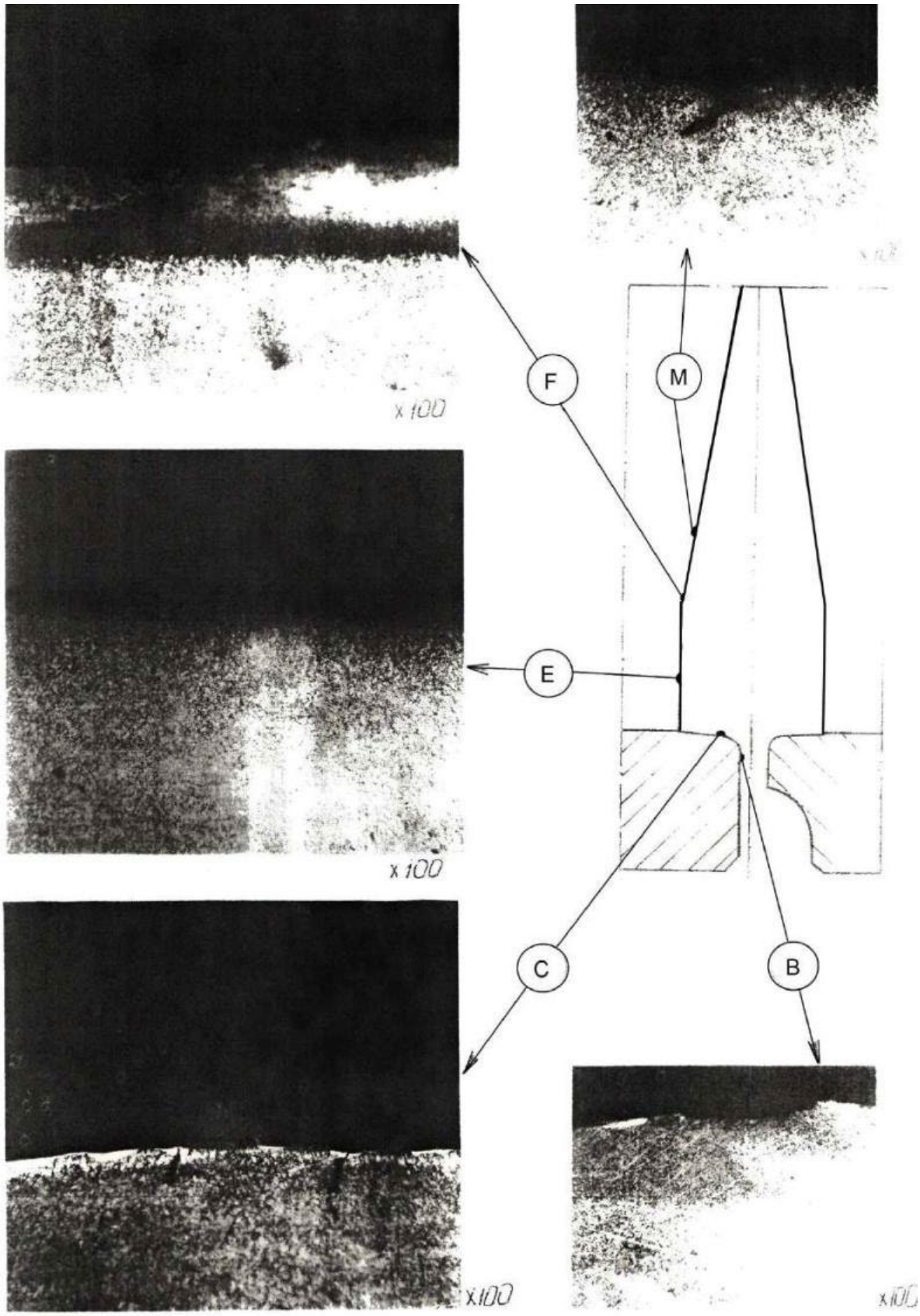

Figure 9.4. Change structures material peaks And bushings hardened by ion-plasma chromium plating

In the metal of the body, bushing, striker and peak , in

areas of metal damage, changes in structure and hardness are noted. Structural changes V zone "IN" corps are observed to the depths 0,1 mm, bushings - 0.3 mm. IN zones "WITH" And "D" structural changes are observed only on into the sleeve to a depth of 0.1 mm.

Hardness V these zones makes up HV 430–500.

On the striker and the pick, structural changes occur mainly in zones "N" and "M" in a layer 0.1 mm deep for the striker and 0.2 mm deep for the pick (HV 460–540). In zones "F", structural changes are visible only on the surface of the pick to a depth of 0.05 mm (HV 420). In zones "E" of the striker and pick, no changes in the metal structure are observed.

On all the examined parts, cracks of 0.1 mm depth are possible on the body in zones “A” and “B”, on the bushing – “B” and “C”, and on striker in zone "M". There are no cracks in other zones.

8.3. Study qualities material details

Hardness material is:

body – HRC 40–41;

sleeve - HRC 40–41.

The hardness of the striker and pick material is not constant in height. At a length of up to 30 mm from the working end, the hardness is HRC 38–39 for the striker and HRC 29–30 for the pick. On the remaining part respectively HRC 42–44 and HRC 36–39.

Microstructure of the material of sorbitol-type parts of different dispersion.

Results of testing the mechanical properties of the material The tensile strength of parts is given in Table 9.1.

Table 9.1

Mechanical properties material details, hardened by ion-plasma chromium plating

Part name	Direction of cutting samples	Mechanical properties			
		σ_{in}, MPa	$\sigma_{0.2}$, MPa	δ, %	ψ, %
frame	axial	1360–1370	1290–1300	14.0–16.0	54.0–56.0
	tangen-cial	1320–1340	1230–1260	14.0–15.0	48.0

Part name	Direction of cutting samples	Mechanical properties			
		σ_{in}, MPa	$\sigma_{0.2}$, MPa	δ, %	ψ, %
striker	axial	1460–1540	1380–1400	13.0–14.5	51.0
	tangen-cial	1430–1490	1360–1380	12.0–13.0	42.0–45.0
sleeve	axial	1285	1210	14.5	59.0
	tangen-cial	1250–1280	1180–1190	13.0–16.0	48.0–54.0
peak	axial	1260	1180–1190	15.0–16.0	54.0–56.0
	tangen-cial	1165–1180	1090–1105	14.5–17.0	42.0–61.0

From Table 9.1 it follows that the mechanical properties of the material of the bushing, body and peak, obtained during tensile testing, do not meet the requirements imposed on the parts **.**

8.4. Conclusion

1. The parts of this test variant were strengthened by ion-plasma chromium plating; the coating thickness of the body and bushing was 35–75 μm, and that of the striker and peak was 10–70 μm.

2. When testing hydraulic hammer parts hardened by ion-plasma chromium plating, no increase in wear resistance was obtained compared to the original version as a result of destruction (chipping) of the coating.

3. Locations of damage zones of parts, strengthened by ion-plasma chromium plating, basically coincide with the destruction zones observed on parts manufactured without additional strengthening.

4. Damage to parts consists of wear and chipping of the chrome coating, work hardening, formation of grooves and nicks and cracks in places.

5. A characteristic feature of damage caused by this type of hardening is the chipping of the coating, which covers a large area of the bushing channel.

6. Structural changes in the surface volumes of metal parts with a depth of 0.1–0.3 mm are observed in places both on uncoated surfaces and under a layer of chromium.

7. The number and depth (up to 0.1 mm) of cracks up to 0.1 mm for this strengthening option is significantly less compared to previous methods.

8. The mechanical properties of the material of all parts, with the exception of the striker, do not meet the requirements imposed on the parts, which is obviously due to the high heating temperature of the parts during the ion-plasma chromium plating process.

9. Considering the small wear of parts hardened by ion-plasma chromium plating before the hardened layer begins to break down, it is advisable to improve the coating application technology by reducing the heating temperature of the parts and selecting the optimal coating application parameters.

9. STUDY WEAR RESISTANCE PARTS STRENGTHENED BY ION-PLASMA CHROME PLATING (BY ADVANCED TECHNOLOGY)

9.1. Terms and Conditions tests details

The results of testing parts hardened by ion-plasma chromium plating showed that the hardened parts have good wear resistance before the coating is destroyed. Therefore, hardening treatment (ion-plasma chromium plating) was performed using an improved technology that eliminates overheating of parts during the coating application process and chipping. him during testing.

Thickness applied chrome coatings compiled 50–60 μm. The roughness parameter of hardened surfaces is R_a 0.8–3.6. After polishing, the roughness of the working surfaces of the parts is achieved within the range of R_a 0.4–0.8.

The wear resistance of the hardened parts was studied using the developed method described in Section 2. Initial signs of coating failure in the form of scoring marks were detected at the peak in zones "M" and "F" after 300 loading cycles, on the striker in the same zones after 450 cycles. In the cavity of the bushing channel, scoring marks appeared after 600 cycles, and in the housing - after 700 loading cycles. In the channels of the housing and bushing (zone B) and their cut, cracks oriented along the axis of the parts formed after 800 cycles. Due to coating wear on the most loaded areas of the device parts, the test was stopped after 1730 loading cycles.

Measurements of worn parts show that the given diameter channels corps And bushings V zone cut increased up to 125.5 mm. The striker is worn in the "N" zone by 0.2 mm, in the "M" zone by 0.5 mm. The peak is 0.3 mm and 0.85 mm, respectively.

9.2. Wear details

The nature of damage to parts hardened by ion-plasma chromium plating using improved technology, in The test process is shown in Fig. 10.1 and 10.2. The locations of the zones of greatest wear and the nature of damage to the parts similar to those observed on the above-studied parts.

In zone "A" of the striker channel (housing) and bushing, wear, work hardening and plastic deformation of the metal are observed. These phenomena are more intense on the bushing. In zone "B" wear and plastic deformation of the surface layer are visible and education grooves and scuffs. On the bushing, the groove tops are smoothed, worn (in some places to the base); on the body, the grooves are rough, without signs of wear. In zone "C", uniform wear, work hardening and peeling of the surface layer are observed. Peeling on the body is significant, on the bushing it is in the initial stage of development. Small areas of preserved hardened layer are noted on the body. The surfaces of the "D" zones are characterized by wear and peeling of the material; on the body and bushing, the coating wears out without signs of chipping or peeling.

The nature of the damage to these strikers and peaks is similar to that observed on previously examined parts, hardened ion-plasma chromium plating using the original technology. In the central part of the striker (zone "N"), a smoothed spot with a preserved coating is noted. On the striker, the coating is worn to a lesser extent than on the peak. Zone "M" is characterized by the presence of a relief of grooves-scratches, developed to a greater extent on the peak. On the striker, as a result of wear, the relief of the grooves is significantly smoothed. It is noted that in terms of the degree of development of the grooves of the striker and peak differ less than striker And peak previously researched options strengthening. Zone
"F" is characterized by wear of the coating, work hardening and smoothing of the surface. The damage in this zone is uniform around the circumference of the parts And practically equally on striker And dive. Traces The wear and cold working of the coating are observed in zone "E". Along the contour of the parts, metal dragging onto the edge of the cylindrical surface is noted.

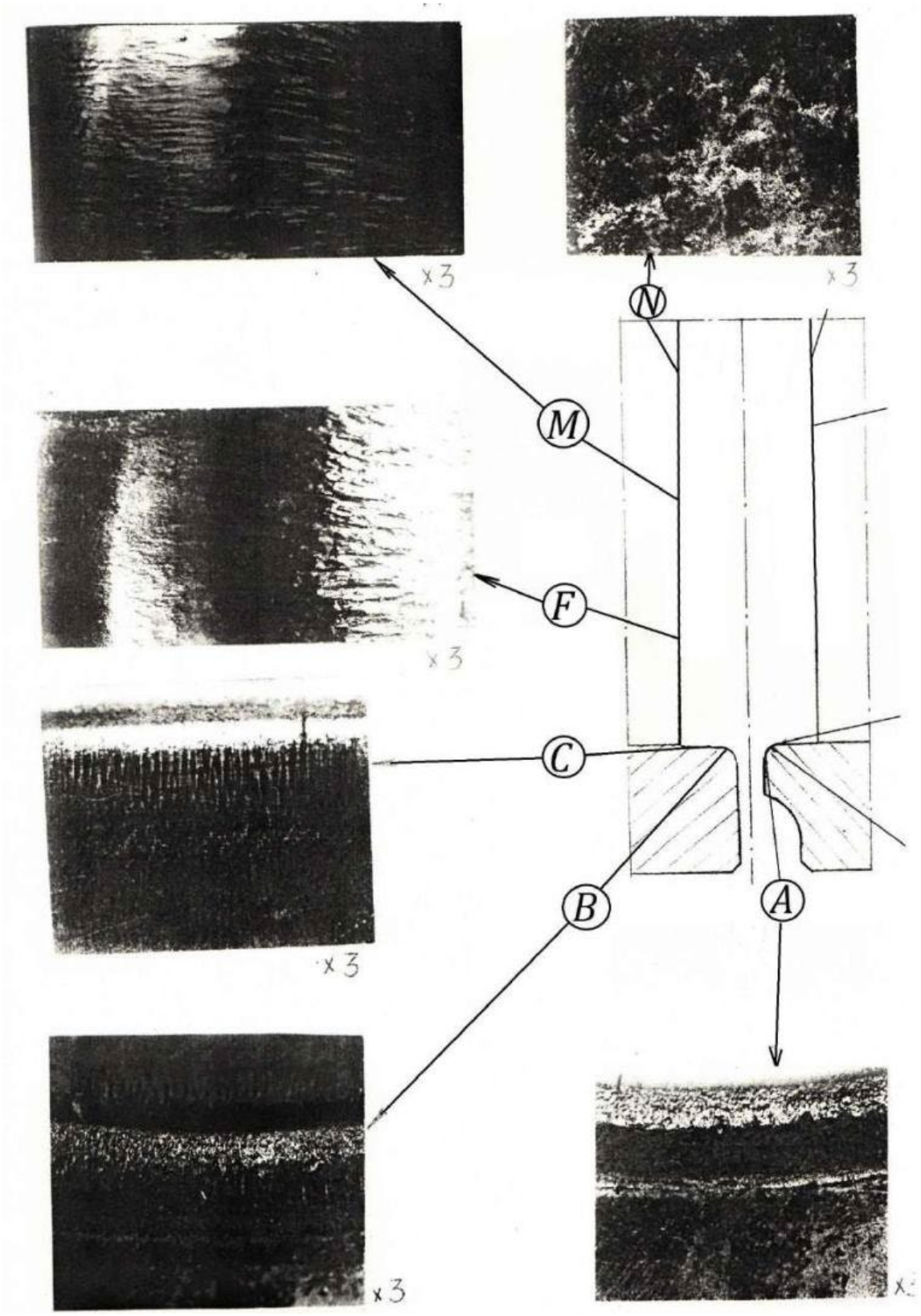

Figure 10.1. Wear peaks And bushings, reinforced ion-plasma chromium plating (using advanced technology)

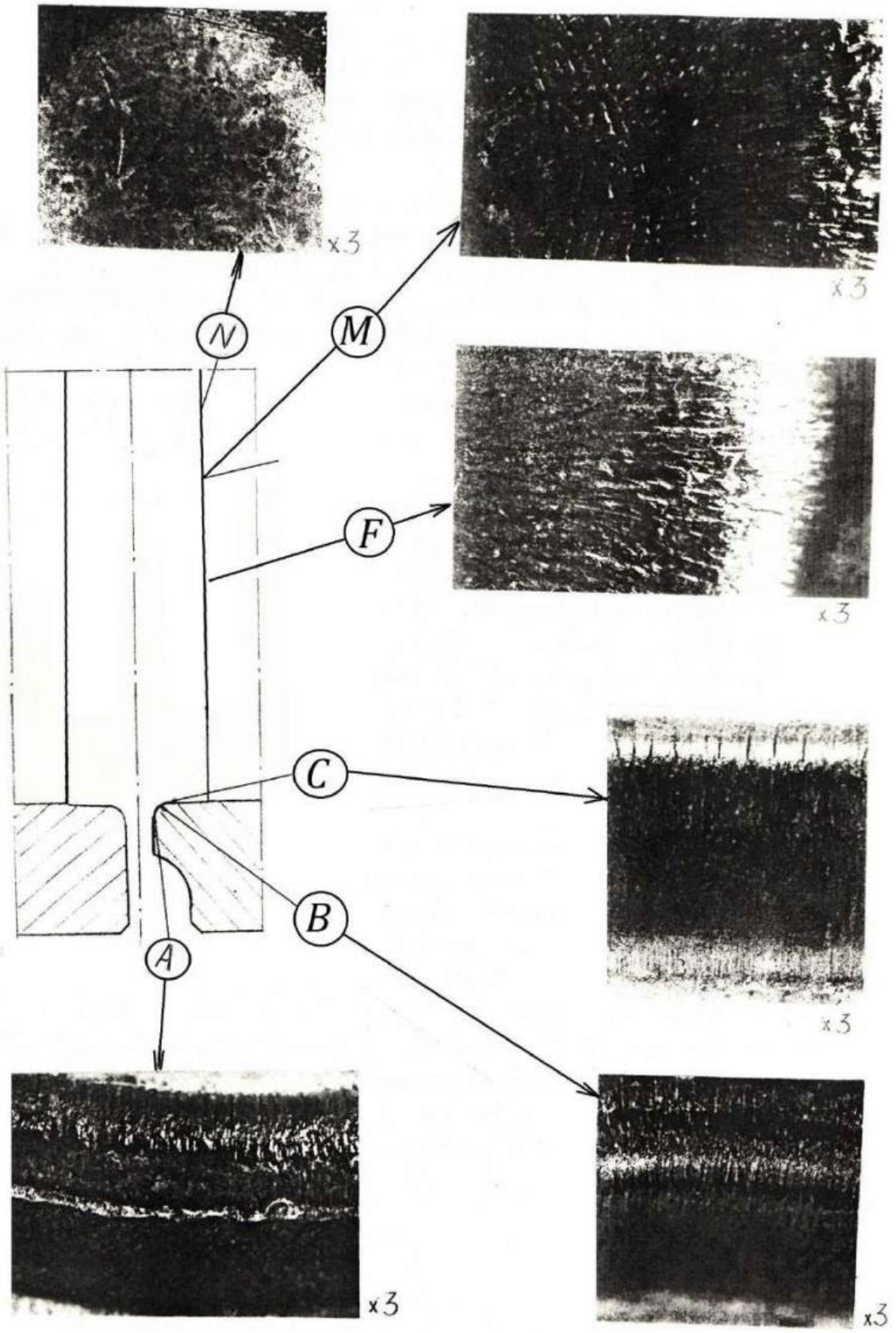

Figure 10.2. Wear corps And striker, reinforced ion-plasma chromium plating (using advanced technology)

9.3. Characteristic crack formation and structural state of the material

Cracks are observed on the test parts of the investigated variant (Fig. 10.3 and 10.4). On the body and bushing, cracks are observed in zones "A" and "B". Their depth on the body reaches 0.55 mm, on the bushing - 0.4 mm. In zones "C" and "D" cracks are absent. On the striker, cracks are recorded in the "N" zone with a depth of up to 0.3 mm and in the "M" zone - up to 0.6 mm. At the peak, cracks are observed only in the "M" zone with a depth of up to 0.6 mm. The appearance of cracks in fractures is similar to those previously observed in other hardening options (outlined contour, oxidation and smoothing of the surface).

On all the studied parts of this method of hardening, significant wear of the hardening coating occurred during the testing process .

On in the body And in the bushing leftovers coatings are observed V zones
"A" and "C", in zone "D" the coating wear is insignificant. The thickness of the remaining coating on the bushing in zones "A" and "C" is 10 μm, in zone "D" - 40 microns. On in the body (channel) V zone "WITH" to 10 μm, V zone
"D" - 20-30 μm. On the striker and peak, the coating is preserved only in zones "N" and "E". The layer thickness on the striker is 10 μm, on the peak up to 5 μm.

Structural changes are observed in the metal of the parts under study in the damage zones. Structural transformations on the bushing on depth 0.25–0.30 mm are celebrated V zones "A" And "B", on the top - to a depth of 0.15-0.20 μm in zones "A", "B" and "C". The hardness of the material in the zones of structural transformations is HV 510-645 .

The material shows peaks of structural changes at a depth of 0.25–0.30 mm are observed in zones "N" and "M". On the striker in these same zones, the depth of structural changes is 0.15–0.20 mm. Hardness material in areas of structural changes – HV 510–585.

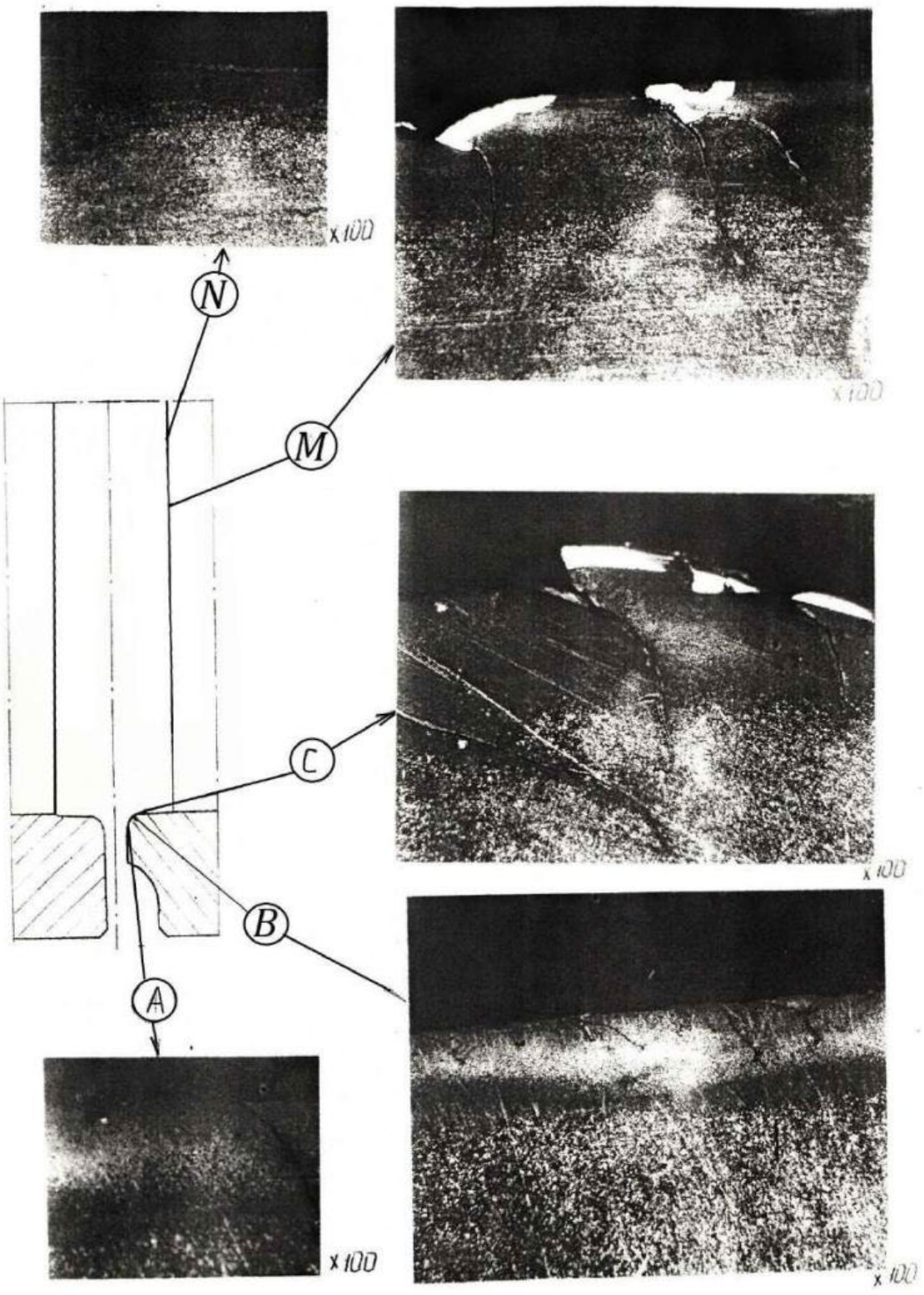

Figure 10.3. Structural changes in the body material and striker, reinforced ion-plasma chromium plating (using advanced technology)

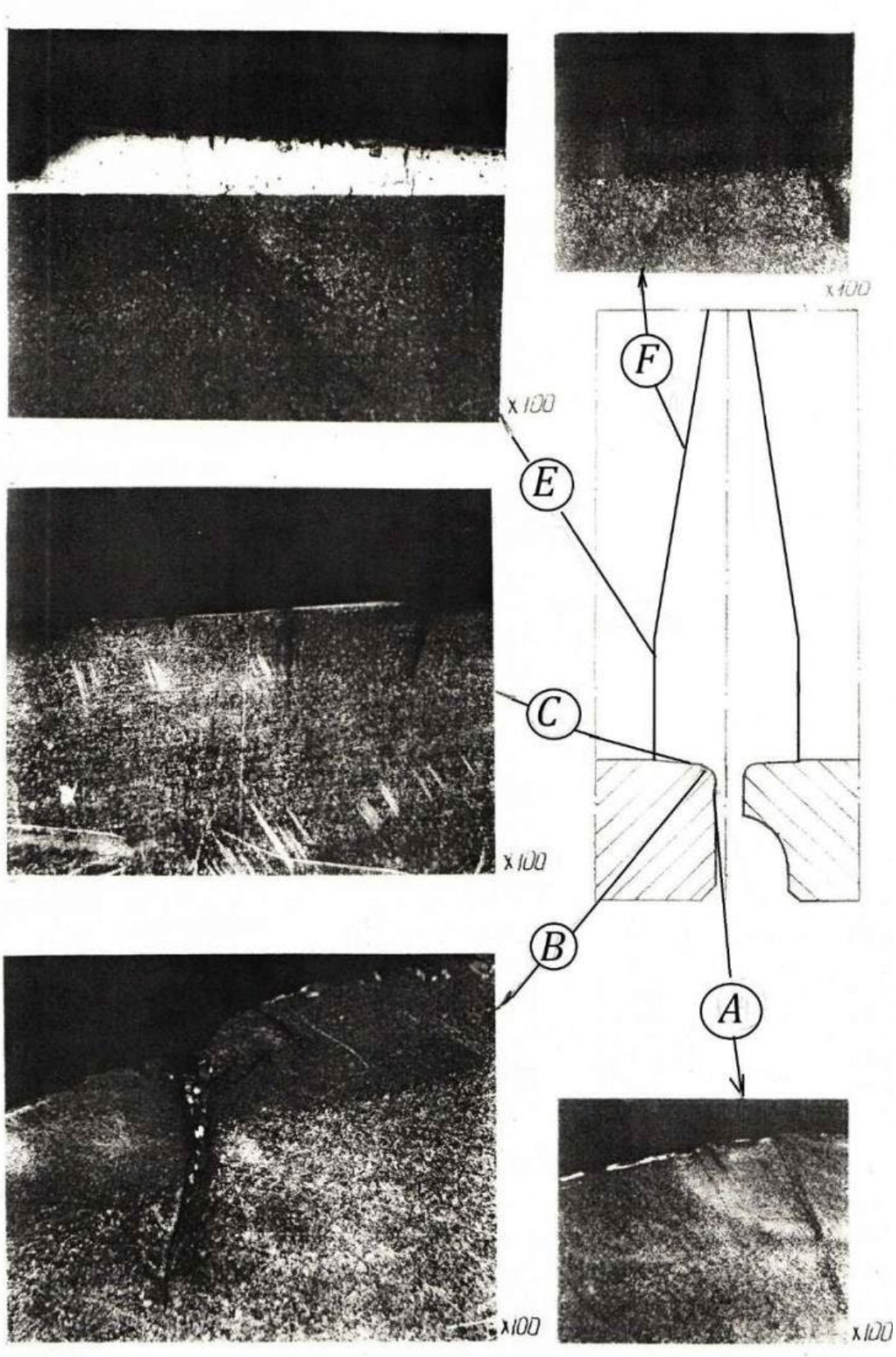

Figure 10.4. Structural changes material peaks And bushings hardened by ion-plasma chromium plating
(By improved technologies)

9.4. Quality material details

Hardness material researched details consists of: sleeve – HRC 40–42;
peak - HRC 40–42;
frame - HRC 40–42;
striker - HRC 40–42.

The microstructure of the material of the parts is of the sorbitol type, with a finely dispersed structure.

Results tests mechanical properties The tensile strength of the material of the parts is presented in Table 10.1.

Table 10.1

Mechanical properties material details, reinforced ion-plasma chromium plating (using advanced technology)

Part name	Direction of cutting samples	Mechanical properties			
		σ_{in}, MPa	$\sigma_{0.2}$, MPa	δ, %	ψ, %
striker	axial	1390.0–1430,0	1310.0–1360,0	8.0	23.0
	tangen-cial	1490,0	1400.0–1430,0	15.0	56.0
peak	axial (def (example)	1460,0	1380,0	6.4–8.0	3.0–15.0
	tangen-cial	1450.0–1510,0	1360.0–1375,0	13.0	51.0–54.0

9.5. Conclusion

1. The results of tests of parts hardened by ion-plasma chromium plating using the improved technology indicate that their wear resistance in ~ 1.75 times compared to the original (not subjected to special hardening).

2. The damage to the working surfaces of the tested parts is similar in nature and location of the zones to the previously examined parts.

3. Damage to parts is characterized by wear of the coating, work hardening of the metal, formation of grooves, nicks and cracks.

In the most heavily loaded parts of the components (in zones “B” and “C” on the striker body and sleeve and “M” and “F” on the striker and peak), the hardening coating is almost completely worn out.

4. Improved ion-plasma chromium plating technology ensures that

hardened parts operate without chipping or peeling of the coating.

5. A special feature of the test results for this type of strengthening is less wear on the lower parts of the device (bushing, peak) compared to the upper parts.

6. In areas of damage to parts, zones of structural transformations of the material to a depth of up to 0.3 mm are observed, which are characteristic of secondary hardening phenomena.

7. There are cracks on all parts of the device: on the body and bushing in zones "A" and "B" up to 0.55 mm, on the striker and peak in the zone up to 0.6 mm. In other areas of damage to the parts, cracks were not detected.

10. STUDY DURABILITY PARTS STRENGTHENED BY CHROME PLATING BY WAY DECOMPOSITIONS CONNECTIONS "BARKHOS"

10.1. Parameters coatings And conditions tests

Hardening of part models for testing wear resistance is achieved by applying a chrome coating, implemented decomposition organochromic connections "Barkhos". The coating thickness is: on the sleeve - 26-30 microns; on the body striker - 123–150 microns; on pique - 25–40 microns; on striker - 73–120 μm. The roughness of the working surfaces of the parts before coating was R_a 0.4–0.8. After chromium plating, the roughness of the surfaces of the parts changed insignificantly (R_a 0.48–0.9), so the parts were not subjected to any finishing treatment before testing.

Initial signs of destruction of the chromium coating in the form of scratches and nicks were detected at the peak after 390 loading cycles. striker similar damage surfaces revealed V zones "M" and "F" in the range of 400-420 cycles. Destruction of the hardening layer in the form of coating chips was detected on the bushing after 400 loading cycles, on the body - 800 cycles. The tests were stopped after 1300 loading cycles due to almost complete wear of the coating on the bushing and striker.

Measurements of the tested parts showed that the reduced diameter of the channels in the cutting zone increased to 125.7 mm. worn out in the "M" zone by 0.45 mm, in the "T" zone – 0.6 mm. The pick was worn in zone “M” – 0.5 mm, in zone “F” – 0.65 mm. After the test, the parts were subjected to a comprehensive materials science study.

10.2. Wear details

The location of the damage zones of the working surfaces of the housing and bushing is similar to that identified in the previously studied hardening options. In the damaged areas, the formation of furrows-scuffs, slander, chips chromium, plasticdeformation of the base metal, crack formation and oxidation of surfaces.

On the bushing in zone "A" there is work hardening and wear of the metal with the formation of a step of wear. On the body in this zone there are small grooves and a slightly higher degree of deformation of the metal. In

zones "B" of both parts there is plastic deformation of the metal and the formation of a smoothed relief (Fig. 11.1, 11.2).

On the surface of the channel (zone "C") of the bushing, the chrome layer is almost completely absent, chipping of the coating is observed. On the body, the chrome coating in this zone is preserved, however, it has a large number of cracks of a grid orientation and individual areas of chipping of the chrome. In zone "D" of both parts, the coating is preserved. Rubbing, wear and smoothing of the chrome coating are noted.

The wear pattern of the striker and the peak is similar to that observed in the previously studied hardening variants. Zone "N" looks like a spot with a worn, smoothed and cold-hardened surface with a diameter of about 26 mm on the striker and 20 mm on the peak. Remains of the chrome coating are preserved in this zone on the peak.

On the striker and peak in the "M" zone, the chrome coating layer is practically absent. Grooves and scuffs are observed on the base metal of the parts and are characterized by a significant smoothing of the relief.

In the "F" zone, the peak shows a chrome coating with individual chips, on the striker the chrome layer has been preserved in the form of isolated small islands. Signs of wear and chrome chips are noted in the "E" zone of both parts. To a large extent, the chrome has been preserved at its peak. The tarnish colors on surface of the chromium layer preserved from destruction in all zones they have a yellowish-bluish tint.

10.3. Characteristic crack formation and structural state of the material

During the testing, cracks formed on all the examined parts of the device. On the body and bushing, cracks with a depth of to 0.3 mm revealed V zones "A", "IN" And V zone "WITH" with

sides cut. On striker And pique cracks depth to 0.35 mm peaks are noted in the “M”, “F” zone and in the “N” zone (Fig. 11.3 and 11.4).

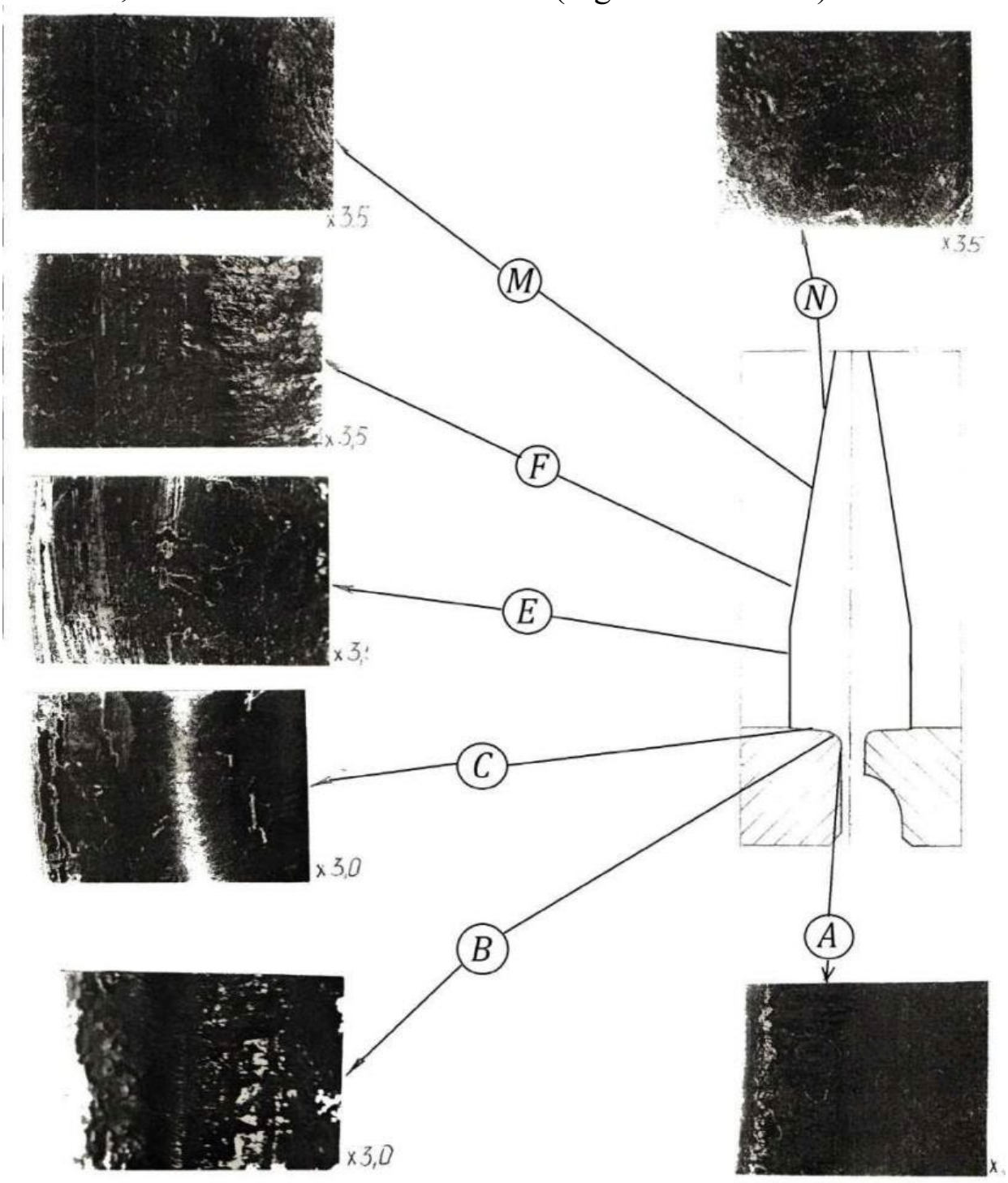

Figure 11.1. Damage peaks And bushings, reinforced chromium plating by decomposition of the organochromium compound "Barkhos"

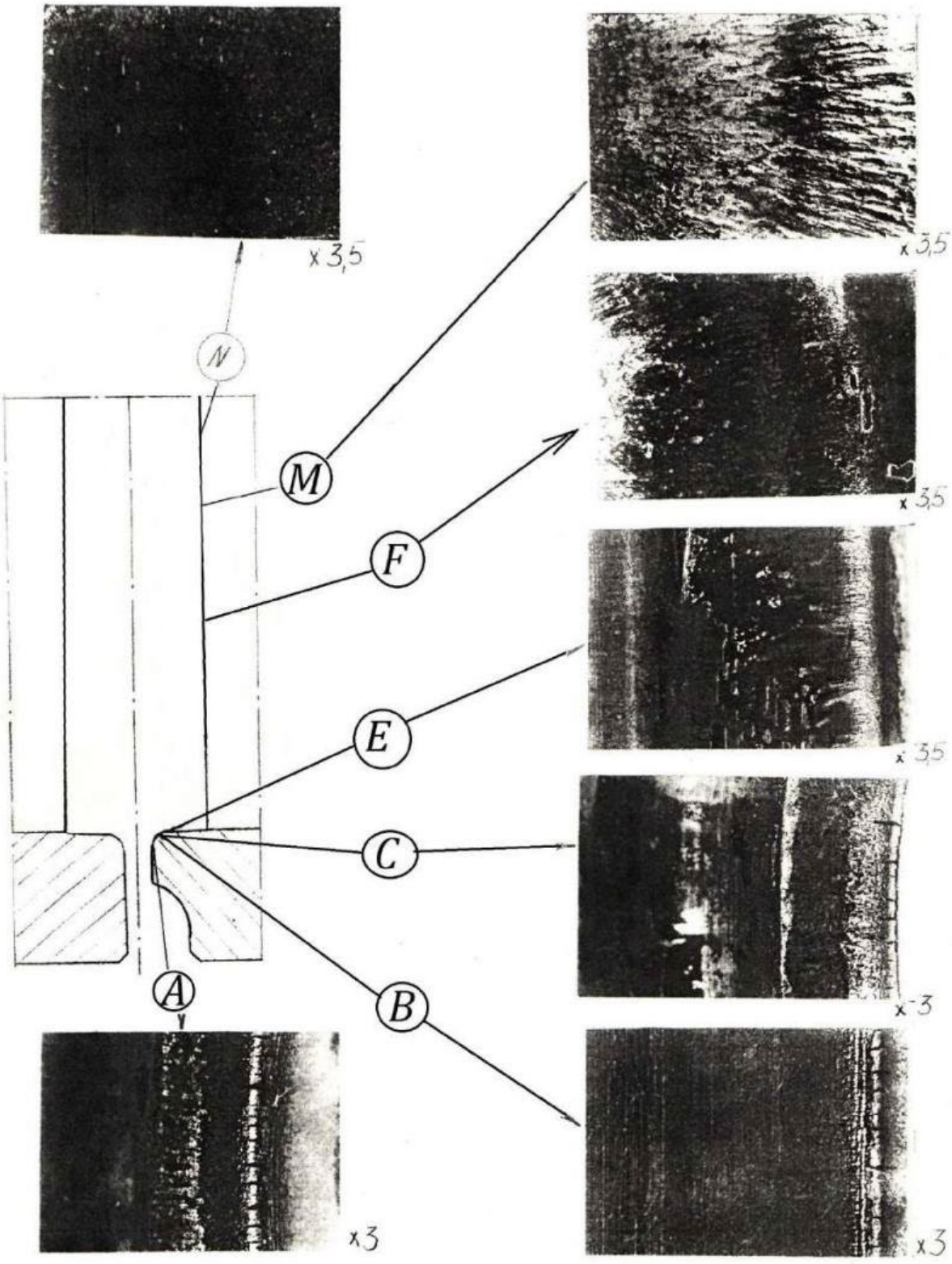

Figure 11.2. Damage corps And striker, reinforced chromium plating by decomposition of the organochromium compound "Barkhos"

In the working areas of all the parts examined, partial or complete removal of the chrome coating occurred. The thickness of the remaining layers on in the bushing makes up V zone "WITH" with sides zones "D" 20 μm, V zone "D" - 15 microns. On in the body V zones "WITH" And "D" near 100 microns. IN zones "A" And "IN" on both in detail coating absent.

On the striker and the pick, the remains of a chromium layer up to 10 μm thick were preserved in all zones (except for zone “E”) of the pick and in zone “E” of the striker.

In some areas of the working surfaces of parts in damage zones, changes in the structure and hardness of the base metal are observed, regardless of the presence or wear of the chromium coating (Fig. 11.3 and 11.4).

On the body and bushing, structural changes are observed in the zones "A", "IN" And "WITH". Depth changes the greatest in zones "A" And "B" - up to 0.30...0.35 mm, in zone "C" - up to 0.10 mm. In zone "D" structural changes Not revealed. Hardness V zones structural changes reach HV 514...540.

On the striker and the peak, changes in the structure of the base metal are observed in zones "N", "M" and "F". The depth of structural changes is up to 0.5 mm at the peak, and up to 0.25 mm at the striker. The hardness of the material in the zones of structural changes is HV 585–645.

10.4. Quality material details

Hardness material details is:
bushing – HRC 42–43 (individual points – HRC44);
body - HRC 42–43 (separate dots - HRC44); peak –
HRC 40–42;
striker - HRC 40–42.

The microstructure of the material of the parts is of the sorbitol type, with a finely dispersed structure.

Results of testing the mechanical properties of the material The tensile strength of parts is given in Table 11.1.

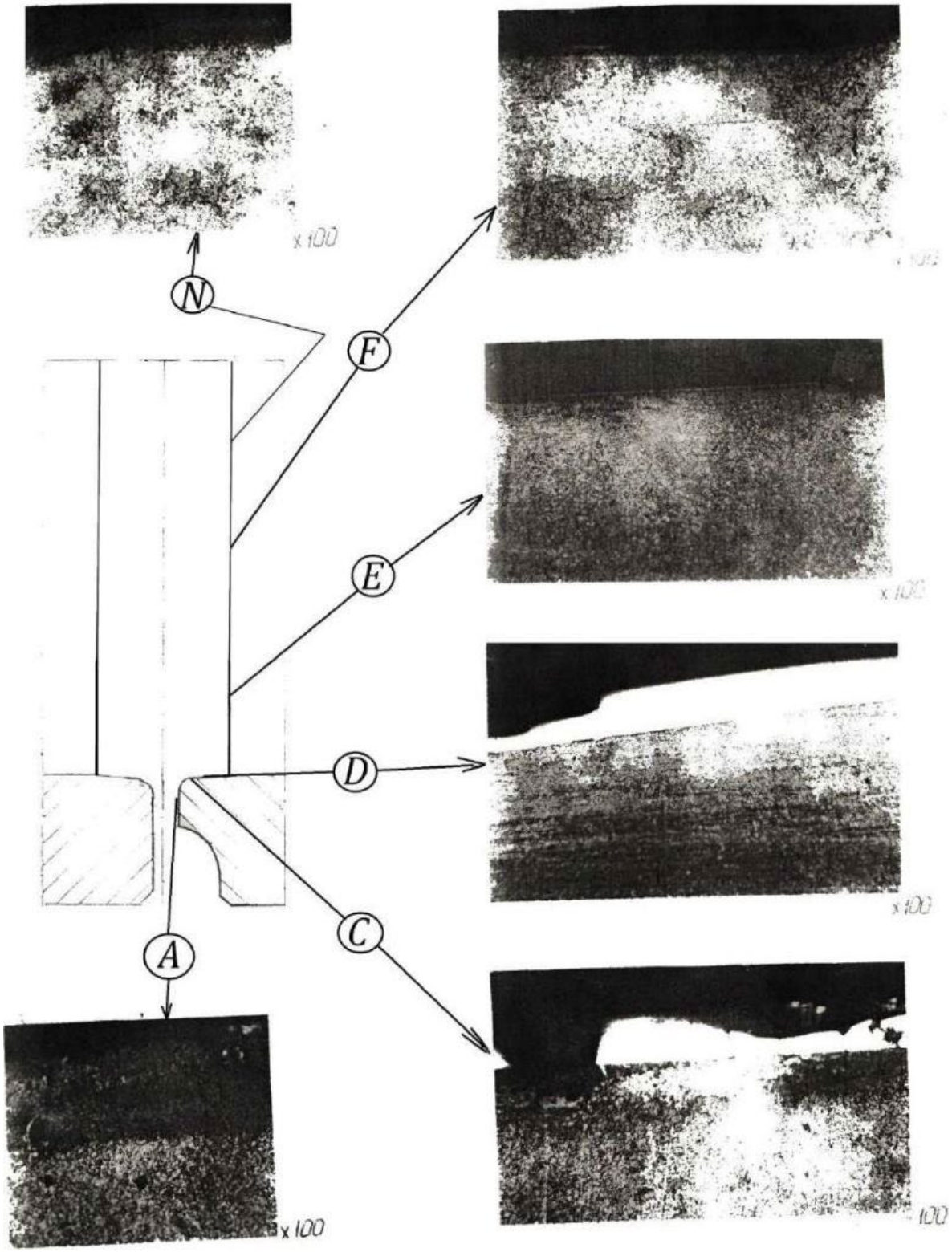

Figure 11.3. Structural changes in the body and striker material, reinforced chromium plating by way decomposition organochromium compound "Barkhos"

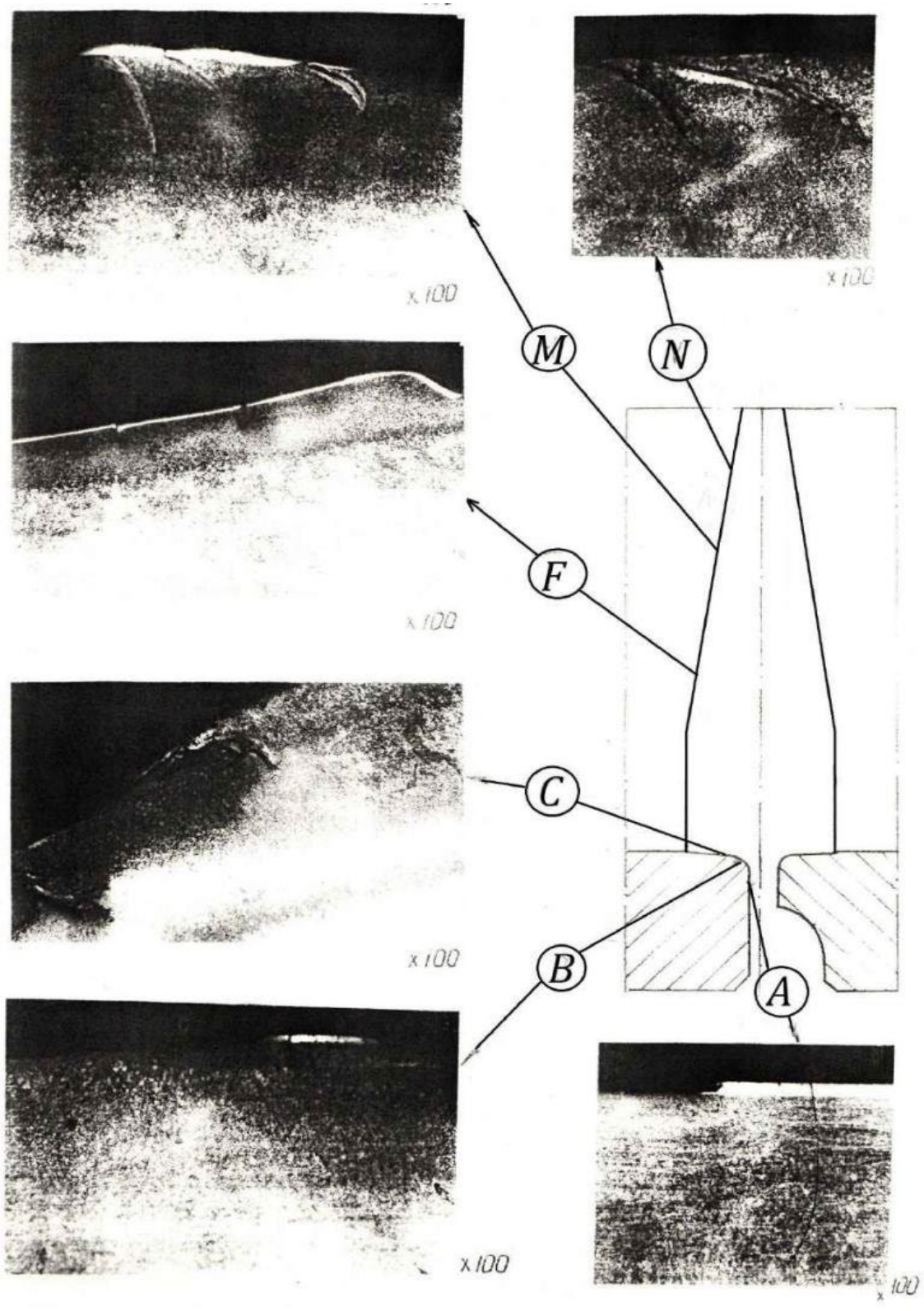

Figure 11.4. Structural changes material peaks And bushings,reinforced chromium plating by way decomposition organochromium compound "Barkhos"

Table. 11.1

Mechanical properties material details, reinforced chromium plating by way decomposition organochromic Barkhos connections

Part name	Direction of cutting samples	Mechanical properties			
		σ_{in}, MPa	$\sigma_{0.2}$, MPa	δ, %	ψ, %
sleeve	axial	1470,0	1400.0–1405,0	12.0	45.0–48.0
	tangen-cial	1470,0	1380.0–1400,0	14.0	54.0–55.0
frame	axial	1410,0	1320,0	8.0–12.0	26.0–51.0
	tangen-cial	1425.0–1430,0	1330.0–1350,0	13.0	54.0–56.0
peak	axial	1440.0–1470,0	1360.0–1370,0	12.0–15.0	51.0–56.0
	tangen-cial	1450.0–1460,0	1380.0–1390,0	6.5–8.0	23.0
striker	axial	1490,0	1405.0–1420,0	10.0–12.0	39.0–42.0
	tangent-al	1480.0–1485,0	1400.0–1400,5	12.0–13.0	56.0

From Table 11.1 it follows that the mechanical properties of the material of the parts after tensile testing meet the requirements.

10.5. Conclusion

1. Results of tests of hardened parts chromium plating by way decomposition organochromic connections

"Barkhos" show that wear resistance is increased by □□1.3 times compared to the original (not subjected to special hardening).

2. Location of damage zones of parts hardened by chromium plating by way decomposition connections "Barkhos", similarly detected on parts manufactured without additional strengthening.

3. Destruction of parts during testing occurs primarily through wear and chipping of the chrome coating.

4. Structural changes and cracks in the base metal occur regardless of the presence or complete wear of the chromium coating

during testing.

5. The thickness of the chrome coating has an ambiguous effect on the wear resistance of the parts: a thicker layer of chrome on the striker body (123–150 μm) increased its wear resistance compared to the sleeve (26–30 μm), but an increased coating thickness on the striker (73–120 μm) caused its more intense destruction compared to the pick, which has a chrome thickness of 25–40 μm.

11. STUDY WEAR RESISTANCE PARTS STRENGTHENED BY CHROME PLATING BY SUMY-SWISS TECHNOLOGIES

11.1. Terms and Conditions strengthening And tests details

Hardening of parts by chromium plating using the Sumy-Swiss technology [137, 138] yielded the following thickness of the chromium coating:

sleeve – 70–80
microns; frame - 60–80
μm; peak – 17–40 μm;
striker – 18–40 μm.

The roughness parameter of chrome-plated surfaces of parts is R_a 0.4–0.8.

The study of wear resistance of parts hardened by chromium plating using the Sumy-Swiss technology was carried out by loading according to the method described above.

Initial signs of wear on the coating appeared at the peak in the form of scratch marks in zones "M" and "F" after 400 loading cycles. Similar damage to the striker was detected after 1900 loading cycles, in the cavity of the bushing channel - 1100 cycles, and in the body - 1600 cycles. The tests were stopped after 1900 loading cycles due to damage to the coating at the peak.

Measurements of the tested parts show that the given diameter channels corps And bushings V zone cut increased to 125.6 mm, peak V zones "M" And "F" worn out on 0.5 mm, striker - on 0.3 mm.

11.2. Damage details V in the process tests

The type of damage to parts hardened by chromium plating using the Sumy-Swiss technology during testing is shown in Fig. 12.1 and 12.2. The damage to parts in terms of the location of intensive wear zones and the general nature is close to that observed in the previously studied hardening variants.

The body and bushing show wear, work hardening, scoring on the working surface, plastic deformation and discoloration. running away.

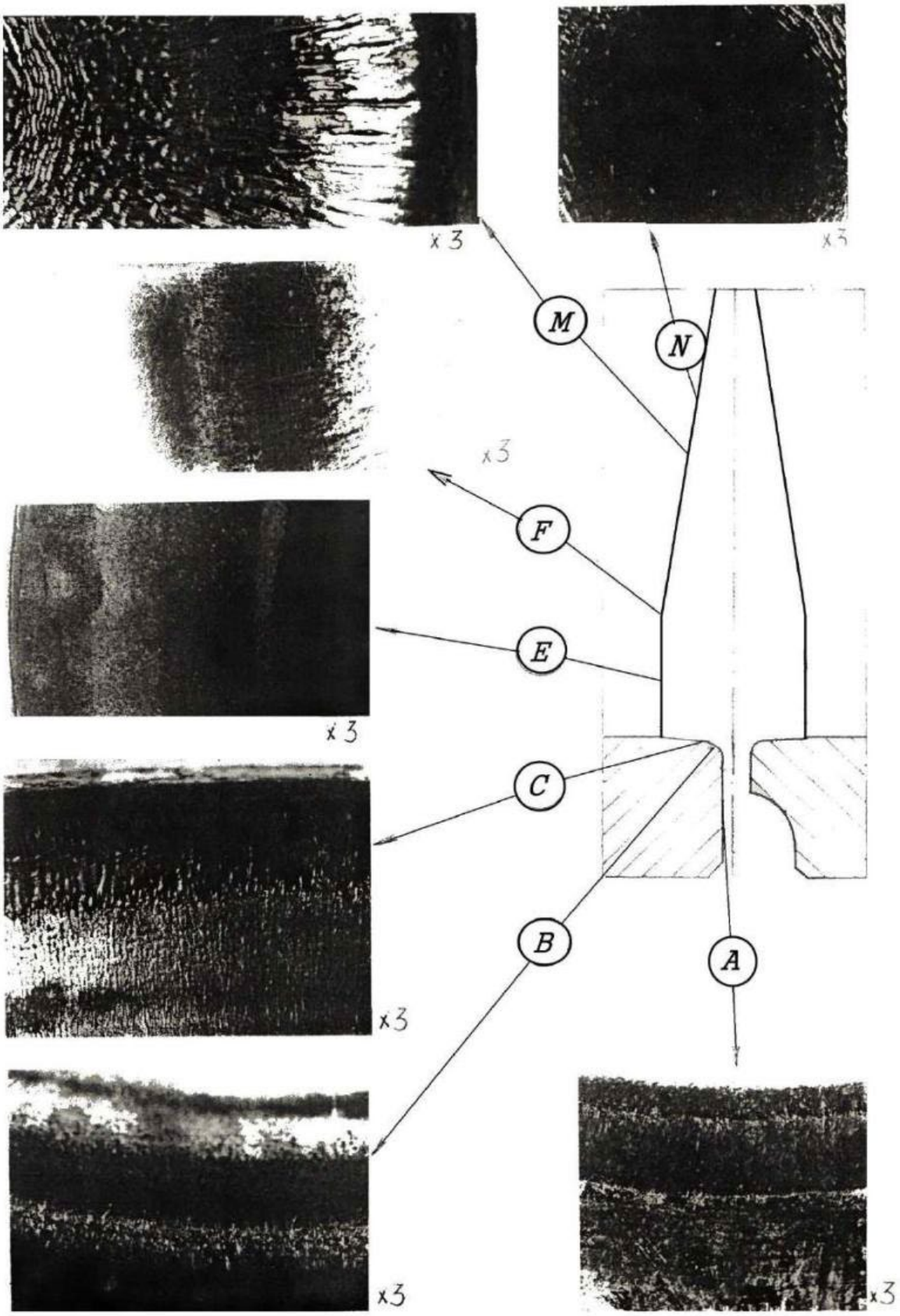

Figure 12.1. Wear peaks And bushings, reinforced chromium plating using Sumy-Swiss technology

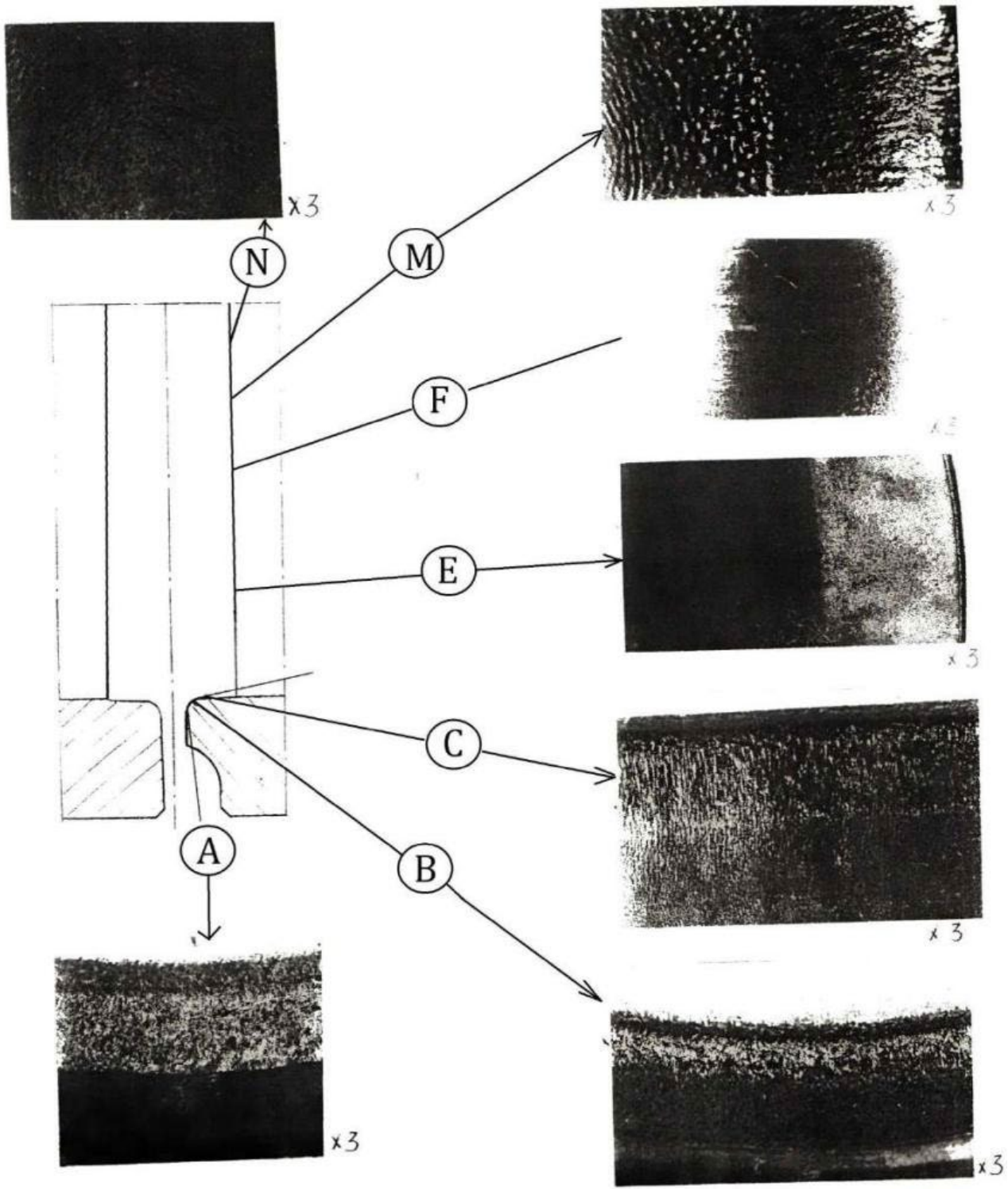

Figure 12.2. Wear corps And striker, reinforced chromium plating using Sumy-Swiss technology

In zone “A” on the bushing, work hardening of the metal and its intensive wear are revealed. with education steps production. In zone "B" a folded relief and intense work hardening are observed, which is more pronounced on the bushing. In zone "C" the surface of the chrome coating is characterized by wear and rubbing. Some peeling with minor signs of wear of the hardened layer is noted in zone "D".

The damage to the working surfaces of the striker and the pick is also not significantly different from those studied above. The degree of damage to the pick is higher than to the striker. Zone "A" looks like a smoothed spot with a diameter of 20 mm on the pick and 26 mm on the striker. Here a layer of chrome up to 10 mm has been preserved.

In the "M" zone, the chrome coating is practically absent. The formation of grooves and nicks is observed directly in the base metal. The grooves are smoothed on the striker, and very clear on the peak.

On the lower half of the surface (zone "F"), the chrome layer on the striker is partially preserved, which gives the surface a matte shade. Rubbing and signs of wear of the coating are noted. At the peak, the coating is worn out, which is confirmed by the picture of wear and scuffs. Chrome coating preserved V view belt width 2–4 mm, adjacent to the outer contour. A network of cracks is observed in the coating. On the rest of the surfaces "E" the chromium layer is missing. The surface of the base metal has traces of wear and tarnish colors. The transition to the remaining belt of chromium coating is sharp. The configuration of the boundary of the remaining chromium layer indicates that What coating on this plot was destroyed by chipping.

11.3. Structural state material details

During the testing, the hardening chromium coating in the working areas of all the parts examined showed complete or partial wear. On the bushing, the chromium layer was preserved in zone "A" with a thickness of up to 10 μm, in zone "C" on the cut side - up to 10 μm, on the remaining part 40-50 μm (Fig. 12.3). On the body, the coating was preserved in zones "A" (30 μm) and "B" (50-60 μm).

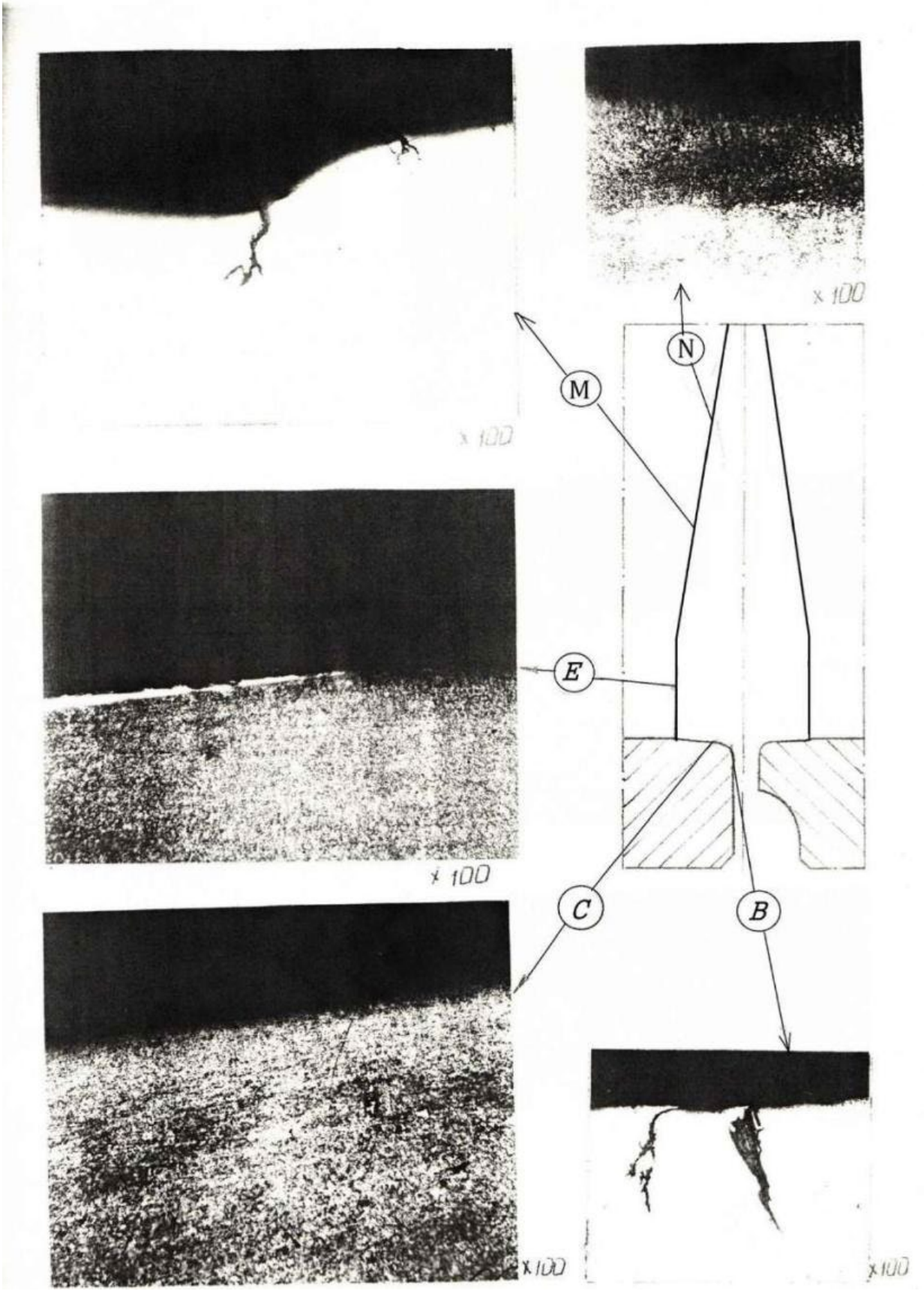

Figure 12.3. Structural changes in the material of the peak and bushing, reinforced chromium plating By Sumy-Swiss technologies

IN zone "IN" chromium preserved on separate areas thickness 10–20 microns (rice. 12.4).

On striker (rice. 12.4) leftovers preserved from wear and tear chromium by microstructure are observed in all zones. The coating thickness in zone "M" is 10-30 μm, in zone "N" - 20 μm. At the peak, a chromium layer up to 100 μm thick was preserved only in zone "C" at the outer contour of the part.

Changes in structure and hardness are observed in the base material of the parts in the area of damage. Structural changes in the base metal of the parts are observed in the working zones both in those areas where the chrome is completely worn out and in areas where the chrome layer is preserved. On the body and bushing, the depth of the zones of structural changes is 0.2–0.3 mm in zones “A” and “B”, respectively. In zone “C” – up to 0.05 mm, in zone “D” structural changes are not observed. The hardness of the material in the zones of structural changes is HV 450–550.

On striker And pique structural changes are observed V zones "N", "M" and "F" to a depth of 0.4 mm at the peak and up to 0.3 at the striker. Hardness in the zones of structural changes is HV 380–450. No structural changes in the base metal in the "E" zones of both parts are noted.

All parts of this set have cracks in the damaged areas, identical in appearance and distribution to those observed in the above-studied hardening variants. On the body, the cracks develop to a depth of up to 1 mm (zone B). On the bushing, the crack depth is up to 0.4 mm. The crack depth at the peak (zones "N" and "M") reaches 0.7 mm. On the striker, cracks are noted in all zones, their depth is 0.1–0.8 mm.

The cracks in the section are oriented at an angle to the surface, smoothly curved, and extend beyond the zones of structural changes. Developing in depth, the cracks pass from the chromium layer into the base metal. Cracks in fractures are characterized by smooth walls, oxidation, and a clearly defined contour; merging of adjacent cracks is possible.

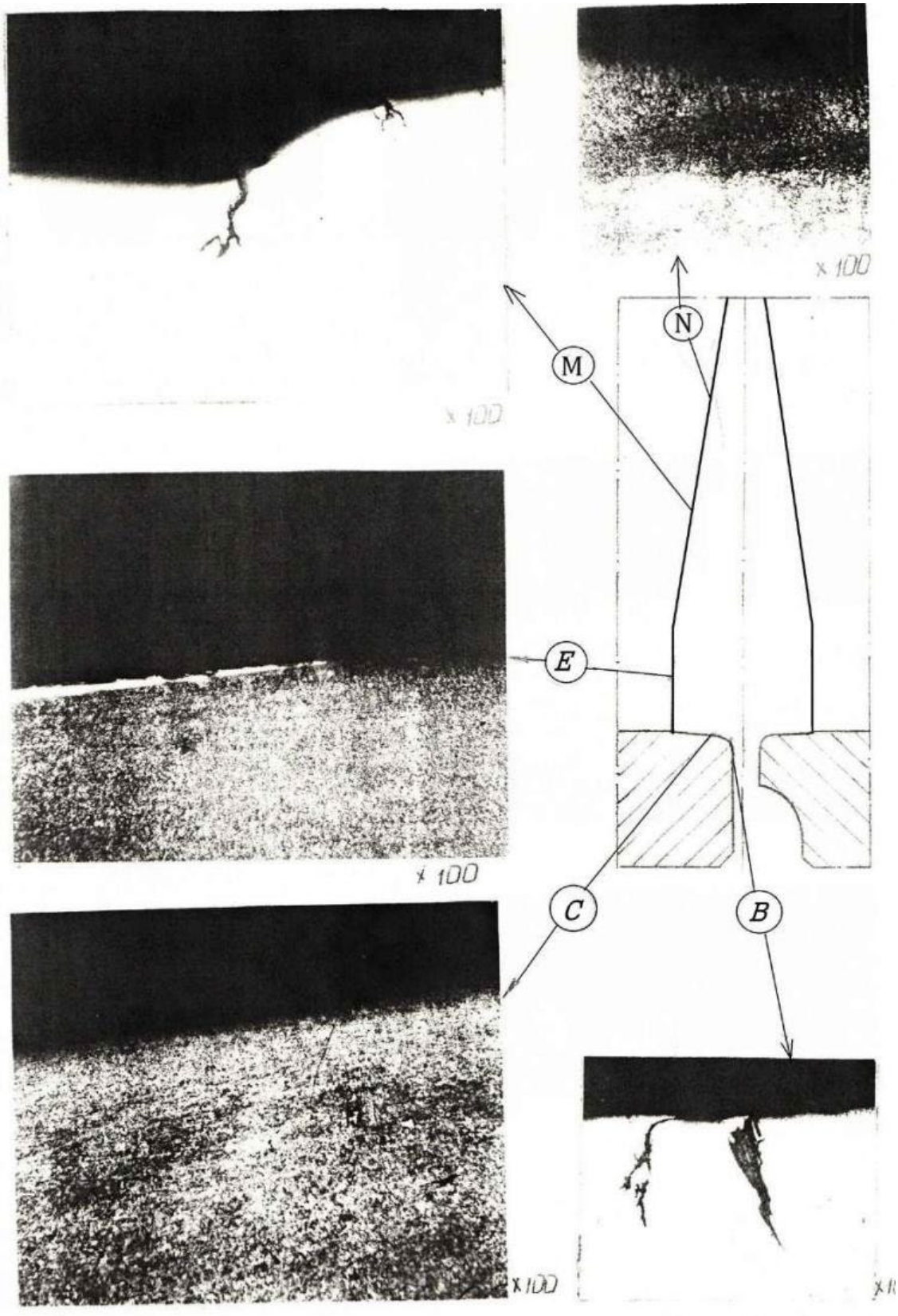

Figure 12.3. Structural changes in the bushing and peak material, reinforced chromium plating By Sumy-Swiss technologies

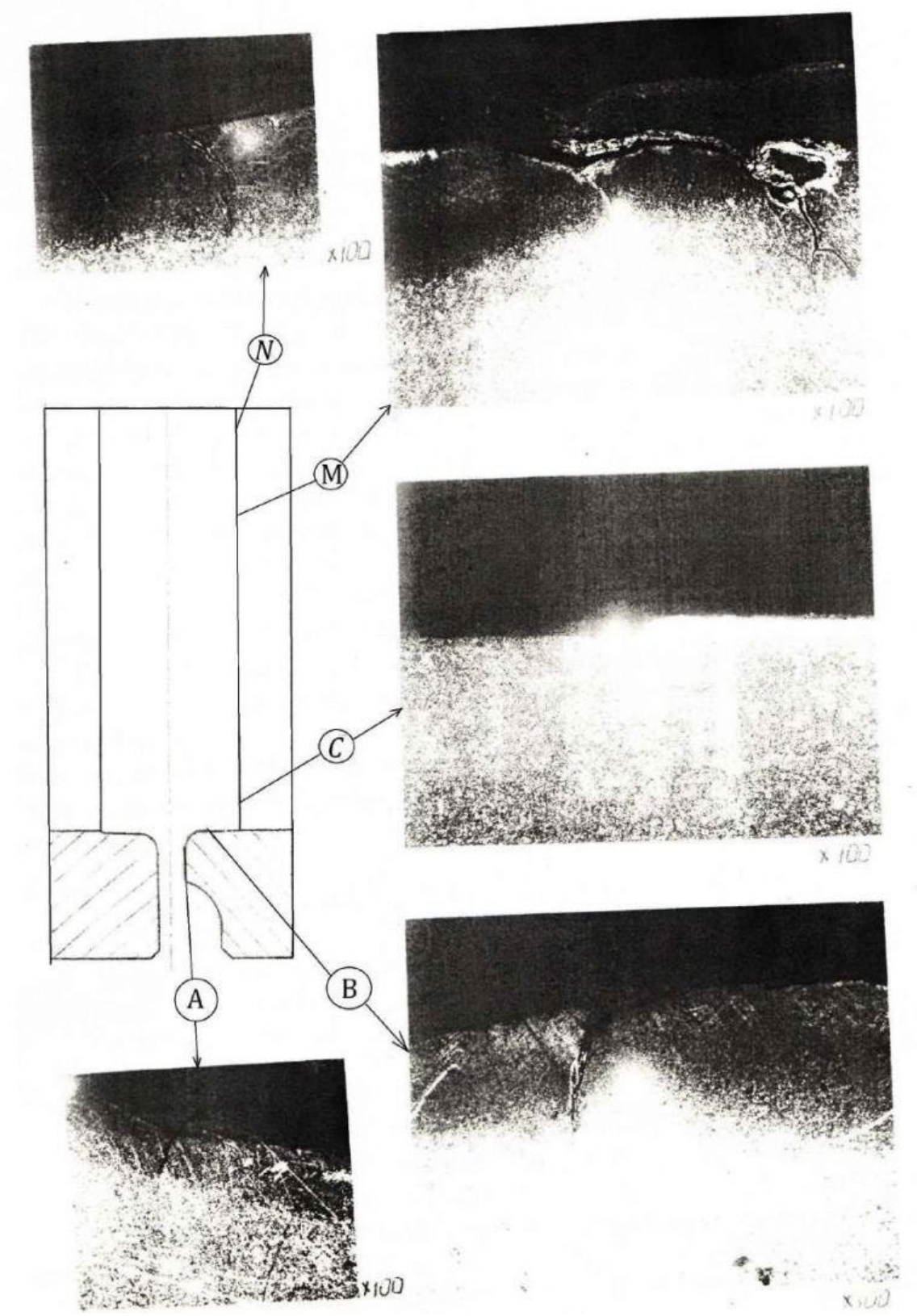

Figure 12.4. Structural changes material corps And striker, hardened chromium plating By Sumy-Swiss technologies

11.4. Study qualities material details

Hardness material details uniform By height And consists of: sleeve – HRC 42–43;
frame striker - HRC 42–44;
peak – HRC 43–44;
striker - HRC 44–45.

The microstructure of the material of the parts is of the sorbitol type, with varying dispersion.

The results of testing the mechanical properties of the material for tension are given in Table 12.1.

Table 12.1

Mechanical properties material details, hardened by chromium plating using Sumy-Swiss technology

Part name	Direction of cutting samples	Mechanical properties			
		σ_{in}, MPa	$\sigma_{0.2}$, MPa	δ, %	ψ, %
sleeve	axial	1490,0	1410.0–1410,5	10.0–12.0	44.0–45.0
	tangen-cial	1460.0–1480,0	1360.0–1390,0	12.0–13.0	48.0–51.0
frame	axial	1470,0	1370.0–1380,0	12.0	44.0–47.0
	tangen-cial	1480.0–1490,0	1380,0	13.0–14.0	50.0–51.0
peak	axial	1480,0	1370.0–1390,0	12.0–13.0	56.0–58
	tangen-cial	1490,0	1390.0–1410,0	8.0–9.0	28.0–36.0
striker	axial	1485.0–1490,0	1380,0	14.0–15.0	54.0–56.0
	tangen-cial	1480.0–1490,0	1390.0–1410,0	10.0–11.0	33.0–39.0

From table. 12.1 follows, What mechanical properties material parts meet the requirements.

11.5. Conclusion

1. The results of tests of a hydraulic hammer equipped with parts hardened by chromium plating using Sumy-Swiss technology show that What achieved increase durability details
~ 1.9 times compared to the original (not subjected to special hardening) version.

2. The location of the damage zones and their nature are similar to those found on parts that were not subjected to additional strengthening.

3. Damage to parts in working areas consists of intensive work hardening of the base metal, wear of the chromium layer and the substrate material (in areas where the chromium coating is completely worn out), and the formation of cracks.

4. A number of features of damage development are noted in the examined set of parts:

5. The destruction of the chrome coating occurs mainly through wear. The exception is the end surface of the pick, where the destruction of the chrome occurs through chipping (flaking).

6. The greatest number of cracks are observed on the body and the striker.

7. A special feature of the coating made using the Sumy-Swiss technology is good adhesion of chromium; peeling or separation of the chromium layer from the base metal is not observed. Joint plastic deformation of the coating with the base metal is noted during testing, pressing of chromium into the cracks formed while maintaining tight contact with the material of the parts.

12. TRIAL AND STUDY DETAILS, REINFORCED SURFACE WELDING ALLOY "HASTELLOY"

12.1. Terms and Conditions tests details

Hardening of parts by surfacing with Hastelloy alloy was carried out to a thickness of 3–5 mm, then mechanical processing and grinding were performed. The roughness parameter of the surfacing surfaces after grinding is R_a 0.8–1.4 μm.

The outer surfaces of the parts outside the hardening zone had tempered colors, the hardness of the material of the parts was 35–37 HRC. The hardness of the deposited Hastelloy alloy was within the range of 240–243 HB.

The wear resistance of the housing, bushing, striker and peak, hardened by surfacing with Hastelloy alloy, was studied using the method described in Section 2. Initial signs of destruction of the hardfaced layer appeared on the striker after 900 loading cycles in the form of scratches in zones "M" and "F". Similar damage to the surfaces was detected at the peak after 1500 loading cycles. Similar damage in zones "A" and "B" in the housing cavity was detected after 1600 cycles, and in the bushing cavity after 1700 loading cycles. The tests were stopped after 2100 loading cycles with a satisfactory condition of the test parts due to better results compared to the previously tested hardening methods.

Measurements of the tested parts show that the diameter of the housing channel in the shear zone increased to 125.3 mm, on the bushing it remained equal to 125 mm. The striker wore out in the zones "M" and "F" by 0.28-0.3 mm, the peak in the same zones by 0.25-0.3 mm.

12.2. Damage welded details

The general appearance of damage to the working surfaces of the tested parts, welded with Hastelloy alloy, during the testing process is shown in Fig. 13.1 and 13.2. The areas of the most intensive wear of the parts coincide with the areas identified in the above-studied variants of hardening of the device parts.

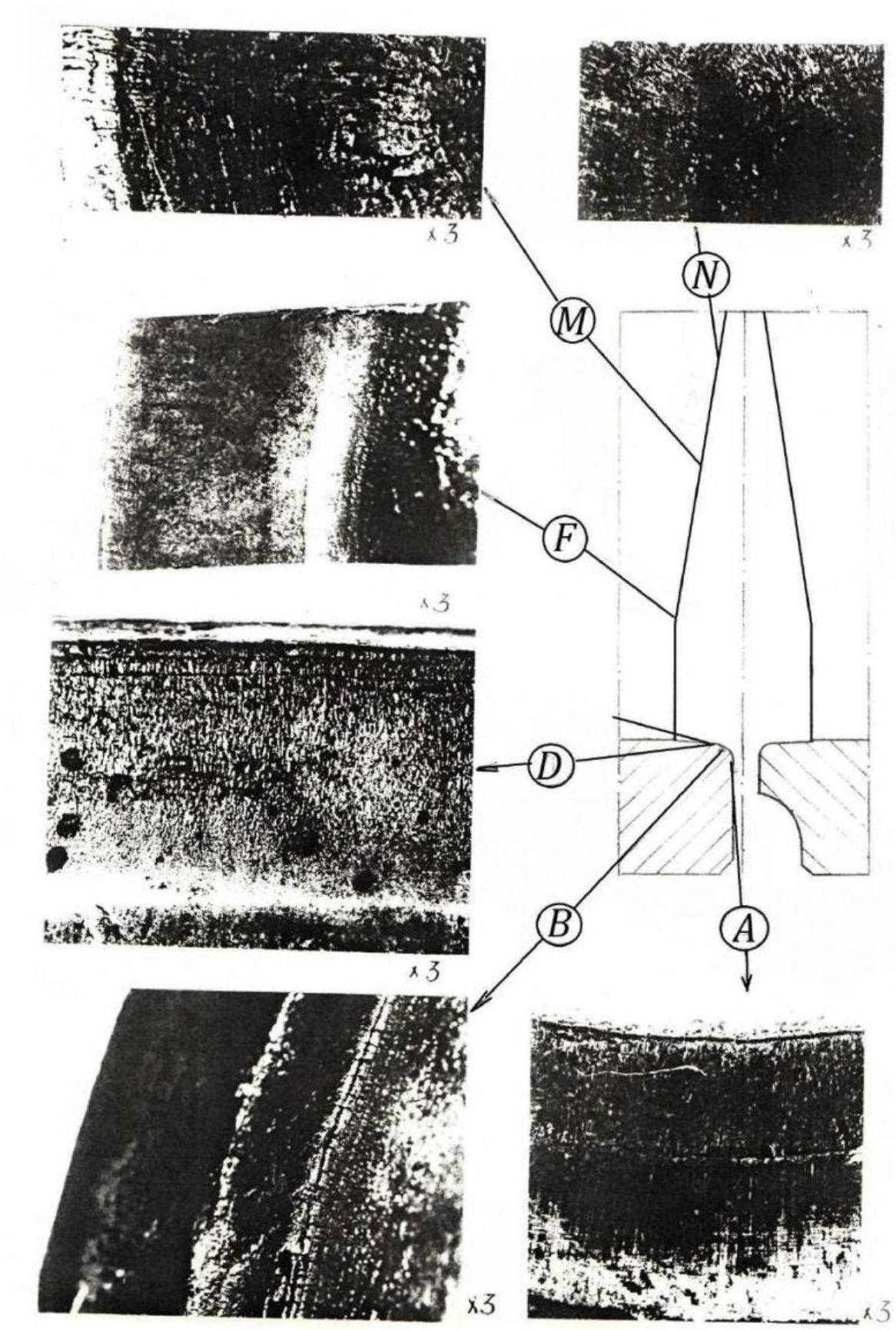

Figure 13.1. Wear of the spear and bushing, hardened by welding alloy "Hastelloy"

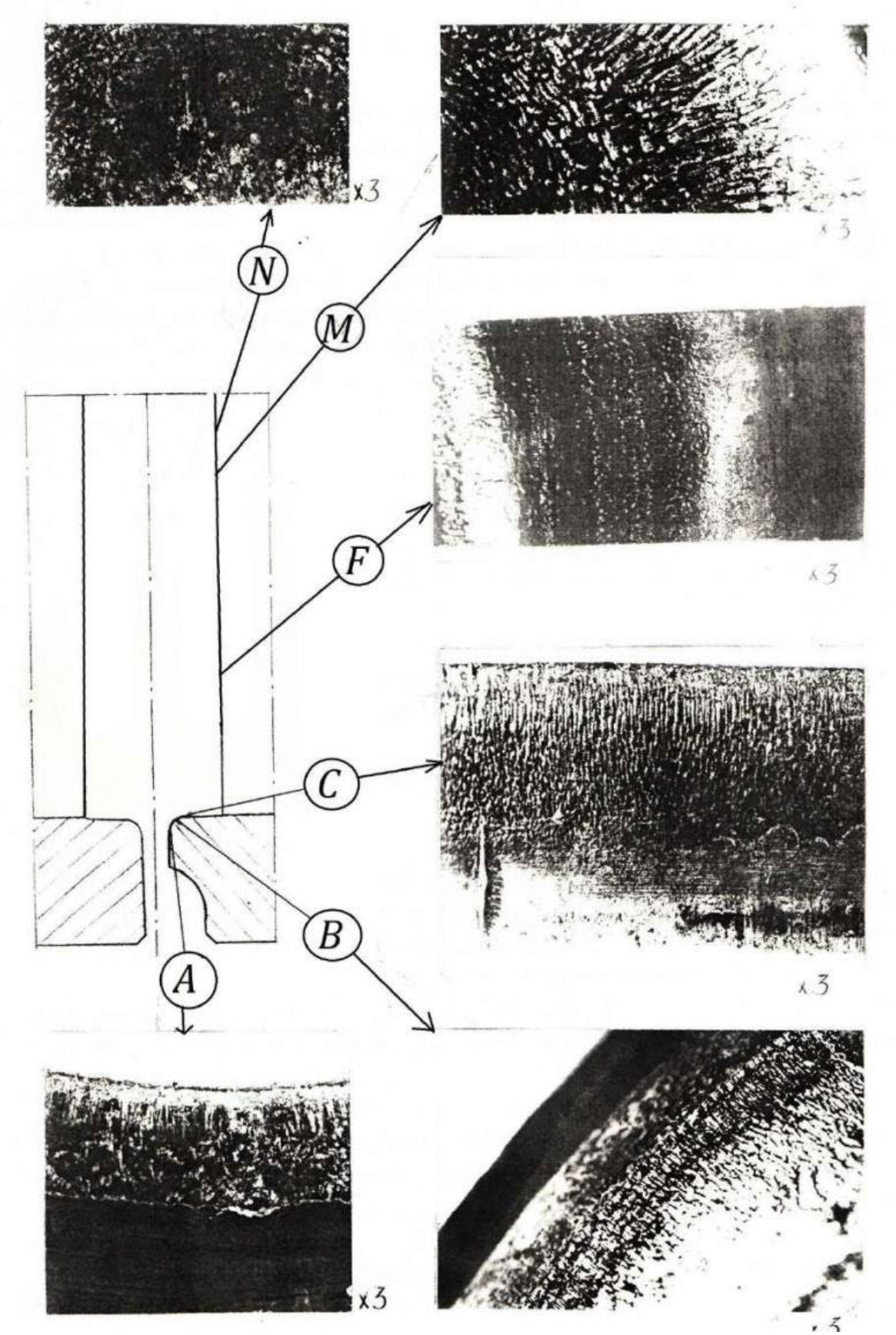

Figure 13.2. Wear of the body and striker, hardened by welding alloy "Hastelloy"

The nature of the damage to the housing and bushing differs from that observed on the parts of previous hardening methods. There are practically no surface burrs. Intensive plastic deformation (crumpling) of the deposited metal, its work hardening, cracking and oxidation are observed. In zones "A", plastic deformation of the deposited metal and cracks of mesh orientation are observed. In zones "B", plastic deformation of the surface volumes of the metal, ring cracks intersected by axial tears are observed. In places on the bushing, small chipping of the deposited metal occurs.

In zones "C" plastic deformation of the deposited metal is observed with the formation of axial folds, more pronounced on the bushing. In zones "D" running-in and some crumpling of the deposited layer is observed.

The damage to the striker and the peak is similar to that found in the previous versions. The weld layer is completely preserved. Zone "N" has view oval ironed out spots diameter of 25...27 mm on the striker and 15 mm on the peak. Radial grooves with a general annular direction, adjacent to the central spot, are clearly expressed on the striker. The surface of the peak in this area is crumpled, cold-worked and smoothed.

Zone "M" is characterized by poorly defined grooves-burrs. Relief of plastic deformation lines and grooves smoothed and intensively work-hardened. At the peak, the grooves are crushed until they disappear completely. Zone "F" is characterized by work-hardening and smoothing of the surface. In zones "N" , "M" and "F" on The peak shows cracks of a grid orientation of varying degrees of development. On the striker, the cracks are weakly visible. In the "N" zones of the striker and peak, the surfaces are worn down, evenly around the circumference.

12.3. Characteristic structural state of the material of the parts

When examining the macrostructure in the diametrical section of the parts, it was found that the metal of the deposited layer is dense. Defects in the form of gas pores, non-metallic inclusions, cavities, slag deposits And cracks are absent. Line fusion reinforcing layer With main metal wavy, depth penetration is 1.5 mm. No defects in the form of discontinuities are observed along the fusion line (Fig. 13.3).

Thickness fused metal is: frame striker –1.4–3.1 mm; sleeve – 2.2–

3.1 mm; striker – 2.3–4.5 mm; peak – 1.2–2.3 mm. The hardness of the deposited metal outside the damage zones is the same for the parts and is HRC 18–20.

The microstructure of the deposited metal outside the damaged zones has a grain structure of columnar orientation (Fig. 13.4).

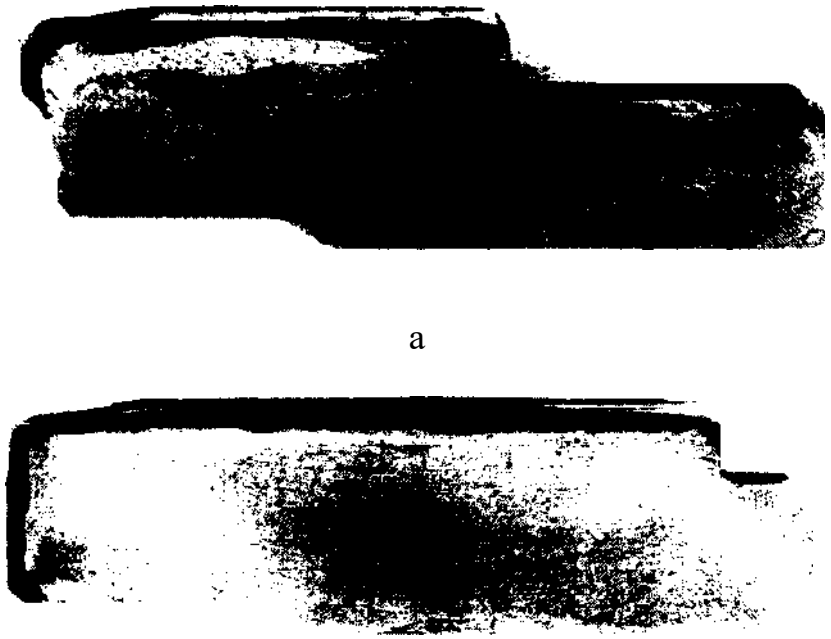

a

b

Figure 13.3. Microstructure corps (a) And bushings (b),
clad with Hastelloy alloy

The grain size varies for different zones of the deposited metal. When identifying the microstructure, it was found that the etchability of the deposited metal varies along the layer height, with more intense etchability observed near the fusion line (see Fig. 13.4, a).

Directly at the fusion line, the heat-affected zone is clearly visible (see Fig. 13.5). The width of this zone outside the areas of damage to the working surfaces is: bushing – 3.0 mm; body – 3.0 mm; peak – 4.0 mm; striker – 5.5 mm.

The hardness of the base metal of the device parts in the heat-affected zones outside the damaged areas of the working zones is: frame - HRC 30–32 (basic metal - HRC 33–35);

bushing – HRC 35–38 (base metal – HRC 30–33); striker – HRC 30–34 (base metal – HRC 25–30); peak – HRC 31–33 (base metal – HRC 25–30). The microstructure of the metal in the heat-affected zones consists of troostosorbite.

a

b

Figure 13.4. Microstructure fused metal:
a - V zone contacts With main metal; b - V average parts

a

b

Figure 13.5.Zones thermal influences V basically metal in the fusion area

On in the body And in the bushing size radius channel increased during testing by 0.5 mm.

All the examined parts of this manufacturing variant show partial wear of the hardening layer and its work hardening. The hardness of the deposited metal in zones “A” and “B” is HRC 28–33 for the bushing and HRC 30–33 for the body. At the peak, the hardness of the deposited layer in zone “N” is HRC 24–28, in zone “M” – HRC 20–28. On the striker, the hardness in these zones is HRC 20–22. In the remaining working zones, the hardness of the deposited metal is at the level of HRC 18–21.

IN base metal lines fusion V areas of all working zones show areas of thermal influence, the width of which is: on in the bushing - 5.0–5.5 mm; on in the body - 5.5–6.0 mm; on pike – 3–10 mm; on the striker – 7–10 mm.

The hardness of the metal in heat-affected zones is presented in Table 13.1.

Table 13.1

Distribution hardness V zones thermal influences on in detail

Part name	Hardness in heat-affected zones By workers surfaces of parts, HRC				Hardness of base metal, HRC	Hardness in the zones of thermal influence of surfacing, HRC
	"A"	"IN"	"WITH"	"D"		
Sleeve	33–35	30–34	34–35	32–35	34–35	35–38
Frame striker	34–36	36–44	38–40	32–33	33–35	30–32
	"N"	"M"	"F"	"E"		
Pika	34–36	36–41	30–32	31–34–	25–30	31–33
The striker	33–36	28–33	25–30	30–33	25–30	30–34

From Table 13.1 it follows that heating of the surface volumes of the metal of the parts during testing has a complex effect on the distribution of hardness in the heat-affected zones induced by the surfacing of the hardening layer.

The microstructure of the metal in the heat-affected zones is troost-sorbitol, sorbitol, and in places very finely dispersed.

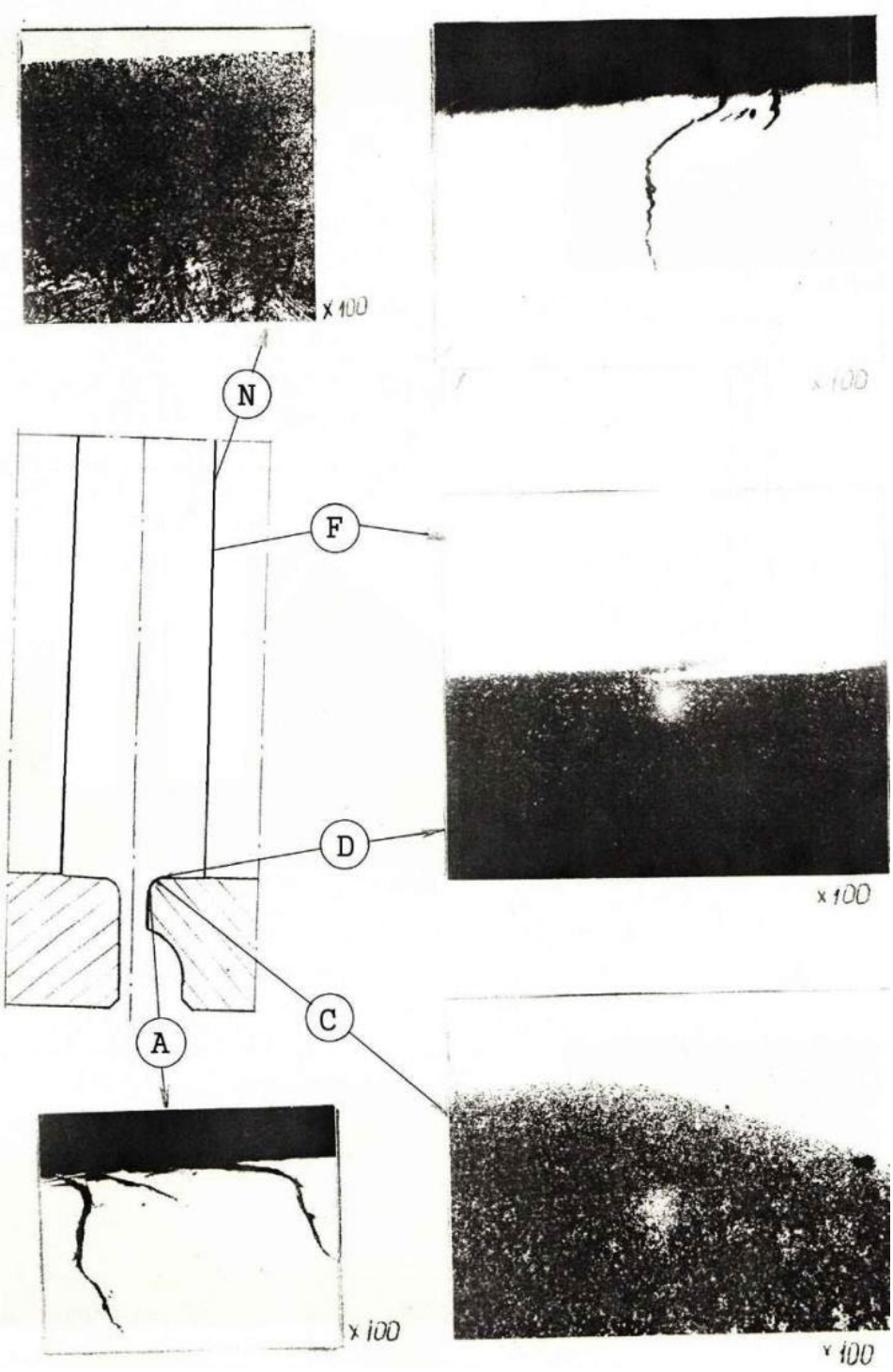

Figure 13.6. Structural changes material corps And striker, welded with Hastelloy alloy

When examining parts strengthened by surfacing with Hastelloy alloy, a large number of cracks were found, located only in the working zones (Fig. 13.6, 13.7).

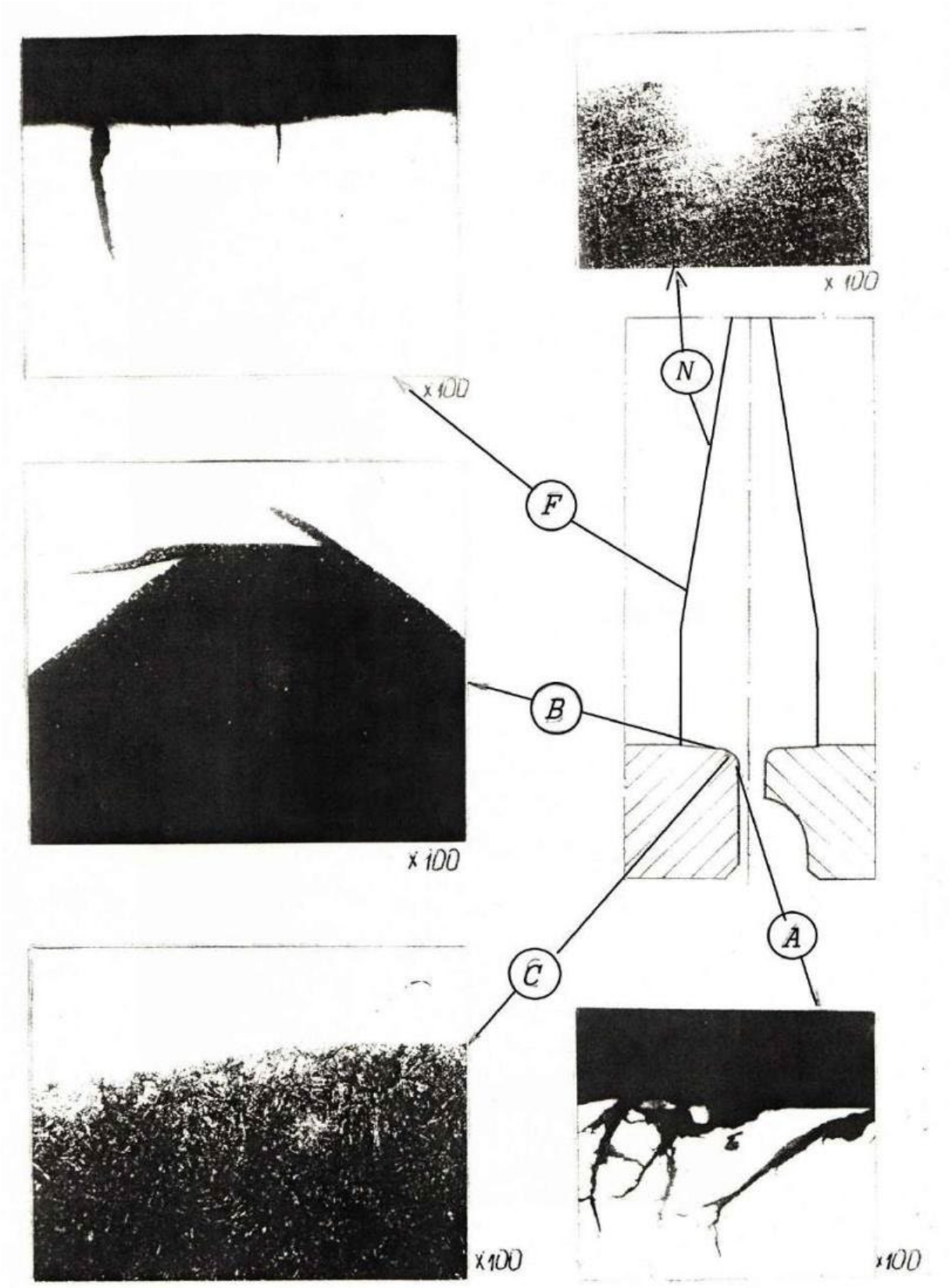

Figure 13.7. Structural changes material peaks And bushings, welded alloy "Hastelloy"

Cracks develop in the weld layer starting from the surface (rice.

13.8). On in the bushing cracks located V zones "A" and "B". The depth of the cracks in zone "A" is 0.4 mm, in zone "B" up to 1 mm. On the body, the depth of the cracks in both zones is up to 0.4 mm. On On the surfaces of the housing and bushing channels, cracks are located in the transition area from zone "B" to zone "C" on a belt up to 5 mm wide. In zones "C" and "D" cracks in the deposited metal are not observed.

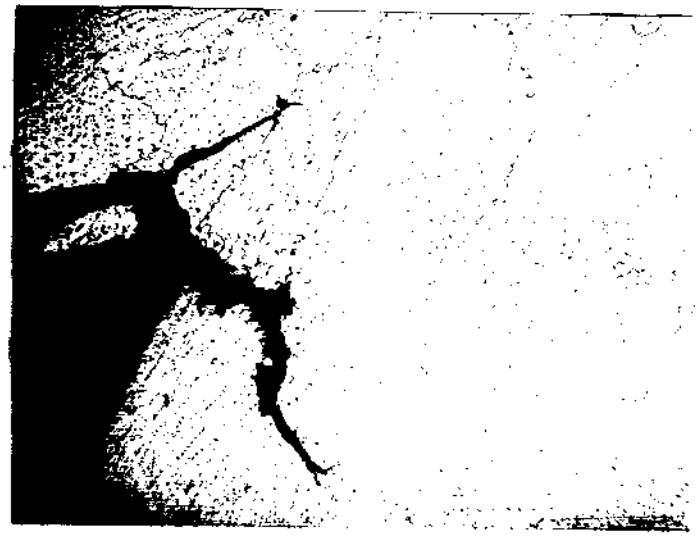

a

b

Figure 13.8. View cracks V Hastelloy alloy

On the striker and peak, cracks are located mainly in zones "N" and "M". On the peak, in zone "D", there are a large number of cracks, their depth is up to 0.9 mm; on the striker, cracks are isolated, up to 0.5 mm. In

the "M" zone, a large number of cracks are noted on both parts. depth to 0.7 mm. IN zone "F" cracks are isolated, A V zone
"E" - absent. No cracks are observed on the striker and peak of metal chipping along the joint.

On in the body And there are cracks in the bushing oriented both in the radial and latitudinal directions; in places they are connected to each other, acquiring a mesh configuration. Chipping of the deposited metal is noted at the intersections of cracks.

The cracks have a clearly defined contour at the fracture, an oxidized smoothed surface (Fig. 13.9).

The type of cracks is similar to those observed in previously studied variants of hardening of parts.

12.4. Study qualities material details

Chemical compound fused metal presented in table 13.2.

Table 13.2

Chemical compound fused layers details

Part name	Content alloying elements , %									
	Ni	C	Mn	Si	Cr	Mo	W	Fe	V	Co
Sleeve	osn.	0.06	0.33	0.23	14.1	14.4	3.0	10.0	-	-
Frame	osn.	0.06	0.32	0.30	13.0	14.8	3.0	13.0	-	-
Reference data										
Hastelloy "IN"	osn.	0.05	1.0	1.0	1.0	26.0–30.0	-	4.0–6.0	0.35	2.5

Hastelloy "WITH"	osn.	0.08	1.0	1.0	14.5–16.5	15.0–17.0	3.0–4.0	4.0–7.0	0.35	2.5

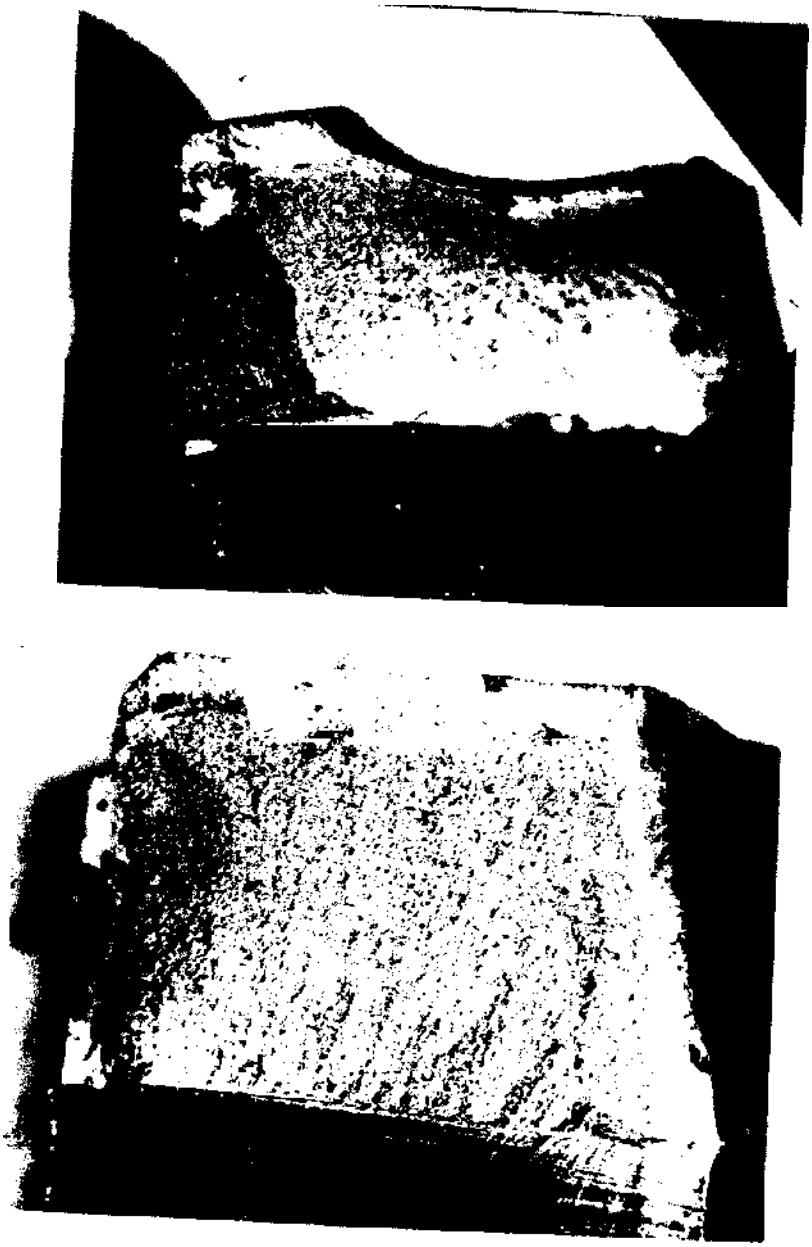

Drawing 13.9. View cracks V fractures: a – body; b – bushings

From Table 13.2 it follows that the deposited metal chemical composition is close to Hastelloy "C" alloy, but differs from it by lower values for silicon and higher values for iron. The hardness of the material of the parts is:

sleeve - HRC 30–33;

frame - HRC 33–35;

peak – HRC 25–30;

striker – HRC 25–30.

The microstructure of the material of the parts is finely dispersed , *sorbitol* type.

The results of testing the mechanical properties of the material of the parts for tension are presented in Table 13.3.

Table 13.3

Mechanical properties material details, reinforced by welding alloy "Hastelloy"

Part name	Direction of cutting samples	Mechanical properties			
		σ_{in}, MPa	$\sigma_{0.2}$, MPa	δ, %	ψ, %
sleeve	axial	1160.0–1170,0	1080.0–1100,0	18.0–19.0	62.0
	tangen-cial	1080,0	900.5–980,0	15.0–17.0	48.0–51.0
frame	axial	1150.0–1160,0	1070.0–1080,5	16.0	51.0
	tangen-cial	1090,0	900.0–940,0	18.0	62.0
striker	axial	1050.0–1050,0	910.0–920,0	18.0–20.0	62.0
	tangen-cial	1050.5–1060,5	920.0–930,0	16.0–18.0	48.0–51.0
peak	axial	1080,0	815.0–920,0	18.0–18.5	64.0
	tangen-cial	1050.0–1060,0	920.5–930,0	16.0–16.5	44.0–47.0

12.5. Conclusion

1. The results of testing models of parts hardened by surfacing with Hastelloy alloy show that the wear resistance of parts is increased by ~ 2.1 times compared to the original (not subjected to special hardening) version.

2. The damage to the working surfaces of the tested parts is similar in nature and location of the zones to the previously studied sets of parts.

3. During the surfacing process with Hastelloy alloy, intensive softening of the base metal occurred.

4. The Hastelloy weld metal layer is preserved on all parts of the kit, with minimal wear compared to the original weld metal layer thickness.

5. Damage to the body and bushing during testing consists of work hardening and plastic deformation of the deposited layer, and to the striker and peak – in the appearance of a weakly expressed relief, grooves and intensive work hardening of the peak.

6. The degree of damage to the sleeve and the peak of the device is higher than that of the body and the striker.

7. Cracks develop only in the weld layer on the body and bushing in zones "A" and "B", on the striker and peak - "N" and "M". The maximum crack depth is up to 1 mm.

13. DISCUSSION RESEARCH RESULTS

The results of the tests show that the durability of parts can be increased by using modern strengthening technologies, resulting in tribotechnical systems with high contact and operational properties of surfaces.

Fig. 14.1 shows the results of wear resistance tests of the housing and bushing, hardened by the methods studied above, in the form of a diagram. It was found that the following types of destruction of the surface layers of the metal of the parts occur during the tests: plastic displacement, work hardening, microcutting, cohesive separation and crack formation. In the case of cohesive separation, the destruction of friction bonds is accompanied by the formation of cracks on the surface that extend deep into the material. In this case, it is advisable to form a third medium on the surface of the parts, which localizes the destruction during friction and transforms the resulting separation crack into a near-surface shear crack. With such wear mechanisms, it is necessary to ensure special scuff-resistant properties of the surface of the part. For these purposes, wear-resistant compounds applied to the friction surfaces are most effective.

Good results (2100 loading cycles) were obtained during testing corps And bushings, reinforced by welding alloy "Hastelloy" (5). The peculiarity of this method of strengthening is the low hardness of the deposited metal (HRC 18–21). However, during the surfacing process, the base material of the part is softened (HRC 30–35) and its mechanical properties are reduced. The low hardness of the deposited layer allows for easier mechanical processing of the product. However, the intensive softening of the base metal of the parts excludes the possibility of using surfacing to strengthen real housings and bushings. Obviously, optimal option use alloy "Hastelloy" for strengthening parts is the use of a liner of this material, connected to the base metal of the product, for example, by welding using explosive energy.

Among the tested methods of strengthening the body and bushing, the most widely used were chromium coatings used to increase the wear resistance of heavily loaded tribosystems. Chromium coatings were applied in a bath with electrolyte mixing (10), using the Sumy-Swiss technology (8), by the ion-plasma deposition method (1) and by decomposition of the organochromium compound "Barkhos" (9).

It has been established that galvanic and ion-plasma chrome coatings provide close enough results by the durability of parts (from 1750 cycles for ion-plasma coating using improved technology, to 1900 cycles for chrome coating obtained using Sumy-Swiss jet technology).

The chromium coating obtained by decomposing the organochromium compound “Barkhos” (9) demonstrated wear resistance that was only 1.3 times greater than the corresponding characteristic of the original (without special types of hardening) version (1330 loading cycles).

Almost identical results in terms of service life of parts were obtained when testing the body and bushing, hardened by laser thermal treatment. processing (3) And detonation gas spraying (7) wear-resistant coating – 1800 cycles. Electric spark microalloying (6) And ion-plasma carbonitride coating

(4) do not provide a significant increase in the service life of parts. This value is 1300 and 1200 loading cycles, respectively.

However, to select the optimal strengthening option, it is not enough to compare the results on the service life of parts obtained during the experimental study. This requires additional analysis of the wear of parts during testing, the service life of parts before the appearance of signs of destruction of the hardened layer, crack formation and structural transformations in the surface volumes of the product material.

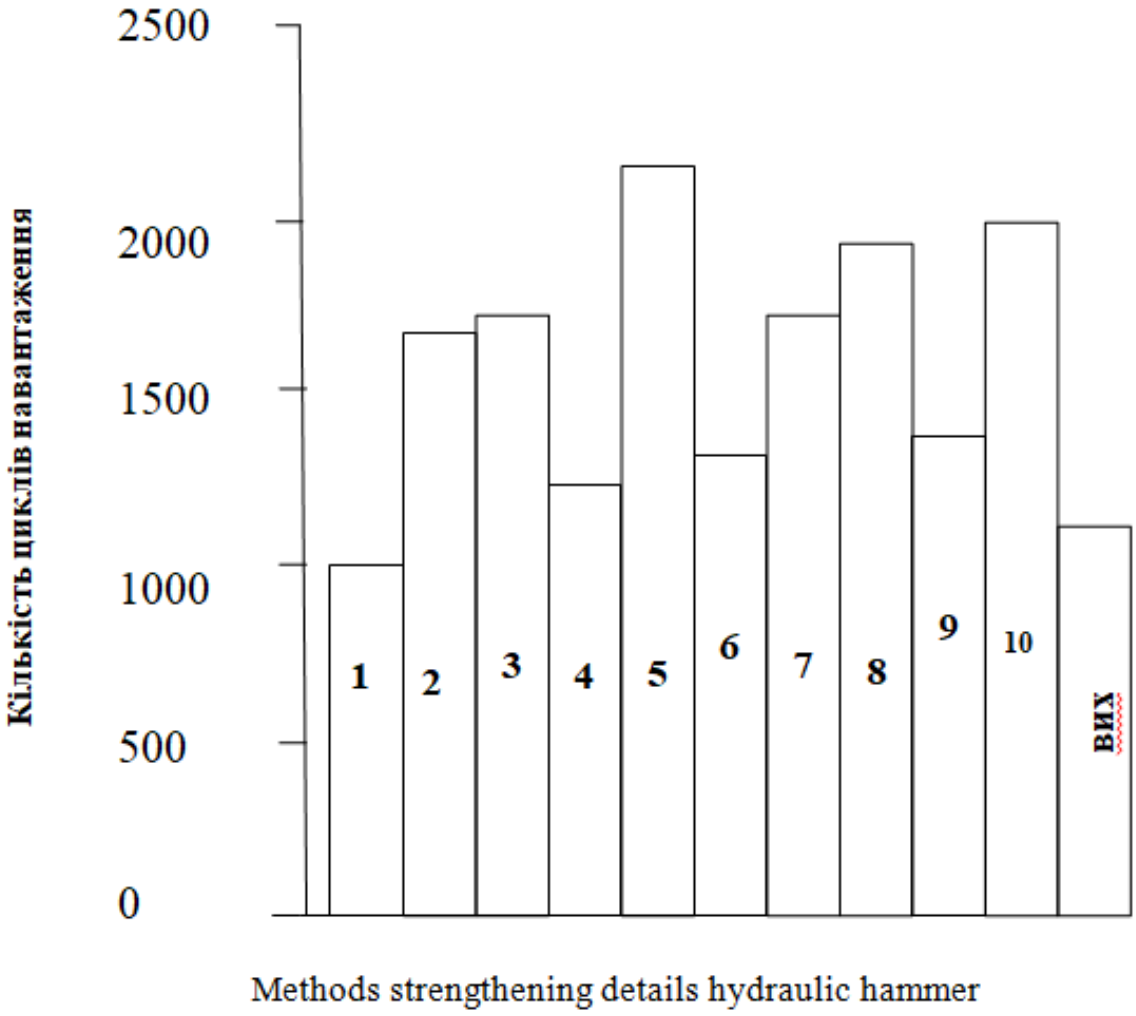

Figure 14.1. Dependence of wear resistance of hydraulic hammer parts on the type of hardening: original – without additional hardening, 1 – ion-plasma chromium plating; 2 – ion-plasma chromium plating using improved technology; 3 – laser heat treatment; 4 – carbonitride coating; 5 – surfacing alloy "Hastelloy"; 6 - electric spark alloying; 7 - detonation hardening; 8 - chromium plating using Sumy-Swiss technology; 9 - chromium plating by decomposition of the "Barkhos" compound; 10 - galvanic chromium plating

The statistical data of wear measurements of housings, bushings, peaks and strikers were calculated and graphically presented as functions. In this case, two main types were distinguished influencing factors, from which first represented by yourself the measured value (wear), and the second is a qualitative factor (the method of strengthening the working surfaces).

Since the durability of parts during testing can be greatly affected by factors such as the pace of testing and interruptions in their implementation,

in addition to statistical processing, instability and interruptions in the testing process were taken into account.

The presentation of the processed research results and the establishment of the relationship between the service life of parts and the influencing factors was carried out in three complexes:

a) bilateral wear of the striker and peak in the “M-M” section and the factors influencing it;

b) wear corps And bushings V channel;

c) the duration of operation of parts before the appearance of initial signs of destruction of hardened surfaces.

As follows from the graphic dependencies of the wear of the striker and the peak on the number of cycles and the type of hardening treatment, positive results in wear resistance are provided by surfacing the working surfaces with Hastelloy alloy (Fig. 14.1). The duration of work increased in comparison with the initial (not subjected to special hardening) condition by 2.1 times, the wear of parts in the controlled section decreased by 3 times.

Good results in wear resistance were obtained when testing parts hardened by chromium plating using the Sumy-Swiss technology. With an increase in durability compared to the original version by 1.9 times, wear in controlled cross-section of the striker and peak decreased by 2.2 times.

The wear process of parts strengthened by detonation gas spraying (7), up to approximately 1200 loading cycles, is practically identical to the wear pattern of parts strengthened by chromium plating using the Sumy-Swiss technology (Fig. 14.1).

However, during further testing, the wear process during detonation hardening is distinguished by an approach to the nature of destruction of the initial (without additional hardening) variant. This is obviously due to the almost complete wear of the sprayed layer after 1200 loading cycles, due to its small thickness (up to 20 μm). Similar results in terms of wear intensity were obtained when testing chromium coatings applied by galvanic methods (10), ion-plasma, vacuum-arc deposition (2) and decomposition of the organochromium compound "Barkhos" (9). Tests of parts strengthened by vacuum-arc deposition using standard technology (1) and decomposition of the compound "Barkhos" (9) showed their low durability. Among the four methods of applying chromium coating noted above, the preferred method is in terms of wear resistance, the coating is obtained by ion- plasma vacuum-arc deposition using improved technology (2).

The complex carbonitride coating, according to literature data,

provides high values of microhardness, adhesion and significant resistance to shear loads. It serves as a screen contact surfaces And allows minimize wear, since it is possible to exclude plastic deformation of the surface and reduce the intensity of crack propagation. Coating (4) showed high wear resistance at the first stage of testing. However, after 450-500 loading cycles, signs of wear and chipping of the coating appeared, which caused the further course of the wear process to be almost identical to the original (without additional strengthening) version.

Testing of a hydraulic hammer with parts hardened by laser heat treatment (3) shows wear stability throughout the entire period of loading. Up to 800 loading cycles, wear of parts is approximately 2.2 times less compared to
the original (additionally non-hardened) version. With further testing from 800 to 1000 cycles, wear is reduced by 2.5 times compared to the original parts. This is due to the creation of a hardened zone of the base metal during the LTO process, characterized by good resistance to destruction regardless of the degree of its wear.

The wear of the material during testing of the striker and pick, hardened by electric spark alloying (6), is directly proportional to the number of loading cycles. This pattern is maintained until the hardened layer is completely worn out. Results measurements testify, What wear reinforced The wear resistance of parts is 1.57–1.62 times less than the wear resistance of parts of the original manufacturing version.

The wear of the parts of the original manufacturing variant (original) first decreases slightly, then, after 800 loading cycles, increases sharply. There is a practically stable wear of the striker material And peaks in progress tests for every loading cycle (Fig. 14.1). Minimal wear was recorded when testing parts hardened by surfacing with Hastelloy alloy (5). Quite close results in wear resistance to the results of testing the hard-faced housing and bushing were shown by parts hardened by the detonation-gas method (7). However, after 1500 loading cycles celebrated increase wear and tear, conditioned, obviously, by destruction (wear) of the hardening coating. Galvanic chromium coating applied by Sumy-Swiss technology (8) showed high wear resistance up to 1600 loading cycles. Further testing showed a sharp increase in wear of the housing and bushings, apparently caused by the onset of coating destruction at the end of zone "C" (at the border with zone "B"). Ion-plasma chromium plating By typical technological scheme (1) on first stage of testing ensures high

wear resistance of the parts. However, after 700 loading cycles, the coating begins to chip, which limited the durability of the housing and bushing of this hardening option to 1000 cycles.

Electric spark alloying (6) and ion-plasma chromium plating By improved technologies (2) provide stable wear resistance of the body and bushing. A directly proportional dependence of wear on the number of loading cycles was recorded during testing of parts hardened by laser heat treatment (3), which indicates the usefulness of hardening the surface volumes of the base metal of the product for these operating conditions, the wear resistance of which is 4.0–5.4 times higher compared to the corresponding characteristic of the base material of parts that have not been subjected to special hardening. Galvanic chromium coating (10) has good wear resistance up to 600 loading cycles. With further testing, wear increases monotonously, reaching a value of 0.55 mm at 1860 loading cycles.

The characteristics of the destruction of the body and bushing, strengthened by chromium plating through the decomposition of the connection, are located separately "Barkhos" (9) And application carbonitride coatings
(4). Both of these coatings are characterized by their destruction in the process tests, which determines significant wear of the channel parts.

Figure 14.2 shows a bar chart characterizing the appearance of visually detectable signs of the onset of destruction of the hardened layer during testing, constructed based on the results of studying the performance of the hydraulic hammer striker.

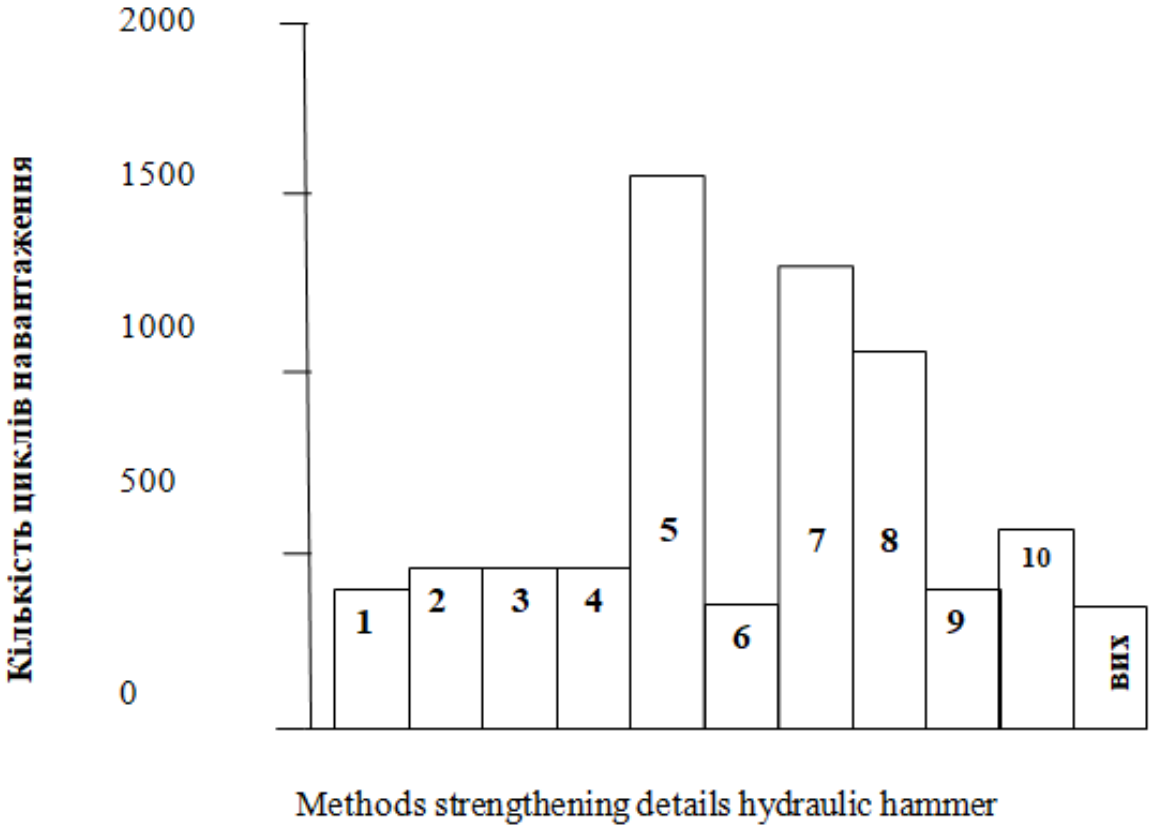

Figure 14.2. Diagram of wear resistance of hydraulic hammer parts depending on the type of hardening: original – without additional hardening, 1 – ion-plasma chromium plating; 2 – ion-plasma chromium plating using improved technology; 3 – laser heat treatment; 4 – carbonitride coating; 5 - surfacing alloy "Hastelloy"; 6 - electric spark alloying; 7 - detonation strengthening; 8 - chromium plating By sumsko-Swiss technologies; 9 - chromium plating decomposition of the compound "Barkhos"; 10 - galvanic chromium plating

It follows from the diagram that the strengthening methods that ensure an increase in the properties of the base metal of the body and

bushing (6, 3), an also big part of chrome coatings (1 and 2, 9, 10) and carbonitride coating (4) provide durability of the hardening layer from 35 to 500 loading cycles. The most significant increase in durability of the hardened layer (by 3.3–5.0 times) compared to the original (without additional hardening) version. This is achieved by chromium plating of parts using Sumy-Swiss technology, detonation-gas spraying of wear-resistant materials and surfacing with Hastelloy alloy (Fig. 14.2).

In a comparative analysis of the damageability of the surfaces of parts during testing in a controlled section of the striker and the peak, the evaluation characteristics were:

1. Damage surfaces (type And intensity).
2. Degree wear and tear(presence) leftovers hardened layer).
3. Quantitative And high quality characteristic cracks.

Nature of damage to the body, bushing, striker and peak various hardening options are practically the same. This was most clearly demonstrated during the study of the striker and the peak.

The degree of damage to the pick is usually higher than to the striker. The exception is parts hardened by chromium plating by decomposing the organochromium compound "Barkhos". When testing this set, more intense damage to the striker was found compared to the pick.

The predominant type of damage to the housing (in zones “C”) of the original (without additional strengthening) version and those strengthened by electric spark alloying, ion-plasma chromium plating and carbonitride coating is wear, the formation of a relief of plastically deformed metal and intensive his slander. On models of the case and bushings, hardened by laser heat treatment and ion-plasma chromium plating using advanced technology, are subject to wear and "peeling" of the surface layer. On the body and bushing, hardened by detonation gas spraying And chromium plating according to the Sumy-Swiss technology, intermediate types of destruction of the surface layers of the material of the parts are noted. The hardened layer of the bushings, treated with chromium plating by decomposing the "Barkhos" compound and ion-plasma chromium plating according to the standard technology, was destroyed with the formation of chips and flaking of the coatings.

On the body and bushing of all manufacturing options, except for those welded with Hastelloy alloy, the channel surface is usually smoothed and has traces of minor plastic deformation. Surface corps And bushings, reinforced by welding "Hastelloy" differs sharply from parts of other

manufacturing options by the formation of a rough, coarse relief without signs of smoothing and axial folds of deformed metal.

The damage to the striker and the peak consists of the formation of a rough relief of folds of deformed metal and their wear. Wear and smoothing of the surface layer of the metal are noted on half the length of the "F" zone.

This is most pronounced in the original (additionally unhardened) version on the striker, as well as on parts hardened by laser heat treatment, carbonitride coating, chromium plating by decomposition of the “Barkhos” compound, and to a lesser extent on peaks treated by electric spark alloying, detonation spraying, ion-plasma chromium plating, galvanic chromium plating and welded with Hastelloy alloy. On strikers with chromium coatings (galvanic, according to Sumy-Swiss technology and deposited by decomposition of the Barkhos compound) damage has developed by chipping of the chromium coating.

The degree of wear of the hardened layers during testing is characterized by the research results presented in Tables 14.1 and 14.2.

Table 14.1 shows that during the wear process, the surface layers of the body and bushing parts hardened by laser heat treatment (3) and surfacing with Hastelloy alloy (5) were preserved to the greatest extent. When testing the body and bushing hardened by ion-plasma chromium plating using standard technology (1), carbonitride coating (4), chromium plating decomposition of the compound "Barkhos" (9), at a certain stage of testing, emergency destruction of the coatings is noted, accompanied by the formation of chips and flaking. Detonation-gas coating (7), ion-plasma chromium coating using improved technology (2) and galvanic chromium coating using Sumy-Swiss technology (8) give wear in the process tests without signs of emergency destruction.

Table 14.1

Change thickness hardened layers And depth development cracks on the body and sleeve models (zone "C")

№№ p/p	Way strengthening	Number of loading cycles	Thickness of the hardened layer, microns		Crack depth, mm
			original	on those that have survived wear and tear areas	
1	2	3	4	5	6
Frame					
1	without strengthening (out)	1000	No	No	0.3
2	LTO (3)	1800	500–550	300–400	0.1–0.5
3	EIL (6)	1300	100–400	less than 10	-
4	ion-plasma chromium plating (1)	1000	50	20	-
5	galvanic chromium plating (8)	1860	30–50	20	0.1–0.3
6	ion-plasma chromium plating using an improved technology technologies (2)	1750	40–50	10	-
7	chromium plating By Sumy-Swiss technology (8)	1900	50–60	20–30	1.0
8	chromium plating decomposition liquids "Barkhos" (9)	1300	100	60–100	0.25
9	carbonitride coating (4)	1200	20	10	-
10	detonation strengthening (7)	1800	-	20	0,1
11	surfacing alloy "Hastelloy" (5)	2100	1400–3100	1050–1800	-
Sleeve					
1	without strengthening (out)	1000	No	No	0,1
2	LTO (3)	1800	450–500	300–400	0.3–0.4
3	EIL (6)	1300	100–400	to 10	-
4	ion-plasma chromium plating (1)	1000	50	20	0,1
5	galvanic chromium plating (8)	1860	20–60	to 3	0.1–0.3

End table. 14.1

1	2	3	4	5	6
6	ion-plasma chromium plating using an improved technology technologies (2)	1750	40–50	10	-
7	chromium plating By sumsko- Swiss technologies (8)	1900	50–60	10–50	0.15
8	chromium plating decomposition liquids "Barkhos" (9)	1300	20	20	0.05
9	carbonitride coating (4)	1200	20	10	-
10	detonation strengthening (7)	1800	-	20	-
11	surfacing alloy "Hastelloy" (5)	2100	2200–3100	2100–2500	-

Table 14.2

Change thickness hardened layers And depth development cracks on the striker (zones "M" and "F")

Item No.	Way strengthening	And to l	a up ro	Zone "M"		Zone "F"	
				Thickness layers on preserved areas, µm	depth cracks, mm	layer on preserved areas, µm	depth cracks, mm
1	2	3	4	5	6	7	8
The striker							
1	without strengthening (out)	1000	No	-	0.3	-	0.3
2	LTO (3)	1800	500–550	100–250	0.5–0.7	-	-
3	EIL (6)	1300	20–50	-	0.1–0.2	30–50	0,1
4	ion-plasma chromium plating (1)	1000	15–12	5–10	0,1	-	-

End table. 14.2

1	2	3	4	5	6	7	8
5	Galvanic chromium plating (8)	1860	20–40	-	0.3–0.4	20	0.1–0.4
6	ion-plasma chromium plating by improvement Noah technologies (2)	1750	50	-	0.6	-	-
7	chromium plating Sumy – Swiss technologies (8)	1900	18–40	30	0.8	20	0,1
8	liquid decomposition chromium plating "Barkhos" (9)	1300	73–120	-	0,1	-	-
9	Carbonitride coating (4)	1200	20	-	0.3–0.8	-	0.3–0.5
10	Detonation hardening(7)	1800	-	-	0.3–0.4	2	0.15
11	surfacing alloy "Hastelloy" (5)	2100	2300–4500	3100	0.7	2500	-

As follows from Table 14.2, the hardened layer was practically preserved on the strikers deposited with Hastelloy alloy (5), treated by electric spark alloying (6) and laser heat treatment (3). On the strikers chromium-plated by the ion-plasma method using the improved technology (2) and with the applied carbonitride coating (4), the hardened layer was practically completely worn out. The coatings applied by detonation-gas spraying (7), ion-plasma chromium plating using the standard technology (1), galvanic chromium plating (10) and using the Sumy-Swiss technology (8), as well as those obtained by decomposition of the Barkhos compound (9), were preserved on the strikers only in the form of individual sections.

On all the studied parts, during wear resistance tests, cracks develop both in the hardened layer (with its partial wear) and in the base metal of the parts (after complete wear of the hardened layer).

On the body, bushing, striker and peak, hardened by surfacing with Hastelloy alloy, cracks are located only within the hardened layer. In parts manufactured using other investigated hardening methods, cracks pass from the hardened layer (in case of its incomplete wear) into the base metal.

The body and bushing, strengthened by electric spark alloying (ESA), carbonitride coating, ion-plasma chromium plating using improved

technology and surfacing with Hastelloy alloy, have no cracks in the “C” zone. The greatest quantity cracks for the body And bushings recorded in cases of their strengthening by galvanic chromium plating, minimal - by detonation spraying, decomposition of the "Barkhos" compound and laser heat treatment (LHT). Cracks of the greatest depth are observed on the body in the case of its strengthening by laser heat treatment, chromium plating (using Sumy-Swiss technology), on the bushing - by laser heat treatment and galvanic chromium plating.

When examining the striker and the pick, it was found that cracks were absent only on the pick, which was strengthened by ion-plasma chromium plating. By typical technologies. The greatest quantity cracks were recorded on the strikers treated with galvanic chromium plating and the Sumy-Swiss technology, decomposition of the Barkhos compound, and detonation-gas spraying, the minimum - treated with ion-plasma chromium plating, carbonitride coating and laser heat treatment. The deepest cracks on the strikers and peaks were recorded for cases of their strengthening by ion-plasma chromium plating using an improved technology, surfacing with Hastelloy alloy, chromium plating, on the strikers - laser heat treatment, carbonitride coating, chromium plating using the Sumy-Swiss technology.

On parts manufactured without additional strengthening (original) maximum quantity cracks noted on the body And striker, minimum on the bushing and peak, which also allows us to consider the condition of the upper parts of the hydraulic hammer as decisive for assessing the effectiveness of strengthening treatments.

Fig. 14.3 shows a bar chart of the dependence of the number of cracks in the striker cross-section (zone "M") on the method of its strengthening. It follows from the figure that all the studied strengthening methods made it possible to reduce the tendency of the material to crack formation. The maximum crack resistance of the striker material was obtained in the case of their strengthening by ion-plasma chromium plating and laser heat treatment. Good results in crack resistance were obtained when testing strikers deposited with Hastelloy alloy and strengthened with a carbonitride coating. The use of electric spark alloying, detonation spraying, galvanic chromium plating and chromium plating by decomposition of the "Barkhos" compound ensures an increase in the crack resistance of the striker material by 1.6–2.0 times.

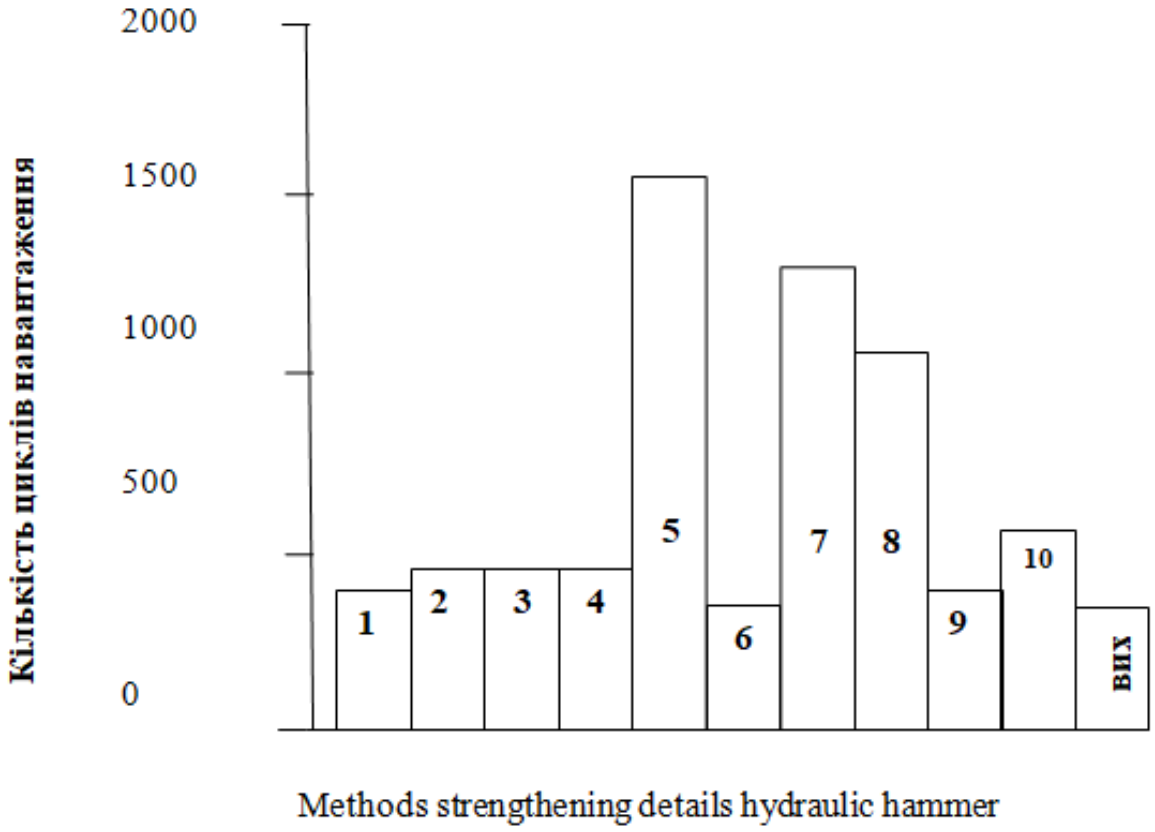

Figure 14.3. Quantity cracks V section striker (zone "M")

4 The dependence of the number of cracks in the section of the housing channel on the method of its strengthening is shown in Fig. 14.4. The data show that when using electric spark alloying, ion-plasma chromium plating, carbonitride coating and surfacing with Hastelloy alloy for strengthening the housing, cracks in the cavity of the channel (zone "C") are not detected. The use of detonation-gas spraying, chromium plating by decomposition of the Barkhos compound and laser heat treatment ensures an increase in the crack resistance of the material of the parts compared to the original (additionally non-strengthened) state. In contrast, the use of galvanic chromium coatings increases the tendency of the materials of the parts to form cracks by 1.8–2.2 times.

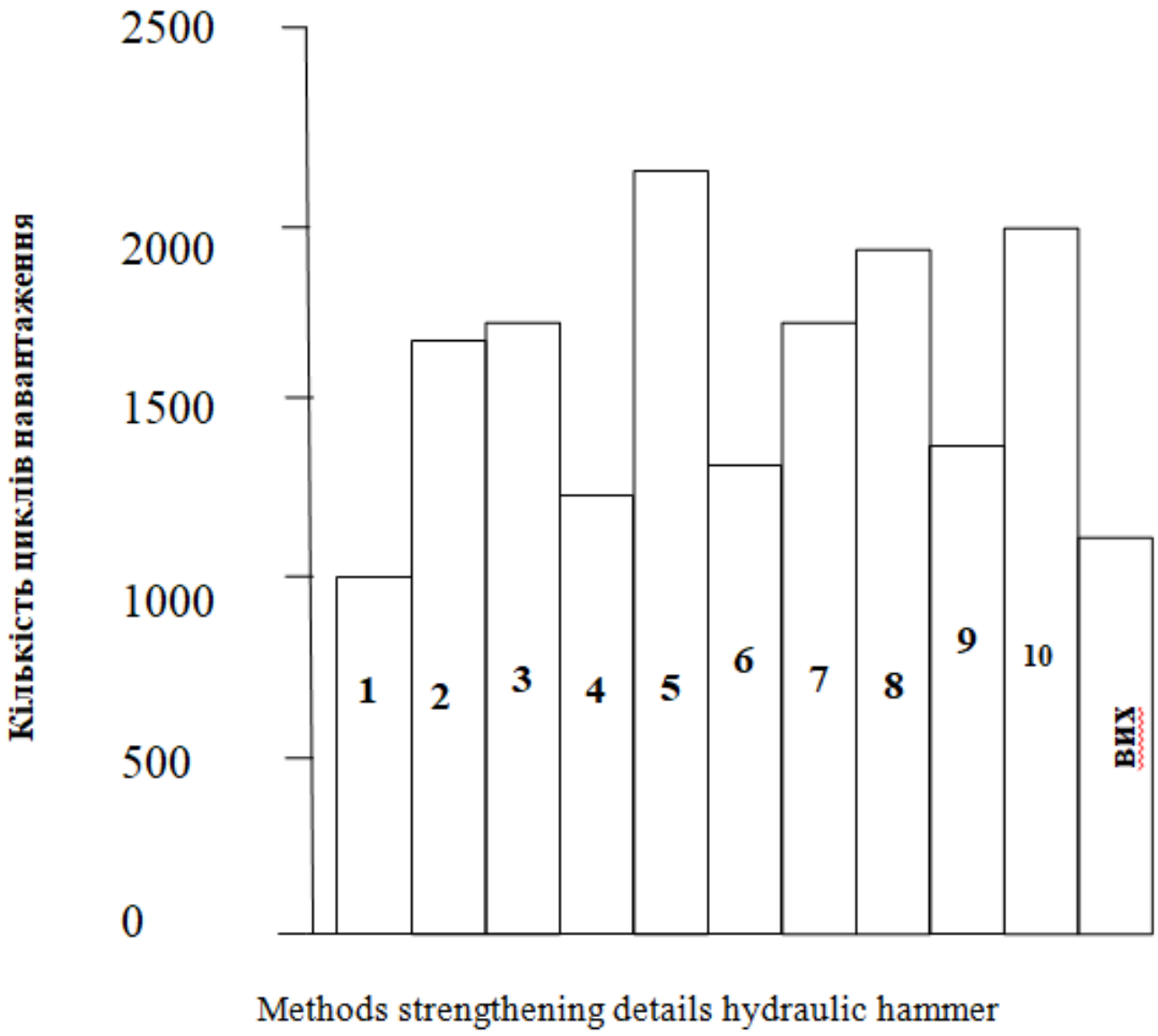

Figure 14.4. Quantity cracks V section channel corps (zone "WITH")

The results of the metallographic study allow us to single out among the studied options for strengthening the body and bushing, surfacing with Hastelloy alloy, laser heat treatment, detonation-gas spraying and ion-plasma chromium plating as the most suitable methods of strengthening treatment of these parts.

A comprehensive comparative assessment of the studied strengthening methods was carried out, the results of which are presented in Table 14.3.

Table 14.3

Advantages And flaws strengthening processing hydraulic hammer parts

Item No.	Type of hardening treatment and her parameters	Number of loading cycles zheniya	Characteristics species	
			advantages	flaws
1	2	3	4	5
1	Original condition, without additional go strengthening	1000	Typical volumetric technology and bushing material	Low value durability, high wear of the striker and picks controlled section 1,75 mm and the housing and bushing channels – 0.8 mm; low wear resistance before the start of destruction of the working surfaces – 300 cycles; significant number of cracks V striker And pique-30/cm, body and sleeve – 12/cm.
2	Laser heat treatment, hardened layer thickness – 0, 50 0,55 mm	1800	The presence of significant remains of the hardened layer after testing – 0,1-0,4, durability 1.5-1.8 times higher than in the original state; a small number of cracks on striker And pique -5/cm And V body channel - 9/cm; high technology ; strengthening by impact on the main material corps and bushings;	Thermal fatigue cracks extending beyond the limits hardened layer; low wear resistance before the onset of destruction of the hardened layer - 450 cycles; the need for additional heat treatment of the body and bushing and honing of hardened surfaces.

3	Electric spark alloying, depth of hardening layers to 0,1 mm	1300	The presence of remains of the hardened layer after testing – 0,001-0,01 mm; no cracks in the channels housings and bushings; shallow depth cracks on the striker and peak–0,1-0,2mm, high technological hardening	Low durability value– V 1.3 times higher than in the original state; significant wear in the controlled section striker And peaks–1.5 mm and the housing and bushing channels – 0.2 mm; low wear resistance before the onset of destruction of the hardened layer – 300 cycles, an insignificant number of cracks in the striker and peak – 15/cm. Necessary grinding and honing hardened surfaces
4	Cr hm, coating thickness 20–150 microns	1800	coating residues after testing: on the body and in the sleeve–3–20 μm; on the striker and peak - areas up to 20 microns; durability is higher than that of the original version without hardening 1.86 times.	High wear in the controlled section of the striker and peak - 1.7 mm and the channels of the body and bushing - 0.55 mm; low wear resistance before the onset of destruction of the coating 500 cycles; the largest number of cracks compared to the methods V body and sleeve - 27/cm, on the striker up to 19/cm; depth 0.3–0.4 mm; chips in the chrome coating; the need to create specialized chromium plating section
5	Ionic-plasma chrome plated nie, thickness coatings 15–75 microns	1000	Availability leftovers coatings on body and sleeve up to 20 microns; on striker And pique–10 μm; absence cracks V channels corps And bushings, insignificant quantity cracks V boykeys pique -3 cm	Absence increases durability (practically And such same as and without strengthening processing ; low wear resistance (to beginning destruction coatings - 400 cycles; coloring hardened layers after 700 cycles loading necessity polishing reinforced surfaces

			depth up to 0.1mm.	before operation, as well as the creation of a specialized area And his equipment complex vacuum equipment
6	Detonation-no strengthening, thickness sprayed layers to 100 microns	1800	Availability leftovers coatings: on cor-puse And in the bushing to 20 microns; on striker And pique to 2 microns; durability approximately 1.8 higher than in original va- riante. High wear resistance before the start destruction coatings – 1300 cycles; good wear resistance (0.2 mm) and small quantity cracks 3/ cm channel corps And bushings depth to 0.3–0.4 mm	High wear V controlled section striker And peaks–1.5 mm, big quantity cracks V striker And pique - 17/cm; necessity dry sand cleaning before strengthening; grinding or honing reinforced surfaces, creations specialized plot
7	Carbonitride no coating, thickness inflicted coatings 20 microns	1200	Availability leftovers coatings on in the body And in the bushing up to 10 microns; absence on in the body And in the bushing cracks, small quantity cracks on striker And pique (8/cm)	Low durability- approximately V 1,2 times higher, how durability details without hardening (original); full wear coatings on striker And peak; low wear resistance to beginning destruction coatings- 450 cycles; big wear V controlled cross-section of the striker and peak - 1.25 mm and the channel of the body and bushing - 1.1 mm; large depth of cracks on striker And pique – 0.3…0.8 mm. The need for honing hardened surfaces, creating a specialized area And his equipped with a complex vacuum equipment

8	Ion-plasma chromium plating using advanced technology, coating thickness 40–60 μm	1750	Availability coating residue on the body And bushing up to 0 microns; durability approx. V 1.75 times higher than non-hardened parts; small amount of cracks on striker and peak (3/cm) and absence of cracks V channels of the body and sleeve.	High wear in the controlled section of the striker and peak - 1.4 mm and the channels of the body and sleeve - 0.4 mm. Complete wear of the coating on the striker and peak; low wear resistance before the coating begins to fail – 450 cycles. Large depth of cracks on the striker and peak up to 0.6 mm. Necessity polishing or honing hardened surfaces, creating a specialized area and equipping it with a complex vacuum equipment.
9	Surfacing alloy "Hastelloy" thickness fused go metal 1.2–4.5 mm	2100	Availability of residues fused layers: on in the body And in the bushing 1.05–2 ,50 mm, on the striker and peak 2.2–3.1 mm. Durability approx. ov 2.1 times higher, how durability of parts without hardening. Minimum wear V controlled section striker And peaks - 0.53 mm channels housings and bushings – 0.035 mm; high wear resistance up to the beginning of destruction deposited layer – 1500 cycles; none action cracks V channels housings and bushings and moderate amount cracks on the striker and pique– 9/cm.	Weakening in process surfacing main material corps and bushings; big depth cracks on striker And pique–do 0 , 7 mm; necessary mechanical processing honing fused layer; absence acceptable technologies application coatings on details hydraulic hammer.

10	Chromium-plated ie in Sumy Swiss technologies, on in the body And in the bushing 13–80 μm, on striker And pique - 17–40 microns	1900	Availability leftovers coatings on the body, in the bushing, striker And pique to 20 - 30 microns; durability approximately V 1,9 times higher, how durability details without strengthening. Small wear V controlled section striker And peaks - 0.8 mm; high wear resistance to beginning destruction coatings – 1000 cycles.	Big wear channels bushings andcorpus–0,6 mm; significant quantity cracks V channels bushings And corps -22/cm and on striker And pique– 17/cm; big depth cracks on in the body And in the bushing to 1 mm; on striker And pique– to 0.8 mm.Necessary polishing coatings And Creation specialized plot chromium plating.
11	Chrome plating decomposition of the compound "Barkhos", on the body and sleeve 26– 150 microns, on the striker and peak – 25–120 microns	1300	Presence of coating residues on body and sleeve – 20–80 μm, on striker and a dive – up to 10 μm; slight wear in the control cross-section of the striker and the peak – 0.85 mm; a small number of cracks along channels corps and bushings - 5/cm and their small depth - 0.05-0.1 mm; no finishing is needed operations on coating.	Low durability value - approximately V 1.3 times higher than durability details in the original condition; significant wear of the housing and bushing channels – 0.55 mm.Low wear resistance before the coating starts to break down – 400 cycles; a greater number of cracks on the striker and peak – 18/cm with a depth of 0.1–0.15 mm; environmental hazard; lack of recycling technology waste.

Continuation table. 14.3

14. CONCLUSIONS AND OFFERS

1. The work created and tested a methodology for comparative evaluation of the effectiveness of strengthening technologies for increasing the durability of hydraulic hammer parts, based on testing parts after various strengthening options, and ensuring the action of pressures during loading, and gas-dynamic characteristics simulating the corresponding parameters of operational loads.

2. Testing of the original (hardened only by volumetric heat treatment) version of the body and sleeve of the hydraulic hammer shows that the main types of damage to the working surfaces are: wear, work hardening, peeling of the surface volumes of the metal, and the formation of cracks.

3. The determination of the optimal method for increasing the durability of the body, bushing, striker and peak was carried out by testing parts subjected to strengthening treatments, including:

– impact on the surface volumes of the body and bushing material (electric spark alloying, laser heat treatment);

– application of wear-resistant coatings (chrome - galvanic using conventional technology and using Sumy-Swiss jet technology, ion-plasma with vacuum-arc deposition,

decomposition of the organochromium compound "Barkhos"; ion-plasma carbonitride coating; detonation gas spraying);

– surfacing wear-resistant materials (alloy "Hastelloy").

4. Comparative tests of the original version of the body and bushing, as well as those strengthened by impact on superficial volumes main product material, application of wear-resistant coatings and surfacing of materials, well resistant to wear, the following coefficients for increasing the service life of parts have been established depending on the method of their strengthening:

– ion-plasma chromium plating By typical technologies 1.0

–carbonitride cover 1.2

–electric spark alloying 1.3

–chromium plating decomposition organochromic connections "Barkhos" 1.3

– ion-plasma chromium plating using advanced technology 1.75

– detonation gas spraying 1.8
– laser thermal processing 1.8
– galvanic chromium plating By conventional technology 1.86
– galvanic chromium plating using Sumy-Swiss technology 1.9
– surfacing alloy Hastelloy 2.1

5. Tests of parts strengthened by the methods studied show that, compared to the original version, a significant increase in wear resistance is achieved:

– in the controlled cross-section of the striker and peak in the case of their strengthening by surfacing with Hastelloy alloy, chromium plating using Sumy-Swiss technology, detonation-gas spraying, ion-plasma chromium plating using improved technology and laser heat treatment;

– housings and bushings in the shear zone during their strengthening by surfacing with Hastelloy alloy, detonation gas spraying, laser heat treatment, ion-plasma chromium plating using improved technology and galvanic chromium plating using Sumy-Swiss technology.

6. A set of studies of parts manufactured without additional strengthening and with the use of strengthening treatments has established that as a result of the application of dynamic loads in the structure of the base metal of the body, bushing, regardless of the type of strengthening treatment (except for surfacing with alloy "Hastelloy") are happening structural-phase transformations that cause the formation of secondary hardening structures, tempering zones and cracks.

7. Metallographic studies of the parts showed that the wear-resistant coating in the controlled (most loaded) section of the peaks and strikers is preserved over almost the entire surface in the case of their strengthening by electric spark alloying, detonation gas spraying, laser heat treatment and surfacing with Hastelloy alloy, and in certain areas by chromium plating using Sumy-Swiss technology and ion-plasma vacuum-arc method using improved technology.

8. During the loading of hydraulic hammer parts, regardless of the method of hardening, a network of cracks is formed in the base metal of the picks and strikers; the greatest number of cracks (30/cm) was recorded in the metal that was not subjected to additional hardening, as well as in the metal hardened by galvanic chromium plating (17–19/cm) and detonation gas spraying (17/cm). The use of ion-plasma chromium plating and laser heat treatment results in a significant reduction in the number of cracks (3–5/cm).

9. A study of crack formation in the housing channel and bushing in the shear zone shows that galvanic chromium coatings increase inclination material details To crack formation by 1.8–2.2 times compared to the initial (additionally non-hardened) state. The use of laser heat treatment and detonation gas spraying leads to an increase in the crack resistance of the material for loading conditions by 1.3–2.4 times compared to the initial state; ion-plasma chromium plating, carbonitride coating and surfacing with Hastelloy alloy provide protection of the base material in the shear zone from crack formation.

10. Evaluation of the effectiveness of hardening treatments based on the durability of the body and bushing, wear in the controlled section of the striker and peak and the channel in the shear zone, wear resistance before the onset of destruction of the hardening coating, the number of cracks in main material. It allows us to recommend as the most acceptable and effective methods of strengthening the parts of a hydraulic hammer by using inserts made of Hastelloy material, chromium plating using Sumy-Swiss technology and ion-plasma chromium plating using advanced technology, detonation-gas spraying of wear-resistant materials and laser heat treatment.

LITERATURE

1. Аулін В. В., Тихий А. А. Трибофізичні основи підвищення зносостійкості і надійності робочих органів ґрунтообробних машин з різальними елементами : монографія. Кропивницький : Лисенко В. Ф. 2017. 278 с
2. Денисенко М. Опальчук А. Зношування та підвищення довговічності робочих органів сільськогосподарських машин. Вісник ТНТУ. 2011. Спецвипуск, Частина 2. С. 201–210.
3. Аулін В. В. Фізичні основи процесів і станів самоорганізації в триботехнічних системах : монографія.Кіровоград: Вид. Лисенко В.Ф., 2014. 370 с.
4. Аулін В. В. Стан самоорганізації середовища ґрунту та закономірності зносу робочих органів ґрунтообробних машин. Проблеми трибології (Problems of tribology). 2013. №1 С.114-119.
5. Аулін В. В. Підвищення надійності трибосистем реалізацією процесів самоорганізації. М-ли III міжнар. наук.-техн. конф.: "Сучасні проблеми триботехніки", 7-9 жовтня 2009р. Миколаїв: НУК, 2009.С 15-17
6. Черновол М. І. Характер зміни напружено-деформованого стану ґрунту під час його взаємодії з робочим органом. Вісник інженерної академії України. 2011. №1. С. 232-237.
7. Fang L. Predicting three-body abrasive wear using Monte Carlo methods. Wear. 2014. V. 256, № 7-8. P. 685-694.
8. О.М. Лосіков «Вид та характер зношення деталей качаючого вузла насоса підживлення аксіальнопоршневої гідромашини». Металлургическая и горнорудная промышленность. -2015.-№7.-С.170-173
9. Патент на корисну модель № 101220 Україна, МПК 8 В 23 В 1/00. Спосіб токарної обробки колодязя корпуса насоса підживлення аксіально-поршневої гідромашини / П. Т. Мельянцов, О. М. Лосіков, В. С. Назарець, В. К. Сидоренко, В. В. Власовець. - заяв. 14.04.2015; опубл. 25.08.2015, Бюл. №16.
10. Патент на корисну модель № 99052 Україна, МПК F04B1/20. Спосіб ремонту корпусу насоса підживлення аксіально-поршневої гідромашини / П.Т. Мельянцов, О. М. Лосіков. - заяв. 30.12.2014; опубл. 12.05.2015, Бюл. №9.
11. Тарельник В.Б. Підвищення довговічності валів відцентрових насосів комбінованими методами / В.Б. Тарельник, В.О. Пирогов // Вісник Національного технічного університету «ХПІ». Серія: Технології в машинобудуванні = Bulletin of the National Technical University "KhPI". Series: Techniques in a machine industry: зб. наук.пр. / Нац. техн. ун-т «Харків. політехн. ін-т». – Харків : НТУ «ХПІ», 2022. – № 2 (6) 2022. – С. 79–87. – ISSN 2079-004X, DOI: 10.20998/2079-004X.2022.2(6).11.
12. Тарельник В.Б. Реновація шийок підшипників ковзання валів відцентрових насосів для зрошення / В.Б. Тарельник, М.Ю. Думанчук, Н.В. Тарельник, Т.П. Волошко, В.О. Пирогов // Вісник Сумського національного аграрного університету. Серія: Механізація та автоматизація виробничих процесів. - № 1(47). – 2022. – С.43-49.
13. Тарельник В.Б., Пирогов В.О. Підвищення довговічності насосних агрегатів,

задіяних в системах зрошення, комбінованими екологічно безпечними технологічними методами // Вісник Сумського національного аграрного університету. Серія: Механізація та автоматизація виробничих процесів – №2(48) – 2022. С. 66-75.

14. V. B. Tarelnyk, O. P. Gaponova, Ie. V. Konoplianchenko, N. V. Tarelnyk, M. Y. Dumanchuk, M. O. Mikulina, V. O. Pirogov, S. O. Gorovoy, and N. K. Medvedchuk, Development the Directed Choice System of the Most Efficient Technology for Improv-ing the Sliding Bearings Babbitt Covers Quality. Pt. 1. Peculiarities of Babbitt Coat-ing Technologies, Metallofiz. Noveishie Tekhnol., 44, No. 1:1475–1493 (2022) (in Ukrainian). https://doi.org/10.15407/mfint.44.11.1475

15. V. B. Tarelnyk, O. P. Gaponova, Ie. V. Konoplianchenko, N. V. Tarelnyk, M. Y. Dumanchuk, V. O. Pirogov, T. P. Voloshko, and D. B. Hlushkova, Development the Directed Choice System of the Most Efficient Technology for Improving the Sliding Bearings Babbitt Covers Quality. Pt. 2. Mathematical Model of Babbitt Coatings Wear. Criteria for Choosing the Babbitt Coating Formation Technology, Metallofiz. Noveishie Tekhnol., 44, No. 12: 1643–1659 (2022) (in Ukrainian). DOI: 10.15407/mfint.44.12.164

16. Ie. Konoplianchenko, V. Tarelnyk, Vas. Martsynkovskyy, O. Gaponova, A. Lazarenko, A. Sarzhanov, M. Mikulina, Zh. Zhengchuan, V. Pirogov. New technology for restoring Babbitt coatings. Journal of Physics: Conference Series. 1741 (2021) pp. 012040-1 – 012040-15. https://doi.org/10.1088/1742-6596/1741/1/012040 (SCOPUS & WoS)

17. Пирогов В.О. Забезпечення протидії фреттинг-корозії деталей пар тертя / В.О. Пирогов // ТЕХНОЛОГІЇ XXI СТОРІЧЧЯ. Збірник тез за матеріалами 27-ої міжнародної науково-практичної конференції (24-26 листопада 2021 р.) Частина 1 «Прогресивні технології в промисловості» Суми – 2021.- С. 236-237.

18. Пирогов В.О. Проблеми підвищення якості машин, задіяних в технологічному циклі зрошення / В.О. Пирогов // Машинобудування очима молодих: прогресивні ідеї – наука – виробництво: матеріали XX Міжнародної науково-технічної конференції (м. Суми, 29 вересня – 1 жовтня 2021 року). – С. 75-78.

19. Тарельник В.Б. Технологічне забезпечення процесу відновлення бабітового покриття на етапі ремонту підшипникових вузлів роторних машин/ В.Б. Тарельник, Є.В. Коноплянченко, В.О. Пирогов В.О., Чжан Чженчуань // Машинобудування очима молодих: прогресивні ідеї – наука – виробництво: матеріали XX Міжнародної науково-технічної конференції (м. Суми, 29 вересня – 1 жовтня 2021 року) – С. 88, 89.

20. Тарельник В. Б., Думанчук М. Ю., Пирогов В. О. Застосування системного підходу для управління якістю поверхневих шарів деталей насосних агрегатів // The 5th International scientific and practical conference ―Modern research in world science‖ (August 7-9, 2022) SPC ―Sci-conf.com.ua‖, Lviv, Ukraine. 2022. pp. 256-262.

21. Тарельник В.Б. Критерії вибору технології нанесення бабітових покрить підшипників ковзання роторних машин/ В.Б. Тарельник, В.О. Пирогов //Матеріалознавство та технології: матеріали міжнародної науково-технічної конференції. – Харків ХНАДУ, 2022. – С. 61-70.

22. Спосіб виготовлення деталей з нержавіючої сталі з комбінованим електроіскровим покриттям на зношувальних плоских і криволінійних поверхнях : пат. 142338 України на корисну модель, МПК (2020.01), B23H 5/00, B23H 9/00 /

Тарельник В. Б., Марцинковський В. С., Гапонова О. П., Коноплянченко Є. В., Тарельник Н. В., Саржанов Б. О., Пирогов В. О., Лазаренко А. Д., Гапон О. О. ; заявл. 11.01.2020 ; опубл. 25.05.2020, Бюл. № 10. 10 с.

23. Спосіб формування покриття на зношувальних поверхнях деталей : пат. 141919 України на корисну модель, МПК (2020.01) B23H 5/00, B23H 9/00 / Тарельник В. Б., Марцинковський В. С., Гапонова О. П., Коноплянченко Є. В., Тарельник Н. В., Саржанов Б. О., Пирогов В. О., Лазаренко А. Д., Гапон О. О. ; заявл. 27.12.2019 ; опубл. 27.04.2020, Бюл. № 8. 8 с.

24. Спосіб формування покриття на зношувальних поверхнях деталей : пат. 141920 України на корисну модель, МПК (2020.01) B23H 5/00, B23H 9/00 / 183 Тарельник В. Б., Марцинковський В. С., Гапонова О. П., Коноплянченко Є. В., Тарельник Н. В., Саржанов Б. О., Пирогов В. О., Лазаренко А. Д., Гапон О. О. ; заявл. 27.12.2019 ; опубл. 27.04.2020, Бюл. № 8. 9 с.

25. Спосіб цементації сталевих деталей електроіскровим легуванням : пат. 142822 України на корисну модель, МПК (2020.01) C23C 8/00, C23C 28/00 / Тарельник В. Б., Марцинковський В. С., Гапонова О. П., Мисливченко О. М., Пирогов В.О., Гапон О. О., Лазаренко А. Д. ; заявл. 11.02.2020 ; опубл. 25.06.2020, Бюл. № 12. 8 с.

26. Спосіб захисту деталей пари тертя пружної муфти від фреттинг-корозії: пат. 142811 України на корисну модель : МПК (2020.01), C23F 15/00, F01D 5/28 (2006.01) / Тарельник В. Б., Марцинковський В. С., Думанчук М. Ю., Коноплянченко Є. В., Гапонова О. П., Тарельник Н. В., Пирогов В.О., Гапон О. О. ; заявл. 05.02.2020 ; опубл. 25.06.2020, Бюл. № 12. 8 с.

27. Спосіб формування покриття на поверхні сталевої деталі методом електроіскрового легування: пат. 144932 України на корисну модель, МПК (2020.01), B23H 1/00, B23H 9/00, C23C 4/00, C23C 6/00, C23C 8/60 (2006.01) / Тарельник В. Б., Марцинковський В. С., Гапонова О. П., Мисливченко О. М., Пирогов В.О., Гапон О. О., Лазаренко А. Д. ; заявл. 26.02.2020 ; опубл. 10.11.2020, Бюл. № 21. 15 с.

28. Спосіб зміцнення поверхонь сталевих деталей пар тертя: пат. 148495 України на корисну модель, МПК (2021.01) B23H 1/00 B23H 7/00 C23C 10/48 (2006.01) C23C 8/70 (2006.01) / Тарельник В.Б., Марцинковський В.С., Гапонова О.П., Мисливченко О.М., Коноплянченко Є.В. Тарельник Н.В., Саржанов О.А., Лазаренко А.Д., Поливаний А.Д., Зенкін М.А., Волошко Т.П. ; заявл. 23.04.2021 ; опубл. 11.08.2021, Бюл. № 32. 11 с.

29. Спосіб формування пакетів гнучких елементів пружних муфт: пат. 151426 України на корисну модель : МПК (2022.01) F16D 3/56 (2006.01) C10M 103/02 (2006.01) C10M 111/00 / Марцинковський В.С., Думанчук М.Ю., Тарельник Н.В., Пирогов В.О., Лазаренко А.Д.; заявл. 25.01.2022; 20.07.2022, Бюл.№ 29. 8 с. 184

30. Спосіб обробки бронзових вкладишів підшипників ковзання: пат. 148005 України на корисну модель, МПК (2021.01), B23H 1/00, B23H 5/00, F16C 33/04 (2006.01) C23C 8/00 C23C 4/00 C23C 14/00 / Тарельник В. Б., Марцинковський В. С., Гапонова О. П., Коноплянченко Є.В., Антошевський Богдан (PL), Роп’як Л.Я., Саржанов О.А., Тарельник Н.В., Мікуліна М. О., Пирогов В. О., Лазаренко А.Д., Поливаний А.Д.; заявл. 22.03.2021 ; опубл. 23.06.2021, Бюл. № 25. 12 с.

31. Спосіб обробки бронзових вкладишів підшипників ковзання: пат. 148006

України на корисну модель, МПК (2021.01), B23H 1/00, B23H 5/00, F16C 33/04 (2006.01) C23C 8/00 C23C 4/00 C23C 14/00 / Тарельник В. Б., Марцинковський В. С., Гапонова О. П., Коноплянченко Є.В., Антошевський Богдан (PL), Роп'як Л.Я., Саржанов О.А., Тарельник Н.В., Мікуліна М. О., Пирогов В. О., Лазаренко А.Д., Поливаний А.Д.; заявл. 22.03.2021 ; опубл. 23.06.2021, Бюл. № 25. 12 с.

32. Спосіб обробки бронзових вкладишів підшипників ковзання: пат. 126517 України на винахід, МПК (2021.01), B23H 1/00, B23H 5/00, F16C 33/04 (2006.01) C23C 8/00 C23C 4/00 C23C 14/00 / Тарельник В. Б., Марцинковський В. С., Гапонова О. П., Коноплянченко Є.В., Антошевський Богдан (PL), Роп'як Л.Я., Саржанов О.А., Тарельник Н.В., Мікуліна М. О., Пирогов В. О., Лазаренко А.Д., Поливаний А.Д.; заявл. 22.03.2021 ; опубл. 19.10.2021, Бюл. № 42. 12 с.

33. Хмара Л.А. Машини для земляних робіт : навч. посібник / Л.А. Хмара, С.В. Кравець, В.В. Нічке, Л.В. Назаров [та ін.] // Під загальною редакцією проф. Хмари Л.А. та проф. Кравця С.В. – Рівне Дніпропетровськ-Харків, 2010. – 557 с.

34. Кириченко І.Г., Назаров Л.В., Нічке В.В. та ін. Наукові основи створення високоефективних землерийно-транспортних машин. - Харків, 2003. - 588 с.

35. Баладінський В.Л. Машини для земляних робіт / В.Л. Баладінський, О.М. Гаркавенко, С.В. Кравець, І.В. Русан, А.В. Фомін. - Рівне: РДТУ, 2000. - 288 с.

36. Фомін А.В., Костенюк О.О., Тетерятник О.А., Боковня Г.І. Конструкція будівельних і меліоративних машин для земляних робіт: Навчальний посібник.– К.: КНУБА, 2005. –93 с.

37. Фомін А.В., Костенюк О.О., Тетерятник О.А., Боковня Г.І. Машини і обладнання для будівництва, утримання і ремонту доріг: Навчальний посібник.–К.: КНУБА, 2005. –125 с.

38. Григоров О. В. Гідравлічний привід підйомно-транспортних, будівельних та дорожніх машин : навч. посібник / О. В. Григоров ; Харківський політехнічний ін-т, нац. техн. ун-т. – Харків : НТУ "ХПІ", 2003. – 264 с. Додаткова література

39. Кузенко Л. М. Дорожньо-будівельні машини : навчальний посібник / Л. М. Кузенко, Д.В. Кузенко, З.З. Вантух, Я.Й. Панюра. – Київ: Видавничий дім «Кондор», 2021. – 236 с.

40. "Institute for SingleCrystals" A fractal approach to estimating the durability of critical parts A.V.Uzhva1, O.V.Orel 1, D.B.Hlushkova1, V.M.Volchuk ISSN 1027-5495. Functional Materials, 31, No.3 (2024), p. 381-386 doi:http://dx.doi.org/10.15407/fm31.03.381 © 2024 — STC

41. Методичні вказівки до виконання лабораторно– практичних занять з дисципліни «Надійність і випробування будівельних і дорожніх машин» / Кіровоград: КНТУ, 2015. – 43 с. 3. Конспект лекцій.

42. Серія стандартів ISO 9000. [Електронний ресурс] : офіційний сайт. – URL: https://www.intercert.com.ua.

43. ДСТУ 3004-95. Надійність техніки. Методи оцінки показників надійності за експериментальними даними. [Електронний ресурс] : офіційний сайт. – URL:https://dnaop.com/html/43855/doc-ДСТУ_3004-95.

TABLE OF CONTENTS

Science vision

HLUSHKOVA Diana
UZHVA Anatoliy
SUMINOV Andrii
SKRYPNIKOV Viktor

TECHNOLOGICAL APPROACHES TO INCREASE PARAMETERS QUALITIES OF A HYDRAULIC HAMMER

Monograph